ICLIAD 65 (3), 265-402, 2024

p-ISSN 0535-5133
e-ISSN 2477-9393

Volumen 65
No. 3
Septiembre
2024

Investigación Clínica

Universidad del Zulia
Facultad de Medicina
Instituto de Investigaciones Clínicas
"Dr. Américo Negrette"
Maracaibo, Venezuela

Investigación Clínica

https://sites.google.com/site/revistainvestigacionesclinicas

Revista arbitrada dedicada a estudios humanos, animales y de laboratorio relacionados con la investigación clínica y asuntos conexos.

La Revista es de Acceso Abierto, publicada trimestralmente por el Instituto de Investigaciones Clínicas "Dr. Américo Negrette", de la Facultad de Medicina, de la Universidad del Zulia, Maracaibo, Venezuela.

Investigación Clínica está indizada en Science Citation Index Expanded (USA), Excerpta Medica/EMBASE y Scopus (Holanda), Tropical Diseases Bulletin y Global Health (UK), Biblioteca Regional de Medicina/BIREME (Brasil), Ulrich's Periodicals, Journal Citation Reports (USA), Index Copernicus (Polonia), SIIEC Data Bases, Sección Iberoamérica (Argentina) e Infobase Index (India), Redalyc y las bases de datos: SciELO (www.Scielo.org.ve), Revencyt, LILACS, LIVECS, PERIODICA y web de LUZ: http://www.produccioncientificaluz.org/revistas

Para cualquier otra información dirigir su correspondencia a:

Dra. Elena Ryder, Editora
Instituto de Investigaciones Clínicas "Dr. Américo Negrette"
Facultad de Medicina, Universidad del Zulia
Maracaibo, Venezuela.

Teléfono:
+58-0414-6305451

Correos electrónicos:
elenaryder@gmail.com
riclinicas@gmail.com

Páginas web:
https://sites.google.com/site/revistainvestigacionesclinicas

http://www.produccioncientificaluz.org/revistas

For any information please address correspondence to:

Dr. Elena Ryder, Editor
Instituto de Investigaciones Clínicas "Dr. Américo Negrette"
Facultad de Medicina, Universidad del Zulia
Maracaibo, Venezuela.

Phone:
+58-0414-6305451

E-mails:
elenaryder@gmail.com
riclinicas@gmail.com

Web pages:
https://sites.google.com/site/revistainvestigacionesclinicas

http://www.produccioncientificaluz.org/revistas

Universidad del Zulia
Publicación auspiciada por el
Vicerrectorado Académico
Serbiluz-CONDES

CODEN: ICLIAD
Versión impresa ISSN: 0535-5133
Depósito legal pp 196002ZU37
Versión electrónica ISSN: 2477-9393 Depósito legal ppi 201502ZU4667

Artes finales:
Lisbeny Valencia
lisbenyvalencia@gmail.com

Invest Clin 65(3): 265 - 266, 2024 https://doi.org/10.54817/IC.v65n3a00

EDITORIAL
Nuestra experiencia con Crossref.

Crossref es una organización sin fines de lucro, orientada a proveer una infraestructura digital a la comunidad académica y de investigación global. Es la mayor agencia de registro de identificadores de objetos digitales (DOI) de la Fundación Internacional DOI. El **identificador de objeto digital**, conocido en inglés como *digital object identifier* y abreviado DOI, es un enlace permanente en forma de código alfanumérico que identifica de forma única un contenido electrónico. Una forma común de emplear el sistema DOI es dar a las publicaciones científicas un número específico que cualquiera puede utilizar para localizar a través de la Red el citado artículo. Constituye una fuente valiosa para la investigación en cienciometría, incluida la medición del crecimiento y el impacto de la ciencia y la comprensión de las nuevas tendencias en las comunicaciones académicas.

Crossref proporciona a los editores de las revistas científicas, un registro mensual de la cantidad de veces que el DOI de un trabajo, publicado en la revista, ha sido visitado por un individuo. Se asume que, si lo visita, es porque tiene interés en el tema tratado en dicho trabajo y, por lo tanto, puede ser una medida del impacto que ese trabajo tiene como referencia para su investigación; puede ser motivo para afianzar sus conocimientos en su profesión o simplemente motivado para conocer sobre un tema, de una forma más sólida que la que pueden brindar las redes sociales, las cuales están plagadas de información sin base científicamente probada. Con más de 106 millones de registros y una tasa de expansión promedio del 11% anual, los metadatos de Crossref se han convertido en una de las principales fuentes de datos académicos para editores, autores, bibliotecarios, financiadores e investigadores [1].

Investigación Clínica se beneficia del servicio de Crossref desde comienzos del 2022. En el Editorial del número correspondiente a diciembre del 2022[2], me referí al impacto de las citaciones *vs l*a lectura de un trabajo, discutiendo algunas posiciones de investigadores sobre este punto. Este tema acerca de la vigencia de las visitas a la Revista, también ha sido objeto de análisis en un estudio sobre la experiencia con nuestra página "Web" [3]. Quiero en este documento expresar nuestra experiencia con Crossref en cuanto a la frecuencia y cantidad de visitas que han recibido los trabajos publicados en la Revista, todos identificados con DOI durante los años 2022 y 2023 y comentar lo que está sucediendo en los primeros 6 meses del 2024. Durante el año 2022 se obtuvo un total de 11.121 visitas, con un promedio mensual de 926, cifras que se elevaron a 13.008 visitas durante el 2023, con un promedio de 1.084 por mes. Los trabajos más frecuentemente citados, identificados por Crossref como "top ten" representaron entre un 20 a 30% del total de cada uno de estos dos años, visitas que variaron entre 12 y 165 veces. Sin embargo, hay que considerar que un buen número de trabajos (70-80%) recibieron al menos 1 visita. No sabemos si estas visitas se transformaran en una citación, pero tal como mencioné en la referencia del editorial del 2022[2], el efecto de leer un trabajo puede ser tan útil como una citación. Como en aquella ocasión, los trabajos más visitados fueron los de Revisión, la mayoría (24/162), fueron investigaciones realizadas en Venezuela y escritos preferentemente en español. Sin embargo, también obtuvieron visitas dentro del "top ten" trabajos de otros países latinoamericanos como México y Perú, además de España y países asiáticos.

Y tal como esperábamos para el 2024[4], en los primeros 6 meses el total de visitas ya alcanza 10.707, con un promedio mensual de 1.784, 65% superior al promedio del 2023 y 93% al del 2022. Las características de los trabajos visitados en estos primeros meses del 2024 se asemejan a lo encontrado en los dos años anteriores.

Esto nos lleva a concluir que la revista tiene más lectores en países de habla hispana, a pesar que la proporción de trabajos en español se mantiene, en los últimos años, en menor proporción que los escritos en inglés. Consideramos que la inclusión del DOI en los trabajos, puede ser efectiva no tan solo para servir de identificador del artículo y para ser referidos en la bibliografía de las publicaciones, sino para que cualquier individuo pueda ubicar el tema de primera mano y así actualizar, transmitir conocimientos o aplicar políticas públicas en salud o en educación.

Elena Ryder
ORCID 0000 0003 4613 6424

REFERENCIAS

1. **Hendricks G, Tkaczyk D, Lin J, Feeney P.** Crossref: The sustainable source of community-owned scholarly metadata. *Quantitative Science Studies* 2020; 1 (1): 414–427. *doi: https://doi.org/10.1162/qss_a_00022.*
2. **Ryder E.** Leer versus citar un trabajo. Análisis de nuestras publicaciones en los últimos años. Invest Clin 2022; 63 (4): 323-325. *https://doi.org/10.54817/IC.v63n4a00.*
3. **Torres Guerra E.** Primera década de la revista Investigación Clínica en la "Web". Invest Clin 2023; 64 (1):123-126. *https://doi.org/10.54817/IC.v64n1a09.*
4. **Ryder E.** Alcances de la revista Investigación Clínica durante el año 2023. Invest Clin 2024; 65 (1): 1-3. *https://doi.org/10.54817/ICv65n1a00.*

Our experience with Crossref

The DOI or digital object identifier gives scientific publications a specific number used to locate them on the Internet. Crossref is the largest DOI registration agency and provides editors of scientific journals with a monthly record of the number of times an individual has visited the DOI of a work published in the Journal. This visit can measure the impact of the work as a reference for your research, to strengthen your professional knowledge, or to learn about a topic more solidly than that provided by social networks, which are full of information without a scientifically proven basis. This Editorial expresses my experience with Crossref regarding the frequency and number of visits the works published in the Journal identified with DOI have received from 2022 and 2023. In 2022, there were 11,121 visits (926/month), which rose to 13,008 visits in 2023 (1,084/month). The most frequently cited works, identified by Crossref as "top ten," represented between 20 and 30% of the total, with a frequency of visits of 12 to 165 times. However, 70-80% received at least one visit. The most visited works were Reviews, with the majority (24/162) realized in Venezuela and in Spanish. However, works from other Latin American countries such as Mexico and Peru, in addition to Spain and Asian countries, also received visits within the "top ten". This leads us to conclude that the Journal has more Spanish-speaking readers, even though the proportion of works in Spanish is lower than those in English. We believe that the inclusion of the DOI in the works can be effective not only to serve as an identifier for the article and to be cited in the bibliography of the publications but also so that any individual can locate a topic firsthand and thus update, transmit knowledge or apply public policies in health or education.

Invest Clin 65(3): 267 - 278, 2024 https://doi.org/10.54817/IC.v65n3a01

Dihydroartemisinin, an artemisinin derivative, reverses oxaliplatin resistance in human colorectal cancer cells by regulating the SIRT3/PI3K/AKT signalling pathway.

Xiaodong Shen, Chencheng Shi, Ming Lei, Rongjian Zhou, Shaoqun Liu and Chang Su

Department of Gastrointestinal Surgery, Minhang Hospital Affiliated to Fudan University, Shanghai, China.

Keywords: dihydroartemisinin; SIRT3; oxaliplatin; colorectal cancer.

Abstract. Dihydroartemisinin (DHA), a derivative of artemisinin, has been shown to act as a chemosensitizer of various cancer chemotherapeutic agents both *in vitro* and *in vivo*. However, in colorectal cancer (CRC), no study has focused on the effect of DHA on oxaliplatin (L-OHP) resistance. Our study aimed to examine the effectiveness of DHA in reversing the resistance of human CRC cells to L-OHP, as well as its underlying molecular mechanisms. LoVo cells were purchased from ATCC, while LoVo/L-OHP cells were obtained by exposing LoVo cells to progressively increasing concentrations of L-OHP. LoVo/L-OHP were treated with various concentrations of DHA, and cell apoptosis ratio and viability were assessed by flow cytometry and CCK-8. Our results showed that DHA treatment remarkably decreased the viability of LoVo/L-OHP cells and increased the apoptosis ratio. As the mechanism of action, we found that DHA enhanced the expression of Sirtuin 3 (SIRT3) and suppressed the phosphatidylinositol 3-kinase (PI3K)/AKT signalling cascade. Silencing of SIRT3 reversed the effect of DHA on cell apoptosis and viability by activating the PI3K/AKT axis in LoVo/L-OHP cells. Overall, our study found that DHA has the ability to counteract L-OHP resistance in LoVo/L-OHP cells through the modulation of the SIRT3/PI3K/AKT signalling pathway, suggesting a new research target for CRC treatment.

Corresponding authors: Shaoqun Liu and Chang Su. Department of Gastrointestinal Surgery, Minhang Hospital Affiliated to Fudan University, Xinzhuang Town, Shanghai 201199, China. E-mail: liushaoqun@fudan.edu.cn
E-mail: surgeon_suchang@fudan

La dihidroartemisinina, un derivado de la artemisinina, revierte la resistencia al oxaliplatino en células humanas de cáncer colorrectal mediante la regulación de la vía de señalización SIRT3/PI3K/AKT.

Invest Clin 2024; 65 (3): 267 – 278

Palabras clave: dihidroartemisinina; SIRT3; oxaliplatino; cáncer colorrectal.

Resumen. Se ha demostrado que la dihidroartemisinina (DHA), un derivado de la artemisinina, actúa como quimiosensibilizador de diversos agentes quimioterapéuticos contra el cáncer tanto *in vitro* como *in vivo*. Sin embargo, en el cáncer colorrectal (CCR), ningún estudio se ha centrado en el efecto del DHA sobre la resistencia al oxaliplatino (L-OHP). El objetivo de nuestro estudio era examinar la eficacia del DHA para revertir la resistencia de las células humanas de CCR al L-OHP, así como sus mecanismos moleculares subyacentes. Las células LoVo se adquirieron a ATCC, mientras que las células LoVo/L-OHP se obtuvieron exponiendo las células LoVo a concentraciones progresivamente crecientes de L-OHP. Las células LoVo/L-OHP se trataron con diversas concentraciones de DHA, y el índice de apoptosis celular y la viabilidad se evaluaron mediante citometría de flujo y CCK-8. Nuestros resultados mostraron que el tratamiento con DHA disminuía notablemente la viabilidad de las células LoVo/L-OHP y aumentaba el índice de apoptosis. Desde el punto de vista de su mecanismo de acción, se observó que el DHA potenciaba la expresión de la sirtuina 3 (SIRT3) y suprimía la cascada de señalización fosfatidilinositol 3-cinasa (PI3K)/AKT. El silenciamiento de SIRT3 revirtió el efecto del DHA sobre la apoptosis y la viabilidad celular a través de la activación del eje PI3K/AKT en las células LoVo/L-OHP. En conjunto, nuestro estudio descubrió la capacidad del DHA para contrarrestar la resistencia a L-OHP en células LoVo/L-OHP a través de la modulación de la vía de señalización SIRT3/PI3K/AKT, lo cual sugiere una nueva foco de investigación para el tratamiento del CCR.

Received: 25-07-2023 Accepted: 27-09-2023

INTRODUCTION

According to the 2020 GLOBOCAN statistics on the incidence and mortality rates of 36 types of cancer worldwide, colorectal cancer (CRC) ranks third in terms of incidence (10.0%) but second in terms of mortality rate (9.4%) [1]. Chemotherapy based on oxaliplatin (L-OHP) is a crucial component of the comprehensive treatment for CRC, which can prolong the survival of patients and improve their quality of life [2-4]. However, primary and/or acquired resistance to L-OHP remains a significant factor limiting the effectiveness of CRC treatment [5,6]. Therefore, it is urgent to clarify the mechanisms of L-OHP resistance in CRC and to find corresponding resistance reversal agents or chemosensitizers.

Previous studies have demonstrated that the mechanisms of resistance to platinum-based chemotherapy drugs may be re-

lated to the abnormal regulation of signalling networks within tumor cells caused by the sustained action of drugs. For example, abnormalities in signalling pathways such as PI3K/AKT and NF-κB give the cells strong anti-apoptotic abilities, leading to resistance to chemotherapy drugs [7,8]. Sirtuin 3 (Sirt3) plays a crucial role in controlling physiological and pathological processes, such as regulating inflammation, oxidative stress, cell proliferation, differentiation, and apoptosis. This protein belongs to the sirtuin protein family, known for its diverse biological functions [9-11]. Research has found that SIRT3 can cause mutant p53 to be deacetylated, leading to cancer cell apoptosis and increased sensitivity to chemotherapeutic drugs [12]. Other evidence also suggested that SIRT3 could improve disease conditions by regulating apoptosis and utilizing the PI3K/Akt pathway in various diseases [13,14]. Dihydroartemisinin (DHA) is a derivative of artemisinin, and there is evidence that DHA can act as a chemosensitizer for various cancer chemotherapeutic drugs both *in vitro* and *in vivo*[15]. The latest research has found that DHA can alleviate acute and chronic pain by increasing the activity of SIRT3 [16]. However, in CRC, no study has focused on the effect of DHA on L-OHP resistance through the SIRT3/PI3K/AKT axis.

Based on previous studies, we hypothesize that DHA may affect the resistance of human CRC cells to L-OHP by regulating the SIRT3/PI3K/AKT axis. Our study aimed to examine the effectiveness of DHA in reversing the resistance of human colorectal cancer cells to L-OHP, as well as its underlying molecular mechanisms.

METHOD

Cell culture and induction of L-OHP resistance

Human CRC cells (LoVo, not resistant to L-OHP) were obtained from the American Type Culture Collection (CCL-229, ATCC) in Manassas, Virginia. The human L-OHP-resistant CRC cells (LoVo/L-OHP, resistant to L-OHP) were obtained by exposing LoVo cells to progressively increased concentrations of L-OHP [17]. The initial concentration of L-OHP was 5 μM, and cells were exposed to L-OHP for two days in each cycle, followed by recovery in L-OHP-free culture medium. The same concentration of L-OHP was repeated for three cycles. After completing three cycles at the same concentration of L-OHP stimulation, the dose was escalated. This procedure was repeated until the final concentration of L-OHP reached 70 μM. Only cells that remained resistant to L-OHP after being cultured in an L-OHP-free medium for at least six months were used for subsequent experiments.

The LoVo/L-OHP and LoVo cells were cultured at 37°C and 5% CO_2 in RPMI-1640 medium (Thermo Fisher Scientific, Inc., MA, USA) that was supplemented with 10% Gibco® fetal bovine serum (FBS) and 100 μg/mL penicillin-streptomycin. Cells were treated with PI3K inhibitor LY294002 (1μM) for 24 hours to inhibit PI3K signaling.

Preparation of Dihydroartemisinin Solution

A stock solution of dihydroartemisinin (obtained from Puyi Biological, Nanjing, China) was prepared by dissolving it in a small quantity of dimethyl sulfoxide (DMSO, procured from Sigma-Aldrich, USA). The resulting stock solution was formulated to have a concentration of either 100 or 300 nmol/L, which was sonicated and stored at 4°C. In subsequent experiments, all cell samples were treated with 30 μM L-OHP or an equivalent amount phosphate-buffered saline (PBS) for treatment.

Cell transfection

The siRNA targeting the SIRT3 gene (si-SIRT3#1, #2, #3) and the negative control (NC) were procured from GeneChem Corp. for cell transfection experiments.

According to the manufacturer's instructions, the LoVo/L-OHP cells were transfected with 5 nM of the aforementioned siRNA or negative controls. Transfection was carried out by using the lipofectamine 3000 (Invitrogen) reagent, following the prescribed protocol, while incubating the cells in a serum-free Opti-MEM medium. After 48 hours of transfection, the transfection efficiency was evaluated through RT-qPCR.

Cell Counting Kit-8 (CCK-8)

LoVo, LoVo/L-OHP, and LoVo/L-OHP+DHA (100nmol/L or 300nmol/L) cells were treated with different concentrations of OHP (5μM-70μM) [17,18]. Cells were cultured into 96-well plates at 5×10^3 cells/well density. After incubating the cells with CCK-8 reagent (10μL, Sangon) for 2 hours, the absorbance at 450 nm was determined on a microplate reader (Thermo Fisher Scientific, MA, USA). The half-maximal inhibitory concentration (IC_{50}) of L-OHP was determined in LoVo and LoVo/L-OHP cells [19].

Reverse transcription-quantitative polymerase chain reaction (RT-qPCR)

RT-qPCR was used to determine the expression of PI3K, SIRT3 and AKT in the cells. We utilized the RNAiso plus kit (procured from Takara, Japan) to obtain RNA from cells and subsequently performed reverse transcription into cDNA using the PrimeScriptTM one-step qRT-PCR kit (obtained from Takara, Dalian, China). For RT-qPCR, we employed the SYBR Premix ExTaq (TaKaRa) and the ABI PRISM7300 Sequence Detection System (from Applied Biosystems). Primer sequences are shown in Table 1. GAPDH served as an internal control. The mRNA expressions were calculated by the $2^{-\Delta\Delta}$Ct method.

Western blot

Total proteins were extracted from the cell lysates and quantified using the Pierce™ BCA Protein Assay Kit (Thermo Scientific).

Table 1
The sequences of all constructs.

Name		Sequence
SIRT3	Forward	5'-CCCCAAGCCCTTTTTCACTTT-3'
	Reverse	5'-CGACACTCTCTCAAGCCCA-3'
PI3K	Forward	5'-TCTAAACCCTGCTCATC-3'
	Reverse	5'-CTTGCCGTAAATCATCCC-3'
AKT	Forward	5'-CTACAACCAGGACCATGAGAAG-3'
	Reverse	5'-ACACGATACCGGCAAAGAAG-3'
GAPDH	Forward	5′-CACCCACTCCTCCACCTTTG-3′
	Reverse	5′-CCACCACCCTGTTGCTGTAG-3′

Then, 20 μg of the extracted proteins were separated by SDS-PAGE and transferred onto PVDF membranes. The PVDF membranes were then incubated with a primary antibody at 4°C overnight. After washing, the membranes were incubated with Goat Anti-Rabbit IgG H&L secondary antibody (ab96899, 1/1000) at 37°C for 45 minutes. The primary antibodies included the SIRT3 antibody ab217319, 1/1000, Abcam), PI3K antibody (ab140307, 1/2000, Abcam), AKT antibody (ab8805, 1/1000, Abcam), bcl-2 antibody (ab32124, 1/1000, Abcam), Bax antibody (ab32503, 1/1000, Abcam), cleaved caspase-3 antibody (ab32042, 1/5000, Abcam), P-gb (ab202976, 1/1000, Abcam), GAPDH antibody (ab8245, 1/1000, Mybiosource), and GAPDH was served as an internal control. We utilized the Pierce ECL Western Blotting Substrate to visualize the protein bands, which was procured from Pierce in Shanghai, China. The membranes were developed and imaged using a chemiluminescence imaging system.

Flow cytometry for cell apoptosis

Cells were incubated at 37°C with 5% CO_2. After the incubation of 24 h, LoVo/L-OHP cells were collected into 1.5 mL tubes with annexin-FITC and propidium iodide (PI) regents, followed by incubation for 10 min. To detect cell apoptosis, 200 μL PI was supplemented with 1 mL phosphate buffer

solution (PBS) into the flow tube. Then, the apoptotic cells were measured using flow cytometry (Beckman Coulter).

Statistical analysis

The data is presented as mean ± SD, and we utilized one-way ANOVA followed by a Tukey post hoc test for statistical comparisons. For significance, a p-value less than 0.05 was considered.

RESULTS

DHA inhibited the proliferation of LoVo/L-OHP cells and induced their apoptosis

We first treated LoVo/L-OHP cells with different concentrations (100 nmol/L or 300 nmol/L) of DHA then used the CCK-8 assay to detect the IC50 of all cells. As shown in Fig. 1-A, the IC_{50} of LoVo/L-OHP cells to L-OHP remarkably declined ($p<0.05$) after DHA treatment. In the next experiment, we treated LoVo/L-OHP cells with 30μM L-OHP or an equal amount of phosphate-buffered saline (PBS) and investigated the changes in cell viability of LoVo/L-OHP cells after DHA treatment. Our findings demonstrated a notable decline in cell viability of LoVo/L-OHP cells following DHA treatment ($p<0.05$, as depicted in Fig. 1-B). Moreover, flow cytometry analysis substantiated a marked rise in apoptotic cells in LoVo/L-OHP cells when treated with 300 nmol/L DHA ($p<0.05$, as illustrated in Fig. 1-C). Furthermore, compared with the LoVo/L-OHP group, the expression of cleaved caspase-3 protein and the Bax/Bcl-2 ratio in the L-OHP +300 nmol/L DHA and L-OHP +100nmol/L DHA groups were remarkably increased, while the expression of P-gb protein was markedly decreased ($p<0.05$, Fig. 1-D). In the subsequent experiments, cells were treated with 300 nmol/L of DHA.

The expression of SIRT3, PI3K, and AKT in LoVo/L-OHP cells after DHA treatment

To further investigate the expression of SIRT3, PI3K, and AKT in LoVo/L-OHP cells after DHA treatment, we examined the expression of SIRT3, PI3K, and AKT in each group of cells using WB and PCR. As shown in Figs 2 A-B, our results indicated a significant decrease in SIRT3 expression level, whereas PI3K and AKT expression levels were significantly elevated in LoVo/L-OHP cells compared to the LoVo group ($p<0.05$). After administering L-OHP to LoVo/L-OHP cells and subsequently treating them with 300 nmol/L DHA, we observed a noteworthy upsurge in the protein and mRNA levels of SIRT3 as compared to the LoVo/L-OHP+L-OHP group ($p<0.05$). Furthermore, we observed a reduction in expression levels of PI3K and AKT in cells following DHA treatment ($p<0.05$).

Silencing SIRT3 promoted L-OHP resistance in LoVo/L-OHP cells after DHA treatment through the PI3K/AKT pathway

To validate the role of the SIRT3/PI3K/AKT signalling pathway in L-OHP resistance of LoVo/L-OHP cells after DHA treatment, we transfected cells with si-SIRT3#1, si-SIRT3#2, si-SIRT3#3, and si-NC and measured the knockdown efficiency of SIRT3. As shown in Figs. 3 A-B, in LoVo/L-OHP cells after DHA treatment, si-SIRT3#1, si-SIRT3#2, and si-SIRT3#3 all markably reduced the expression of SIRT3, and we selected si-SIRT3#2 with the highest knockdown efficiency for subsequent experiments. In addition, we also used the PI3K inhibitor LY294002 to inhibit the PI3K/AKT pathway and divided the cells into groups: conctrl (LoVo/L-OHP+L-OHP+DHA), si-NC (conctrol+si-NC), si-SIRT3 (conctrol+si-SIRT3), and si-SIRT3+LY294002 (conctrol+si-SIRT3+LY294002). As shown in Fig. 3-C, compared with the si-NC group, silencing SIRT3 remarkably increased cell viability and reduced the proportion of cell apoptosis ($p<0.05$). However, the addition of the PI3K agonist LY294002 reversed this effect. Compared with the si-SIRT3 group, the si-SIRT3+LY294002 group had significantly reduced cell viability and increased apoptosis (Fig. 3-D).

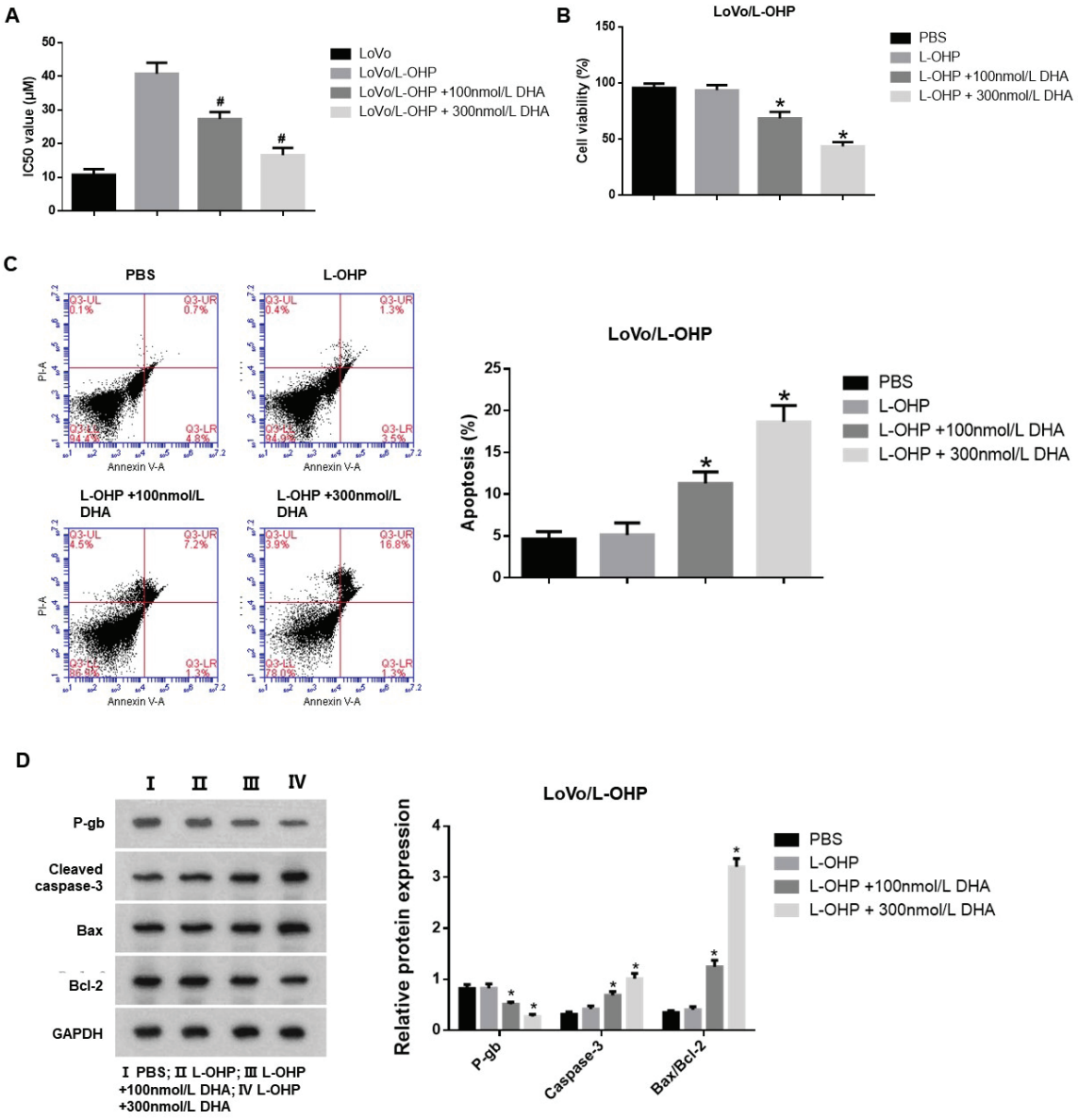

Fig. 1. DHA inhibited the proliferation of LoVo/L-OHP cells and induced their apoptosis. (A) The IC50 of all groups of cells were detected by CCK-8 assay. (B) Cell viability of all groups of cells was detected by CCK-8 assay. (C) The apoptosis rate of all groups of cells was analyzed by flow cytometry. (D) The expression of P-gp protein related to drug resistance and apoptosis-related proteins, cleaved caspase-3 protein, Bax, and Bcl-2, was detected by Western blot. Continuous data were compared using ANOVA. *$p<0.05$ compared with the L-OHP group. #$p<0.05$ compared with the LoVo/L-OHP group.

Effects of SIRT3 knockdown on relevant proteins in LoVo/L-OHP cells after DHA treatment

Finally, we used WB to measure the protein expression of the SIRT3/PI3K/AKT signalling pathway proteins, the drug-resistant protein P-gb, and the apoptosis-related proteins cleaved caspase-3, Bax and Bcl-2. As illustrated in Fig. 4, our data demonstrated that transfection with si-SIRT3 resulted in a notable decline in SIRT3 protein expression and increased protein expression of PI3K and AKT ($p<0.05$).

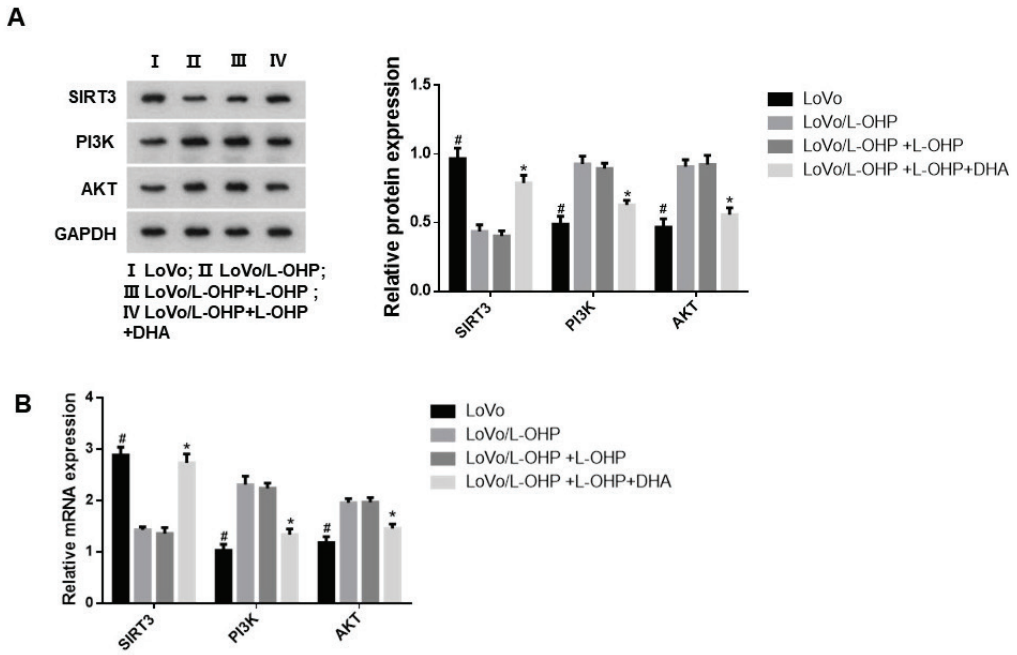

Fig. 2. The expression of SIRT3, PI3K and AKT in LoVo/L-OHP cells after DHA treatment. The SIRT3, PI3K and AKT expression in each group were measured by WB (A) and PCR (B). ANOVA was used to compare the groups. #p<0.05 compared with the LoVo/L-OHP group. *p<0.05 compared with the LoVo/L-OHP+L-OHP group.

On the other hand, treatment with PI3K inhibitor LY294002 remarkably reduced the protein expression levels of PI3K and AKT (p<0.05). Silencing SIRT3 markedly enhanced the expression of P-gb while reducing the protein expression of cleaved caspase-3 and the ratio of Bax/Bcl-2. However, the PI3K inhibitor LY294002 reversed this effect. In the si-SIRT3+LY294002 group, the protein expression of P-gb decreased, while the expression of cleaved caspase-3 and the ratio of Bax/Bcl-2 significantly increased (p<0.05).

DISCUSSION

For researchers, the mechanism of L-OHP resistance in CRC is still elusive. Despite many molecular medicine studies to explain the resistance mechanisms of CRC, it is challenging to distinguish genuinely effective targets for regulating resistance. In addition, most existing multidrug resistance reversal agents have issues such as incomplete resistance reversal, high technical requirements, and significant adverse reactions [20, 21]. Therefore, finding new sensitizers to combine with L-OHP to treat CRC patients is still necessary. We demonstrated that DHA could inhibit the L-OHP resistance in LoVo human colorectal cancer cells by regulating the SIRT3/PI3K/AKT axis.

Studies conducted in the past have demonstrated that DHA can hinder the growth of cancer cells and trigger apoptosis in pancreatic cancer, ovarian cancer, and colorectal cancer. An added advantage of DHA is its low toxicity towards normal tissue cells [22, 23]. In addition, DHA also has a killing effect on multidrug-resistant tumor cells [24]. In our study, we treated CRC-resistant cells LoVo/L-OHP with different concentrations of DHA and found that the viability of LoVo/L-OHP cells marked decrease, and the proportion of apoptotic cells increased significantly after DHA treatment. This phenomenon was

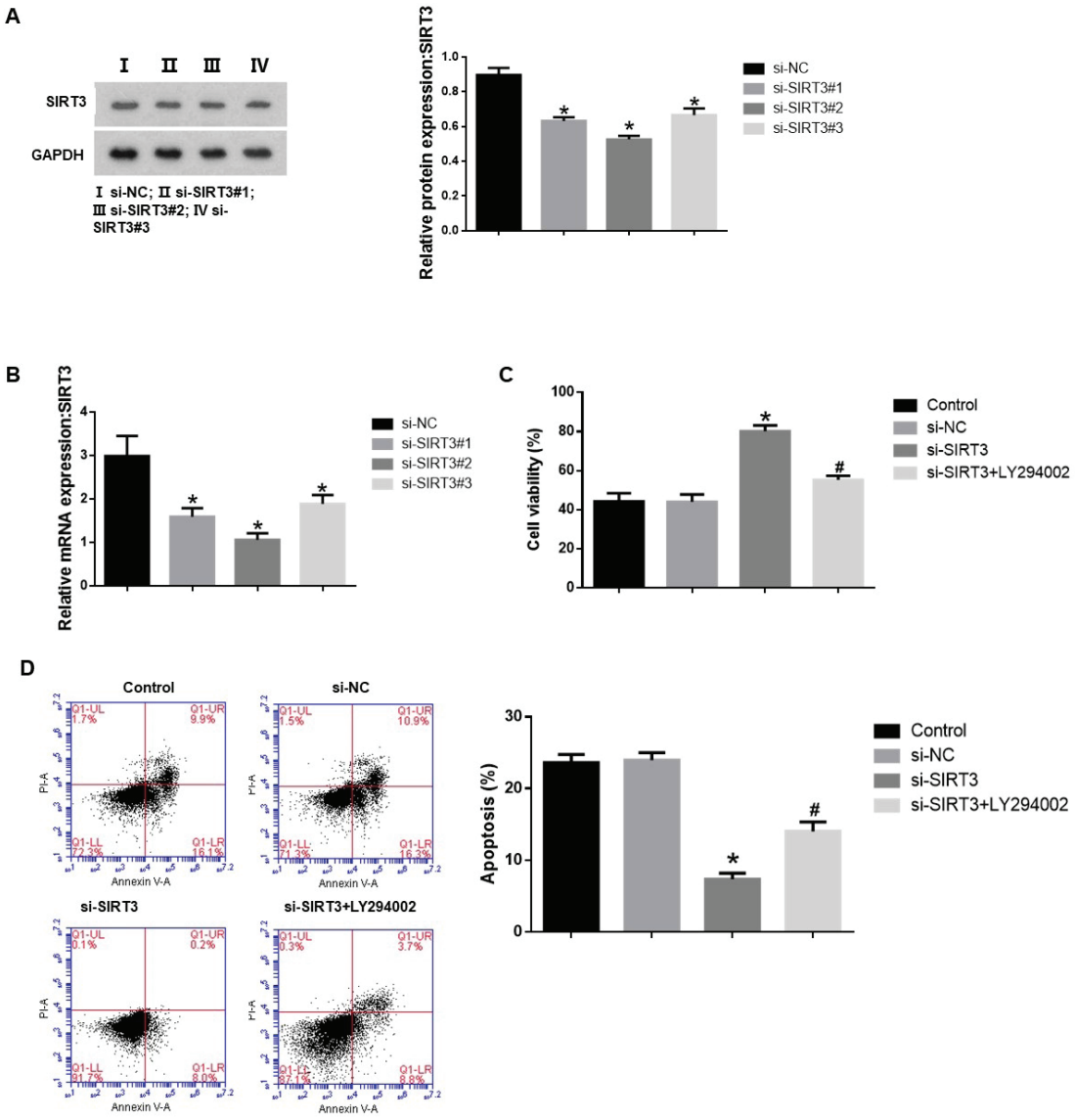

Fig. 3. Silencing SIRT3 promotes L-OHP resistance in LoVo/L-OHP cells after DHA treatment through the PI3K/AKT pathway. The expression of SIRT3 was measured by WB (A) and PCR (B). (C) Cell viability of all groups of cells was detected by CCK-8 assay. (D) The apoptosis rate of all groups of cells was analyzed by flow cytometry. ANOVA was used to compare the groups. *p<0.05 vs si-NC group. #p<0.05 vs si-SIRT3 group.

more pronounced in the group with higher concentrations of DHA, indicating that DHA can inhibit the resistance of LoVo/L-OHP to L-OHP. Similar results have been obtained in other cancers. In non-small-cell lung cancer (NSCLC), DHA can eliminate radiation resistance of NSCLC cell lines and xenograft models by inhibiting the TGF-β, PI3K/Akt, and STAT3 signalling pathways, and enhance the anti-tumor effect of radiotherapy [25]. In breast cancer, DHA regulates the STAT3/DDA1 axis to inhibit the proliferation of breast cancer tumor cells [26]. In addition, Yao *et al.* confirmed that DHA can effectively sensitize CRC cells to 5-fluorouracil (5-FU) by mediating ROS-induced apoptosis [27]. Wang *et al.* also showed that DHA inhibits the characteristics of cancer stem-like cells (CSLCs)

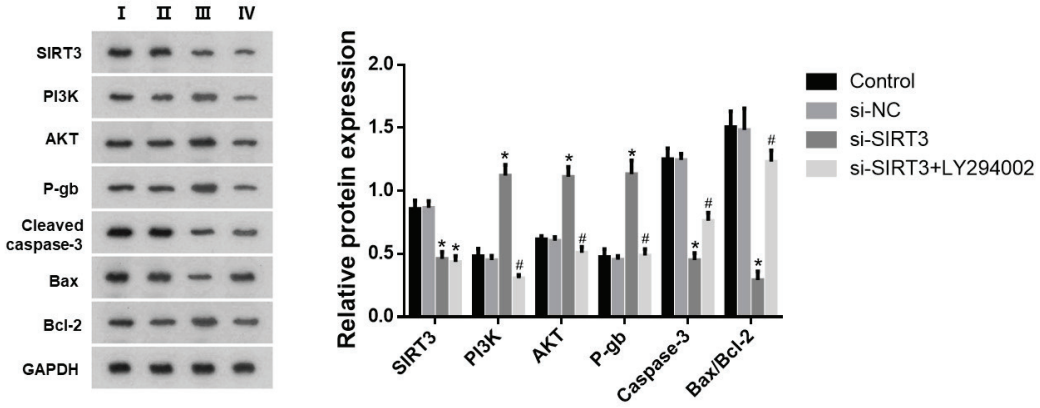

Fig. 4. Effects of SIRT3 knockdown on relevant proteins in LoVo/L-OHP cells after DHA treatment. The protein expression of SIRT3, PI3K, AKT, P-gb, cleaved caspase-3, Bax and Bcl-2 were measured by WB. ANOVA was used to compare the groups. *$p<0.05$ vs si-NC group. #$p<0.05$ vs si-SIRT3 group.

in CRC through the AKT/mTOR signalling pathway [28]. These results suggested that DHA can be a sensitizing cancer treatment agent.

The protein and mRNA levels of SIRT3 were enhanced in LoVo/L-OHP cells after treatment with DHA, indicating that SIRT3 may be involved in the sensitization of LoVo/L-OHP by DHA. Cao *et al.* found that activation of SIRT3 inhibits cisplatin resistance in lung cancer cells and reduces the proliferation and invasion of lung cancer cells [29]. Another research showed that the activity of SIRT3 in colon cancer cells can be enhanced by nitric oxide synthase (NOS), which helps to promote cell apoptosis [30]. To study the mechanism of action, we silenced SIRT3 and found that the viability of LoVo/L-OHP cells improved, and the proportion of apoptotic cells and apoptotic proteins cleaved caspase-3 and the ratio of bax/bcl-2 decreased significantly, indicating that the knockdown of SIRT3 affected the resistance of LoVo/L-OHP cells to L-OHP after DHA treatment. Furthermore, we confirmed that silencing SIRT3 enhanced the expression of PI3K and AKT in LoVo/L-OHP cells. The aberrant activation of the PI3K/AKT pathway acts against chemotherapy-induced apoptosis by increasing the expression of anti-apoptotic genes (bcl-2 and XIAP) and reducing the expression of pro-apoptotic genes (bax) [31]. In our study, we inhibited the PI3K/AKT axis with LY294002 and found that the viability of LoVo/L-OHP cells decreased while apoptosis increased. This also reversed the effect of knocking down SIRT3 on the viability and apoptosis of LoVo/L-OHP cells. Zhang *et al.* [32] found that inhibiting the PI3K/AKT signalling pathway in CRC cells can inhibit cell proliferation and activate apoptosis, thereby reversing oxaliplatin resistance, consistent with our research results.

Limitation

Our research also has some limitations. Whether other genes regulate SIRT3 is not clear. We also did not perform *in vivo* experiments to confirm the apoptosis results. All these need further studies to illustrate.

Our study found that DHA could inhibit the L-OHP resistance in LoVo human colorectal cancer cells by regulating the SIRT3/PI3K/AKT axis. The results might provide a new integrated treatment approach for CRC treatment in clinical practice.

Ethics approval and consent to participate

The ethic approval was obtained from the Ethic Committee of The Minhang Hospital, Affiliated with Fudan University, and

written informed consent was obtained from all patients.All of the authors have Consented to publish this research.

Availability of data and materials

The data are free to access and available upon request.

Competing interests

All authors declare no conflict of interest.

Funding

Project of Health Commission of Minhang District, Shanghai, Grant No. 2021MW23.

ORCID number of authors

- Xiaodong Shen: 0009-0000-0520-8896
- Chencheng Shi: 0009-0008-1369-2946
- Ming Lei: 0009-0000-8480-197X
- Rongjian Zhou: 0009-0007-5598-0834
- Shaoqun Liu: 0000-0002-2016-0947
- Chang Su: 0009-0004-6481-2638

Authors' contributions

Each author has made an important scientific contribution to the study and assisted with drafting or revising the manuscript.

REFERENCES

1. **Sung H, Ferlay J, Siegel RL, Laversanne M, Soerjomataram I, Jemal A, Bray F.** Global cancer statistics 2020: GLOBOCAN estimates of incidence and mortality worldwide for 36 cancers in 185 countries. CA Cancer J Clin 2021;71(3):209-249.
2. **Cvitkovic E, Bekradda M.** Oxaliplatin: a new therapeutic option in colorectal cancer. Semin Oncol 1999;26(6):647-662.
3. **Rovers KP, Wassenaar ECE, Lurvink RJ, Creemers G-JM, Burger JWA, Los M, Huysentruyt CJR, van Lijnschoten G, Nederend J, Lahaye MJ.** Pressurized intraperitoneal aerosol chemotherapy (oxaliplatin) for unresectable colorectal peritoneal metastases: a multicenter, single-arm, phase II trial (CRC-PIPAC). Ann Surg Oncol 2021: 28(9):5611-5616.
4. **Ranieri G, Laforgia M, Nardulli P, Ferraiuolo S, Molinari P, Marech I, Gadaleta CD.** Oxaliplatin-based intra-arterial chemotherapy in colorectal cancer liver metastases: a review from pharmacology to clinical application. Cancers 2019;11(2):141.
5. **Zhang Y, Li C, Liu X, Wang Y, Zhao R, Yang Y, Zheng X, Zhang Y, Zhang X. c**irc-cHIPK3 promotes oxaliplatin-resistance in colorectal cancer through autophagy by sponging miR-637. EBioMedicine 2019;48:277-288.
6. **Lai M, Liu G, Li R, Bai H, Zhao J, Xiao P, Mei J.** Hsa_circ_0079662 induces the resistance mechanism of the chemotherapy drug oxaliplatin through the TNF-α pathway in human colon cancer. J Cell Mol Med 2020;24(9):5021-5027.
7. **Mitsuuchi Y, Johnson SW, Selvakumaran M, Williams SJ, Hamilton TC, Testa JR.** The phosphatidylinositol 3-kinase/AKT signal transduction pathway plays a critical role in the expression of p21WAF1/CIP1/SDI1 induced by cisplatin and paclitaxel. Cancer Research 2000;60(19):5390-5394.
8. **Selfe J, Goddard NC, McIntyre A, Taylor KR, Renshaw J, Popov SD, Thway K, Summersgill B, Huddart RA, Gilbert DC.** IGF1R signalling in testicular germ cell tumour cells impacts on cell survival and acquired cisplatin resistance. J Pathol 2018;244(2):242-253.
9. **Lee S, Jeon Y-M, Jo M, Kim H-J.** Overexpression of SIRT3 suppresses oxidative stress-induced neurotoxicity and mitochondrial dysfunction in dopaminergic neuronal cells. Exp Neurobiol 2021;30(5):341.

10. **Dikalova AE, Pandey A, Xiao L, Arslanbaeva L, Sidorova T, Lopez MG, Billings Iv FT, Verdin E, Auwerx J, Harrison DG.** Mitochondrial deacetylase Sirt3 reduces vascular dysfunction and hypertension while Sirt3 depletion in essential hypertension is linked to vascular inflammation and oxidative stress. Circ Res 2020;126(4):439-452.
11. **Gao J, Feng Z, Wang X, Zeng M, Liu J, Han S, Xu J, Chen L, Cao K, Long J.** SIRT3/SOD2 maintains osteoblast differentiation and bone formation by regulating mitochondrial stress. Cell Death Differ 2018;25(2):229-240.
12. **Guo R, Li Y, Xue Y, Chen Y, Li J, Deng X, Su J, Liu Y, Sun L.** SIRT3 increases cisplatin sensitivity of small-cell lung cancer through apoptosis. Gene 2020;745:144629.
13. **Xu K, He Y, Moqbel SAA, Zhou X, Wu L, Bao J.** SIRT3 ameliorates osteoarthritis via regulating chondrocyte autophagy and apoptosis through the PI3K/Akt/mTOR pathway. Int J Biol Macromol 2021;175:351-360.
14. **Wang Z, Li Y, Wang Y, Zhao K, Chi Y, Wang B.** Pyrroloquinoline quinine protects HK-2 cells against high glucose-induced oxidative stress and apoptosis through Sirt3 and PI3K/Akt/FoxO3a signalling pathway. Biochem Biophys Res Commun 2019;508(2):398-404.
15. **Li Q, Ma Q, Cheng J, Zhou X, Pu W, Zhong X, Guo X.** Dihydroartemisinin as a sensitizing agent in cancer therapies. OncoTargets Ther 2021;14:2563.
16. **Zhang L, Wang Z, Wang C, Li J, Zhao Y, Zhang H, Yu Y, Wang G, Li Y.** Dihydroartemisinin protects against acute and chronic pain via SIRT3-dependent inhibition of peroxiredoxin-3 hyperacetylation and peroxynitrite accumulation in mice. Research Square 2022. *https://doi.org/10.21203/rs.3.rs-1607556/v1*
17. **Wang Q, Wei J, Wang C, Zhang T, Huang D, Wei F, He F, Cai W, Yang P, Zeng S.** Gambogic acid reverses oxaliplatin resistance in colorectal cancer by increasing intracellular platinum levels. Oncol Lett 2018;16(2):2366-2372.
18. **Wang C-H, Baskaran R, Ng SS-C, Wang T-F, Li C-C, Ho T-J, Hsieh DJ-Y, Kuo C-H, Chen M-C, Huang C-Y.** Platycodin D confers oxaliplatin resistance in colorectal cancer by activating the LATS2/YAP1 axis of the hippo signalling pathway. J Cancer 2023;14(3):393.
19. **Liu X, Wu B, Chen H, Sun H, Guo X, Sun T, Zhou D, Yang S.** Intense endoplasmic reticulum stress (ERS)/IRE1α enhanced Oxaliplatin efficacy by decreased ABCC10 in colorectal cancer cells. BMC Cancer 2022;22(1):1369.
20. **Krishna R, Mayer LD.** Multidrug resistance (MDR) in cancer: mechanisms, reversal using modulators of MDR and the role of MDR modulators in influencing the pharmacokinetics of anticancer drugs. Eur J Pharm Sci 2000;11(4):265-283.
21. **Liang Y, Zhu D, Zhu L, Hou Y, Hou L, Huang X, Li L, Wang Y, Li L, Zou H.** Dichloroacetate overcomes oxaliplatin chemoresistance in colorectal cancer through the miR-543/PTEN/Akt/mTOR pathway. J Cancer 2019;10(24):6037.
22. **Aung W, Sogawa C, Furukawa T, Saga T.** Anticancer effect of dihydroartemisinin (DHA) in a pancreatic tumor model evaluated by conventional methods and optical imaging. Anticancer Res 2011;31(5):1549-1558.
23. **Jiao Y, Ge Cm, Meng Qh, Cao Jp, Tong J, Fan Sj.** Dihydroartemisinin is an inhibitor of ovarian cancer cell growth 1. Acta Pharmacol Sin 2007;28(7):1045-1056.
24. **Michaelis M, Kleinschmidt MC, Barth S, Rothweiler F, Geiler J, Breitling R, Mayer B, Deubzer H, Witt O, Kreuter J.** Anticancer effects of artesunate in a panel of chemoresistant neuroblastoma cell lines. Biochem Pharmacol 2010;79(2):130-136.
25. **Zhang H, Zhou F, Wang Y, Xie H, Luo S, Meng L, Su B, Ye Y, Wu K, Xu Y.** Eliminating radiation resistance of non-small cell lung cancer by dihydroartemisinin through abrogating immunity escaping and promoting radiation sensitivity by inhibiting PD-L1 expression. Front Oncol 2020;10:595466.

26. **Zhang J, Li Y, Wang J-G, Feng J-Y, Huang G-D, Luo C-G.** Dihydroartemisinin affects STAT3/DDA1 signalling pathway and reverses breast cancer resistance to cisplatin. Am J Chin Med 2023;51(02):445-459.
27. **Yao Z, Bhandari A, Wang Y, Pan Y, Yang F, Chen R, Xia E, Wang O.** Dihydroartemisinin potentiates antitumor activity of 5-fluorouracil against a resistant colorectal cancer cell line. Biochem Biophys Res Commun 2018;501(3):636-642.
28. **Wang Y, Yang Z, Zhu W, Chen Y, He X, Li J, Han Z, Yang Y, Liu W, Zhang K.** Dihydroartemisinin inhibited stem cell-like properties and enhanced oxaliplatin sensitivity of colorectal cancer via AKT/mTOR signalling. Drug Dev Res 2023;84(5):988-998.
29. **Cao Y, Li P, Wang H, Li L, Li Q.** SIRT3 promotion reduces resistance to cisplatin in lung cancer by modulating the FOXO3/CDT1 axis. Cancer Med 2021;10(4):1394-1404.
30. **Wang Q, Ye S, Chen X, Xu P, Li K, Zeng S, Huang M, Gao W, Chen J, Zhang Q.** Mitochondrial NOS1 suppresses apoptosis in colon cancer cells through increasing SIRT3 activity. Biochem Biophys Res Commun 2019;515(4):517-523.
31. **Liu R, Chen Y, Liu G, Li C, Song Y, Cao Z, Li W, Hu J, Lu C, Liu Y.** PI3K/AKT pathway as a key link modulates the multidrug resistance of cancers. Cell Death Dis 2020;11(9):797.
32. **Zhang Y, Xu Z, Sun Y, Chi P, Lu X.** Knockdown of KLK11 reverses oxaliplatin resistance by inhibiting proliferation and activating apoptosis via suppressing the PI3K/AKT signal pathway in colorectal cancer cell. OncoTargets Ther 2018:809-821.

Invest Clin 65(3): 279 - 293, 2024 https://doi.org/10.54817/IC.v65n3a02

A comparative study on the clinical effectiveness of core decompression with bone grafting for treating alcohol-induced and traumatic osteonecrosis of the femoral head: a population-specific investigation in alcoholism.

Zhensong Wu[1,2], Da Song[3], Qi Xu[3] and Dawei Wang[3]

[1] School of Medicine, Shandong University, Jinan, China.
[2] Zaozhuang Municipal Hospital, Zaozhuang, China.
[3] Department of Joint Surgery, Liaocheng People's Hospital Affiliated to Shandong University, Liaocheng, China.

Keywords: core decompression; bone grafting; traumatic osteonecrosis of the femoral head; alcoholic-induced osteonecrosis of the femoral head.

Abstract. Osteonecrosis of the femoral head (ONFH) is a debilitating orthopedic condition with two primary categories: traumatic osteonecrosis (TONFH) and non-traumatic ONFH, including alcoholic-induced osteonecrosis (AIONFH). Core decompression combined with bone grafting is a common treatment approach, but its efficacy and influencing factors in these two categories remain unclear. We conducted a study involving 50 patients (25 TONFH, 25 AIONFH) who underwent this procedure. Demographic data and clinical assessments were collected. The average age was 47.2 years, with 72% males. AIONFH patients had a higher BMI and more comorbidities like diabetes, hyperlipidemia, hypertension, and immune-related diseases. TONFH had a higher prevalence of osteoporosis and fracture history. Bilateral hip necrosis was more frequent in TONFH, while left hip necrosis dominated in AIONFH. Both groups mainly had JIC classifications C1 and C2. Preoperatively, most cases were ARCO grade III and IV, with lower Harris, PCS, and MCS scores. Both groups improved at the six-month postoperative assessment, with better results in AIONFH. The last follow-up was 16.62 months after treatment. In the final follow-up, AIONFH cases were mainly ARCO type I, and HHS, PCS, and MCS scores were significantly better than TONFH. Core decompression combined with bone grafting effectively treats AIONFH and TONFH, with superior outcomes in AIONFH. Factors influencing postoperative efficacy include BMI, JIC classification, and PCS score. These findings provide valuable insights for tailoring treatment strategies to specific ONFH categories.

Corresponding author: Dawei Wang, Department of Joint Surgery, Liaocheng People's Hospital Affiliated to Shandong University, Liaocheng, China. E-mail: wangdawei0120@126.com

Análisis comparativo de la eficacia clínica de la descompresión central combinada con injerto óseo en el tratamiento de la osteonecrosis traumática o inducida por alcohol de la cabeza femoral.

Invest Clin 2024; 65 (3): 279 – 293

Palabras clave: descompresión central; injerto óseo; osteonecrosis traumática de la cabeza femoral; osteonecrosis inducida por alcohol de la cabeza femoral.

Resumen. La osteonecrosis de la cabeza femoral (ONFH) es una afección ortopédica clasificada en dos categorías principales: osteonecrosis traumática (TONFH) y osteonecrosis no traumática, incluida la osteonecrosis inducida por alcohol (AIONFH). Un estudio con 50 pacientes (25 AIONFH, 25 TONFH) sometidos a descompresión central con injerto óseo evaluó su eficacia y factores influyentes. La edad promedio fue de 47,2 años, con un 72% de hombres y el seguimiento promedio fue de 16,62 meses. Los pacientes con AIONFH tenían un IMC más alto y más comorbilidades como diabetes, hiperlipidemia, hipertensión y enfermedades inmunológicas. La TONFH tenía una mayor prevalencia de osteoporosis y antecedentes de fracturas. La necrosis bilateral de cadera fue más frecuente en la TONFH, mientras que la necrosis de cadera izquierda dominaba en la AIONFH. Ambos grupos tenían principalmente clasificaciones JIC C1 y C2. Preoperatoriamente, la mayoría de los casos eran de grado ARCO III y IV, con puntajes de Harris, PCS y MCS más bajos. A los 6 meses de la evaluación posoperatoria, ambos grupos mejoraron, con resultados superiores en la AIONFH. El seguimiento promedio fue de 16,62 meses. En la última evaluación de seguimiento, la mayoría de los casos de AIONFH eran del tipo ARCO I, y los puntajes de HHS, PCS y MCS fueron significativamente mejores que en la TONFH. La descompresión central con injerto óseo trata eficazmente ambas categorías de ONFH, con resultados superiores en la AIONFH. Los factores que influyen en la eficacia posoperatoria incluyen el IMC, la clasificación JIC y el puntaje PCS. Estos hallazgos informan sobre la adaptación de las estrategias de tratamiento a las categorías de ONFH.

Received: 22-09-2023 Accepted: 21-04-2024

INTRODUCCIÓN

Osteonecrosis of the femoral head (ONFH), or aseptic or avascular necrosis of the femoral head, is a progressive and painful orthopedic disease [1,2]. It can be categorized into traumatic and non-traumatic osteonecrosis based on its etiology. Non-traumatic ONFH is associated with various factors, including alcohol consumption, glucocorticoid use, infection, bone marrow infiltrative diseases, blood coagulation disorders, and certain autoimmune diseases [3]. According to a cross-sectional epidemiological study on ONFH in China, alcohol, steroids, and trauma are the three most common causes, with alcohol-induced non-traumatic osteonecrosis accounting for 37.15% and trauma-induced osteonecrosis accounting for 15.73%[4]. Regardless of the cause, with-

out timely and effective treatment, the disease can lead to excruciating pain, the collapse of the femoral head, and impaired hip joint movement, significantly affecting the patient's quality of life [5].

Currently, clinical treatments for ONFH primarily focus on preserving hip joint function and halting disease progression. Various treatment modalities exist, including total hip arthroplasty, core decompression, vascularized and non-vascularized bone transplantation, and different osteotomy procedures [6]. Each treatment approach presents its advantages and drawbacks. Among these options, core decompression stands out as an ideal method, particularly for patients with early-stage ONFH [7]. This technique entails the removal of necrotic tissue from the femoral head, thereby reducing intraosseous pressure, promoting vascular reconstruction, facilitating bone regeneration within the necrotic region, relieving bone edema, and improving blood supply to the femoral head to foster lesion repair [8-10].

However, it should be noted that both thick channel core decompression and fine needle multi-hole drilling decompression procedures may inadvertently compromise the mechanical properties of the already fragile subchondral bone during the operation. Consequently, this may accelerate the collapse of the load-bearing surface of the femoral head or lead to subchondral bone fractures [11,12]. Combining core decompression with bone grafting has emerged as a viable solution to address this issue. Incorporating bone grafts into the necrotic segment after decompression provides structural support, facilitating subchondral bone reconstruction in the femoral head and mitigating the risk of cartilage collapse [13]. It is essential to recognize that the etiology of ONFH may vary, potentially impacting the clinical efficacy of core decompression combined with bone grafting. Thus, this study aims to analyze patients with alcohol-related ONFH (AIONFH) and traumatic ONFH (TONFH) to compare the clinical outcomes of core decompression combined with bone grafting in both types of patients and identify relevant factors. This research offers valuable insights to enhance the accuracy of the clinical application of core decompression and bone grafting for patients with ONFH.

MATERIAL AND METHODS

Subject Recruitment and Surgical Procedure

For this study, 50 patients were recruited based on strict inclusion and exclusion criteria. Twenty-five patients (35 hips) with TONFH were randomly selected to form the TONFH group, while another 25 patients (34 hips) diagnosed with AIONFH were chosen to constitute the AIONFH group.

All recruited patients underwent surgery under general anesthesia, assuming a supine position. The iliac crest served as the designated operation site. Prior to surgery, routine disinfection and towel laying were performed. The surgical procedure commenced with a layered tissue incision to expose the iliac crest. Subsequently, the iliac bone was removed using a bone knife, crushed with rongeurs, and rinsed with normal saline. Following this, a guide needle was used to puncture the necrotic site along the vertex of the greater trochanter of the femur, approximately 2 cm in length. Necrotic tissue was carefully scraped off from the site. Bone grafting material, composed of a mixture of the just removed bone tissue and artificial bone, was then crushed and implanted into the necrotic area, ensuring complete filling. Attention was given to confirm adequate filling of the bone graft, and any remaining bone tissue was placed into the channel. The wound was finally rinsed and sutured. Postoperatively, all patients were required to remain in bed for one month, after which they resumed limited activity combined with appropriate functional exercise. From three months post-surgery to six months post-surgery, patients utilized walking aids to increase weight-bearing ex-

ercise gradually. Whole weight-bearing exercise was used after six months post-surgery.

Inclusion criteria

1. Patients with a confirmed diagnosis of ONFH through imaging and clinical examinations. 2. Patients with ONFH caused either by alcohol consumption or traumatic incidents. 3. Patients who underwent core decompression combined with bone grafting as a treatment modality. 4. Patients who provided informed consent after being informed about the study.

Exclusion criteria

1. Patients with ONFH caused by hormonal imbalances or inflammation. 2. Patients who underwent treatment methods unrelated to core decompression combined with bone grafting. 3. Patients with an insufficient matching degree or lacking relevant case data. 4. Patients with severe conditions such as malignant tumors or hemorrhagic diseases.

Main observation index

This study utilized the hospital medical record system to gather crucial patient information, medical records during hospitalization, preoperative and postoperative imaging data, postoperative adverse reactions, and follow-up records. The primary data of patients, including sex, age, height, weight, body mass index (BMI), and complications, were collected. All patients underwent an impact examination upon admission, and regular follow-ups were conducted after the operation to assess the presence of necrosis and collapse of the femoral head. The classification system used for ONFH was based on the Japanese Investigation Committee, JIC classification.

The clinical efficacy was evaluated through the Association Research Circulation Osseous (ARCO) classification, Harris Hips score (HHS), and SF-36 scale before the operation and the follow-up at six months after and at the last follow-up.

The ARCO classification served as a means to categorize ONFH, providing insight into the surgical effect and enabling targeted adjustments to the treatment plan. In this study, the ARCO 2019 staging method was employed [14], dividing patients into four stages (I, II, III and IV) based on imaging examination results and pathological changes in the femoral head. Stage I showed abnormalities in X-ray examination, while MRI indicated a banded low signal surrounding the necrotic area. Stage IV was characterized by evident osteoarthritis, with an X-ray examination revealing bone-joint space narrowing, acetabular changes, and joint destruction.

HHS was utilized to evaluate the hip joint function, encompassing four aspects: pain degree (44 points), joint function (47 points), deformity (4 points), and range of motion (5 points). A higher score indicated better hip joint function, with scores less than 70 points indicating poor function, scores between 70 and 79 indicating medium-level function, scores between 80 and 89 indicating good function, and scores of 90-100 indicating excellent function.

The SF-36 scale was employed to assess patients' quality of life, covering eight aspects: physiological function, emotional function, physical pain, general health status, experience, social function, and mental health. The SF-36 conversion equation of the Chinese population published by Lam et al. was used to convert the questionnaire responses into physical health score (PCS) and mental health score (MCS), with higher scores indicating a better quality of life.

Additionally, the therapeutic effect was evaluated based on the results of the last follow-up, with patients without data at the last follow-up being analyzed using data from 6 months after the operation. The effectiveness of treatment was categorized as follows: "Extremely effective", indicating increased bone mineral density in the focus, with the cystic light transmission area and fissure sign returning to normal, and

no collapse of the femoral head; "Effective", indicating increased bone mineral density in the focus, with the cystic light transmission area and fissure sign decreased, and femoral head collapse < 2mm; and "Ineffective," indicating femoral head collapse ≥ 2mm. The effective rate of treatment was calculated by summing the number of patients classified as "Extremely effective" and "Effective".

Statistical analysis

Data entry and collation of the questionnaire were performed using Excel software, while statistical data analysis was conducted using Statistic Package for Social Science (SPSS) 25.0 ® (IBM, Armonk, NY, USA). Continuous variables and classified variables in the study were described and analyzed in the form of "average ± standard deviation" and "cases (proportion)," respectively. For continuous variables conforming to the normal distribution, the independent sample T-test was employed to analyze differences between groups, while those not conforming to the normal distribution were analyzed using the Mann-Whitney U test. The classified variables were subjected to statistical analysis using the chi-square test or Fisher exact test. Univariate Logistic regression analysis was used to identify risk factors affecting treatment efficacy, while multivariate logistic regression analysis was employed to analyze significant indicators. Statistical results with $p<0.05$ were considered to have a significant difference in the data.

RESULTS

Study Characteristics

This study presents the patients' basic information and clinical characteristics, as outlined in Table 1. The average age of the patients included in the study was 47.2 ± 7.4 years, with a majority of male patients (72.0%). The BMI of the patients in the AIONFH group was significantly higher than that of the patients in the TONFH group ($p<0.05$). The prevalence of diabetes, hyperlipidemia, hypertension, and immune-related diseases was higher in the AIONFH group compared to the TONFH group, while the history of osteoporosis and fracture was more frequent in the TONFH group. Regarding postoperative adverse reactions, both groups experienced a higher occurrence of severe pain and deep venous thrombosis at the last follow-up, and there was no significant difference between the two groups ($p>0.05$).

Imaging Features

The imaging results for both groups are detailed in Table 1. Among the patients in the TONFH group, 40.00% exhibited necrosis in both hip joints, while in the AIONFH group, 40.00% displayed necrosis in the left hip joint. According to the JIC classification, many patients in both groups were categorized as C1 and C2 types. Specifically, the TONFH group had a higher proportion of C2 type (45.71%) compared to C1 type (34.29%), whereas both C1 and C2 types were equally distributed in the AIONFH group (38.24%). No significant difference between the two groups was observed in hip joint pathological changes and JIC classification.

Comparison of ARCO classification, HHS and SF-36 score between the two groups before operation

Results of ARCO classification, HHS, and SF-36 score for both groups before the operation are presented in Table 2. No significant difference was found in the above indexes between the two groups before the operation ($p>0.05$). The most common ARCO classification in both groups was Grade IV. In terms of Harris score, the scores for both groups were significantly lower than 70, indicating poor hip joint function.

Table 1
Basic information and clinical characteristics of patients.

Variables		Total	TONFH Group	AIONFH Group	$t/Z/\chi^2/F$	p
Patients/hips		50/69	25/35	25/34		
Age (year, mean ± SD)		47.2±7.4	45.6±8.2	48.8±6.2	1.528	0.133
Gender n (%)	Male	36 (72)	16 (64)	20(80)	1.587	0.208
	Female	14 (28)	9 (36)	5(20)		
BMI (kg/m^2, mean ± SD)		23.81±2.49	22.85±2.54	24.78±2.06	2.949	0.005
Smoking n (%)		27(54)	13(52)	14(56)	0.081	0.777
Alcohol n (%)		40(80)	15(60)	25(100)	12.500	<0.001
Pathogeny n (%)	Alcohol	25(50)	-	25(100)	-	-
	Trauma	21(42)	21(84)	-		
	Others	4(8)	4(16)	-		
Complications / existing medical history n (%)	Diabetes	23(46)	9(36)	14(56)	22.543	<0.001
	Hyperlipidemia	27(54)	9(36)	18(72)		
	Hypertension	28(56)	10(40)	16(64)		
	Immune-related diseases	19(38)	7(28)	12(48)		
	Osteoporosis	26(52)	14(56)	12(48)		
	Fracture	23(46)	21(84)	2(8)		
Necrotic hip joint n (%)	Left	18(26.09)	8(32)	10(40)	0.352	0.839
	Right	13(18.84)	7(28)	6(24)		
	Both	19(27.54)	10(40)	9(36)		
JIC classification n (%)	A	7(10.14)	4(11.43)	3(8.82)	0.985	0.805
	B	8(11.59)	3(8.57)	5(14.71)		
	C1	25(36.23)	12(34.29)	13(38.24)		
	C2	29(42.03)	16(45.71)	13(38.24)		
Postoperative adverse reactions n (%)	Severe pain	8(16)	4(16)	4(16)	0.287	0.963
	Infected	2(4)	1(4)	1(4)		
	Deep venous thrombosis	6(12)	3(12)	3(12)		
	Hematoma	3(6)	1(4)	2(8)		
Follow-up time (month, mean ± SD)		16.62±5.21	17.04±5.22	16.2±5.28	0.566	0.574

$p<0.05$ indicates statistical significance.

For continuous variables conforming to the normal distribution, the independent sample T-test was employed to analyze differences between groups, while those not conforming to the normal distribution were analyzed using the Mann-Whitney U test. The classified variables were subjected to statistical analysis using the chi-square test or Fisher exact test; Traumatic osteonecrosis (TONFH); non-traumatic- alcoholic-induced osteonecrosis (AIONFH). BMI: body mass index; JIC: Japanese Investigation Committee Classification.

Table 2
Comparison of ARCO classification, HHS and SF-36 score between the two groups before operation.

Variables		TONFH Group	AIONFH Group	$t/Z/\chi^2$	p
Patients/hips		25/35	25/34		
ARCO n (%)	I/II	3 (8.57)	3 (8.82)	0.825	0.662
	III	8 (22.86)	11(32.35)		
	IV	24 (68.57)	20 (58.82)		
HHS (score, mean ± SD)	Pain	21.4±2.72	21.09±3.18	0.691	0.490
	Function	23.31±3.34	23.65±2.59	0.461	0.646
	Deformity	4±0	4±0	-	-
	Range of motion	0.6±0.65	0.59±0.5	0.190	0.849
	Total scores	49.31±5.11	49.32±5.76	0.007	0.994
SF-36 (score, mean ± SD)	PCS	32.64±2.89	32.04±2.73	0.755	0.454
	MCS	43.48±1.85	43.04±3.52	0.553	0.583

$p<0.05$ indicates statistical significance.

For continuous variables conforming to the normal distribution, the independent sample T-test was employed to analyze differences between groups, while those not conforming to the normal distribution were analyzed using the Mann-Whitney U test. The classified variables were subjected to statistical analysis using the chi-square test or Fisher exact test.

Traumatic osteonecrosis (TONFH) ; non-traumatic-alcoholic-induced osteonecrosis (AIONFH). ARCO: Association Research Circulation Osseous; HHS: Harris Hip Score; SF-36: 36-Item Short Form Health Survey.

Comparison of ARCO classification, HHS and SF-36 score between the two groups of the follow-up at 6 months after operation

Six months after the operation, the results of ARCO classification, HHS, and SF-36 score for both groups are shown in Table 3. However, it is worth noting that one patient in the TONFH group could not be reached for follow-up, reducing the number of patients/hips to 24/34 in this group.

In terms of ARCO typing, a majority of patients in the AIONFH group were classified as type III (61.76%), while those in the TONFH group still belonged to grade IV (38.24%). This difference between the two groups was statistically significant ($p < 0.05$). The total HHS for the AIONFH group was (73.24 ± 8.45), indicating a significant improvement in hip joint function for these patients. On the other hand, the Harris score for the TONFH group remained lower than 70 ($p<0.05$), indicating persistent poor hip joint function. Moreover, the scores of PCS and MCS in the AIONFH group were higher compared to those in the TONFH group, and the difference in MCS scores was found to be significant. This suggests that patients with AIONFH experienced better physical and mental health outcomes compared to those with TONFH.

Comparison of ARCO classification, HHS and SF-36 score between the two groups at the last follow-up

At the last follow-up, the results of ARCO classification, Harris score, and SF-36 score for both groups are presented in Table 4. It should be noted that during the last follow-up, two patients in the TONFH group and four patients in the AIONFH group could not be contacted normally, reducing the number of patients/hip joints to 22/31 and 21/29.

At the last follow-up, significant differences were observed in the results of all three indexes between the AIONFH and TONFH

Table 3
Comparison of ARCO classification, HHS and SF-36 score between the two groups 6 months after operation.

Variables		TONFH Group	AIONFH Group	$t/Z/\chi 2$	p
Patients/Hips		24/34	25/34		
ARCO n (%)	I	1(2.94)	5(14.71)	15.156	0.002
	II	11(32.35)	5(14.71)		
	III	9(26.47)	21(61.76)		
	IV	13(38.24)	4(11.76)		
HHS (score, mean ± SD)	Pain	25.59±2.73	32.85±3.81	5.881	<0.001
	Function	27.76±3.96	34.76±4.63	6.701	<0.001
	Deformity	4±0	4±0	-	-
	Range of motion	1.26±0.45	1.62±0.92	1.416	0.157
	Total scores	61.62±5.83	73.24±8.45	6.600	<0.001
SF-36 (score, mean ± SD)	PCS	36.21±4.49	38.08±4.73	1.529	0.126
	MCS	45.25±2.77	47.52±4.82	2.030	0.049

$p<0.05$ indicates statistical significance.

For continuous variables conforming to the normal distribution, the independent sample T-test was employed to analyze differences between groups, while those not conforming to the normal distribution were analyzed using the Mann-Whitney U test. The classified variables were subjected to statistical analysis using the chi-square test or Fisher exact test.

Traumatic osteonecrosis (TONFH); non-traumatic- alcoholic-induced osteonecrosis (AIONFH). ARCO: Association Research Circulation Osseous; HHS: Harris Hip Score; SF-36: 36-Item Short Form Health Survey.

groups ($p<0.05$). In the AIONFH group, most patients were classified as type I according to the ARCO classification (43.33%), while most patients in the TONFH group were classified as type II (38.71%). This difference in ARCO classification between the two groups was statistically significant. The HHS of patients in both groups were higher than 70, indicating improved hip joint function. However, the Harris scores in the AIONFH group were notably higher than 80. Furthermore, the scores of PCS and MCS in the AIONFH group were significantly higher than those in the TONFH group.

Therapeutic effect of two groups of patients

The therapeutic effects of the two groups are shown in Table 5. The total effective rate of the AIONFH group was 76.47%, which was higher than that of TONFH group (55.88%).

Analysis of the related factors affecting the prognosis of patients

Table 6 presents the results of the Logistic regression analysis conducted to identify possible factors related to the prognosis of patients. The univariate Logistic analysis examined several factors, including BMI, immune-related diseases, history of osteoporosis, JIC classification, HHS, PCS, and MCS. The analysis revealed that these factors showed statistical significance concerning the prognosis of patients.

Upon further analysis using multivariate Logistic regression, three factors were statistically significant predictors of prognosis. These factors were BMI, JIC classification, and PCS.

Table 4
Comparison of ARCO/ classification, HHS and SF-36 score between the two groups at six months after the last follow-up.

Variables		TONFH Group	AIONFH Group	Z/χ^2	p
Patients/Hips		22/31	21/29		
ARCO▲ n (%)	I	3(9.68)	13(43.33)	10.806	0.013
	II	12(38.71)	10(33.33)		
	III	5(16.13)	3(10)		
	IV	11(35.48)	4 (13.33)		
HHS▲ (score, mean ± SD)	Pain	32.58±5.1	36.83±6.29	3.225	0.001
	Function	35.39±7.28	40.00±6.26	3.100	0.002
	Deformity	3.77±0.43	3.86±0.35	0.872	0.383
	Range of motion	3.13±1.71	3.59±1.4	0.713	0.476
	Total scores	74.87±14.17	84.28±13.99	2.791	0.005
SF-36▲ (score, mean ± SD)	PCS	41.86±8.35	45.86±7.32	2.296	0.022
	MCS	47.26±3.78	50.27±5.48	2.088	0.037

▲ The results were compared with the corresponding indexes of this group before operation, $p< 0.05$; $p<0.05$.

For continuous variables conforming to the normal distribution, the independent sample T-test was employed to analyze differences between groups, while those not conforming to the normal distribution were analyzed using the Mann-Whitney U test. The classified variables were subjected to statistical analysis using the chi-square test or Fisher exact test.

Traumatic osteonecrosis (TONFH); non-traumatic- alcoholic-induced osteonecrosis (AIONFH). ARCO: Association Research Circulation Osseous; HHS: Harris Hip Score; SF-36: 36-Item Short Form Health Survey.

Table 5
Clinical treatment of patients in two groups.

Groups	Extremely effective	Effective	Ineffective	Total efficiency
TONFH Group (34 hips)	15(44.12)*	4(11.76)	15 (44.12)	19 (55.88)
AIONFH Group (34 hips)	23(67.65)	3(8.82)	8 (23.53)	26 (76.47)
χ^2 *value*				3.219
p value				0.073

* n (%).

$p<0.05$ indicates statistical significance.

Traumatic osteonecrosis (TONFH); non-traumatic- alcoholic-induced osteonecrosis (AIONFH).
The classified variables were subjected to statistical analysis using the chi-square test or Fisher exact test.

DISCUSSION

Core decompression combined with bone grafting is ideal for treating AIONFH and TONFH

ONFH is a challenging orthopedic condition with a high disability rate, necessitating timely and effective treatment to preserve patients' health and quality of life [15]. Among various treatment approaches, core decompression and bone grafting are considered favorable surgical methods [16]. The combination of these techniques not only reduces internal pressure in the femoral head, alleviates bone marrow edema, and enhances intraosseous microcirculation through

Table 6
Logistic regression analysis of factors related to prognosis of patients.

Predictor	Univariables OR (95% CI)	*p*	Multivariables OR (95% CI)	*p*
Pathogeny	2.566(0.905-7.275)	0.076		
Gender	0.653(0.21-2.027)	0.461		
Age	0.979(0.906-1.059)	0.602		
BMI	0.723(0.571-0.915)	0.007	0.692(0.507-0.944)	0.020*
Smoking	2.141(0.771-5.945)	0.144		
Alcohol	0.389(0.128-1.181)	0.096		
Diabetes	2.612(0.902-7.569)	0.077		
Hyperlipidemia	1.146(0.418-3.138)	0.791		
Hypertension	1.95(0.705-5.394)	0.198		
Immune-related diseases	0.28(0.097-0.805)	0.018	0.133(0.007-2.47)	0.176
Osteoporosis	0.222(0.07-0.703)	0.011	3.365(0.536-21.125)	0.195
Fracture	0.429(0.153-1.198)	0.106		
JIC	5.526(1.726-17.692)	0.004	14.275(1.117-182.387)	0.041*
HHS	0.811(0.707-0.93)	0.003	0.779(0.594-1.023)	0.072
PCS	0.581(0.432-0.78)	<0.001	0.419(0.192-0.913)	0.029*
MCS	0.674(0.52-0.875)	0.003	0.781(0.475-1.284)	0.330

*p<0.05.

Univariate Logistic regression analysis was used to identify risk factors affecting treatment efficacy, while multivariate Logistic regression analysis was employed to analyze significant indicators.

Body mass index (BMI); JIC: Japanese Investigation Committee; HHS: Harris Hip Score; Physical Health Score (PCS); Mental Health Score (MCS).

improved muscle and pulse reflux but also facilitates osteogenesis, bone repair, and provides structural support to the femoral head, thereby reducing the risk of postoperative femoral head collapse [17].

Prior research by Larson et al. indicated that using core decompression alone to treat ONFH yields variable clinical success rates, with the lowest rate being only 20%, leading to uncertain therapeutic outcomes [18]. However, our study demonstrates that combining core decompression with bone grafting yields better therapeutic results for patients with AIONFH and TONFH, achieving 55.88% and 76.47% success rates. By comparing various indices before surgery, at six months after the operation, and at the last follow-up, we observed an improvement in the ARCO classification from grade III/IV to grade I/II in both groups. The HHS and SF-36 scores were also significantly enhanced, indicating notable improvements in hip joint function and overall quality of life. The ARCO classification system is widely used to assess ONFH and reflects the occurrence of femoral head collapse [5,19]. The HHS provides a comprehensive evaluation of post-surgery hip joint function. The combination of these assessments effectively captures the hip joint's recovery and the overall well-being of the patients [20]. The SF-36 scale is a reliable tool for measuring health-related quality of life [21], and when combined with the other measures, it highlights the substantial positive impact of the surgical intervention on the patient's functional recovery and psychological well-being.

Core decompression combined with bone grafting has a better therapeutic effect on AIONFH

Upon further analysis, we observed that the therapeutic efficacy of core decompression combined with bone grafting was superior in patients with AIONFH compared to those with TONFH. TONFH is generally caused by direct trauma to the femoral head, leading to the disruption of blood supply, ischemia, and hypoxia of osteocytes, ultimately resulting in necrosis [22]. The blood supply to the femoral head is primarily from the medial and lateral circumflex femoral arteries, which supply blood to the lateral anterior superior region and the area below the femoral head. Fractures, particularly in the femoral neck region, can damage these arteries, increasing the likelihood of ONFH.

On the other hand, AIONFH arises mainly from an imbalance in osteogenesis/osteoclast activity and abnormal lipid metabolism, causing ischemia, hypoxia, venous stasis, and elevated intraosseous pressure in the femoral head [23,24]. Considering the unique characteristics of core decompression combined with bone grafting and the distinct pathological nature of the two diseases, this treatment approach holds greater promise for managing AIONFH. Our study supports this notion, as the total effective rate in the AIONFH group was higher than that in the TONFH group. Moreover, starting from six months after the operation, many indices in the AIONFH group showed better outcomes than those in the TONFH group. At the last follow-up, except for "deformity" and "range of motion" in the Harris score, all other indices demonstrated significant improvement in the AIONFH group compared to the TONFH group. These findings suggest that core decompression combined with bone grafting yields superior clinical efficacy in treating AIONFH, leading to more pronounced improvements in the patients' quality of life.

Overall, the results indicate that the chosen treatment approach is more advantageous for AIONFH patients due to its ability to address the disease's specific pathological mechanisms. This study highlights the importance of selecting appropriate treatment strategies tailored to the unique characteristics of different types of femoral head necrosis, ultimately leading to better clinical outcomes and improved patient well-being.

BMI, JIC classification and PCS score are the risk factors affecting the prognosis of patients

Our results also indicated that BMI, JIC classification, and PCS score could be potential risk factors influencing the prognosis of patients with AIONFH and TONFH. BMI is a commonly used indicator to assess body weight and is employed to evaluate various health conditions [25], including obesity and the risk of fractures [26], hypertension [27], and kidney disease [28]. Prior studies have highlighted the crucial role of lipid metabolism in the development of femoral head osteonecrosis. Lowering body fat content has been shown to enhance osteogenesis, while lipid metabolism disorders may lead to fat entering the bloodstream and spreading throughout the body, potentially affecting bone marrow and increasing intramedullary pressure. This process could obstruct venous reflux and impede blood circulation within bone tissue, ultimately influencing the clinical effectiveness of intramedullary decompression combined with bone grafting. Hence, higher BMI levels may impact the treatment outcomes of this surgical approach.

Additionally, the location of the necrotic area within the femoral head is closely associated with femoral head collapse and pain [29,30]. When the osteonecrosis area is located inside the weight-bearing region, the subchondral bone remains more intact, enhancing femoral head stability and reducing pain and collapse rates during weight-bearing [31,32]. On the contrary, when the JIC classification of the patient indicates type C, where the necrotic area is situated outside the weight-bearing region, patients tend to

experience more severe pain, and the probability of postoperative femoral head collapse is higher. Therefore, the JIC classification serves as an effective index for predicting the prognosis of patients.

Furthermore, the PCS score reflects patients' physical health and indirectly indicates the impact of femoral head osteonecrosis on their life. Patients' quality of life is often closely related to the severity and duration of the disease and the stress caused by it [33]. As a result, the PCS score can provide insights into the patient's overall condition and prognosis, helping to gauge the severity of the disease and its impact on the patient's well-being.

Considering BMI, JIC classification, and PCS score as potential risk factors in the prognosis of AIONFH and TONFH patients can aid in understanding their clinical outcomes and developing appropriate treatment strategies tailored to their specific conditions. The findings of this study underscore the efficacy of core decompression combined with bone grafting in treating avascular necrosis of the femoral head (ONFH), particularly in the context of alcohol-induced ONFH. While the results of this study support the positive outcomes of this surgical technique, it is essential to acknowledge that the focus on alcohol-induced ONFH necessitates specific consideration of the population studied. Given the epidemiological significance of alcohol-induced ONFH in specific populations, it is crucial to emphasize the specificity of this study's findings to the alcoholism-related etiology in the title of the manuscript. By recognizing the unique epidemiological aspects of the study population, the results and implications can be more accurately contextualized and better aligned with the specific medical-metabolic origins of alcohol-induced ONFH.

While the current study included assessments at preoperative, six months postoperative, and a final follow-up, we acknowledge the need for more frequent and intermediate medical controls during the postoperative period. Therefore, it is recommended to incorporate interim assessments at specific intervals, such as three months and 12 months postoperatively, to provide a more comprehensive understanding of the progression and outcomes of the surgical treatment. These additional checkpoints will allow for a more nuanced evaluation of the patient's recovery and the effectiveness of the intervention, particularly in the context of the described surgical treatment approach for osteonecrosis of the femoral head. Further, it is imperative to acknowledge the significance of utilizing additional assessment scales, including imaging-based evaluations, alongside standard clinical rating scales for a comprehensive evaluation of treatment outcomes in osteonecrosis of the femoral head. While the study incorporated reliable and internationally recognized clinical rating scales such as the Association Research Circulation Osseous (ARCO) classification, Harris Hip Score (HHS), and SF-36 scale, the inclusion of imaging-based assessments, such as MRI and X-ray evaluations, would provide valuable insights into the structural changes and healing progression within the femoral head post-surgery. The integration of imaging assessments will offer a more holistic understanding of the treatment response and aid in determining the success of the surgical intervention from both functional and anatomical perspectives. Therefore, it is recommended to consider including imaging-based evaluation tools as supplementary measures to augment the comprehensive assessment of treatment outcomes in future research endeavors. Besides, this study included its focus on a specific population and etiological factors, which may restrict the generalizability of the findings to other populations and ONFH etiologies.

In conclusion, core decompression combined with bone grafting has demonstrated promising therapeutic outcomes for AIONFH and TONFH, with particularly significant results observed in AIONFH cases.

This treatment approach improves hip joint function and effectively enhances patients' overall quality of life while mitigating the risk of postoperative femoral head collapse. Consequently, it is a recommended surgical method for managing these conditions.

Moreover, our findings suggest that BMI, JIC classification, and PCS score may serve as potential risk factors influencing the prognosis of patients with AIONFH and TONFH. Patients who present with specific indicators related to these factors should receive heightened attention and suitable treatment measures to improve the surgery's clinical effectiveness and prognostic outcomes. Furthermore, as medical advancements continue to progress, the availability of various bone grafting options has expanded. Building upon the established efficacy of core decompression combined with bone grafting in treating AIONFH, further exploration into different types of bone grafts may offer additional opportunities for treatment optimization.

Conflict of interests

The authors declared no conflict of interest.

Author's ORCID numbers

- Zhensong Wu (ZW): 0009-0009-2940-0781
- Da Song (DA): 0009-0004-2242-2498
- Qi Xu (QX): 0009-0001-5704-582X
- Dawei Wang (DW): 0009-0001-4508-790X

Participation in development and writing of the paper

Concept and design: ZW and DW. Acquisition of data, literature review, and refinement of manuscript: All authors. Analysis and interpretation of data: DS and QX. Manuscript writing: ZW. Review of final manuscript: DW.

Funding

No funds, grants, or other support was received.

REFERENCES

1. **Yue J, Gao H, Guo X, Wang R, Li B, Sun Q, Liu W, Chen J, Li Y.** Fibula allograft propping as an effective treatment for early-stage osteonecrosis of the femoral head: a systematic review. J Orthop Surg Res 2020; 15(1):206. *doi: 10.1186/s13018-020-01730-6.*
2. **Yan Z, Zhan J, Qi W, Lin J, Huang Y, Xue X, Pan X.** The protective effect of luteolin in glucocorticoid-induced osteonecrosis of the femoral head. Front Pharmacol 2020; 11:1195. *doi: 10.3389/fphar.2020.01195.*
3. **Assouline-Dayan Y, Chang C, Greenspan A, Shoenfeld Y, Gershwin ME.** Pathogenesis and natural history of osteonecrosis. Semin Arthritis Rheu 2002; 32(2):94-124.
4. **Tan B, Li W, Zeng P, Guo H, Huang Z, Fu F, Gao H, Wang R, Chen W.** Epidemiological study based on China osteonecrosis of the Femoral Head Database. Orthop Surg 2021; 13(1):153-160. *doi: 10.1111/os.12857.*
5. **Konarski W, Poboży T, Śliwczyński A, Kotela I, Krakowiak J, Hordowicz M, Kotela A.** Avascular necrosis of femoral head-Overview and current state of the art. Int J Environ Res Public Health. 2022;19(12):7348. *doi: 10.3390/ijerph19127348.*
6. **Hines JT, Jo WL, Cui Q, Mont MA, Koo KH, Cheng EY, Goodman SB, Ha YC, Hernigou P, Jones LC, Kim SY, Sakai T, Sugano N, Yamamoto T, Lee MS, Zhao D, Drescher W, Kim TY, Lee YK, Yoon BH, Baek SH, Ando W, Kim HS, Park JW.** Osteonecrosis of the femoral head: an updated review of ARCO on pathogenesis, staging and treatment. J Korean Med Sci. 2021;36(24):e177. *doi: 10.3346/jkms.2021.36.e177.*

7. **Wu P, Xiao Y, Qing L, Tang J, Huang C, Cao Z.** Comparison of retrograde anatomy iliac bone flap grafting versus anterograde anatomy iliac bone flap grafting for treatment of osteonecrosis of the femoral head. J Orthop Surg Res 2023; 18(1):130. *doi: 10.1186/s13018-023-03617-8.*
8. **Sai Krishna MLV, Kar S, Kumar R, Singh H, Mittal R, Digge VK.** The role of conservative management in the avascular necrosis of the femoral head: A review of systematic reviews. Indian J Orthop. 2023;57(3):410-420. *doi: 10.1007/s43465-023-00818-5.*
9. **Singh M, Singh B, Sharma K, Kumar N, Mastana S, Singh P.** A molecular troika of angiogenesis, coagulopathy and endothelial dysfunction in the pathology of avascular necrosis of femoral head: A comprehensive review. Cells. 2023 ;12(18):2278. *doi: 10.3390/cells12182278.*
10. **Anand A, Jha CK, Singh PK, Sinha U, Ganesh A, Bhadani PP.** Avascular necrosis of femur as a complication of Cushing's syndrome due to adrenocortical carcinoma. Am Surg. 2023;89(6):2701-2704.
11. **Petek D, Hannouche D, Suva D.** Osteonecrosis of the femoral head: pathophysiology and current concepts of treatment. Efort Open Rev 2019; 4(3):85-97. *doi: 10.1302/2058-5241.4.180036.*
12. **Zhu S, Zhang X, Chen X, Wang Y, Li S, Qian W.** Comparison of cell therapy and other novel adjunctive therapies combined with core decompression for the treatment of osteonecrosis of the femoral head: a systematic review and meta-analysis of 20 studies. Bone Joint Res 2021; 10(7):445-458. *doi: 10.1302/2046-3758.107.BJR-2020-0418.R1.*
13. **Mont MA, Salem HS, Piuzzi NS, Goodman SB, Jones LC.** Nontraumatic osteonecrosis of the femoral head: where do we stand today?: A 5-year update. J Bone Joint Surg Am 2020; 102(12):1084-1099. *doi: 10.2106/JBJS.19.01271.*
14. **Yoon BH, Mont MA, Koo KH, Chen CH, Cheng EY, Cui Q, Drescher W, Gangji V, Goodman SB, Ha YC, Hernigou P, Hungerford MW, Iorio R, Jo WL, Jones LC, Khanduja V, Kim H, Kim SY, Kim TY, Lee HY, Lee MS, Lee YK, Lee YJ, Nakamura J, Parvizi J, Sakai T, Sugano N, Takao M, Yamamoto T, Zhao DW.** The 2019 Revised Version of Association Research Circulation Osseous Staging System of Osteonecrosis of the Femoral Head. J Arthroplasty 2020; 35(4):933-940. *doi: 10.1016/j.arth.2019.11.029.*
15. **Peng WX, Ye C, Dong WT, Yang LL, Wang CQ, Wei ZA, Wu JH, Li Q, Deng J, Zhang J.** MicroRNA-34a alleviates steroid-induced avascular necrosis of femoral head by targeting Tgif2 through OPG/RANK/RANKL signaling pathway. Exp Biol Med 2017; 242(12):1234-1243. *doi: 10.1177/1535370217703975.*
16. **Algarni AD, Al MH.** Clinical and radiological outcomes of extracorporeal shock wave therapy in rarly-stage femoral head osteonecrosis. Adv Orthop 2018; 2018:7410246. *doi: 10.1155/2018/7410246.*
17. **Zhao Y, Zhang G, Song Q, Fan L, Shi Z.** Intramedullary core decompression combined with endoscopic intracapsular decompression and debridement for pre-collapse non-traumatic osteonecrosis of the femoral head. J Orthop Surg Res 2023; 18(1):6. *doi: 10.1186/s13018-022-03477-8.*
18. **Larson E, Jones LC, Goodman SB, Koo KH, Cui Q.** Early-stage osteonecrosis of the femoral head: where are we and where are we going in year 2018? Int Orthop 2018; 42(7):1723-1728. *doi: 10.1007/s00264-018-3917-8.*
19. **Li G, Li B, Li B, Zhao J, Wang X, Luo R, Li Y, Liu J, Hu R.** The role of biomechanical forces and MALAT1/miR-329-5p/PRIP signaling on glucocorticoid-induced osteonecrosis of the femoral head. J Cell Mol Med 2021; 25(11):5164-5176. *doi: 10.1111/jcmm.16510.*
20. **Ma JX, Kuang MJ, Fan ZR, Xing F, Zhao YL, Zhang LK, Chen HT, Han C, Ma XL.** Comparison of clinical outcomes with InterTan vs Gamma nail or PFNA in the treatment of intertrochanteric fractures: A meta-analysis. Sci Rep-Uk 2017; 7(1):15962. *doi: 10.1038/s41598-017-16315-3.*
21. **Jayasinghe UW, Harris MF, Taggart J, Christl B, Black DA.** Gender differen-

ces in health-related quality of life of Australian chronically-ill adults: patient and physician characteristics do matter. Health Qual Life Out 2013; 11:102. *doi: 10.1186/1477-7525-11-102.*

22. **Bachiller FG, Caballer AP, Portal LF.** Avascular necrosis of the femoral head after femoral neck fracture. Clin Orthop Relat R 2002(399):87-109. *doi: 10.1097/00003086-200206000-00012.*
23. **Qin X, Jin P, Jiang T, Li M, Tan J, Wu H, Zheng L, Zhao J.** A Human chondrocyte-derived in vitro model of alcohol-induced and steroid-induced femoral head necrosis. Med Sci Monitor 2018; 24:539-547. *doi: 10.12659/msm.907969.*
24. **Liu Y, Zhao D, Wang W, Zhang Y, Wang B, Li Z.** Efficacy of core decompression for treatment of canine femoral head osteonecrosis induced by arterial ischaemia and venous congestion. Hip Int 2017; 27(4):406-411. *doi: 10.5301/hipint.5000462.*
25. **Laimer J, Holler A, Pichler U, Engel R, Neururer SB, Egger A, Griesmacher A, Bruckmoser E.** Nutritional status in patients with medication-related osteonecrosis of the jaw (MRONJ). Nutrients 2021; 13(5):1585. *doi: 10.3390/nu13051585.*
26. **Gkastaris K, Goulis DG, Potoupnis M, Anastasilakis AD, Kapetanos G.** Obesity, osteoporosis and bone metabolism. J Musculoskel Neuron 2020; 20(3):372-381.
27. **Tan L, Long LZ, Ma XC, Yang WW, Liao FF, Peng YX, Lu JM, Shen AL, An DQ, Qu H, Fu CG.** Association of body mass index trajectory and hypertension risk: A systematic review of cohort studies and network meta-analysis of 89,094 participants. Front Cardiovasc Med 2022; 9:941341. *doi: 10.3389/fcvm.2022.941341.*
28. **Hosseinpanah F, Barzin M, Golkashani HA, Nassiri AA, Sheikholeslami F, Azizi F.** Association between moderate renal insufficiency and cardiovascular events in a general population: Tehran lipid and glucose study. BMC Nephrol 2012; 13:59. *doi: 10.1186/1471-2369-13-59.*
29. **Huang Z, Tan B, Ye H, Fu F, Wang R, Chen W.** Dynamic evolution of osseous structure in osteonecrosis of the femoral head and dynamic collapse risks: a preliminary CT image study. J Orthop Surg Res 2020; 15(1):539. *doi: 10.1186/s13018-020-02069-8.*
30. **Hong G, Huang X, Lv T, Li X.** An analysis on the effect of the three-incision combined approach for complex fracture of tibial plateau involving the posterolateral tibial plateau. J Orthop Surg Res 2020; 15(1):43. *doi: 10.1186/s13018-020-1572-4.*
31. **Wu Z, Wang B, Tang J, Bai B, Weng S, Xie Z, Shen Z, Yan D, Chen L, Zhang J, Yang L.** Degradation of subchondral bone collagen in the weight-bearing area of femoral head is associated with osteoarthritis and osteonecrosis. J Orthop Surg Res 2020; 15(1):526. *doi: 10.1186/s13018-020-02065-y.*
32. **Asada R, Abe H, Hamada H, Fujimoto Y, Choe H, Takahashi D, Ueda S, Kuroda Y, Miyagawa T, Yamada K, Tanaka T, Ito J, Morita S, Takagi M, Tetsunaga T, Kaneuji A, Inaba Y, Tanaka S, Matsuda S, Sugano N, Akiyama H.** Femoral head collapse rate among Japanese patients with pre-collapse osteonecrosis of the femoral head. J Int Med Res 2021; 49(6):675883032. *doi: 10.1177/03000605211023336.*
33. **Carta MG, Maggiani F, Pilutzu L, Moro MF, Mura G, Sancassiani F, Vellante V, Migliaccio GM, Machado S, Nardi AE, Preti A.** Sailing can improve quality of life of people with severe mental disorders: results of a cross over randomized controlled trial. Clin Pract Epidemiol Ment Health 2014; 10:80-86. *doi: 10.2174/1745017901410010080.*

Invest Clin 65(3): 294 - 307, 2024 https://doi.org/10.54817/IC.v65n3a03

La eficacia de los aceites ozonizados en el tratamiento de pacientes con micosis superficiales.

Natalia Soucre[1], Verónica Bracho[1], Primavera Alvarado[2,3] y Elsy Cavallera[1]

[1]Servicio de Dermatología. Instituto de Biomedicina ''Dr. Jacinto Convit''. Hospital Vargas de Caracas, Venezuela.
[2]Laboratorio de Micología. Instituto de Biomedicina ''Dr. Jacinto Convit''. Hospital Vargas de Caracas. Venezuela.
[3]Facultad de Medicina Universidad Central de Venezuela, Caracas, Venezuela.

Palabras clave: micosis superficiales; aceites ozonizados; antifúngico; ozono.

Resumen. Las micosis superficiales constituyen uno de los principales motivos de consulta en el área dermatológica. En los últimos años se ha comprobado en diferentes países la efectividad terapéutica de los aceites ozonizados en infecciones micóticas por su amplio espectro germicida y antifúngico. El objetivo fue evaluar la eficacia del uso de aceite de girasol ozonizado en el tratamiento de micosis superficiales en pacientes de la consulta externa de Micología en el Servicio de Dermatología del Hospital Vargas de Caracas, Instituto Autónomo de Biomedicina Dr. Jacinto Convit. Se realizó un estudio experimental descriptivo transversal, donde se evaluaron 36 pacientes con diagnóstico de micosis superficial y 10 sujetos sanos. Del grupo de 36 pacientes, 26 fueron tratados con aceite de girasol ozonizado (AGO) y 10 pacientes con aceite de girasol sin ozonizar (AGNO). Los 10 individuos sanos representaron el control de sensibilidad al AGO. Las micosis superficiales más frecuentes evaluadas en el grupo de AGO fue *tinea corporis* (31%), seguido de estomatitis subprotésica (23%) y para el grupo de AGNO *tinea pedis* (50%); en cuanto al agente etiológico se evidenció una mejoría con el tratamiento de AGO del 86% para *Candida albicans* y 60% para el complejo *Trichophyton rubrum* a la semana 8 de tratamiento. Se concluyó que el efecto antifúngico del AGO es mayor para el género *Candida* spp que para los dermatofitos, evidenciándose una mejoría total de las lesiones con seis semanas de tratamiento.

Autor de correspondencia: Primavera Alvarado, Laboratorio de Micología. Instituto de Biomedicina "Dr. Jacinto Convit''. Caracas, Venezuela. Correo electrónico: Prima558@gmail.com

The efficacy of ozonated oils in the treatment of patients with superficial mycosis.

Invest Clin 2024; 65 (3): 294 – 307

Keywords: superficial mycoses; ozonated oils; antifungal; ozone.

Abstract. Superficial mycoses are one of the main reasons for consultation in the dermatological area. In recent years, the therapeutic effectiveness of ozonated oils in fungal infections has been verified in different countries due to its broad germicidal and antifungal spectrum. The objective is to evaluate the efficacy of the use of ozonated sunflower oil in the treatment of superficial mycoses in patients of the Mycology consultation at the Dermatology Service of the Hospital Vargas de Caracas, Instituto Autonómo de Biomedicina "Dr. Jacinto Convit". A cross-sectional descriptive, experimental study was conducted, where 36 patients diagnosed with superficial mycosis and ten healthy subjects were evaluated. Of the group of 36 patients, 26 were treated with ozonated sunflower oil (AGO) and ten patients with non-ozonized sunflower oil (AGNO). Ten healthy individuals represented the AGO sensitivity control. The most frequent superficial mycosis evaluated in the AGO group was *tinea corporis* (31%), followed by denture stomatitis (23%) and for the AGNO group, *tinea pedis* (50%). Regarding the etiological agent, an improvement with the AGO treatment of 86% for *Candida albicans* and 60% for the *Trichophyton rubrum complex* was evidenced at week eight of treatment. It is concluded that the antifungal effect of AGO is more significant for the genus *Candida* spp than for dermatophytes, evidencing a total improvement of the lesions with six weeks of treatment.

Recibido: 05-09-2023 Aceptado: 26-04-2024

INTRODUCCIÓN

Las micosis superficiales son infecciones fúngicas que afectan la piel, las uñas y el cabello. Son causados por dermatofitos, mohos y levaduras. Estas infecciones fúngicas son de distribución geográfica cosmopolita y predominan en las regiones tropicales y subtropicales [1,2]. En cuanto a los factores predisponentes se encuentran los malos hábitos higiénicos, el hacinamiento, acondicionamiento físico, el uso de zapatos cerrados y ropa sintética [3,4]. En el caso de pacientes con procesos crónicos o debilitantes como la diabetes, las micosis superficiales se incrementan y se extienden con facilidad. Aunque no causa mortalidad, se sabe que se asocia con una alta morbilidad que puede ser psicológica o física. Esto afecta la calidad de vida de las personas infectadas lo que repercute negativamente en su situación laboral, afectiva y social. Tales infecciones están aumentando a escala mundial y, por lo tanto, son motivo de grave preocupación en todo el mundo [5].

A lo largo de los años se han incluido diferentes métodos terapéuticos para las micosis superficiales, entre las cuales existe la ozonización de aceites vegetales, lo cual se logra utilizando el ozono (O_3), el cual se caracteriza por ser una molécula inestable compuesta por tres átomos de oxígeno. Cada átomo de oxígeno liberado se une a otra mo-

lécula de oxígeno (O_2) formando moléculas de O_3. En condiciones normales es muy soluble en agua, 20 veces más soluble que el oxígeno, como es una molécula bastante inestable, su vida media en agua es de 20 minutos aproximadamente, limitando su uso por este medio. Por otro lado, es soluble en aceites comerciales, al unirse la molécula de ozono a los dobles enlaces de los ácidos insaturados, hace que esta se vuelva más estable y puede permanecer unida inclusive hasta dos años. El potencial de oxidación del ozono es de 2,07 Voltios, es uno de los potenciales más elevado en la tabla de los potenciales de oxidación, superado solamente por el potencial del flúor cuyo valor es de 2,87 Voltios [6,7]. El gas ozono (O_3) es un potente oxidante lo que lo convierte en un potente agente germicida, fungicida y viricida. Actualmente, se conoce sus efectos antiinflamatorios [8], antioxidantes [9] y cicatrizantes [10]. Por lo tanto, la ozonoterapia se ha sugerido como un tratamiento alternativo en odontología y en campos médicos, como la dermatología. Se ha propuesto su uso en casos de acné, eczema, dermatitis atópica, psoriasis, herpes zoster, pioderma, micosis, y también en la cicatrización de heridas en la piel [10].

En la búsqueda de tratamientos alternativos para las micosis superficiales, se planteó un ensayo clínico para evaluar la eficacia del uso de aceites de girasol ozonizado en el tratamiento de micosis superficiales en pacientes de la consulta externa de Micología en el Servicio de Dermatología del Hospital Vargas de Caracas, Instituto Autónomo de Biomedicina Dr. Jacinto Convit.

MATERIALES Y MÉTODOS

Se trata de un estudio del tipo experimental, descriptivo y de corte transversal, para evaluar pacientes con diagnóstico presuntivo de micosis superficiales. Estos fueron atendidos en la consulta externa de Micología del Servicio de Dermatología del Hospital Vargas de Caracas, Instituto de Biomedicina Dr. Jacinto Convit.

Población y muestra: Se evaluaron 36 pacientes con diagnóstico presuntivo de micosis superficiales, 26 fueron tratados con aceite de girasol ozonizado (AGO), 10 con aceite de girasol sin ozonizar (AGNO). Adicionalmente, se incluyeron 10 individuos sanos, como controles, a quienes se les colocó aceite de girasol ozonizado para evaluar la sensibilidad del producto, durante el lapso de octubre a diciembre de 2019.

Con aprobación del comité de Bioética del Instituto autónomo de Biomedicina Dr. Jacinto Convit y, previo consentimiento informado de cada paciente, se recolectó la información clínico-epidemiológica de cada paciente (edad, sexo, procedencia, antecedentes personales, presentación clínica, mejoría clínica, duración del tratamiento, efectos adversos y recidivas).

Criterios de inclusión:

- Se seleccionaron pacientes con micosis superficiales no complicadas, que no comprometían la salud ni la vida de los pacientes, mientras se realizó el estudio.
- Pacientes de ambos géneros. En edades entre 5 y 70 años.
- Los pacientes en edad pediátrica (<12 años) recibieron solo el tratamiento de aceite de girasol ozonizado.
- Pacientes que aceptaron voluntariamente participar en el estudio, previo consentimiento informado.
- Sin tratamientos previos con antimicóticos tópicos y sistémicos.

Criterios de exclusión:

- Pacientes con enfermedades mentales que impidieran su colaboración con el estudio y condiciones del mismo.
- Pacientes con micosis superficiales muy extensas o que afectaran uñas y pelo ya que éstas ameritan tratamiento sistémico.

- Pacientes VIH positivos.
- Pacientes menores de 2 años o mayores de 80 años.

Preparación del aceite ozonizado: Se utilizaron aceites purificados refinados de girasol de uso comestible. El equipo TA-600 fue el elegido para la ozonización del mismo. La capacidad de generación de ozono fue de 6 gr/hora. El método de ozonización fue de difusión por burbujeo y agitación. Se sumergió un difusor poroso en una mezcla agua-aceite y se agitó mecánicamente de forma constante durante todo el tiempo de ozonización. Los poros del difusor fueron de tamaño controlado, a fin de proporcionar burbujas que pudieron interaccionar, con cierta eficacia, con las gotas del aceite de girasol dispersas en la fase acuosa [6].

Toma de muestra: Una vez seleccionado el paciente, se realizó la limpieza de la zona afectada con alcohol isopropílico al 70% para remover contaminantes, luego se practicó escarificado de la piel afectada utilizando hoja de bisturí número 15, recolectando el material (polvo o escama) sobre un porta-objeto.

Estudio micológico:

Examen directo: Las muestras obtenidas se impregnaron con una gota del colorante clorazol Black-E y encima se colocó un cubre objeto, se esperó 5 minutos y se observó al microscopio de luz, para la detección de estructuras fúngicas (hifas y blastoconidias).

Cultivo micológico: El material recolectado (escamas), se cultivó en los medios agar Sabouraud o de lactrimel, ambos suplementados con cloranfenicol al 5%. Los cultivos fueron incubados de 25 a 30°C durante 4 semanas aproximadamente. Posteriormente, en los cultivos donde hubo crecimiento, se determinó el agente etiológico, según las características macroscópicas y microscópicas [11].

Ensayo clínico: El tratamiento con aceite ozonizado se indicó una frecuencia de dos veces al día en la zona afectada, por un máximo de 8 semanas. La evolución clínica de los pacientes fue evaluada por dos residentes del último año del postgrado de Dermatología y un especialista en Dermatología del Instituto de Biomedicina Dr. Jacinto Convit.

Los pacientes tratados con aceite de girasol ozonizados y sin ozonizar después de 2 semanas sin mejoría clínica, tuvieron tratamiento convencional asegurado.

Registro fotográfico: Se realizó registro fotográfico estricto de los pacientes con cámara digital de 8 megapíxeles, previo al inicio del tratamiento y luego a la semana 2, 4, 6 y 8.

Análisis estadístico

Se realizó análisis de varianza, el cual permitió determinar si los diferentes tratamientos mostraron diferencias significativas o, por el contrario, puede suponerse que sus medias poblacionales no difieren. Se utilizó la prueba exacta de Fisher para analizar los datos categóricos, examinando la significancia de la asociación entre los dos tipos de clasificación. Se consideraron estadísticamente significativas aquellas comparaciones con valores de $p<0,05$.

RESULTADOS

En este trabajo se encontró que en ambos grupos el sexo predominante fue el femenino, con 62% (16/26) para el grupo AGO y 60% (6/10) para el grupo de AGNO. El grupo etario predominante en ambos grupos fue de 31 a 40 años (35,5 ± 4,5), con un porcentaje de 30,8% (8/26) en el primero y 40% (4/10) en el segundo. El fototipo cutáneo predominante fue el IV con 73% (19/26) y 90% (9/10) respectivamente (Tabla 1).

El Distrito Capital fue el lugar de mayor procedencia de los pacientes para ambos grupos, con 84,61% (22/26) para AGO y 70% (7/10) AGNO; otras procedencias fueron los estados Miranda, Vargas y Aragua (Tabla 1).

Del total de pacientes evaluados en el grupo de AGO, solo 42,3% (11/26) presentaron comorbilidades asociada, entre ellas, psoriasis 7,6 % (2/26), penfigoide ampollar

Tabla 1
Datos epidemiológicos de los pacientes tratados con aceite de girasol ozonizado y aceite de girasol sin ozonizar.

	AGO		AGNO	
Sexo	Número	Porcentaje %	Número	Porcentaje %
Femenino	16	62 (16/26)	6	60 (6/10)
Masculino	10	38 (10/26)	4	40 (4/10)
Total	26	100 (26)	10	100 (10)
Grupo etario				
0 a 10	2	7,7 (2/26)	0	0
11 a 20	2	7,7 (2/26)	0	0
21 a 30	1	3,8 (1/26)	0	0
31 a 40	8	30,8 (8/26)	4	40 (4/10)
41 a 50	3	11,5 (3/26)	0	0
51 a 60	2	7,7 (2/26)	2	20 (2/10)
61 a 70	4	15,3 (4/26)	3	30 (3/10)
>70	4	15,3 (4/26)	1	10 (1/10)
Total	26	100 (26)	10	100 (10)
Fototipo				
I	0	0	0	0
II	1	4 (1/26)	0	0
III	4	15 (4/26)	0	0
IV	19	73 (19/26)	9	90 (9/10)
V	2	8 (2/26)	1	10 (1/10)
VI	0	0	0	0
Total	26	100 (26)	10	100(10)
Procedencia				
Distrito Capital	22	84,61 (22/26)	7	70 (7/10)
Miranda	3	11,53 (3/26)	2	20 (2/10)
Vargas	0	0 (0/0)	1	10 (1/10)
Aragua	1	3,84 (1/26)	0	0 (0/0)
Total	26	99,98 (26)	10	100 (10)

AGO: Pacientes tratados con aceite de girasol ozonizado; AGNO: Pacientes tratados con aceite de girasol sin ozonizar.

3,8% (1/26), lupus eritematoso cutáneo crónico 3,8% (1/26), hipertensión arterial 19,2% (5/26), adenocarcinoma faríngeo 3,8% (1/26). Para el grupo de AGNO se presentó un solo paciente con psoriasis ,10% (1/10) y dos con hipertensión arterial, 20% (2/10) (Tabla 1).

El diagnóstico clínico encontrado en el grupo de pacientes tratado con AGO en orden de mayor a menor frecuencia fue: *Tinea corporis* 31% (8/26), estomatitis subprotésica 23% (6/26), *tinea pedis* y *tinea cruris* 15% (4/15), *tinea faciei* 8% (2/26), intertrigo y queilitis 4% (1/26). Para el grupo AGNO, fue *tinea pedis* 50% (5/10), estomatitis sub-

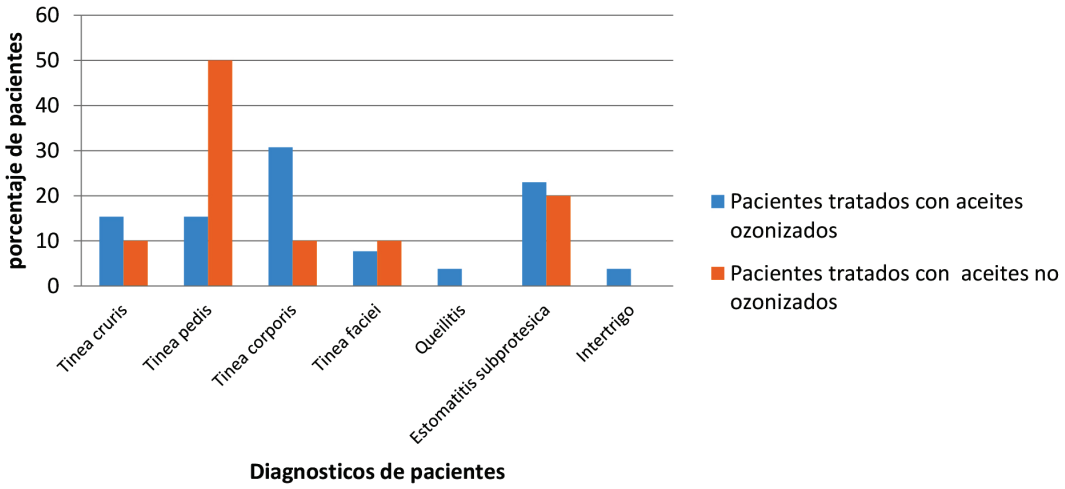

Fig 1. Diagnóstico clínico de pacientes tratados con aceite de girasol ozonizado y aceite de girasol sin ozonizar.

protésica 20% (2/10), *tinea corporis, tinea faciei* y *tinea cruris* 10% (1/10) respectivamente (Fig. 1).

Con relación al examen directo micológico fue positivo en todos los casos estudiados, para el grupo de AGO se visualizaron, hifas 50% (13/26), blastoconidias 27% (7/26) y ambas estructuras 23% (6/26). Para el grupo de AGNO, hifas 80% (8/10), blastoconidias 10% (1/10) y ambas estructuras 10% de los casos (1/10).

Al observar, por patología, el agente etiológico más frecuente en el grupo de AGO, para *tinea corporis* fue el complejo *Trichophyton rubrum*. En los casos de estomatitis subprotésica fueron *Candida albicans* y *Candida tropicalis*. Para *tinea pedis*, complejo *Trichophyton mentagrophytes* y en *tinea cruris*, complejo *Trichophyton rubrum*. En los dos casos de *tinea* no se aisló el agente. Se reportó un solo caso de intertrigo y un caso de queilitis aislándose *Candida albicans* en ambos casos (Tabla 2).

Para el grupo de AGNO, el agente etiológico más frecuente según la patología fue, para *tinea corporis* el complejo *Trichophyton rubrum*, en estomatitis subprotésica dos pacientes en los cuales se aisló *Candida no albicans*; en los cinco casos de *tinea pedis*, se reportó un caso del complejo *Trichophyton rubrum* y 4 casos sin crecimiento. En *tinea cruris* se aisló complejo *Trichophyton rubrum*, en *tinea faciei*, no se aisló el agente (Tabla 2).

Para evaluar la evolución clínica con los aceites, se usó una escala de puntuación de mejoría clínica, cuyo significado fue, 1: mejoría total (100%), 2: mejoría moderada (50%-70%), 3: mejoría leve (25%), 4: sin mejoría (0%). En la evolución clínica del grupo de los 26 pacientes tratados con AGO, en la segunda semana de tratamiento, el 73% (19/26) de los pacientes obtuvieron una mejoría moderada. En la cuarta semana, el 23% (6/26) de los pacientes alcanzaron mejoría total. En la sexta semana, el 57,7% (15/26) tuvieron mejoría total y se observó que el número de pacientes con mejoría total fue significativamente mayor ($p<0,001$), que aquellos que tuvieron mejoría moderada o leve. Finalmente, en la semana 8 se encontró que los pacientes tratados con AGO 61,5% (16/26) tuvieron mejoría total, seguido por 7,7% (2/26) con mejoría moderada; 23% (6/26) con mejoría leve y 7,7% (2/26) sin mejoría (Fig. 2).

Con respecto a la evolución clínica del grupo de AGNO, no se observó mejoría en ninguno de los 10 pacientes.

En cuanto a la mejoría de los pacientes según el agente etiológico tratados con AGO, a la semana 8 de tratamiento, se obser-

Tabla 2
Agentes etiológicos aislados en cultivos de pacientes tratados con aceite de girasol ozonizado y aceite de girasol sin ozonizar.

Diagnóstico clínico	AGO		AGNO	
	Agente etiológico	Porcentaje de aislamiento	Agente etiológico	Porcentaje de aislamiento
Tinea corporis	Complejo *Trichophyton rubrum*	58%	Complejo *Trichophyton rubrum*	100%
	No se aisló el agente	50%		
Estomatitis subprotésica	*Candida albicans*	83.30%	*Candida no albicans*	100%
	Candida tropicalis	16.70%		
Tinea pedis	Complejo *Trichophyton mentagrophytes*	25%	Complejo *Trichophyton rubrum*	56%
	Complejo *Trichophyton rubrum*	75%	No se aisló el agente	44%
Tinea cruris	Complejo *Trichophyton rubrum*	100%	Complejo *Trichophyton rubrum*	100%
Tinea faciei	-	-	-	-
Intertrigo	*Candida albicans*	100%	-	-
Queilitis	*Candida albicans*	100%	-	-

AGO: Pacientes tratados con aceite de girasol ozonizado; AGNO: Pacientes tratados con aceite de girasol sin ozonizar.

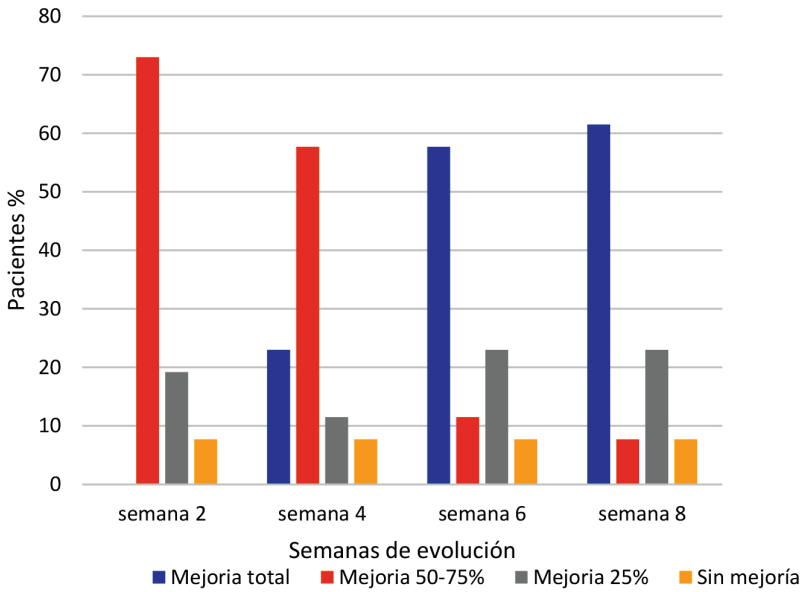

Fig. 2. Evolución clínica en pacientes tratados con aceite de girasol ozonizado.
Escala de puntuación de mejoría clínica en pacientes tratados con aceites ozonizados: 1: mejoría total (100%), 2: mejoría moderada (50%-70%), 3: mejoría leve (25%), 4: sin mejoría (0%).

vó que los pacientes con reporte de *Candida albicans*, tuvieron una mejoría total en 86% (6/7) de los casos y solo 14% (1/7) restante con mejoría moderada. La mejoría total se obtuvo en los pacientes a partir de la semana 4 de tratamiento y se completó a la semana 6 de tratamiento.

En cambio, aquellos pacientes donde se le aisló el complejo *Trichophyton rubrum* presentaron una respuesta variable al tratamiento reflejada en 60% (3/5) mejoría total, 20% (1/5) mejoría moderada y 20% (1/5) mejoría leve. Solo se observó mejoría total en los pacientes a quienes se le aisló el complejo *Trichophyton mentagrophytes* y *Candida tropicalis* (Figs. 3,4 y 5).

En la evaluación del control de sensibilidad al producto, representado por 10 sujetos sanos, a los cuales se les aplicó aceite de girasol ozonizado en el dorso de la mano diariamente por una semana, ninguno de ellos presentó reacción adversa al mismo.

En cuanto a las recidivas, se observó que de los 26 pacientes tratados con AGO, 9 (34%) recidivaron antes de los 6 meses de culminado el tratamiento. Los agentes etiológicos involucrados fueron: complejo *Trichophyton mentagrophytes*, complejo *Trichophyton rubrum*; es importante destacar que no se observó recidiva en el género *Candida*. Cuando se evaluó por patología, las recidivas fueron: *tinea cruris* (2/4), *tinea pedis* (3/4), *tinea corporis* (3/8) y *tinea faciei* (1/2). En los pacientes que presentaron estomatitis subprotésica y queilitis no se observó recidiva.

DISCUSIÓN

En este estudio, se evaluó la eficacia antifúngica del aceite de girasol ozonizado (AGO) en el tratamiento de micosis superficiales. En la actualidad existen reportes que aseguran su propiedad curativa. Bocci, explica el mecanismo de acción principal del ozono, el cual no actúa sobre receptores específicos, sino de forma indirecta, es decir, por la producción de "estrés oxidativo" que induce posteriores respuestas adaptativas [12]. El O_3 reacciona rápidamente con los antioxidantes y ácidos grasos poliinsaturados y los resultados son productos de oxidación lipídica e inducción de segundos mensajeros intracelulares, de los cuales los más importantes son el peróxido de hidrógeno (H_2O_2) y alquenales (principalmente 4- hidroxinonenal, 4-HNE). Estos segundos mensajeros conducen a la activación de factores transcripcionales nucleares como el factor nuclear (derivado de eritroide 2) como 2 (Nrf2), que resulta en transcripción de elementos de respuesta antioxidante (ARE) y la producción posterior de enzimas antioxidantes incluyendo superóxido dismutasa, glutatión-peroxidasa, proteínas de choque térmico (HSP70) y hemo oxigenasa-1 (HO-1) [12,13]. Además, Nrf2 puede conducir a la

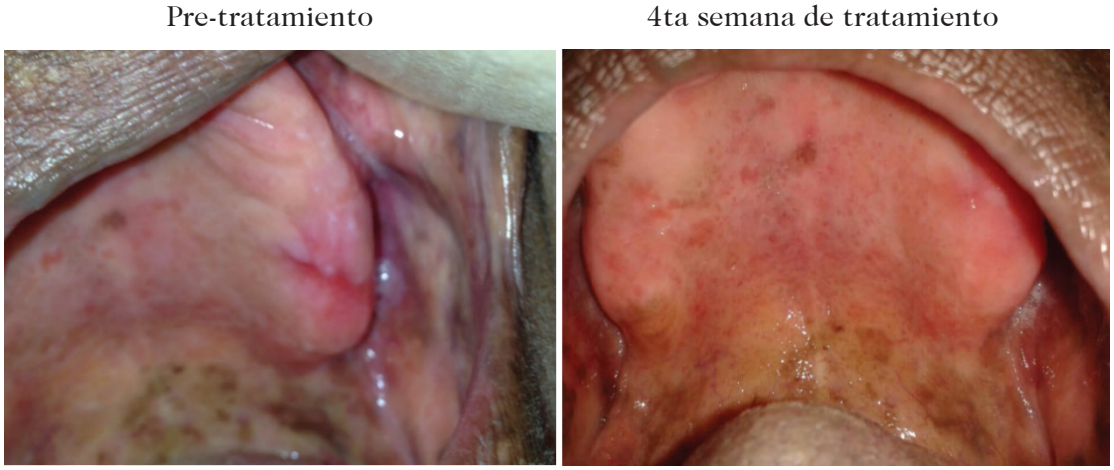

Fig. 3. Paciente con estomatitis subprotésica tratada con aceite de girasol ozonizado.
Paciente femenina de 73 años, con estomatitis subprotésica, por uso de prótesis dental. Directo micológico: blastoconidias, cultivo micológico: *Candida tropicalis*. Mejoría completa tras aplicar aceite de girasol ozonizado (AGO) a las 4 semanas de tratamiento.

Fig. 4. Paciente con *tinea corporis* en glúteo tratada con aceite de girasol ozonizado.
Paciente femenina de 34 años, con *tinea corporis* en ambos glúteos. Directo micológico: Hifas gruesas ramificadas, cultivo micológico: complejo *T. rubrum*. Mejoría completa tras aplicar aceite de girasol ozonizado (AGO) a las 6 semanas de tratamiento.

Fig. 5. Paciente con *tinea corporis* en abdomen tratada con aceite de girasol ozonizado.
Paciente femenina de 11 años, con *tinea corporis*. Directo micológico: Hifas gruesas tortuosas y septadas, cultivo micológico: negativo. Mejoría completa tras aplicar aceite de girasol ozonizado (AGO) a las 6 semanas de tratamiento.

supresión del factor nuclear kappa β (NFκB) que tiene un efecto proinflamatorio, produciendo un estrés oxidativo controlado. La ozonoterapia (O_3T) puede modular la respuesta inmune mediante la supresión de NFκB y la inducción de otros factores de transcripción nuclear, como el factor nuclear de células T activadas (NFAT) y proteína activada-1 (AP-1), así como una mayor modulación de los interferones e interleucinas [14].

Con relación a la acción de aceites vegetales, se ha reportado que, extractos alcohólicos, aceites esenciales y compuestos aislados de los bulbos de ajos (*Allium sativum*), tienen un efecto antimicótico contra algunos géneros de hongos. El aceite de girasol ozonizado, siendo el ozono la unidad alotrópica del oxígeno, constituido por moléculas triatómicas de este elemento, es el responsable de potenciar la actividad antimicrobiana debido a su poder oxidante, mediante acción directa por radicales libres[15].

En el presente estudio, se tomó una población total de 36 pacientes, de los cuales 26 fueron tratados con AGO y 10 con AGNO. Existen pocos estudios publicados a nivel

clínico acerca de la eficacia de este aceite ozonizado a nivel mundial y hasta la fecha, ninguno publicado en Venezuela; la mayoría muestran su eficacia *in vitro*.

En este trabajo se observó que ambos grupos fueron similares en cuanto a su predominio del sexo femenino, promedio de edad 31 a 40 años (35,5 ± 4,5), fototipo cutáneo IV, procedencia Distrito Capital, lo cual ayudó a minimizar los sesgos. Con respecto al grupo etario predominante, concuerda con lo descrito por otros autores [16,17], donde el grupo trabajador comprendido en este rango de edades, es el más afectado por estas micosis. Distrito Capital fue el lugar de mayor procedencia de los pacientes, debido a que el estudio se realizó en Caracas.

Del total de pacientes con comorbilidad asociada, del grupo tratado con aceite de girasol ozonizado, entre ellas: penfigoide ampollar, lupus eritematoso cutáneo crónico, adenocarcinoma faríngeo y una paciente con 30 semanas de gestación, mostraron una curación completa. Se necesitan estudios a posteriori con una muestra poblacional mayor, para demostrar su efectividad en estos pacientes con compromiso del sistema inmunológico.

Sin embargo, algunos informes han indicado el éxito de las aplicaciones tópicas de ozonoterapia (O_3T). En el estudio de Clavo y col. [14], se tomó un grupo de 12 pacientes y se realizaron insuflaciones rectales de O_3 y aplicación tópica de aceite ozonizado, en el manejo de la persistencia de hemorragia rectal inducida por radiación, en pacientes con cáncer de próstata. El aceite ozonizado no penetra a través de las membranas mucosas, pero, en cambio, reacciona para inducir la producción celular de peróxido de hidrógeno, que actúa como segundos mensajeros en la curación de heridas. Al final de este estudio, de los 12 pacientes tratados, se observó mejoría del 100% en 7 pacientes, del 75% en 3 pacientes y del 50% en los otros dos pacientes, mejorando notablemente la calidad de vida de los mismos [14].

Los agentes etiológicos más frecuentemente aislados en los cultivos micológicos, para ambos grupos, fueron el complejo *Trichophyton rubrum* y *Candida albicans*, coincidiendo estos, como los principales agentes causantes de dermatofitosis y estomatitis subprotésica, respectivamente, según diferentes autores [1,17]. El agente etiológico más frecuente según la patología, para el grupo AGO, en *tinea corporis*, fue el complejo *Trichophyton rubrum*; sin embargo, en el 42% de los cultivos no se obtuvo crecimiento, lo que pudo ser consecuencia de que los pacientes tuvieron tratamiento previo y no lo revelaron al momento del interrogatorio. Estos resultados coinciden con la literatura, autores como Tangarife y col. reportan que hasta 40% de los cultivos resultan negativos, del total de casos positivos por examen micológico directo (microscopía) [18].

En estomatitis subprotésica, intertrigo y queilitis, el agente etiológico fue *Candida albicans;* para tinea pedís el complejo *Trichophyton mentagrophytes;* para *tinea cruris,* complejo *Trichophyton rubrum*. Para el grupo AGNO, el agente etiológico más frecuente según la patología fue para *tinea corporis*, *tinea pedís* y *tinea cruris*, complejo *Trichophyton rubrum* y para estomatitis subprotésica, *Candida no albicans*. En ambos grupos estudiados, los agentes etiológicos encontrados son los más comunes para las patologías estudiadas. Estos resultados concuerdan con varios estudios, entre ellos el de Arosemena y col. quienes evaluaron 51 pacientes de la consulta de Micología con *tinea pedis*, de los cuales el 51% consultaron por la *tinea pedis per se* y un 49% por otras dermatomicosis distintas, siendo la *tínea unguis* la más frecuente con 65% [19]. Se observó la forma clínica crónica interdigital como la más frecuente y el agente etiológico comúnmente aislado fue el complejo *Trichophytum rubrum* [19]. Por otro lado, Angulo y col. revisaron 2623 casos de dermatofitosis de los registros del departamento de Micología del Instituto de Biomedicina Caracas, en donde 1363 casos correspondieron al complejo *T.*

rubrum (52%), siendo *tinea unguium, tinea corporis* y *tinea pedis* las patologías más frecuente asociadas [20].

Con respecto a la evolución clínica se observó que en la semana 2, la mayoría de los pacientes presentaron mejoría moderada, 73%, y al transcurrir el tiempo, en la semana 4, se observó la mejoría total en el 23% de los pacientes, que fue aumentando hasta llegar a la semana 8 de mejoría total (61,5%). Estos resultados concuerdan con el ensayo aleatorizado controlado de fase III de Menéndez y col. acerca de la eficacia del aceite de girasol ozonizado (Oleozon®) en 200 pacientes con *tinea pedis*, observando su efectividad cuando fue administrado dos veces al día durante un período de 6 semanas y comparado con ketoconazol [7]. La curación clínica y micológica total se alcanzó en el 75% y 81% de los casos tratados con Oleozon® y ketoconazol, respectivamente, sin diferencias significativas entre los dos grupos y sin reportes de efectos adversos. Los autores de ese estudio consideraron el aceite ozonizado como un medicamento antimicótico eficaz y de bajo costo. Además, evidenciaron los efectos fungicidas del aceite de girasol ozonizado en un porcentaje del 75%, comparables con el del presente trabajo que fue de 61,5% para todas las patologías estudiadas [7].

Al mencionar el grupo de pacientes con micosis superficiales y tratados con aceite de girasol no ozonizado (AGNO), se observó que no hubo mejoría clínica con el mismo, con lo cual se puede demostrar que la ozonización es la que provee la actividad antifúngica, así como lo refiere Travagali y col. quienes mencionan que la reacción del ozono con los ácidos grasos insaturados, que componen los triglicéridos presentes en los aceites y grasas vegetales, se forma toda una gama de productos oxigenados (hidroperóxidos, ozónidos, diperóxidos, peróxidos y poliperóxidos) que son los responsables de la amplia actividad biológica de estos aceites vegetales ozonizados [21].

En cuanto a la mejoría de los pacientes según el agente etiológico, tratado con AGO a la semana 8 de tratamiento, se demostró que para *Candida albicans* hubo una mejoría total del 86% y sólo el 14% restante con mejoría moderada, lo cual significa que este agente es sensible al tratamiento, encontrando similitud con lo descrito por Kumar y col. [22] en el ensayo clínico donde evaluaron la eficacia del aceite de oliva ozonizado en el manejo de lesiones y condiciones bucales aplicado dos veces al día, con masaje con torunda o guante durante 1 min sobre la lesión, todos los pacientes con candidiasis oral y queilitis angular mostraron curación total.

Por otro lado, Ouf y col. [23], estudiaron el efecto del ozono y aceite ozonizado en la esporulación, pérdida de micelio, manano, nutrientes y la actividad de las enzimas hidrolíticas de cinco dermatofitos diferentes. Se encontró que el aceite ozonizado era más eficaz que el ozono gaseoso. Los agentes más susceptibles fueron *Nannizzia gypsea* y *Microsporum canis* (la CMI fue de de 4 μg/mL para ambos hongos en el caso del ozono aplicado como gas y fue de 0,5 y 0,25 μg/mL para los mismos ítems en el caso de aceite ozonizado); mientras que *Trichophyton interdigitale* y *Trichophyton mentagrophytes* fueron relativamente resistentes (la CMI fue 16 μg/mL en el caso del ozono gaseoso y 2,0 μg/mL para el aceite ozonizado en el caso de ambos hongos) [23].

El estudio reveló una disminución constante en la producción de esporas de *Nannizzia gypsea* y *Microsporum canis* en la aplicación de aceite ozonizado. El hecho de que los dermatofitos sean más resistentes en su pared celular y en su producción de esporas que *Candida* spp, puede ser la razón por la cual el tratamiento no sea tan efectivo en estos [23,24].

En el presente estudio solo el 60% de los pacientes positivos para el complejo *Trichophyton rubrum* presentaron mejoría completa y dos pacientes con el complejo *Trichophyton mentagrophytes* y *Microsporum canis* mejoraron totalmente. Weitzman y col

reportaron que la resistencia del complejo *T. rubrum* a la erradicación está relacionada con su pared celular, esta barrera protectora contiene manano, que puede inhibir la inmunidad mediada por células, obstaculizar la proliferación de queratinocitos y mejorar la resistencia del organismo a las defensas naturales de la piel [25]. Por otro lado, Geweely y col. en su estudio *in vitro* sobre la actividad antifúngica del aceite de oliva ozonizado (oleozon®) demostró la actividad antimicrobiana contra todas las especies de dermatofitos y no dermatofitos analizados, con una CMI que van desde 0,53 a 2,0 mg/mL [26].

En nuestro trabajo, se observó que la mejoría clínica, de acuerdo al agente etiológico por semanas de tratamiento, fue con *Candida* spp siendo las más rápidas en responder al tratamiento. Los pacientes mostraron mejoría total en la semana 4, comparado con los dermatofitos, en donde se observó una mejoría total a partir de la semana 6. En cuanto a la evaluación del control de sensibilidad al producto, representado por 10 individuos sanos, a los cuales se les aplicó aceite de girasol ozonizado, ninguno de ellos presentó reacción adversa al mismo, al igual que ninguno de los 36 pacientes con micosis superficial, tal como han reportado otros autores tales como Menedez y col. en pacientes con onicomicosis [27].

Se observó recidiva de las lesiones en 34% de los pacientes tratados con AGO luego de los 6 meses de culminado el tratamiento y los agentes etiológicos involucrados fueron los dermatofitos y ninguna especie del género *Candida*. Las patologías por estomatitis subprotésica y queilitis causadas por la especie *Candida* no recidivaron durante este lapso de tiempo. Esto coincide con los estudios de Menéndez y col., donde a los 6 meses posterior al uso del tratamiento recidivaron pacientes con *tinea pedis* [7], y el de Kumar y col. donde pacientes con estomatitis subprotésica y queilitis ocasionadas por el género *Candida*, no recidivaron [22].

Este es el primer estudio preliminar que se realiza en Venezuela utilizando aceites ozonizados en pacientes, destacándose que el aceite de girasol ozonizado (AGO) fue efectivo para el género *Candida* y con resultados poco satisfactorios para los dermatofitos según la muestra estudiada. Se recomienda, realizar un ensayo clínico con un mayor número de pacientes para corroborar la eficacia de los aceites ozonizados en micosis superficiales no extensas.

Conflicto de intereses

Los autores declaran no tener conflictos de intereses.

Financiamiento

El trabajo no recibió financiamiento externo.

Número ORCID de autores

- Natalia Soucre (NS): 0009-0004-0808-7507
- Verónica Bracho (VB): 0009-0005-6157-2832
- Primavera Alvarado (PA): 0000-0002-5965-6827
- Elsy Cavallera (EC): 0009-00083040-6622

Participación de autores

NS y EC: Participaron en ensayos clínicos, y escritura de manuscrito. VB: Participo en ensayos clínicos, elaboro la parte estadística. PA: Diseño de metodología, ensayos clínicos, escritura de manuscrito.

REFERENCIAS

1. **Gupta C, Das S, Gaurav V, Singh P.K, Rai G, Datt S, Tigga R.A, Pandhi D, Bhattacharya S, Ansari M.A, Dar S.A.** Review on host-pathogen interaction in dermatophyte infections. J Mycol Med

2023; 33(1):101331. *doi: 10.1016/j.mycmed.2022.101331.*

2. **Chiacchio N, Madeira C, Humaire C, Silva C.S, Gomes Fernandes L, Dos Reis A.** Superficial mycoses at the Hospital do Servidor Público Municipal de São Paulo between 2005 and 2011. An Bras Dermatol 2014; 89:67-71. *doi: 10.1590/abd1806-4841.20141783.*
3. **Havlickova Blanka, Czaika Viktor, Friedrich Markus.** Epidemiological trends in skin mycoses worldwide. Mycoses 2008;51 Suppl 4:2-15. *doi: 10.1111/j.1439-0507. 2008.01606. x.*
4. **Das Saibal, Bandyopadhyay Sanjib, Sawant Sanket Chaudhuri S.** The epidemiological and mycological profile of superficial mycoses in India from 2015 to 2021: A systematic review. Indian J Public Health 2023;67(1):123-135. *doi: 10.4103/ijph.ijph_987_22.*
5. **Sharma Bharti, Nonzom Skarma.** Superficial mycoses, a matter of concern: Global and Indian scenario-an updated analysis. Mycoses 2021; 64(8):890-908. *doi: 10.1111/myc.13264.*
6. **Schwartz A, Kontorchnikova C, Malesnikov O, Martínez -Sánchez G.** Guía para el uso médico del ozono: fundamentos terapéuticos e indicaciones. Vol 1. 1ra ed. Madrid: Asociación Española de Profesionales Médicos en Ozonoterapia. AEPROMO; 2011.
7. **Menéndez S, Falcón L, Simón D, Landa N.** Efficacy of ozonized sunflower oil in the treatment of tinea pedis. Mycoses 2002; 45(8):329-332. *doi: 10.1046/j.1439-0507.2002.00780.x.*
8. **Tartari AP, Moreira FF, Pereira MC, Carraro E, Cidral-Filho FJ , Inoue Salgado A, Ilvan Kerppers I.** Anti-inflammatory effect of ozone therapy in an experimental model of rheumatoid arthritis. Inflammation 2020; 43:985–993. *doi: 10.1007/s10753-020-01184-2.*
9. **Rodríguez ZB, Álvarez RG, Guanche D, Merino N, Hernández Rosales F, Menéndez Cepero S, González Y, Schulz S.** Antioxidant mechanism is involved in the gastroprotective effects of ozonized sunflower oil in ethanol-induced ulcers in rats. Mediators Inflamm 2007; 2007:65873. *doi: 10.1155/2007/65873.*
10. **Urbano Machado A, Vidor Contri R.** Effectiveness and safety of ozone therapy for dermatological disorders: a literature review of clinical trials. Indian J Dermatol. 2022; 67(4): 479. *doi: 10.4103/ijd.ijd_152_22.*
11. **Camacaro L, De Arbeloa M, Fernández A, Cavallera E, Alvarado P.** PCR multiplex en la detección de *Tinea unguium* en pacientes de Caracas –Venezuela. Invest Clin 2019; 60 (2): 160-170. *doi.org/10.22209/IC.v60n2a05.*
12. **Bocci V. Ozone.** A New Medical Drug. 2da ed. Italia: Springer editors; 2011. p.227-237.
13. **Güner M, Görgülü T, Olgun A, Torun M, Kargi E.** Effects of ozone gas on skin flaps viability in rats: an experimental study. J Plast Surg Hand Surg 2016; 50:291-297. *doi: 10.3109/2000656X.2016.1170024.*
14. **Clavo B, Santana-Rodriguez N, Llontop P, Gutiérrez D, Ceballos D, Charlin Méndez C, Rovira G, Suarez G, Rey-Baltar D, García L, Martínez-Sánchez G, Fiuza D.** Ozone therapy in the management of persistent radiation-induced rectal bleeding in prostate cancer patients. J Evid Based Complementary Altern Med 2015; 2015:1-7. *doi: 10.1155/2015/480369.*
15. **Sechi LA, Lezcano I, Nunez N, Espim M, Duprè I, Pinna A, Molicotti P, Fadda G, Zanetti S.** Antibacterial activity of ozonized sunflower oil (Oleozon) J Appl Microbiol 2001;90(2):279-284. *doi: 10.1046/j.1365-2672.2001.01235. x.*
16. **Arenas R, Bonifaz A, Padilla M, Arce M, Atoche C, Barba J, Campos P, Fernández R, Mayorga J, Nazar D, Ocampo J.** Onychomycosis. A Mexican survey Eur J Dermatol 2010;20(5):611-4. *doi: 10.1684/ejd.2010.1023.*
17. **Weitzman I, Summerbell R.** The dermatophytes. Clin Microbiol Rev 1995; 8:240–259. *doi: 10.1128/CMR.8.2.240.*
18. **Tangarife C, Verónica J, Flórez M, Sindy V, Mesa Arango, Ana C.** Diagnóstico micológico: de los métodos convencionales a

los moleculares. Med Lab 2015; 21: 211-242. *doi.org/10.36384/issn.0123-2576.*

19. **Arosemena R, Halmai O, González M.** Estudio prospectivo de pacientes con *tinea pedis* de la consulta de micología durante el segundo trimestre de 1989. Dermat Venez 1990; 28:65-67.
20. **Angulo A, Bravo N, Falco A, Pulido A, Rivera Z, Cavallera E.** Dermatofitosis por *Trichophyton rubrum.* Experiencia de 10 años en el Departamento de Micología del Instituto de Biomedicina. Dermat Venez 2008; 46:12-17.
21. **Travagli V, Zanardi I, Valacchi G, Bocci V.** Ozone and ozonated oils in skin diseases: a review. Hind Publish Corp. Med Inflam 2010; 2010:1-9. *doi: 10.1155/2010/610418.*
22. **Kumar T, Arora N, Puri G, Aravinda K, Dixit A, Jatti D.** Efficacy of ozonized olive oil in the management of oral lesions and conditions: A clinical trial. Contemp Clin Dent 2016; 7:51-54. *doi: 10.4103/0976-237X.177097.*
23. **Ouf S, Moussa T, Abd-Elmegeed A, Eltahlawy S.** Anti-fungal potential of ozone against some dermatophytes. Braz J Microbiol 2016; 47: 697-702. *doi: 10.1016/j.bjm.2016.04.014.*
24. **Thomson P, Anticevic S, Rodríguez H, Silva V.** Actividad antifúngica y perfil de seguridad del producto natural derivado del aceite de maravilla ozonizado (AMO3) en dermatofitos. Rev Chil Infect 2011; 28:512-519.
25. **Weitzman I, Summerbell R.** The dermatophytes. Clin Microbiol Rev 1995; 8:240–259. *doi: 10.1128/CMR.8.2.240.*
26. **Geweely N.** Antifungal activity of ozonized olive oil (Oleozone). Int J Agri Biol 2006;8: 671-678. *doi: 1560–8530/2006/08–5–670–675.*
27. **Menéndez S, Falcón L, Maqueira Y.** Therapeutic efficacy of topical OLEOZON® in patients suffering from onychomycosis. Mycoses 2011;54(5):e272-7. *doi: 10.1111/j.1439-0507.2010. 01898.x*

Invest Clin 65(3): 308 - 320, 2024 https://doi.org/10.54817/IC.v65n3a04

Elevated CA125 values predict adverse outcomes in acute heart failure.

Ji Zhang[1], Wenhua Li[1], Jie Hui[2] and Jianqiang Xiao[1]

[1]Department of Cardiology, Wujin Hospital Affiliated with Jiangsu University, the Wujin Clinical College of Xuzhou Medical University, Changzhou City, Jiangsu Province, China.

[2]Department of Cardiology, The First Affiliated Hospital of Soochow University, Suzhou, China.

Keywords: carbohydrate antigen 125; risk prediction; N-terminal pro-B-type natriuretic peptide; acute heart failure.

Abstract. In acute heart failure (AHF), elevated carbohydrate antigen 125 (CA125) and N-terminal pro-B-type natriuretic peptide (NTproBNP) have been shown to correlate with adverse events. We sought to quantify their prognostic usefulness in predicting the six-month combined death/heart failure readmission endpoint. The study included 352 patients admitted for AHF. The primary endpoint was the six-month combined endpoint of death/AHF rehospitalization. CA125 and NTproBNP were dichotomized according to the best cut-offs to predict the six-month primary endpoint. The independent association of CA125 and NTproBNP with the primary endpoint was assessed by multivariate Cox regression analysis, and their incremental prognostic utility was evaluated by net reclassification improvement (NRI) and integrated discrimination improvement (IDI) index. Forty-seven (13.4%) deaths and 113 (32.1%) AHF rehospitalizations were identified at the six-month follow-up. The subjects with CA125≥39.7 U/mL and NTproBNP≥3900 pg/mL had significantly higher cumulative event rates (56.1% vs. 33.3% and 53.3% vs. 33.8%, both $p<0.001$). Elevated CA125 (HR 1.93; 95% CI [1.32-2.83]; $p=0.001$) was associated with a higher HR (hazard ratio) than NTproBNP≥3900 pg/mL (HR 1.71; 95% CI [1.19-2.48]; $p=0.004$) after adjusting for established risk factors. Elevated CA125 still independently predicted adverse events when CA125 and NTproBNP entered the same multivariate model. Furthermore, risk reclassification analyses demonstrated significant improvements in NRI of 22.3% ($p=0.014$) and IDI of 2.7% ($p=0.012$) when adding CA125 to the base model + NTproBNP. Elevated CA125 and NTproBNP predicted adverse outcomes in AHF patients. CA125 added prognostic value to NTproBNP; thus, their combination conferred greater predictive capacity.

Corresponding author: Ji Zhang, Department of Cardiology, Wujin Hospital Affiliated with Jiangsu University, the Wujin Clinical College of Xuzhou Medical University, No. 2, Changzhou City, Jiangsu Province, China. Telephone number: +86 519 8557 9192. E-mail: js_zhangji@126.com

Valores elevados de CA125 predicen resultados adversos en la insuficiencia cardíaca aguda.

Invest Clin 2024; 65 (3): 308 – 320

Palabras clave: antígeno carbohidrato 125; predicción del riesgo; péptido natriurético tipo pro-B N-terminal; insuficiencia cardíaca aguda.

Resumen. En la insuficiencia cardíaca aguda, se ha demostrado que el antígeno de carbohidratos 125 (CA125) elevado y el péptido natriurético tipo B N-terminal (NTproBNP) se correlacionan con eventos adversos. Intentamos cuantificar su utilidad pronóstica al predecir el punto final combinado de 6 meses de readmisión por muerte/insuficiencia cardíaca. El estudio incluyó a 352 pacientes ingresados por insuficiencia cardíaca aguda. El punto final principal fue el punto final combinado de 6 meses de muerte/rehospitalización aguda. CA125 y NTPROBNP se dicotomizaron de acuerdo con los mejores límites para predecir el punto final primario de 6 meses. La asociación independiente de CA125 y NTPROBNP con el punto final primario se evaluó mediante análisis multivariado de regresión de Cox, y su utilidad pronóstica incremental se evaluó mediante la mejora de la reclasificación neta (NRI) y el índice de mejora de la discriminación integrada (IDI). En el seguimiento a los 6 meses se identificaron un total de 47 (13,4%) muertes y 113 (32,1%) rehospitalizaciones por insuficiencia cardíaca aguda. Los sujetos con CA125≥39,7 U/mL y NTproBNP≥3900 pg/mL presentaron tasas de acontecimientos acumulativos significativamente más altas (56,1% frente a 33,3% y 53,3% frente a 33,8%, p<0,001 en ambos casos). CA125 elevado (HR: 1,93; IC del 95% [1,32-2,83]; p = 0,001) se asoció con un HR superior al NTproBNP ≥3900 pg/mL (HR 1,71; IC del 95% [1,19-2,48]; p = 0,004) después del ajuste por los factores de riesgo establecidos. CA125 elevado aún predijo de forma independiente los acontecimientos adversos cuando tanto CA125 como NTproBNP se introdujeron juntos en el mismo modelo multivariante. Además, los análisis de reclasificación del riesgo demostraron mejoras significativas en el NRI del 22,3% (p = 0,014) y en el IDI del 2,7% (p = 0,012) al añadir CA125 al modelo base + NTproBNP. Los niveles elevados de CA125 y NTproBNP predijeron los resultados adversos en los pacientes con insuficiencia cardíaca aguda. CA125 añadió valor pronóstico al NTproBNP y, por lo tanto, su combinación confirió una mayor capacidad predictiva.

Received: 30-10-2023 Accepted: 18-06-2024

INTRODUCTION

Given the variations in clinical presentation and the impact of comorbidities in acute heart failure (AHF) patients, risk prediction remains challenging. Identifying high-risk subjects will help in further management by optimizing diuretic therapy, increasing the frequency of monitoring visits, and other therapeutic measures.

Published studies indicate that high levels of several biomarkers [1], including natriuretic peptides [2,3], sST-2 [4-6], cardiac troponins [7,8], and carbohydrate antigen 125 (CA125) [9,10], correlate with AHF severity and adverse outcomes. Based on different patho-

physiological pathways involving heart failure progression and response patterns for modification over time, we speculate that integrating multiple biomarkers will improve prognostic power in subjects admitted for AHF. As a widely used biomarker for monitoring ovarian cancer [11], CA125 has been studied in heart disease patients [10,12-14] and especially in heart failure [10,12,15], emerging as a surrogate for fluid overload and/or cytokine production in AHF [16].

Our study was performed to evaluate the prognostic utility of CA125 in predicting the six-month combined endpoint of death/AHF rehospitalization among AHF patients.

METHODS

Study population and design

This prospective, observational cohort study from a single centre included 352 patients consecutively admitted to the cardiology ward from December 2019 to September 2020 due to AHF following current guidelines [17,18]. AHF was the primary diagnosis of hospitalization for our study. Patients with a diagnosis of severe hepatic disease, sepsis, ongoing dialysis treatment for end-stage renal disease, pulmonary embolism, or acute rheumatic and autoimmune diseases were excluded by design. Demographic information, vital signs, medications, and medical history were collected, along with standard echocardiographic evaluation, laboratory results and 12-lead electrocardiogram during index admission. Intravenous furosemide or torasemide was used in all patients at least 24 h after admission. 11.4% and 4.5% of the patients received intravenous treatment with vasodilators and vasopressors, respectively. The established treatment guidelines were followed [17-19]. Time to death/AHF readmission, whichever occurred first, was the primary endpoint at the six-month follow-up.

Subjects were followed up through outpatient service or by telephone. Three patients were lost to follow-up during the study period. Patients were censored free of events or lost to follow-up at last contact within this period or at six months. The local ethics committee approved this study, and all patients provided informed consent for their participation following the Declaration of Helsinki.

Biomarker measurement

CA125 serum levels were obtained between 5:30 and 8:00 h on the second day of admission. In contrast, N-terminal pro-B-type natriuretic peptide (NTproBNP) serum levels were immediately determined after admission using commercially available immunoassay kits (Elecsys CA125 II assay, Roche Diagnostics and Vitros Immunodiagnostic Products NT-proBNP Reagent Pack, Ortho-Clinical Diagnostics, respectively). A technician blinded to the clinical information performed the biomarker assay.

Statistical analysis

Categorical variables are presented as frequencies and percentages, and continuous variables are summarized as the mean ± standard deviation or median (interquartile range). We dichotomized both biomarkers according to the best predictive cut-offs and compared between-group baseline characteristics using the t-test, Mann–Whitney test, chi-square or Fisher exact test, as appropriate. The resulting cut-off values were 39.7 U/mL for CA125 and 3900 pg/mL for NTproBNP. The cumulative rate of events (death or AHF readmission) among CA125 or NTproBNP categories was estimated and compared using the Kaplan–Meier method and log-rank test. Univariate and multivariate Cox analyses determined the relationship of CA125 and NTproBNP with the primary endpoint. Candidate variables in the initial multivariate model included clinical characteristics such as age, sex, weight, history of atrial fibrillation, diabetes, hypertension and acute myocardial infarction on admission. The biochemical variables included were serum creatinine, blood hemoglobin, and serum sodium. We also included left ventricular ejection fraction (LVEF>50% [reference], 36%-50%, and ≤35%), admission heart rate, admission

systolic blood pressure, evidence of pleural effusion, peripheral oedema, and AHF category (worsening heart failure [WHF] or new-onset heart failure) in our analyses. For multivariate Cox regression analyses, we retained factors with $p<0.15$ in univariate Cox analysis and those clinically relevant. Given the number of events available, the included variables were carefully chosen, and a parsimonious multivariate Cox model was derived. CA125, NTproBNP, or both biomarkers were first entered individually in the multivariate model. The Schoenfeld residuals were used to test the assumption of proportional hazards over time.

Harrell's C-statistics measured the discriminative ability of the models. The incremental prognostic utility of CA125 for NTproBNP and baseline variables was evaluated using integrated discrimination improvement (IDI) and net reclassification improvement (NRI) with the corresponding P values. We performed two multiple linear analyses to examine the relations of log-transformed CA125 and NTproBNP to clinical variables.

A 2-sided p value of <0.05 was considered statistically significant in all analyses. The principal analysis was performed using SPSS 26.0. Risk reclassification was calculated in R 4.0.3.

RESULTS

Baseline characteristics

Of 352 subjects, 49.4% had LVEF>50%. Heart failure with preserved ejection fraction predominated in our population, with only 17.0% and 21.2% exhibiting LVEF≤35% for patients with CA125<39.7 U/mL and patients with CA125≥39.7 U/ mL, respectively. The sample consisted of 46.9% females, and the mean age was 76±11 years. The median baseline levels of CA125 and NTproBNP in the entire population were 43.2 U/mL (21.6-102.7) and 5170 pg/mL (2748-10000), respectively. The baseline characteristics of the study participants by CA125 categories are shown in Tables 1, 2 and 3. Patients with elevated CA125 (CA125≥39.7 U/mL) exhibited a worse clinical profile. Lower LVEF and pleural effusion were more prevalent when CA125 was elevated. Subjects with CA125 ≥39.7 U/mL had a higher proportion of treatment with digitalis at discharge and a lower proportion with sodium-glucose cotransporter 2 inhibitor. Lower LVEF, pleural effusion, peripheral edema and paroxysmal nocturnal dyspnea were more prevalent when CA125 was elevated. No differences were detected in the presence of orthopnea and moist rales in lung fields.

Clinical predictors of CA125 and NTproBNP

Table 4 lists those variables independently correlated with log-transformed CA125 and NTproBNP. We identified different clinical predictors of these two biomarkers in the AHF setting. For lnCA125, the most important predictors were pleural effusion and WHF (standardized β coefficients 0.392 and 0.231, respectively). The most important predictors of lnNTproBNP were serum creatinine, weight and LVEF (standardized β coefficients 0.382, -0.306 and -0.286, respectively).

Moreover, we found differential associations of CA125 and NTproBNP with clinical presentations of AHF. A presentation as WHF was associated with higher CA125 levels; conversely, admission for new-onset heart failure was independently and positively related to NTproBNP values.

CA125 levels, NTproBNP levels, and the primary endpoint

In total, 47 patients (13.4%) died (12 deaths occurred during the index admission and 35 post-discharge), and 113 (32.1%) AHF rehospitalizations were identified at the six-month follow-up. CA125 and NTproBNP values in subjects experiencing death/AHF rehospitalization were significantly higher when compared with those free of events (56.3 U/mL [27.2-135.6] vs. 33.9 U/mL [18.4-79.8] and 6255 pg/mL [3425-6255] vs. 4085 pg/mL [2390-8015], respectively, $p<0.001$ for both).

Table 1
Demographic and medical characteristics stratified by CA125 categories.

	CA125<39.7U/mL (n=159)	CA125≥39.7U/mL (n=193)	*p*
Age, years	77±9	75±12	0.085
Female, n (%)	83 (52.2)	82 (42.5)	0.069
Weight, kg	60.4±12.3	59.4±12.1	0.425
Hypertension, n (%)	108 (67.9)	112 (58.0)	0.056
Diabetes mellitus, n (%)	44 (27.7)	55 (28.5)	0.864
Atrial fibrillation, n (%)	76 (47.8)	107 (55.4)	0.153
Previous coronary artery disease, n (%)	38 (23.9)	33 (17.1)	0.114
Previous myocardial infarction, n (%)	19 (11.9)	15 (7.8)	0.187
Acute myocardial infarction, n (%)	25 (15.7)	11 (5.7)	0.002
Previous PCI, n (%)	15 (9.4)	9 (4.7)	0.077
Valvular heart disease, n (%)	17 (10.7)	24 (12.4)	0.612
WHF, n (%)	131 (82.4)	182 (94.3)	<0.001
Previous pacemaker, n (%)	4 (2.5)	5 (2.6)	1.000
Anemia, n (%)	43 (27.0)	51 (26.4)	0.896
Previous stroke, n (%)	17 (10.7)	22 (11.4)	0.833
COPD, n (%)	35 (22.0)	45 (23.3)	0.771
Previous malignancy, n (%)	2 (1.3)	12 (6.2)	0.018
Pleural effusion, n (%)	59 (37.1)	140 (72.5)	<0.001
Peripheral oedema, n (%)	38 (23.9)	96 (49.7)	<0.001

CA125, carbohydrate antigen 125; PCI, percutaneous coronary intervention; WHF, worsening heart failure; COPD, chronic obstructive pulmonary disease. Anemia, defined as a hemoglobin level <120g/L in men and <110g/L in women.

By the Kaplan–Meier method, subjects with CA125≥39.7 U/mL and NTproBNP≥3900 pg/mL exhibited significantly higher cumulative event rates (56.1% vs. 33.3% and 53.3% vs. 33.8%, both p<0.001, Fig. 1A, B). When combined (Fig. 1C), patients with both biomarkers elevated had the highest cumulative event rate (61.5%); intermediate when only one of them was elevated: 44.2% for those with only CA125 elevated and 40.5% for subjects with only NTproBNP elevated, respectively, and lower (25.3%) for patients with values below the chosen biomarker cutpoints, p trend <0.001.

Table 5 displays the results of univariate and multivariate modelling. In the multivariate Cox analysis, elevated CA125 (HR 1.93; 95% CI [1.32-2.83]; p=0.001) was associated with a higher adjusted HR than NTproBNP≥3900 pm/mL (HR 1.71; 95% CI [1.19-2.48]; p=0.004). Elevated CA125 still independently predicted adverse events when CA125 and NTproBNP entered in the same multivariate model. In the final Cox model, serum creatinine and NTproBNP≥3900 pm/mL were other independent predictors. No interactions were found when these two biomarkers were included in the final Cox model (p=0.508).

We compared the performance of each regression model by using Harrell's C-statistic as a discrimination measure. Compared with the model including NTproBNP alone (0.623), CA125 alone (0.635) or none (0.606), the Cox model including CA125 and NTproBNP had a higher C-statistic (0.648).

Table 2
Vital signs, laboratory and echocardiography data stratified by CA125 categories.

	CA125<39.7U/mL (n=159)	CA125≥39.7U/mL (n=193)	*p*
Heart rate, b.p.m.	87±22	93±24	0.033
Systolic blood pressure, mmHg	136±24	135±23	0.564
Diastolic blood pressure, mmHg	80±16	83±15	0.150
Haemoglobin, g/L	123.6±24.0	126.3±25.6	0.314
Serum creatinine, umol/L	86 (69–117)	83 (66–114)	0.340
Sodium, mmol/L	140.1±5.3	139.0±5.3	0.057
NTproBNP, pg/mL	4200 (2510–7940)	5990 (3245–11400)	0.002
CA125, U/mL	21 (13-27)	91 (56-173)	<0.001
LVEF, %	50±13	47±13	0.020
LVEF ≤ 35%, n (%)	27 (17.0)	41 (21.2)	0.313
LVEF ≤ 50%, n (%)	43 (27.0)	67 (34.7)	0.122
LVDD, mm	53±9	53±10	0.802
LVSD, mm	39±10	40±11	0.317
LAD, mm	46±8	48±9	0.035

CA125, carbohydrate antigen 125; NTproBNP, N-terminal pro-B-type natriuretic peptide; LVEF, left ventricular ejection fraction; LVDD, left ventricular diastolic diameter; LVSD, left ventricular systolic diameter; LAD, left atrial diameter.

Table 3
Medical treatment stratified by CA125 categories

	CA125<39.7U/mL	CA125≥39.7U/mL	*p*
Intravenous administration of vasopresors , n (%)	8(5.0)	8(4.1)	0.691
Intravenous administration of vasodilators, n (%)	21(13.2)	19(9.8)	0.322
Medication before admission			
Loop diuretic, n (%)	61(38.4)	64(33.2)	0.310
Spironolactone, n (%)	55(34.6)	60(31.1)	0.486
ACEI/ARB/ARNI, n (%)	48(30.2)	50(25.9)	0.372
Beta-blocker, n (%)	46(28.9)	48(24.9)	0.391
Digitalis, n (%)	17(10.7)	25(13.0)	0.515
SGLT2 inhibitor, n (%)	20(12.6)	17(8.8)	0.251
Medication at discharge (340 cases discharged after improvement)			
Loop diuretic, n (%)	138(89.0)	172(93.0)	0.202
Spironolactone, n (%)	122(78.7)	159(85.9)	0.079
ACEI/ARB/ARNI, n (%)	105(67.7)	112(60.5)	0.169
Beta-blocker, n (%)	106(68.4)	130(70.3)	0.649
Digitalis, n (%)	30(19.4)	56(30.3)	0.021
SGLT2 inhibitor, n (%)	61(39.4)	47(25.4)	0.006

CA125, carbohydrate antigen 125; ACEI, angiotensin converting enzyme inhibitors; ARB, angiotensin receptor blockers; ARNI, angiotensin receptor neprilysin inhibitor; SGLT2, sodium-glucose co-transporter 2.

Table 4
Clinical predictors of lnCA125 and lnNTproBNP.

	Standardized β regression coefficient	*p*
Ln (CA125)		
Pleural effusion, n (%)	0.392	<0.001
WHF, n (%)	0.231	<0.001
Peripheral oedema, n (%)	0.173	<0.001
Weight, kg	-0.154	0.002
Age, years	-0.151	0.003
LVEF, %	-0.132	0.006
Sodium, mmol/L	-0.106	0.018
Ln (NTproBNP)		
Serum creatinine, umol/L	0.382	<0.001
Weight, kg	-0.306	<0.001
LVEF, %	-0.286	<0.001
Pleural effusion, n (%)	0.154	<0.001
WHF, n (%)	-0.141	0.001
LVDD, n (%)	0.139	0.019

Ln(CA125), antigen carbohydrate 125 natural logarithm; Ln(NTproBNP), N-terminal pro–B-type natriuretic peptide natural logarithm; WHF, worsening heart failure; LVEF, left ventricular ejection fraction; LVDD, left ventricular diastolic diameter.

IDI and NRI values were significantly higher when adding each biomarker or both to the baseline variables model. Furthermore, a significant improvement in NRI of 22.3% (p=0.014) and IDI of 2.7% (p=0.012) was observed when adding CA125 to the base model + NTproBNP, supporting the incremental prognostic effect on top of NT-proBNP (Table 6).

DISCUSSION

Our study compared the risk prediction capacity of NTproBNP and CA125 in the setting of AHF. After multivariate adjustment, the elevation of CA125 and NTproBNP had a positive prognostic effect on adverse events. Not only elevated NTproBNP but also CA125 remained independent predictors of poor outcomes by combining both biomarkers. Additionally, adding CA125 to the model, including NTproBNP, significantly improved the predictive power.

Congestion, as a strong predictor of heart failure-related readmission and death [20], is responsible for most heart failure decompensation and is an essential therapeutic target in AHF [17,18]; however, evaluation of congestion remains a challenge in the routine management of AHF [21]. Perhaps due to the limited accuracy of signs and symptoms for quantifying fluid overload severity [22,23], signs of congestion (peripheral edema, pleural effusion, and other signs) are not routinely used for risk stratification. Suitable biomarkers would optimize risk prediction. CA125 levels correlate well with signs of fluid congestion[9,10,16] and pulmonary artery wedge pressure [10,16]. In this study, the most important clinical predictor of serum CA125 levels was the presence of pleural effusion. As a marker of congestion, CA125 is related to adverse events in heart failure patients [9,10] and indicates heart failure severity. However, in the BIOSTAT-CHF study, CA125 levels were highly predictive of adverse outcomes, beyond and independently of surrogates of congestion [9]. We also confirmed the predictive value of CA125 in stage D heart failure independently of pleural effusion or ascites. Therefore, we think CA125 could provide added prognostic value over surrogates of congestion [24]. Elevated CA125 is an independent predictor with incremental prognostic value over traditional prognosticators and natriuretic peptides [9], and thus, combining both biomarkers improved risk stratification in AHF [10].

Interestingly, although CA125 has been shown to be a potential tool for treatment guidance in AHF [12,25], little support is available regarding the benefits of NP-guided therapy over usual care [26]. In the CHANCE-HF trial, compared to the standard of care, a CA125-guided therapy characterized by a higher frequency of furosemide equivalent dose adjustments and ambulatory intravenous furosemide administrations according to CA125 response and clinical

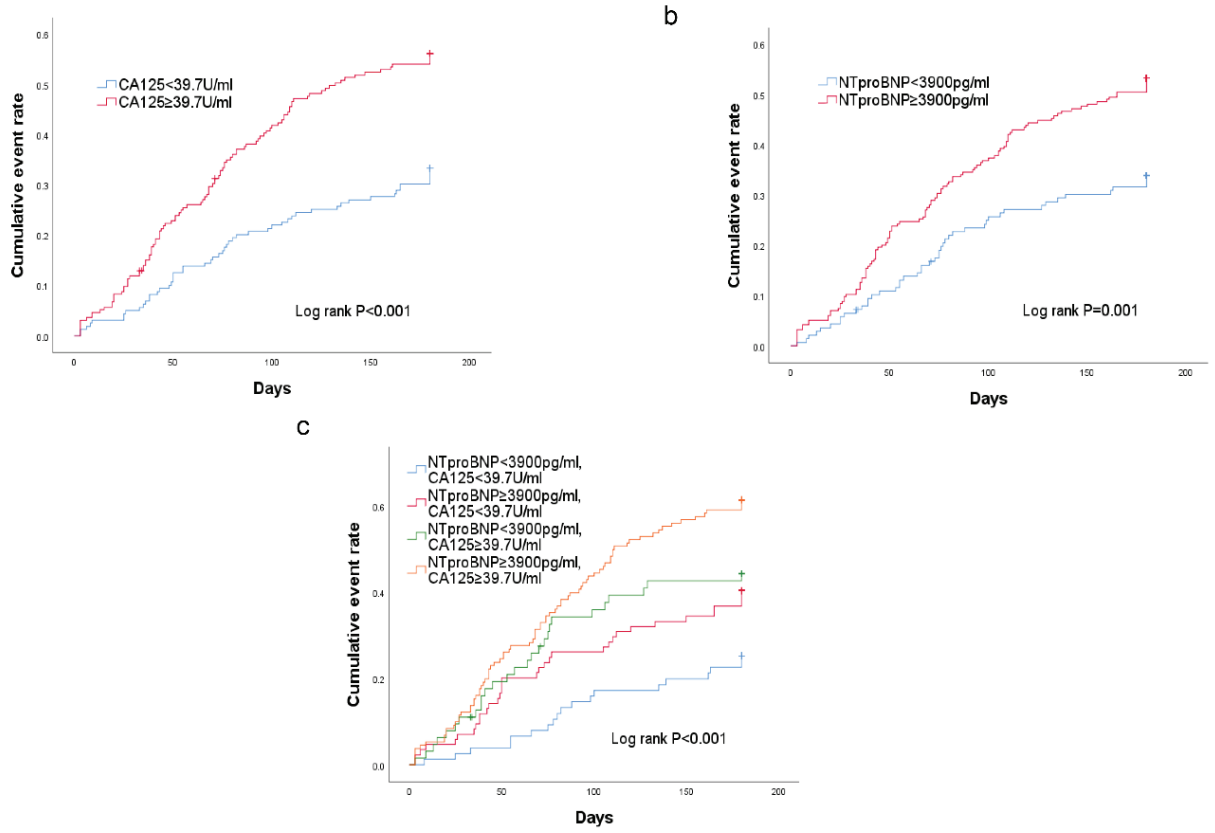

Fig. 1. Kaplan–Meier estimates for the six-month combined endpoint of death/AHF rehospitalization stratified by CA125 (A), NTproBNP (B) and the combination of CA125 and NTproBNP (C). AHF: acute heart failure.

Table 5

CA125 and NTproBNP hazard ratios for 6-month combined endpoint of death/AHF readmission.

Variables	Univariate		Multivariate	
	HR (95% CI)	*p*-value	HR (95% CI)	*p*-value
Age, /10 years increase	1.10 (0.96-1.29)	0.167	1.06 (0.90-1.24)	0.457
Atrial fibrillation, n (%)	1.38 (1.01-1.89)	0.046	1.21 (0.85-1.71)	0.291
Serum creatinine, /SD increase	1.20 (1.00-1.01)	0.004	1.20 (1.04-1.38)	0.014
LVEF≤35%, n (%)	0.76 (0.48-1.21)	0.251	0.75 (0.45-1.27)	0.285
LVEF≤50%, n (%)	1.37 (0.98-1.92)	0.069	1.30 (0.92-1.86)	0.142
Systolic blood pressure, /10 mmHg increase	0.93(0.87-1.00)	0.042	0.96(0.90-1.03)	0.222
Sodium, /SD increase	0.90 (0.79-1.03)	0.112	0.92 (0.79-1.06)	0.243
WHF, n (%)	1.39 (0.80-2.40)	0.244	1.15 (0.63-2.08)	0.647
Pleural effusion, n (%)	1.32 (0.96-1.82)	0.086	0.99 (0.69-1.42)	0.955
Peripheral oedema, n (%)	1.40 (1.04-1.91)	0.034	1.14 (0.82-1.60)	0.430
CA125≥39.7U/mL, n (%)	2.00 (1.44-2.79)	<0.001	1.78 (1.22-2.61)	0.003
NTproBNP≥3900pg/mL, n (%)	1.78 (1.26-2.50)	0.001	1.57 (1.08-2.27)	0.018

HR from Cox regression analysis. Multivariate HR from the model containing CA125 + NTproBNP + baseline variables. HR, hazard ratio; CI, confidence intervals; SD, standard deviation.

Table 6
Reclassification results for 6-month combined endpoint of death/AHF rehospitalization.

	NRI (%) (*p*-value)	IDI (%) (*p*-value)
Model 2 vs. 1	16.2(0.014)	2.6(0.010)
Model 3 vs. 1	23.8(0.008)	3.5(0.002)
Model 4 vs. 1	27.0(0.002)	5.3(<0.001)
Model 4 vs. 2	22.3(0.024)	2.7(0.020)

NRI, net reclassifification improvement; IDI, integrated discrimination improvement. Model 1 = base model. Model 2 = base model + NTproBNP categories. Model 3 = base model + CA125 categories. Model 4 = base model + NTproBNP categories + CA125 categories.

profile indicated a significantly reduced risk of 1-year mortality or AHF readmission [12]. In a recent multicentre randomized study of 160 AHF subjects with renal dysfunction, a CA125-guided diuretic strategy with an admission loop diuretics dose determined based on CA125 levels significantly improved 72-h eGFR [25]. Briefly, in subjects with high CA125 levels, high-intensity diuretic treatment and/or closer follow-up were advocated. When CA125 was low or decreased, a down-titration was recommended in both trials, which endorsed the role of CA125-guided decongestion treatment in AHF.

This study included a non-selected hospitalized population of patients with AHF. Based on this, we think many patients hospitalized for AHF have preserved ejection fraction in the real world. Although we pay more attention to heart failure with reduced ejection fraction, Dunlay *et al.* reported that two-thirds of advanced heart failure subjects had LVEF>40% [27]. The predominance of preserved ejection fraction in our population may explain a slightly lower proportion of treatment with renin–angiotensin system inhibitors and beta-blockers. Advanced heart failure occurs primarily in the elderly, and the cardiorenal syndrome is common. Sodium-glucose cotransporter 2 inhibitors may carry a higher risk of hypotension in older adults, in patients with renal dysfunction and taking loop diuretics. We know that patients with elevated CA125 had a worse clinical profile, which may be one possible explanation for a lower proportion of treatment with sodium-glucose cotransporter 2 inhibitor and a higher proportion of treatment with digitalis in patients with elevated CA125 values.

In this study, we used a cut-off value of 39.7 U/mL for CA125, but our previous paper confirmed that CA125≥65.7 U/mL was highly predictive of adverse outcomes in stage D heart failure patients [24]. We noticed that some researchers divided patients based on the normal CA125 levels (<35 U/mL) derived primarily from cancer studies[28]. The optimal cut-off for defining normal vs. elevated values in different heart failure scenarios has not been established. We think the value of CA125 we obtained could provide a particular reference value in the setting of AHF and stage D heart failure.

Given the long half-life of CA125 (approximately 5-12 days) [16] and the shorter mean half-life of NTproBNP (60-120 min) [29], CA125 potentially provides pathophysiological information several weeks prior, and NTproBNP could provide acute hemodynamic information, similar to glycated hemoglobin and serum glucose in diabetes. One study reported that levels of CA125 and NTproBNP represent distinct pathophysiological states related to heart failure severity [10]. The combined use of CA125 and NTproBNP improved risk stratification, and this multimarker approach holds promise in guiding depletion therapy, showing the need to incorporate CA125 into daily clinical practice. In addition, conversely to natriuretic peptides, age, sex, body weight, and renal function did not significantly influence CA125 levels [12,21]. In the current study, we found that NTproBNP strongly depended on serum creatinine, weight, and LVEF, while CA125 appeared not to be significantly influenced by these factors. Beyond these considerations, additional benefits for implementing CA125

testing in daily clinical practice arise from its standardized measurement, low cost, and wide availability.

Our study had some limitations. First, its observational design makes it susceptible to confounding factors and bias. Second, it is a single-centre study that precludes the extrapolation of results. Third, it is impossible to extrapolate findings to patients undergoing renal dialysis because this study included patients with baseline serum creatinine values ≤360 μmol/L. Finally, we measured CA125 levels at the one-time point after an overnight fast on the second day of admission; however, peak CA125 levels might better reflect fluid overload in patients with AHF.

In conclusion, in AHF patients, elevated CA125 levels were highly predictive of six-month death/AHF readmission, adding prognostic value to NTproBNP and clinical risk factors. Measuring simultaneously these two biomarkers conferred greater predictive capacity when compared with either of them alone. Hence, this glycoprotein should be considered a complement for optimal risk prediction. The underlying mechanisms of CA125 in AHF syndromes remain unclear, and more research is needed.

Conflict of interest

The authors have no conflicts of interest to declare.

Funding

Not applicable.

ORCID numbers authors

- Ji Zhang (JZ): 0000-0001-6099-9336
- Wenhua Li (WHL): 0000-0001-5496-0435
- Jie Hui (JH): 0000-0001-6517-5977
- Jianqiang Xiao (JZ): 0000-0002-7513-2230

Participation of the authors

JZ and WHL wrote and designed the study. JZ and JH wrote and revised the manuscript. JQX collected data. All authors read and approved the final manuscript.

REFERENCES

1. **Levy WC, Mozaffarian D, Linker DT, Sutradhar SC, Anker SD, Cropp AB, Anand I, Maggioni A, Burton P, Sullivan MD, Pitt B, Poole-Wilson PA, Mann DL, Packer M.** The Seattle Heart Failure Model: prediction of survival in heart failure. Circulation 2006; 113:1424-33. *doi:10.1161/CIRCULATIONAHA.105.584102.*
2. **Stienen S, Salah K, Eurlings LW, Bettencourt P, Pimenta JM, Metra M, Bayes-Genis A, Verdiani V, Bettari L, Lazzarini V, Tijssen JP, Pinto YM, Kok WE.** Challenging the two concepts in determining the appropriate pre-discharge N-terminal pro-brain natriuretic peptide treatment target in acute decompensated heart failure patients: absolute or relative discharge levels? Eur J Heart Fail 2015; 17:936-44. *doi:10.1002/ejhf.320.*
3. **Kociol RD, Horton JR, Fonarow GC, Reyes EM, Shaw LK, O'Connor CM, Felker GM, Hernandez AF.** Admission, discharge, or change in B-type natriuretic peptide and long-term outcomes: data from Organized Program to Initiate Lifesaving Treatment in Hospitalized Patients with Heart Failure (OPTIMIZE-HF) linked to Medicare claims. Circ Heart Fail 2011; 4:628-36. *doi:10.1161/CIRCHEARTFAILURE.111.962290.*
4. **Aleksova A, Paldino A, Beltrami AP, Padoan L, Iacoviello M, Sinagra G, Emdin M, Maisel AS.** Cardiac biomarkers in the emergency department: the role of soluble ST2 (sST2) in acute heart failure and acute coronary syndrome-There is meat on the bone. J Clin Med 2019; 8:270. *doi:10.3390/jcm8020270.*
5. **van Vark LC, Lesman-Leegte I, Baart SJ, Postmus D, Pinto YM, Orsel JG, Westenbrink BD, Brunner-la Rocca HP, van**

Miltenburg AJM, Boersma E, Hillege HL, Akkerhuis KM; TRIUMPH Investigators. Prognostic value of Serial ST2 measurements in patients with acute heart failure. J Am Coll Cardiol 2017; 70:2378-2388. *doi:10.1016/j.jacc.2017.09.026.*

6. **Morrow DA, Velazquez EJ, DeVore AD, Prescott MF, Duffy CI, Gurmu Y, McCague K, Rocha R, Braunwald E.** Cardiovascular biomarkers in patients with acute decompensated heart failure randomized to sacubitril-valsartan or enalapril in the PIONEER-HF trial. Eur Heart J 2019; 40:3345-3352. *doi:10.1093/eurheartj/ehz240.*
7. **Peacock WF 4th, De Marco T, Fonarow GC, Diercks D, Wynne J, Apple FS, Wu AH; ADHERE Investigators**. Cardiac troponin and outcome in acute heart failure. N Engl J Med 2008; 358:2117-1126. *doi:10.1056/NEJMoa0706824.*
8. **Felker GM, Mentz RJ, Teerlink JR, Voors AA, Pang PS, Ponikowski P, Greenberg BH, Filippatos G, Davison BA, Cotter G, Prescott MF, Hua TA, Lopez-Pintado S, Severin T, Metra M.** Serial high sensitivity cardiac troponin T measurement in acute heart failure: insights from the RELAX-AHF study. Eur J Heart Fail 2015; 17:1262-1670. *doi:10.1002/ejhf.341.*
9. **Núñez J, Bayés-Genís A, Revuelta-López E, Ter Maaten JM, Miñana G, Barallat J, Cserkóová A, Bodi V, Fernández-Cisnal A,** Núñez E, Sanchis J, Lang C, Ng LL, Metra M, Voors AA. Clinical role of CA125 in worsening heart failure: A BIOSTAT-CHF Study Subanalysis. JACC Heart Fail 2020; 8:386-397. *doi:10.1016/j.jchf.2019.12.005*.
10. **Núñez J, Sanchis J, Bodí V, Fonarow GC, Núñez E, Bertomeu-González V, Miñana G, Consuegra L, Bosch MJ, Carratalá A, Chorro FJ, Llàcer A.** Improvement in risk stratification with the combination of the tumour marker antigen carbohydrate 125 and brain natriuretic peptide in patients with acute heart failure. Eur Heart J 2010; 31:1752-1763. *doi:10.1093/eurheartj/ehq 142.*
11. **Marcus CS, Maxwell GL, Darcy KM, Hamilton CA, McGuire WP**. Current approaches and challenges in managing and monitoring treatment response in ovarian cancer. J Cancer 2014; 5:25-30. *doi:10.7150/jca.7810.*
12. **Núñez J, Llàcer P, Bertomeu-González V, Bosch MJ, Merlos P, García-Blas S, Montagud V, Bodí V, Bertomeu-Martínez V, Pedrosa V, Mendizábal A, Cordero A, Gallego J, Palau P, Miñana G, Santas E, Morell S, Llàcer A, Chorro FJ, Sanchis J, Fácila L; CHANCE-HF Investigators.** Carbohydrate Antigen-125-Guided Therapy in Acute Heart Failure: CHANCE-HF: A Randomized Study. JACC Heart Fail 2016; 4:833-843. *doi:10.1016/j.jchf.2016.06.007.*
13. **Rheude T, Pellegrini C, Schmid H, Trenkwalder T, Mayr NP, Joner M, Kasel AM, Holdenrieder S, Nunez J, Sanchis J, Bodi V, Schunkert H, Kastrati A, Hengstenberg C, Husser O.** Comparison of carbohydrate antigen 125 and N-Terminal pro-brain natriuretic peptide for risk prediction after transcatheter aortic valve implantation. Am J Cardiol 2018; 121:461-468. *doi:10.1016/j.amjcard.2017.11.020.*
14. **Falcão F, Oliveira F, Cantarelli F, Cantarelli R, Brito Júnior P, Lemos H, Silva P, Camboim I, Freire MC, Carvalho O, Sobral Filho DC**. Carbohydrate antigen 125 for mortality risk prediction following acute myocardial infarction. Sci Rep 2020; 10:11016. *doi:10.1038/s41598-020-67548-8.*
15. **Falcão F, de Oliveira FRA, da Silva MCFC, Sobral Filho DC.** Carbohydrate antigen 125: a promising tool for risk stratification in heart diseases. Biomark Med 2018; 12:367-381. *doi:10.2217/bmm-2017-0452.*
16. **Núñez J, Miñana G, Núñez E, Chorro FJ, Bodí V, Sanchis J.** Clinical utility of antigen carbohydrate 125 in heart failure. Heart Fail Rev 2014; 19:575-584. *doi:10.1007/s10741-013-9402-y.*
17. **Ponikowski P, Voors AA, Anker SD, Bueno H, Cleland JGF, Coats AJS, Falk V, González-Juanatey JR, Harjola VP, Jankowska EA, Jessup M, Linde C, Nihoyannopoulos P, Parissis JT, Pieske B, Riley JP, Rosano GMC, Ruilope LM, Ruschitzka F, Rutten FH, van der Meer P; ESC Scientific Document Group.** 2016

ESC Guidelines for the diagnosis and treatment of acute and chronic heart failure: The Task Force for the diagnosis and treatment of acute and chronic heart failure of the European Society of Cardiology (ESC)Developed with the special contribution of the Heart Failure Association (HFA) of the ESC. Eur Heart J 2016; 37:2129-2200. *doi:10.1093/eurheartj/ehw128.*

18. **Yancy CW, Jessup M, Bozkurt B, Butler J, Casey DE Jr, Colvin MM, Drazner MH, Filippatos GS, Fonarow GC, Givertz MM, Hollenberg SM, Lindenfeld J, Masoudi FA, McBride PE, Peterson PN, Stevenson LW, Westlake C.** 2017 ACC/AHA/HFSA Focused Update of the 2013 ACCF/AHA Guideline for the Management of Heart Failure: A Report of the American College of Cardiology/American Heart Association Task Force on Clinical Practice Guidelines and the Heart Failure Society of America. Circulation 2017; 136:e137-e161. *doi:10.1161/CIR.0000000000000509.*
19. **Ibanez B, James S, Agewall S, Antunes MJ, Bucciarelli-Ducci C, Bueno H, Caforio ALP, Crea F, Goudevenos JA, Halvorsen S, Hindricks G, Kastrati A, Lenzen MJ, Prescott E, Roffi M, Valgimigli M, Varenhorst C, Vranckx P, Widimský P; ESC Scientific Document Group.** 2017 ESC Guidelines for the management of acute myocardial infarction in patients presenting with ST-segment elevation: The Task Force for the management of acute myocardial infarction in patients presenting with ST-segment elevation of the European Society of Cardiology (ESC). Eur Heart J 2018; 39:119-177. *doi:10.1093/eurheartj/ehx393.*
20. **Rubio-Gracia J, Demissei BG, Ter Maaten JM, Cleland JG, O'Connor CM, Metra M, Ponikowski P, Teerlink JR, Cotter G, Davison BA, Givertz MM, Bloomfield DM, Dittrich H, Damman K, Pérez-Calvo JI, Voors AA.** Prevalence, predictors and clinical outcome of residual congestion in acute decompensated heart failure. Int J Cardiol 2018; 258:185-191. *doi:10.1016/j.ijcard.2018.01.067.*
21. **Mullens W, Damman K, Harjola VP, Mebazaa A, Brunner-La Rocca HP, Martens P, Testani JM, Tang WHW, Orso F, Rossignol P, Metra M, Filippatos G, Seferovic PM, Ruschitzka F, Coats AJ.** The use of diuretics in heart failure with congestion - a position statement from the Heart Failure Association of the European Society of Cardiology. Eur J Heart Fail. 2019;21(2):137-155. *doi:10.1002/ejhf.1369.*
22. **Parrinello G, Torres D, Paterna S, di Pasquale P, Licata G.** The pathophysiology of acute heart failure: the key role of fluid accumulation. Am Heart J 2008; 156:e19. *doi:10.1016/j.ahj.2008.04.031.*
23. **Gheorghiade M, Follath F, Ponikowski P, Barsuk JH, Blair JE, Cleland JG, Dickstein K, Drazner MH, Fonarow GC, Jaarsma T, Jondeau G, Sendon JL, Mebazaa A, Metra M, Nieminen M, Pang PS, Seferovic P, Stevenson LW, van Veldhuisen DJ, Zannad F, Anker SD, Rhodes A, McMurray JJ, Filippatos G; European Society of Cardiology; European Society of Intensive Care Medicine.** Assessing and grading congestion in acute heart failure: a scientific statement from the acute heart failure committee of the heart failure association of the European Society of Cardiology and endorsed by the European Society of Intensive Care Medicine. Eur J Heart Fail 2010; 12:423-433. *doi:10.1093/eurjhf/hfq045.*
24. **Zhang J, Li W, Xiao J, Hui J, Li Y.** Prognostic significance of carbohydrate antigen 125 in stage D heart failure. BMC Cardiovasc Disord 2023; 23:108. Published 2023 Feb 25. *doi:10.1186/s12872-023-03139-5.*
25. **Núñez J, Llàcer P, García-Blas S, Bonanad C, Ventura S, Núñez JM, Sánchez R, Fácila L, de la Espriella R, Vaquer JM, Cordero A, Roqué M, Chamorro C, Bodi V, Valero E, Santas E, Moreno MDC, Miñana G, Carratalá A, Rodríguez E, Mollar A, Palau P, Bosch MJ, Bertomeu-González V, Lupón J, Navarro J, Chorro FJ, Górriz JL, Sanchis J, Voors AA, Bayés-Genís A.** CA125-guided diuretic treatment versus usual care in patients with acute heart

failure and renal dysfunction. Am J Med 2020; 133:370-380.e4. *doi:10.1016/j.amjmed.2019.07.041.*

26. Felker GM, Anstrom KJ, Adams KF, Ezekowitz JA, Fiuzat M, Houston-Miller N, Januzzi JL Jr, Mark DB, Piña IL, Passmore G, Whellan DJ, Yang H, Cooper LS, Leifer ES, Desvigne-Nickens P, O'Connor CM. Effect of natriuretic peptide-guided therapy on hospitalization or cardiovascular mortality in high-risk patients with heart failure and reduced ejection fraction: A randomized clinical trial. JAMA 2017; 318:713-720. *doi:10.1001/jama.2017.10565.*

27. Dunlay SM, Roger VL, Killian JM, Weston SA, Schulte PJ, Subramaniam AV, Blecker SB, Redfield MM. Advanced heart failure epidemiology and outcomes: a population-based study. JACC Heart Fail 2021; 9:722-732. *doi: 10.1016/j.jchf.2021.05.009.*

28. Lorenzo M, Palau P, Llàcer P, Domínguez E, Ventura B, Núñez G, Miñana G, Solsona J, Santas E, De La Espriella R, Bodí V, Núñez E, Sanchis J, Bayés-Genís A, Núñez J. Clinical utility of antigen carbohydrate 125 for planning the optimal length of stay in acute heart failure. Eur J Intern Med 2021; 92:94-99. *doi: 10.1016/j.ejim.2021.05.037.*

29. Clerico A, Carlo Zucchelli G, Pilo A, Passino C, Emdin M. Clinical relevance of biological variation: the lesson of brain natriuretic peptide (BNP) and NT-proBNP assay. Clin Chem Lab Med 2006; 44:366-378. *doi:10.1515/CCLM.2006.063.*

Invest Clin 65(3): 321 - 334, 2024 https://doi.org/10.54817/IC.v65n3a05

Protective effects of thiamine pyrophosphate and cinnamon against oxidative liver damage induced by an isoniazid and rifampicin combination in rats.

Bahtınur Yeter[1], Renad Mammadov[2], Zeynep Koc[3], Seval Bulut[2], Tugba Bal Tastan[4], Mine Gulaboglu[5] and Halis Suleyman[2]

[1]Department of Child Health and Diseases, Faculty of Medicine, Erzincan Binali Yildirim University, Erzincan, Turkey.
[2]Department of Pharmacology, Faculty of Medicine, Erzincan Binali Yildirim University, Erzincan, Turkey.
[3]Department of Biochemistry, Faculty of Medicine, Erzincan Binali Yıldırım University, Turkey.
[4]Department of Histology and Embryology, Faculty of Medicine, Erzincan Binali Yildirim University, Erzincan, Turkey.
[5]Department of Biochemistry, Faculty of Pharmacy, Ataturk University, Turkey.

Keywords: isoniazid; rifampicin; thiamine pyrophosphate; cinnamon extract; oxidative stress; inflammation.

Abstract. Isoniazid and rifampicin (IRC) have been shown to cause hepatotoxicity in both clinical and preclinical studies. Oxidative stress and inflammation have been held responsible for the pathogenesis of IRC-induced hepatotoxicity. Antioxidative and anti-inflammatory effects of thiamine pyrophosphate (TPP) and cinnamon extract (CE) have been shown in previous studies. Therefore, our study investigated the protective effects of TPP and CE on possible liver damage caused by IRC treatment in rats. Twenty-four albino Wistar rats were categorized into four groups: a healthy group (HG), an IRC group (IRG), a TPP+IRC group (TIRG), and a CE+IRC group (CIRG). TPP (25 mg/kg) was administered intraperitoneally to TIRG, while CE (100 mg/kg) was administered orally to CIRG. In IRG, TIRG, and CIRG, isoniazid (50 mg/kg) and rifampicin (50 mg/kg) were administered orally one hour after these treatments. For seven days, this procedure was repeated once a day. After this period, blood samples were taken from the tail veins, and the rats were sacrificed. The removed liver tissues were analyzed for oxidant, antioxidant, and proinflammatory cytokines and subjected to histopathological evaluation. Serum alanine aminotransferase and aspartate aminotransferase activities

Corresponding Author: Halis Suleyman, Erzincan Binali Yildirim University, Faculty of Medicine, Department of Pharmacology, Erzincan, Turkey, Phone: +90 530 9211909, Fax: +90 446 2261819. E-mail: halis.suleyman@gmail.com

were also measured. An increase in malondialdehyde, nuclear factor kappa B, tumor necrosis factor-alpha, interleukin 1 beta, and interleukin-6 levels, a decrease in total glutathione levels, superoxide dismutase and catalase activities, and an increase in alanine aminotransferase and aspartate aminotransferase activities were found with IRC treatment ($p<0.001$). The histopathological analysis of the IRG suggested hepatotoxicity ($p<0.001$). TPP and CE administered with IRC inhibited the biochemical changes ($p<0.001$). In the TIRG, this inhibition was higher than in the CIRG ($p<0.05$). Histological damage was inhibited by TPP ($p<0.001$). CE prevented biochemical changes but not histological changes except inflammatory cell infiltration. Therefore, TPP may be better than CE in preventing IRC-induced hepatotoxicity.

Efectos protectores del pirofosfato de tiamina y la canela contra el daño hepático oxidativo inducido por la combinación de isoniazida y rifampicina en ratas.

Invest Clin 2024; 65 (3): 321 – 334

Palabras clave: isoniazida; rifampicina; pirofosfato de tiamina; extracto de canela; estrés oxidativo; inflamación.

Resumen. Se ha demostrado que la isoniazida y la rifampicina (IRC) causan hepatotoxicidad tanto en estudios clínicos como preclínicos. El estrés oxidativo y la inflamación se han considerado responsables de la patogénesis de la hepatotoxicidad inducida por IRC. En estudios anteriores se han demostrado los efectos antioxidantes y antiinflamatorios del pirofosfato de tiamina (TPP) y del extracto de canela (CE). Por lo tanto, en nuestro estudio se investigaron los efectos protectores del TPP y el CE sobre el posible daño hepático causado por el tratamiento con IRC en ratas. Se clasificaron 24 ratas Wistar albinas en cuatro grupos: un grupo sano (HG), un grupo IRC (IRG), un grupo TPP+IRC (TIRG) y un grupo CE+IRC (CIRG). El TPP (25 mg/kg) se administró por vía intraperitoneal al TIRG, mientras que el CE (100 mg/kg) se administró por vía oral al CIRG. En IRG, TIRG y CIRG, se administró isoniazida (50 mg/kg) y rifampicina (50 mg/kg) por vía oral una hora después de estos tratamientos. Durante siete días, este procedimiento se repitió una vez al día. Tras este periodo, se tomaron muestras de sangre de las venas de la cola y se sacrificaron las ratas. Los tejidos hepáticos extraídos se analizaron en busca de citocinas oxidantes, antioxidantes y proinflamatorias y se sometieron a una evaluación histopatológica. También se midieron las actividades séricas de la alanina aminotransferasa y la aspartato aminotransferasa. Con el tratamiento con IRC se observó un aumento de los niveles de malondialdehído, factor nuclear kappa B, factor de necrosis tumoral alfa, interleucina 1 beta e interleucina 6, una disminución de los niveles totales de glutatión y de las actividades de superóxido dismutasa y catalasa, y un aumento de las actividades de alanina aminotransferasa y aspartato aminotransferasa ($p<0,001$). El análisis histopatológico del IRG sugirió hepatotoxicidad ($p<0,001$). El TPP y el CE

administrados con el IRC inhibieron los cambios bioquímicos (p<0,001). En el TIRG, esta inhibición fue mayor que en el CIRG (p<0,05). El daño histológico fue inhibido por el TPP (p<0,001). El CE previno los cambios bioquímicos pero no los histológicos, excepto la infiltración de células inflamatorias. Por lo tanto, TPP puede ser una mejor opción que CE para la prevención de la hepatotoxicidad inducida por IRC.

Received: 24-01-2024 *Accepted: 28-04-2024*

INTRODUCTİON

Isoniazid and rifampicin are anti-mycobacterial drugs that are part of the World Health Organisation's recommended combination treatment regimen for tuberculosis[1]. Treatment for tuberculosis consists of a quartet of anti-mycobacterial medications, including isoniazid, rifampicin, ethambutol, and pyrazinamide. Furthermore, the isoniazid and rifampicin combination (IRC) includes the supportive phase of tuberculosis treatment [1,2]. Although effective in treating tuberculosis, these drugs may cause serious side effects. During treatment, there may be toxic effects on the dermatology, gastrointestinal system, hypersensitivity, neurology, hematology, and renal system [3]. Antituberculosis drugs can cause liver toxicity, which can result in the discontinuation of the drug as well as morbidity and mortality [4]. A primary antituberculosis drug, isoniazid, has been reported to cause liver injury through oxidative stress [5]. The role of lipid peroxidation (LPO) in the pathogenesis of isoniazid-associated oxidative liver injury has been documented [6]. Severe oxidative liver damage is believed to be initiated by reactive oxygen species (ROS) [7]. According to the literature, isoniazid has hepatotoxic effects due to the formation of the acetylhydrazine metabolite due to its acetylation [1]. Although rifampicin alone has a low hepatotoxicity potential [6], it exhibits additive and synergistic hepatotoxicity when used with isoniazid in treating tuberculosis [4]. This has been attributed to the stimulation of hydrolases by rifampicin and the formation of hepatotoxic reactive metabolites from isoniazid [8].

The protective effect of thiamine pyrophosphate (TPP), thiamine's active metabolite, was evaluated in IRC-induced hepatotoxicity in rats [9]. Evidence in the literature shows that TPP protects various organs from oxidative and proinflammatory cytokine damage [10-12]. Cinnamon, which we also investigate in our study against the possible toxicity of IRC on the liver, is the bark of some *Cinnamomum (Lauraceae)* species [13]. Cinnamon has been shown to have anti-inflammatory, antioxidant, and many other beneficial biological properties in the literature [14]. It has been reported that cinnamon protects the heart, liver, kidney, blood, brain, and spleen from the toxicity of chemicals through its antioxidant, radical-scavenging, and LPO-suppressing properties[15]. The anti-inflammatory effect of cinnamon extract (CE) has been associated with inhibition of proinflammatory cytokines [16]. This information suggests that TPP and CE may be helpful in treating IRC-induced liver injury. This study was designed to investigate the protective effects of TPP and CE against IRC-induced liver injury in rats.

MATERİALS AND METHODS

Animals

Twenty-four male albino Wistar rats (282-294 g, 5-6 months old) purchased from the Experimental Animal Research and Ap-

plication Centre of Erzincan Binali Yildirim University were used in the study. The rats were housed in an environment with appropriate temperature (22±2°C), humidity (50-60%) and 12-h light-dark cycle and fed ad libitum. Experimental procedures were carried out after the approval of the local Animal Experiments Ethics Committee of Erzincan Binali Yıldırım University (Date: 31.08.2023, Decision number: 29).

Chemical substances

Isoniazid and Rifampicin were procured from Koçak Farma Ilaç ve Kimya Sanayi (Istanbul, Turkey), Thiamine pyrophosphate was procured from BioPharma (Moscow, Russia), Cinnamon extract was procured from Solgar (Leonia, USA), and thiopental sodium used for the experiment was procured from IE Ulagay (Istanbul, Turkey).

Experimental groups

The rats (n=6/each group) were randomly divided into healthy control (HG), isoniazid + rifampicin (IRG), TPP + isoniazid + rifampicin (TIRG), and CE + isoniazid + rifampicin (CIRG) groups.

Experimental process

In the experiment, TPP (25 mg/kg) was administered intraperitoneally to the TIRG. CE (100 mg/kg) was administered orally by gavage to the CIRG. In both the HG and IRG, distilled water was administered the same way. To the IRG, TIRG, and CIRG, isoniazid (50 mg/kg) and rifampicin (50 mg/kg) were given orally one hour after the TPP, CE, and distilled water were given. The indicated treatment protocol was administered once daily for seven days. At the end of the seventh day, blood samples were collected from the tail vein of the rats for alanine aminotransferase (ALT) and aspartate aminotransferase (AST) analyses. The rats were then euthanized with 50 mg/kg thiopental sodium intraperitoneally, and liver tissues were collected. Malondialdehyde (MDA), total glutathione (tGSH), superoxide dismutase (SOD), catalase (CAT), nuclear factor kappa B (NF-κB), tumor necrosis factor-alpha (TNF-α), interleukin 1 beta (IL-1β), and interleukin 6 (IL-6) were analyzed in the liver tissues. Liver tissues were also examined histopathologically.

Biochemical analyses

Preparation of the samples

The tissues were cleaned of blood using physiological saline and pulverized by adding liquid nitrogen. Powdered tissues were dissolved in 50 mM phosphate buffer (pH=7.4). For MDA, tGSH, SOD, CAT, NF-κB, TNF-α, IL-1β, and IL-6 analyses, the supernatants obtained after centrifugation were used.

Tissue MDA, tGSH, SOD, and CAT determination

MDA and tGSH levels and SOD activities in tissues were determined by measuring each with Enzyme-Linked ImmunoSorbent Assay (ELISA) kit (product nos. 10009055, 703002, and 706002, respectively, Cayman Chemical Company) according to the instructions. The CAT analysis was conducted according to the method recommended by Goth [17].

Tissue NF-κB, TNF-α, IL-1β, and IL-6 determination

TNF-α, IL-1β, and IL-6 levels were determined with ELISA kits purchased from Eastbiopharm Co Ltd (China), and NF-κB levels were measured with commercial ELISA kits purchased from SunRed Biological Technology Co. Ltd (China). The analyses were performed according to the kit instructions.

Determination of ALT and AST in serum. Tubes without anticoagulants were used for blood samples, and serum was used for analyses. After centrifugation, the clear filtrate was separated and stored at -80°C. ALT and AST activities were determined spectrophotometrically using a Cobas 8000 autoanalyzer (Roche Diagnostics GmBH, Germany) with kits (Roche Diagnostics).

Histopathological analysis

Tissue samples were fixed in formalin (10%). Subsequently, tissue samples were washed. Tissues were embedded in paraffin after ethanol (70-100%) and xylol procedures. Sections (4-5 μ) were prepared and stained with hematoxylin-eosin (H&E). Sections were photographed and analyzed using a light microscope (Olympus Inc., Tokyo, Japan) and the DP2-SAL firmware program. Histopathological changes in liver tissue were defined as hepatocyte degeneration, Kupffer cell activation, capillary congestion, and the presence of polymorphonuclear cell (PMNL) infiltration. Each section was graded 0-3 for each criterion (0, absent; 1, mild; 2, moderate; 3, severe). The evaluation was performed by a pathologist who was unaware of the study groups' assignments.

Statistical analyses

The statistical procedures were conducted using "SPSS for Windows, 22.0" statistical software. It was determined that the numerical data were normally distributed by the Shapiro-Wilk test; therefore, one-way ANOVA was used for the analysis. According to the results of Levene's test, Tukey HSD or Games Howell tests were used as post hoc tests for intergroup comparisons. The biochemical data were presented as mean ± standard deviation (X±SD). The Kruskal-Wallis test was preferred for analyzing semiquantitative histopathologic grading data, and then the post-hoc Dunn's test was employed for the analysis. Statistical results were presented as median (quartile 1- quartile 3). The significance level was set at $p<0.05$.

RESULTS

Analysis of MDA, tGSH, SOD and CAT levels in liver tissue

It can be seen from Fig. 1A that MDA levels in liver tissue increased in the IRG group (5.48±0.20) compared to healthy rats (2.39±0.18) ($p<0.001$). The increase in MDA was observed to be suppressed in the TIRG (2.67±0.24) and CIRG (4.06±0.15) ($p<0.001$). Compared with CE, TPP suppressed the increase in MDA more effectively ($p<0.001$). The MDA levels in TIRG and HG were not significantly different ($p=0.100$).

In IRG, a decrease in tGSH levels and SOD and CAT activities (3.42±0.24, 5.33±0.15, 3.78±0.12, respectively) were detected with the increase in MDA compared to HG (6.34±0.18, 9.19±0.12, 7.51±0.21, respectively) ($p<0.001$). TPP (5.80±0.10, 8.76±0.13, 7.09±0.26, respectively) and CE (4.48±0.09, 6.66±0.16, 5.39±0.37, respectively) inhibited the decrease in tGSH levels and SOD and CAT activities ($p<0.001$). TPP treatment prevented the decrease in antioxidants more effectively than CE ($p<0.001$) (Fig. 1B-D).

Analysis of NF-κB, TNF-α, IL-1β and IL-6 levels in liver tissue

As presented in Fig. 2A-D, the levels of NF-κB, TNF-α, IL-1β, and IL-6 in the liver tissues of rats in the IRG group (4.86±0.09, 4.68±0.09, 6.29±0.15, 5.70±0.12, respectively) were higher than those in the HG group (2.38±0.11, 2.13±0.07, 3.37±0.19, 2.49±0.24, respectively) ($p<0.001$). Compared to the IRG group, both TPP (2.57±0.12, 2.37±0.11, 3.68±0.26, 2.77±0.11, respectively) and CE (3.25±0.15, 3.31±0.14, 5.00±0.48, 4.02±0.22, respectively) inhibited these increases in NF-κB, TNF-α, IL-1β and IL-6 ($p<0.05$). However, this inhibition was more significant in the TPP than in the CE group ($p<0.05$). There were similarities between TIRG and HG in terms of NF-κB ($p=0.315$), IL-1β ($p=0.157$) and IL-6 ($p=0.064$) levels.

Analysis of ALT and AST activities in serum samples

As presented in Fig. 3A-B, ALT and AST activities measured from the serum of rats in the IRG (86.67±4.55, 220.00±7.72, respectively) were found to be increased according to HG (29.17±4.02, 39.17±4.92, respec-

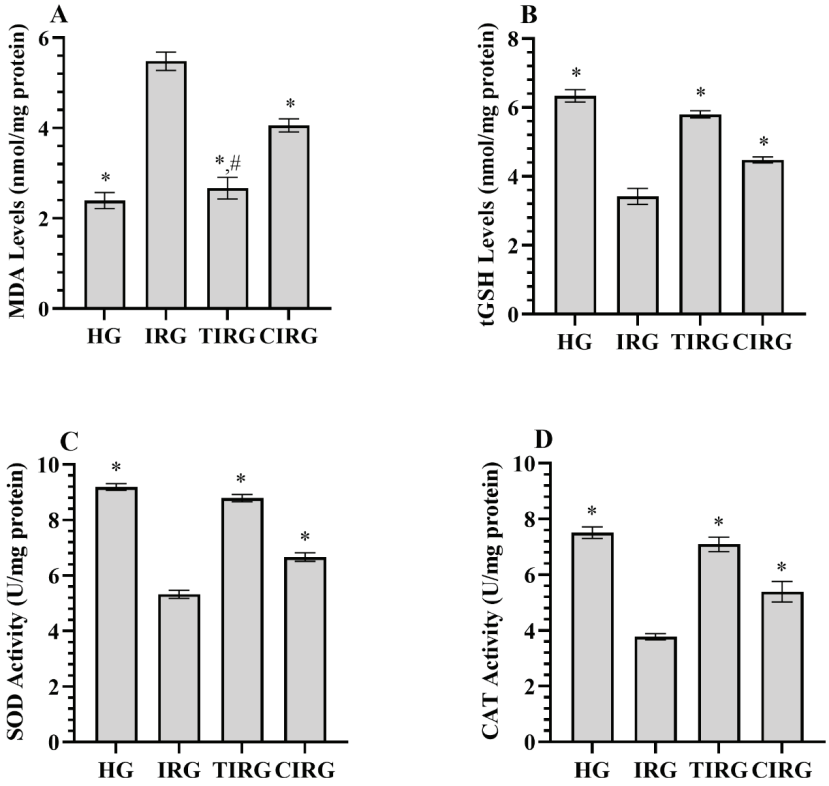

Fig. 1(A-D). Results of analyses of MDA (A), tGSH (B), SOD (C) and CAT (D) data measured from liver tissues. *; $p<0.001$ vs IRG, # $p>0.05$ vs HG. MDA: malondialdehyde, tGSH: total glutathione, SOD: superoxide dismutase, CAT: catalase, HG: healthy group, IRG: isoniazid+rifampicin applied group, TIRG: thiamine pyrophosphate+izoniazid+rifampisin applied group, CIRG: Cinnamon extract+izoniazid+rifampisin applied group.

tively) ($p<0.001$). The increase in ALT and AST activities in the IRG appeared to be suppressed in TIRG (32.83±3.55, 45.83±4.62, respectively) and CIRG (56.50±2.43, 92.50±4.51, respectively) ($p<0.001$). TPP inhibited this increase in ALT and AST activities more effectively than CE ($p<0.001$). Serum ALT ($p=0.165$) and AST ($p=0.200$) activities of TIRG and HG were similar.

Histopathologic findings

There were normal central arteries in the liver tissue sections, radially arranged hepatic cords in the lobules, and normal tissue structure in the HG group, as presented in Fig. 4A and Table 1.

Upon examination of the liver tissue of the IRG group, it was observed that the hepatocytes around the central artery had lost their typical morphology, were degenerating, their nuclei bulged and appeared pyknotic on occasion. A noticeable phenomenon was the loss of radial arrangement of hepatic cords, which resulted in irregular and spiralized cords. There was a marked and moderate degree of congestion in both the central artery and surrounding blood vessels. A significant increase was observed in the number of Kupffer cells. Many PMNLs were detected infiltrating the pericapillary area (Fig. 4B and Table 1).

Notably, in the TIRG group treated with TPP, the arrangement of hepatic cords and hepatocytes was generally normal, and the Kupffer cell population was relatively similar to the control group. PMNL infiltration was rare throughout the tissue (Fig. 4C and Table 1).

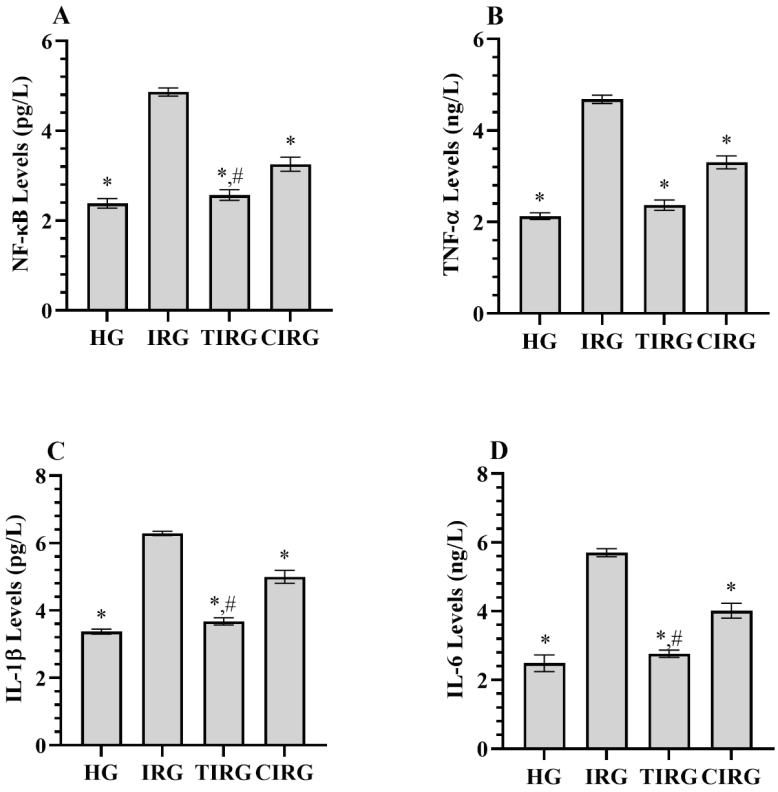

Fig. 2 (A-D). Results of analyses of NF-κB (A), IL-1β (B), TNF-α (C), and IL-6 (D) data measured from liver tissues. *; p<0.05 vs IRG, #, p>0.05 vs HG.
NF-κB: nuclear factor kappa-B, IL-1β: interleukin 1-beta, TNF-α: tumor necrosis factor-alpha, IL-6: interleukin-6, HG: healthy group, IRG: isoniazid+rifampicin group, TIRG: thiamine pyrophosphate +izoniazid+rifampisin group, CIRG: Cinnamon extract+izoniazid+rifampisin group.

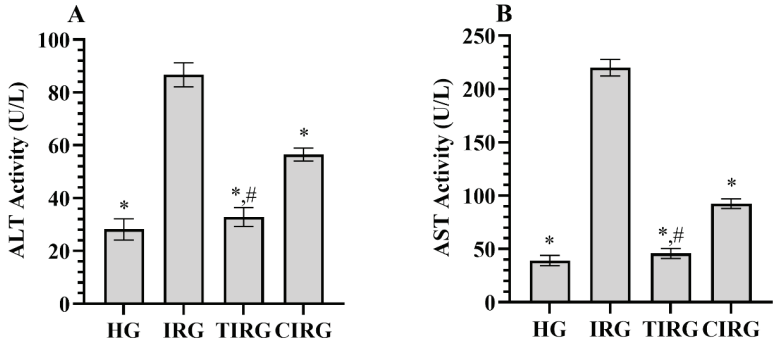

Fig. 3 (A-B). Results of analyses of ALT (A) and AST (B) data measured from serum. *; $p<0.001$ vs IRG, #, $p>0.05$ vs HG.
ALT: alanine aminotransferase, AST: aspartate aminotransferase HG: healthy group, IRG: isoniazid+rifampicin group, TIRG: thiamine pyrophosphate+izoniazid+rifampisin group, CIRG: cinnamon extract+izoniazid+rifampisin group.

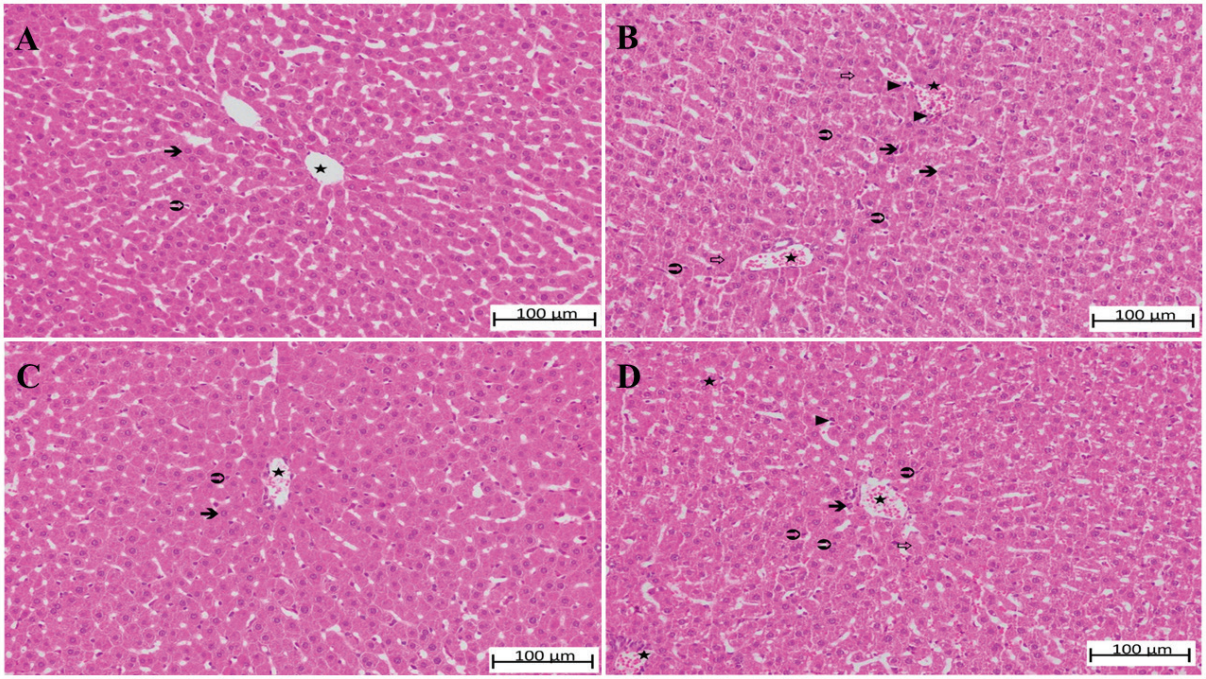

Fig. 4 (A-D). A. Liver tissue belonging to the HG. ➔; hepatocyte, ➲; Kupffer cell, ★; normal appearance of blood vessels (H&E x200). **B.** Liver tissue belonging to the IRG. ➔; degenerated hepatocyte, ⇨; irregularity in hepatic cords, ➲; increased Kupffer cells, ►; polymorphonuclear cell infiltration, ★; moderately congested blood vessel (H&E x 200). **C.** Liver tissue belonging to the TIRG. ➔; hepatocyte with normal morphology, ➲: Kupffer cell, ★; slightly congested blood vessel (H&E x 200). **D.** Liver tissue belonging to the CIRG. ➔; moderately degenerated hepatocytes, ➲; increased Kupffer cells, ⇨; irregularity in the hepatic cords, ►; weakly polymorphonuclear cell infiltration, ★; moderately congested blood vessels (H&E x200). HG: healthy group, IRG: isoniazid+rifampicin group, TIRG: thiamine pyrophosphate+izoniazid+rifampisin group, CIRG: Cinnamon extract+izoniazid+rifampisin group.

Table 1

Analysis results of histopathological grading data of liver tissues from rats.

Parameters	Groups (n=6/each groups)				H / *p* values
	HG (n=6)	IRG (n=6)	TIRG (n=6)	CIRG (n=6)	
	Median (quartile 1-quartile 3)				
Degeneration	0(0-0)*	3(2-3)	0(0-0)$^{*,\#}$	2(2-2)$^{\&}$	129.013<0.001
Kupffer cell activation	0(0-0)*	3(2-3)	0(0-0)$^{*,\#}$	2(2-2)$^{\&}$	129.151/<0.001
Congestion	0(0-0)*	2(2-3)	0.5(0-1)$^{*,\#}$	2(2-2)$^{\&}$	122.132/<0.001
PMNL infiltration	0(0-0)*	3(3-3)	1(1-1)*	1(0.25-2)*	114.468/<0.001

Histopathological grading (0-3): 0: absent, 1: mild damage, 2: moderate damage, 3: severe damage. * p<0.001 vs. IRG, #; p>0.05 vs. HG, &; p>0.05 vs. IRG, HG: healthy group, IRG: isoniazid+rifampicin group, TIRG: thiamine pyrophosphate + izoniazid + rifampisin group, CIRG: Cinnamon extract + izoniazid + rifampisin group. Statistical analysis was done using the Kruskal-Wallis test. Then, Dunn's test was applied. Data are presented as median (quartile 1-quartile 3). p<0.05 was considered significant.

In the CE-treated CIRG group, it was remarkable that hepatic cords were irregular, and hepatocyte degeneration was at a moderate level. In general, it was observed that the congestion in the blood vessels was at a moderate level, and the Kupffer cell population was increased. Mild PMNL infiltration was also determined in the pericapillary area (Fig. 4D and Table 1).

DİSCUSSİON

The primary treatment protocol for tuberculosis consists of isoniazid, rifampicin, pyrazinamide, and ethambutol for six months [18]. Increased dosages of these drugs have been tried to overcome resistance, which has increased the incidence of side effects [19]. Drug-related side effects often result in a change in treatment, which can adversely affect the treatment's effectiveness. One of the most common side effects of antituberculosis treatment is hepatotoxicity [18]. In the literature, mitochondrial dysfunction and oxidative stress have been reported to be involved in the mechanism of IRC-induced hepatotoxicity [19]. In this study, TPP [10] and CE [14], both with antioxidative activity, were examined biochemically and histopathologically for their protective effects on IRC-induced hepatotoxicity. Our biochemical analysis revealed that IRC use caused an increase in oxidant (MDA) and inflammatory markers (NF-κB, TNF-α, IL-1β, and IL-6), a decrease in antioxidants (tGSH, SOD, and CAT), and an increase in ALT and AST activities.

As mentioned above, the role of LPO in the pathogenesis of isoniazid-induced oxidative liver injury was demonstrated [6]. Rifampicin, on the other hand, was reported to exhibit additive and even synergistic hepatotoxicity when used in combination with isoniazid [4]. The cause of this condition has been attributed to rifampicin stimulating hydrolases and the formation of hepatotoxic reactive metabolites from isoniazid [8]. As is well known, MDA is an LPO product used as a biomarker of oxidative stress [20]. MDA exhibits a toxic effect; additionally, converting ROS into active substances causes cell membrane damage, leading to apoptosis and liver necrosis [21]. An experimental study has found that four weeks of IRC treatment has increased MDA in rat livers [22]. By suppressing the increase in MDA in the group administered TPP in conjunction with IRC, it is evident that TPP displays antioxidant properties. It was suggested in the literature that thiamine interacted with free radicals and hydroperoxides and inhibited LPO [23]. Previously, TPP was also tested in oxidative liver injury induced by propofol 11 and metazimol [24] and was found to inhibit the increase in MDA levels in rat livers, similar to our study. In our study, CE suppressed the increase in MDA levels. However, CE suppressed the increase in MDA levels less than TPP. Moselhy *et al*. reported that aqueous and ethanol extracts of cinnamon could prevent the increase in MDA levels by reducing LPO in carbon tetrachloride-induced oxidative liver injury in rats [25].

The liver tissues of the animals were also analyzed in terms of antioxidants. For this purpose, tissue tGSH levels and SOD and CAT activities were determined. GSH represented the most important endogenous nonenzymatic antioxidant. GSH plays a role in the protection of cells from ROS.10 The literature reported that hydrazine reacted with the sulfhydryl group of GSH, depleting its levels in hepatocytes and causing cell death [26]. In our study, tGSH levels were found to be decreased in the IRC group. Similarly, Zhang *et al.* found that IRC decreased GSH levels in liver tissue and serum samples [27]. During the metabolism of antituberculosis drugs, toxic metabolites and free radicals deplete endogenous antioxidants, making the liver susceptible to further damage [28]. According to the literature, external administration of agents with antioxidant activity could contribute to tissue defense in such cases [29]. Our study determined that TPP administered with IRC prevented the decrease in tGSH levels and even maintained them at healthy levels for

the healthy group. Delen et al. similarly concluded that TPP inhibited the depletion of tGSH in the liver caused by propofol use 11. The decrease in tGSH levels in CE-treated animals was suppressed, although not as much as in TPP-treated animals. In a previous study, CE was found to possess antioxidant properties and to suppress GSH depletion in liver tissue [29].

Results of our analysis indicated that SOD and CAT activities were also decreased in the IRC group in which tGSH levels were low. By accelerating the conversion of oxygen to hydrogen peroxide (H_2O_2), SOD was the first antioxidant enzyme to fight ROS [27]. CAT, on the other hand, converted the toxic H_2O_2 into H_2O and oxygen [30]. As a result, SOD and CAT acted as mutually supportive antioxidant enzymes that protected ROS [27]. It was demonstrated in previous preclinical studies that IRC decreased the activity of SOD and CAT in the liver [31,32]. The results of this study revealed that TPP treatment was able to prevent the decline in SOD and CAT activities. Throughout the body, TPP catalyzes various chemical reactions. As a cofactor of enzymes involved in maintaining cell redox, it synthesized reduced nicotinamide adenine dinucleotide phosphate and glutathione and increased the synthesis of antioxidants [24]. In addition, Bedir *et al.* found that TPP prevented metamizole-induced decreases in the activities of SOD and CAT in the liver tissues of rats [24]. El-Kholy *et al.* used CE, another therapeutic drug, to treat oxidative liver damage induced by amoxicillin/clavulanate and found that it inhibited the decrease in SOD and CAT activity, similar to our results [29].

Previously, it was reported that IRC treatment caused inflammation. This leads to activation of macrophages and infiltration of circulating immune cells into the tissue [28]. In contrast, sterile inflammation also contributed to hepatotoxicity by increasing oxidative stress. NF-κB was a transcription factor that modulated inflammation [28,33]. According to our biochemical results and previous studies, increased NF-κB levels with IRC treatment confirmed inflammatory activity [28,31]. In the TPP-treated group, the increase in NF-κB levels seemed to be prevented. Similarly, Ozer *et al.* found that TPP suppressed the increase of NF-κB in damaged ovarian tissue [34]. In our CE-treated group, NF-κB levels were higher than the TPP group and lower than the IRC group. A recent study found that this increase was suppressed in obese rats treated with Cinnamon powder compared to rats with increased hepatic NF-κB expression with obesity [35]. Our study also investigated liver tissues for the levels of proinflammatory cytokines such as TNF-α, IL-1β, and IL-6.

Increased ROS released inactive NF-κB through a series of reactions. Activated NF-κB induced gene transcription of TNF- α and IL-1β [21]. On the other hand, TNF-α, which is considered the primary mediator inducing the inflammatory response, has been reported to activate NF-κB by binding to the TNF receptor [31,36]. In addition, it was pointed out that TNF-α increased ROS production that triggered liver injury through various pathways [31]. IL-1β had intense proinflammatory activity like TNF-α [37]. Although IL-6 also prevented acute liver inflammation, its prolonged stimulation resulted in tissue damage to the liver [38]. Our study discovered that TNF-α, IL-1β, and IL-6 levels were similarly increased in the IRC group in which NF-κB levels were increased. Patel *et al.* also found an increase in TNF-α, IL-1β, and IL-6 levels in their study on the effects of IRC on the liver [38]. Cytokine levels in rats administered with TPP and CE were lower than those of the IRC group. No studies have been conducted in the literature on the effect of TPP on tissue cytokine levels in oxidative liver injury. However, it was reported that TPP prevented the increase in TNF-α and IL-1β levels due to ethanol toxicity in optic nerve tissue [39]. In the literature, studies also reported that CE, another therapeutic agent, exhibited anti-inflammatory activity by suppressing the increase in TNF-α, IL-1β, and IL-6 levels induced by various causes in the liver [40,41].

In this study, the ALT and AST activities of blood samples obtained from animals were measured. These transaminases were sensitive markers of liver cell damage, and these biomarkers have been widely used in the past and present to assess liver function [42]. In both clinical and experimental studies, it has been demonstrated that IRC treatment increases the levels of ALT and AST [18,26,42]. Our study also demonstrated increased ALT and AST activity after IRC treatment. A lower enzyme activity was observed in both TPP and CE-treated groups, but a lower activity was observed in the TPP-treated group. As previously reported, TPP inhibited the increase in ALT, AST, and lactate dehydrogenase activities following acetaminophen [43] and cisplatin-induced liver injury [12]. Mosely *et al.* also demonstrated that CE inhibited the increase in ALT and AST activities [25].

A histologic analysis of liver tissues confirmed our biochemical findings. Degeneration of hepatocytes and marked congestion of blood vessels were observed in the IRC group. In addition, an increase in the number of Kupffer cells and PMNL was observed. According to previous studies, IRC induced changes in the liver, such as sinusoidal dilatation, infiltration of immune cells, inflammation in the portal system, and necrosis of the liver [27,28]. Our histopathological analysis showed that the hepatocytes and Kupffer cell populations of the TPP-treated group were similar to those of the control group, and rare evidence of PMNL infiltration was observed. Several studies demonstrated that TPP protected liver tissue from oxidative damage and prevented structural changes such as cellular degeneration, necrosis, and infiltration of inflammatory cells [11,43]. In the CE group, there was moderate hepatocyte degeneration and vascular congestion. In addition, there was a moderate increase in the Kupffer cell population and mild PMNL infiltration. However, some previous studies reported that CE treatment altogether [44] or almost entirely [25] prevented tissue damage in oxidative liver injury. However, our histopathologic evaluation indicated that TPP protected the histologic structure of the liver better than CE, similar to our biochemical results.

Limitations

In the future, total oxidant levels and antioxidant levels should be measured to investigate the mechanism of hepatoprotective effect of TPP and CE in greater detail. Additionally, we believe that anti-inflammatory cytokine levels should be evaluated.

Our results revealed that IRC induced an increase in oxidants and proinflammatory cytokines and a decrease in antioxidants in the liver tissues of the animals. Moreover, IRC treatment caused an increase in liver function parameters and damage to the histological structure of the liver. TPP and CE inhibited both biochemical and histopathologic changes. However, TPP protected liver tissue from IRC-induced damage better than CE. The results of our study indicated that adding TPP to the treatment might be an effective therapeutic strategy for preventing IRC-induced hepatotoxicity. Moreover, based on the results of our literature review, our study was the first to compare the antioxidant and anti-inflammatory properties of TPP and CE. As a result of our current study, we are likely to contribute to future experimental and clinical studies on diseases where oxidative stress and inflammation are involved in the pathogenesis.

Competing interest

The authors declared no conflict of interest.

Data availability

Study data can be obtained from the corresponding author upon request.

Funding

None.

ORCID numbers

- Bahtinur Yeter (BY): 0000-0003-0336-8161
- Renad Mammadov (RM): 0000-0002-5785-1960
- Zeynep Koc (ZK): 0000-0002-0716-7773
- Seval Bulut (SB): 0000-0003-4992-1241
- Tugba Bal Tastan(TBT): 0000-0001-8257-8639
- Mine Gulaboglu (MG): 0000-0002-3248-1502
- Halis Suleyman (HS): 0000-0002-9239-4099

Author Contributions

BY: research concept and design, writing the article, critical revision of the article, final approval; RM: collection and/or assembly of data, final approval; ZK: collection and/or assembly of data, final approval; SB: data analysis and interpretation, writing the article, critical revision of the article, final approval; TBT: collection and/or assembly of data, final approval; MG: collection and/or assembly of data, final approval; HS: research concept and design, writing the article, final approval.

REFERENCES

1. **Combrink M, du Preez I.** Metabolomics describes previously unknown toxicity mechanisms of isoniazid and rifampicin. Toxicol Lett 2020;322:104-110.
2. **Suárez I, Fünger SM, Kröger S, Rademacher J, Fätkenheuer G, Rybniker J.** The diagnosis and treatment of tuberculosis. Dtsch Arztebl Int 2019;116:729-735.
3. **Forget EJ, Menzies D**. Adverse reactions to first-line antituberculosis drugs. Expert Opin Drug Saf 2006;5:231-249.
4. **Yew WW, Chang KC, Chan DP**. Oxidative stress and first-line antituberculosis drug-induced hepatotoxicity. Antimicrob Agents Chemother 2018;62:e02637-17
5. **Song L, Zhang ZR, Zhang JL, Zhu XB, He L, Shi Z, Gao L, Li Y, Hu B, Feng FM**. MicroRNA-122 is involved in oxidative stress in isoniazid-induced liver injury in mice. Genet Mol Res 2015;14:13258-13265.
6. **Ahadpour M, Eskandari MR, Mashayekhi V, Haj Mohammad Ebrahim Tehrani K, Jafarian I, Naserzadeh P, Hosseini MJ.** Mitochondrial oxidative stress and dysfunction induced by isoniazid: study on isolated rat liver and brain mitochondria. Drug Chem Toxicol 2016;39:224-232.
7. **Shuhendler AJ, Pu K, Cui L, Uetrecht JP, Rao J.** Real-time imaging of oxidative and nitrosative stress in the liver of live animals for drug-toxicity testing. Nat Biotechnol 2014;32:373-380.
8. **Askgaard DS, Wilcke T, Døssing M.** Hepatotoxicity caused by the combined action of isoniazid and rifampicin. Thorax 1995;50:213-214.
9. **Sica DA**. Loop diuretic therapy, thiamine balance, and heart failure. Congest Heart Fail 2007;13:244-247.
10. **Altuner D, Cetin N, Suleyman B, Aslan Z, Hacimuftuoglu A, Gulaboglu M, Isaoglu N, I Demiryilmaz I, Suleyman H.** Effect of thiamine pyrophosphate on ischemia-reperfusion induced oxidative damage in rat kidney. Indian J Pharmacol 2013;45:339-343.
11. **Acun Delen L, Korkmaz Dişli Z, Taş HG, Kuyrukluyildiz U, Yazici GN, Süleyman B, Kuzucu M, Gürsu C, Suleyman H.** The effects of thiamine pyrophosphate on propofol-induced oxidative liver injury and effect on dysfunction. Gen Physiol Biophys 2022;41:63-70.
12. **Turan MI, Cayir A, Cetin N, Suleyman H, Siltelioglu Turan I, Tan H.** An investigation of the effect of thiamine pyrophosphate on cisplatin-induced oxidative stress and DNA damage in rat brain tissue compared with thiamine: thiamine and thiamine pyrophosphate effects on cisplatin neurotoxicity. Hum Exp Toxicol 2014;33:14-21.
13. **Yanakiev S.** Effects of cinnamon (Cinnamomum spp.) in dentistry: A review. Molecules 2020;25:4184.

14. **Gruenwald J, Freder J, Armbruester N**. Cinnamon and health. Crit Rev Food Sci Nutr 2010;50:822-834.
15. **Dorri M, Hashemitabar S, Hosseinzadeh H.** Cinnamon (Cinnamomum zeylanicum) as an antidote or a protective agent against natural or chemical toxicities: a review. Drug Chem Toxicol 2018;41:338-351.
16. **Ho SC, Chang KS, Chang PW**. Inhibition of neuroinflammation by cinnamon and its main components. Food Chem 2013;138:2275-2282.
17. **Góth L.** A simple method for determination of serum catalase activity and revision of reference range. Clin Chim Acta 1991;196(2-3):143-151.
18. **Tostmann A, Boeree MJ, Aarnoutse RE, de Lange WC, van der Ven AJ, Dekhuijzen R.** Antituberculosis drug-induced hepatotoxicity: concise up-to-date review. J Gastroenterol Hepatol 2008;23(2):192-202.
19. **Enriquez-Cortina C, Almonte-Becerril M, Clavijo-Cornejo D, Palestino-Domínguez M, Bello-Monroy O, Nuño N, López A, Bucio L, Souza V, Hernández-Pando R, Muñoz L, Gutiérrez-Ruiz MC, Gómez-Quiroz LE.** Hepatocyte growth factor protects against isoniazid/rifampicin-induced oxidative liver damage. Toxicol Sci 2013;135:26-36.
20. **Aynaoglu Yildiz G, Yapca OE, Dinc K, Gursul C, Gundogdu B, Aktas M, Suleyman Z, Bulut S, Suleyman H.** Stress-associated ovarian damage, infertility, and delay in achieving pregnancy and treatment options. Invest Clin 2023;64:513-523. *doi.org/10.54817/IC.v64n4a08*
21. **Zhuang X, Li L, Liu T, Zhang R, Yang P, Wang X, Dai L.** Mechanisms of isoniazid and rifampicin-induced liver injury and the effects of natural medicinal ingredients: A review. Front Pharmacol 2022;13:1037814.
22. **Pelapelapon AA, Rohmawaty E, Herman H**. Evaluation of the hepatoprotective effect of *Plantago major* extract in a rifampicin-isoniazid induced hepatitis rat model. Trends in Sciences 2023;20:6331-6331.
23. **Sarandol E, Tas S, Serdar Z, Dirican M.** Effects of thiamine treatment on oxidative stress in experimental diabetes. Bratislavske Lekarske Listy 2020;121:235-241.
24. **Bedir Z, Erdem KTO, Can A,** Çiçek B**, Gülaboğlu M, Süleyman Z, Gürsul C, Mokhtare B,** Özçiçek F**, Süleyman H.** Effect of thiamine pyrophosphate upon possible metamizole-induced liver injury in rats. Int J Pharmacol 2023;19:139-146.
25. **Moselhy SS, Ali HK.** Hepatoprotective effect of cinnamon extracts against carbon tetrachloride induced oxidative stress and liver injury in rats. Biol Res 2009;42:93-98.
26. **Naji KM, Al-Khatib BY, Al-Haj NS, D'souza MR.** Hepatoprotective activity of melittin on isoniazid-and rifampicin-induced liver injuries in male albino rats. BMC Pharmacol Toxicol 2021;22:1-11.
27. **Zhang G, Zhu J, Zhou Y, Wei Y, Xi L, Qin H, Rao Z, Han M, Ma Y, Wu X.** Hesperidin alleviates oxidative stress and upregulates the multidrug resistance protein 2 in isoniazid and rifampicin-induced liver injury in rats. J Biochem Mol Toxicol 2016;30:342-349.
28. **Sanjay S, Girish C, Toi PC, Bobby Z**. Gallic acid attenuates isoniazid and rifampicin-induced liver injury by improving hepatic redox homeostasis through influence on Nrf2 and NF-κB signalling cascades in Wistar Rats. J Pharm Pharmacol 2021;73:473-486.
29. **El-Kholy M, Faried A, Ghada M**. Role of cinnamon extract in the protection against amoxicillin/clavulanate-induced liver damage in rats. IOSR-JPBS. 2019;14:14-21.
30. **Kaya A, Ceylan AF, Kavutcu M, Santamaria A, Šoltésová Prnová M, Stefek M, Karasu Ç.** A dual-acting aldose reductase inhibitor impedes oxidative and carbonyl stress in tissues of fructose-and streptozotocin-induced rats: comparison with antioxidant stobadine. Drug ChemToxicol 2023;5:1-11.
31. **He X, Song Y, Wang L, Xu J.** Protective effect of pyrrolidine dithiocarbamate on isoniazid/rifampicin–induced liver injury in rats. Mol Med Rep 2020;21:463-469.
32. **Yang J, Li G, Bao X, Suo Y, Xu H, Deng Y, Feng T, Deng G.** Hepatoprotective effects

of phloridzin against isoniazid-rifampicin induced liver injury by regulating CYP450 and Nrf2/HO-1 pathway in mice. Chem Pharm Bull 2022;70:805-811.

33. **Wang N, Jiang D, Zhou C, Han X.** Alpha-solanine inhibits endothelial inflammation via nuclear factor kappa B signaling pathway. Adv Clin Exp Med. 2023;32:909-920.
34. **Ozer M, Ince S, Gundogdu B, Aktas M, Uzel K, Gursul C, Suleyman H, Suleyman Z.** Effect of thiamine pyrophosphate on cyclophosphamide-induced oxidative ovarian damage and reproductive dysfunction in female rats. Adv Clin Exp Med 2022;31:129-137.
35. **Li B, Li J, Hu S**. Cinnamon could improve hepatic steatosis caused by a high-fat diet via enhancing hepatic beta-oxidation and inhibiting hepatic lipogenesis, oxidative damage, and inflammation in male rats. J Food Biochem 2022;46:e14077.
36. **Zhai H, Yang B, Fu Y, Zhang D, Li Y, Huang J.** Effects of somatostatin in combination with early hemoperfusion on inflammatory, hemorheological and oxidative parameters during the treatment of acute pancreatitis. Invest Clín. 2023;64:41-52.
37. **Wang Y, Che M, Xin J, Zheng Z, Li J, Zhang S.** The role of IL-1β and TNF-α in intervertebral disc degeneration. Biomed Pharmacother 2020;131:110660.
38. **Patel S, Chaturvedi A, Dubey N, Shrivastava A, Ganeshpurkar A.** Ascorbic acid ameliorates isoniazid-rifampicin-induced hepatocellular damage in rats. iLIVER. 2022;1:72-77.
39. **Ucak T, Karakurt Y, Tasli G, Cimen FK, Icel E, Kurt N, Ahiskali I, Süleyman H.** The effects of thiamine pyrophosphate on ethanol induced optic nerve damage. BMC Pharmacol Toxicol 2019;20:40.
40. **Kanuri G, Weber S, Volynets V, Spruss A, Bischoff SC, Bergheim I.** Cinnamon extract protects against acute alcohol-induced liver steatosis in mice. J Nutr 2009;139:482-487.
41. **Hussain S, Ashafaq M, Alshahrani S, Siddiqui R, Ahmed RA, Khuwaja G, Islam F**. Cinnamon oil against acetaminophen-induced acute liver toxicity by attenuating inflammation, oxidative stress and apoptosis. Toxicol Rep 2020;7:1296-1304.
42. **Yilmaz I, Demiryilmaz I, Turan M, Cetin N, Gul M, Süleyman H.** The effects of thiamine and thiamine pyrophosphate on alcohol-induced hepatic damage biomarkers in rats. Eur Rev Med Pharmacol Sci 2015;19:664-670.
43. **Uysal HB, Dağlı B, Yılmaz M, Kahyaoğlu F, Gökçimen A, Ömürlü İK, Demirci B.** Biochemical and histological effects of thiamine pyrophosphate against acetaminophen-induced hepatotoxicity. Basic Clin Pharmacol Toxicol 2016;118:70-76.
44. **Eidi A, Mortazavi P, Bazargan M, Zaringhalam J.** Hepatoprotective activity of cinnamon ethanolic extract against CCI4-induced liver injury in rats. Excli Journal. 2012;11:495.

Invest Clin 65(3): 335 - 345, 2024 https://doi.org/10.54817/IC.v65n3a06

Benefits of recombinant human brain natriuretic peptide to improve ventricular function and hemodynamics in patients with ST-elevation myocardial infarction.

Dahuan Shi[1], Xin Li[1], Lantao Yang[1], Chunmei Luo[1] and Jing Ma[2]

[1]Department of Emergency Medicine, Baoding No. 2 Central Hospital, Baoding, China.
[2]Department of Cardiovascular Medicine, Affiliated Hospital of Hebei University, Baoding, China.

Keywords: ST-segment elevation myocardial infarction; recombinant human brain natriuretic peptide; tirofiban; primary percutaneous coronary intervention.

Abstract. This study aimed to assess the impact of recombinant human brain natriuretic peptide (rh-BNP) on ventricular function and hemodynamics in post-ST-segment elevation myocardial infarction (STEMI). We compared the outcomes of 65 STEMI patients treated with rh-BNP to an equal cohort given tirofiban following percutaneous coronary intervention (PCI). Data collected pre- and post-intervention included biochemical markers, TIMI (Thrombolysis In Myocardial Infarction) grade, hemodynamics, thrombotic score (TS), left ventricular ejection fraction (LVEF), high-sensitivity C-reactive protein (CRP) levels, liver and kidney function, and ECG. The TIMI level ($p=0.03$), the ratio of TIMI myocardial perfusion grade III ($p=0.04$), and the thrombus score ($p<0.001$) in the rh-BNP group after the intervention markedly exceeded those in the tirofiban group. After correction, the TIMI frame count (CTFC) ($p=0.02$), the incidence of slow flow ($p=0.02$), thrombus score ($p<0.001$), stent length ($p=0.02$) as well as times of administration of sodium nitroprusside medication in the rh-BNP group were markedly below those in the tirofiban group ($p=0.01$). Creatine kinase (CK) ($p<0.001$), CK-MB ($p=0.01$), and N-terminal pro-b-type natriuretic peptide (NT-proBNP) ($p<0.02$) in the rh-BNP group were markedly below those the in tirofiban group 24 hours after intervention; and the sum-STR ($p<0.03$) immediately after intervention markedly exceeded that in the tirofiban group. No significant differences were found in major cardiac adverse events (MACE) between the treatments. At the 30-day follow-up, rh-BNP showed a more effective enhancement of blood flow status, with the safety profiles of both treatments being comparable. The findings suggest that the rh-BNP has significant potential for treating PPCI-related slow flow.

Corresponding author: Jing Ma. Department of Cardiovascular Medicine, Affiliated Hospital of Hebei University, Baoding, China. E-mail: MJ0111MJ@163.com

Beneficios del péptido natriurético cerebral humano recombinante para mejorar la función ventricular y la hemodinámica en pacientes con infarto de miocardio con elevación del segmento ST.

Invest Clin 2024; 65 (3): 335 – 345

Palabras clave: infarto de miocardio con elevación del segmento ST; péptido natriurético recombinante del cerebro humano; tirofibán; intervención coronaria percutánea primaria.

Resumen. El objetivo de este estudio fue evaluar el impacto del péptido natriurético cerebral humano recombinante (rh-BNP) sobre la función ventricular y la hemodinámica después de un infarto de miocardio con elevación del segmento ST (STEMI). Comparamos los resultados de 65 pacientes con STEMI tratados con rh-BNP con un grupo equivalente tratado con tirofiban tras la intervención coronaria percutánea (PCI). Los datos recopilados antes y después de la intervención incluyeron marcadores bioquímicos, grado TIMI (Trombolisis en infarto del miocardio), hemodinámica, puntuación trombótica (TS), fracción de eyección del ventrículo izquierdo (LVEF), niveles de proteína C reactiva de alta sensibilidad (CRP), función hepática y renal y ECG. El nivel de TIMI (p=0,03), la proporción de grado de perfusión miocárdica TIMI III (p=0,04) y la puntuación trombótica (p<0,001) en el grupo rh-BNP después de la intervención superaron significativamente a aquellos en el grupo de tirofiban. Tras la corrección, el conteo de fotogramas TIMI (CTFC) (p=0,02), la incidencia de flujo lento (p=0,02), la puntuación trombótica (p<0,001), la longitud del stent (p=0,02) así como las veces de administración de la medicación de nitroprusiato de sodio en el grupo rh-BNP fueron notablemente inferiores a los del grupo de tirofiban (p=0,01). La CK (p<0,001), la CK-MB (p=0,01) y la NT-proBNP (p<0,02) en el grupo rh-BNP fueron significativamente inferiores a los del grupo de tirofiban 24 horas después de la intervención, y la sum- ST-segment resolution (STR) (p<0,03), inmediatamente después de la intervención superó significativamente a la del grupo de tirofiban. No se encontraron diferencias significativas en los eventos adversos cardiacos mayores (MACE) entre los tratamientos. En el seguimiento de 30 días, el rh-BNP mostró una mejora más efectiva del estado del flujo sanguíneo, siendo los perfiles de seguridad de ambos tratamientos comparables. Los hallazgos sugieren que el rh-BNP tiene un potencial significativo para tratar el flujo lento relacionado con PPCI.

Received: 20-08-2023 Accepted: 11-02-2024

INTRODUCTION

ST-segment elevation myocardial infarction (STEMI) is a severe form of heart attack characterized by a prolonged period of blocked blood supply that affects a large area of the heart muscle [1]. The mean age of a first MI is 65.1 for men, while for women, it is 72. An ST-elevation myocardial infarction affects around 38% of patients with acute coronary syndrome when they arrive at the hospital [2].

STEMI is commonly caused by the rupture of an atherosclerotic plaque in a coronary artery, leading to the formation of a blood clot that completely blocks the artery and interrupts blood flow to the heart muscle. This results in myocardial ischemia and, if not promptly treated, irreversible damage to the heart muscle [1,2].

The symptoms of STEMI can include chest pain or discomfort, shortness of breath, nausea, lightheadedness, and pain or discomfort in other areas of the upper body, such as the arms, back, neck, jaw, or stomach [3].

Diagnosis of STEMI is primarily based on the clinical presentation, ECG findings, and the elevation of cardiac biomarkers. An ECG demonstrating ST-segment elevation is considered diagnostic, particularly when complemented by symptoms indicative of ischemia. Furthermore, cardiac enzymes such as troponins are utilized to confirm myocardial damage [1,4].

Treatment of STEMI focuses on the timely restoration of coronary blood flow, typically achieved through reperfusion therapies such as percutaneous coronary intervention (PCI) or thrombolytic therapy [5]. Adjuvant therapies include antiplatelet agents, anticoagulants, beta-blockers, and angiotensin-converting enzyme inhibitors to reduce myocardial oxygen demand and prevent further thrombus formation [6,7].

In this context, recombinant human brain natriuretic peptide (rhBNP) therapy emerges as a novel adjunct in managing STEMI. rhBNP, a synthetic form of the naturally occurring brain natriuretic peptide, has shown promise in improving ventricular function and hemodynamics [8]. Its mechanisms of action include vasodilation, natriuresis, and the inhibition of the renin-angiotensin-aldosterone system, which collectively contribute to reduced cardiac load and improved myocardial recovery [9]. According to a study by Zhou *et al.* [10], rhBNP has shown promise in improving ventricular function and hemodynamics in patients with end-stage renal disease and type 4 cardiorenal syndrome. Another study by Liang *et al.* suggests that rhBNP combined with catheter-directed therapy may improve right ventricular dysfunction and stabilize hemodynamics in patients with acute pulmonary embolism [11].

Given the high stakes of STEMI management and the potential impact on patient outcomes, a comprehensive evaluation of rhBNP's efficacy and safety is warranted. Since limited studies have been conducted in this field, especially in the Middle East, this study was essential to elucidate the effect of the therapeutic effect of recombinant human brain natriuretic peptide in patients with myocardial infarction by increasing the ST piece.

MATERIALS AND METHODS

General information

The research is a retrospective study using case data. The criteria for selecting patients in this study were as follows: the diagnosis of STEMI symptoms following views of the "STEMI Diagnosis and Treatment Guidelines" [6]; patients received PCI treatment within 12 h after admission; treatment with tirofiban (TIF) or rh-BNP after PCI; no allergic reactions were observed after treatment with TIF or rh-BNP; did not receive intravenous thrombolysis treatment before PCI; Killip level exceeds that of Grade III or cardiogenic shock patients. Exclusion criteria: patients with comorbidities of organ and tissue diseases such as brain, heart, kidney, and liver; patients with severe aortic stenosis; patients with mental or other cognitive impairments or who refuse to cooperate with the experiment; patients with pulmonary hypertension caused by pulmonary heart disease or other reasons; patients with a history of MI, valvular heart disease, dilated cardiomyopathy, HF, hypertrophic cardiomyopathy, or other general diseases. Given the above standards, this study collected the medical history information of 142 STEMI patients

admitted to our hospital from June 2021 to June 2023, with 130 participants included in the experimental study. In the queue, 65 patients received treatments with TIF, while the remaining cases received treatments with rh-BNP. All sufferers had clinical and pathological features taken and signed an informed consent form to use this information. This research was approved by the Ethics Committee of the Medical Center to collect relevant information from sufferers (approval number: MEC-2021-06). All work was carried out following the provisions of the Declaration of Helsinki. The research process is demonstrated in Fig. 1.

Treatment strategies

All patients took 300 mg aspirin orally, clopidogrel 300 mg/ticagrelor 180 mg, and intravenous heparin 5000 IU at admission. Coronary artery angiography (CAG) was carried out before intervention to determine the quantity of the pathological branches, for patients who received treatments with rh-BNP, 5 mg of medication was injected intravascularly during the intervention period, followed by implantation of a stent and re-administration of 5 mg of rh-BNP. If the symptoms of slow BF persisted, they were given a last 5 mg dose of rh-BNP. Sufferers who received treatments with TIF were slowly injected 5 mg/kg through the CA during the intervention period. After the stent implantation, 5 mg/kg TIF was administered via CA again. 3 mg/kg TIF was injected through the CA for sufferers with slow BF symptoms. After 24 hours of intervention, all patients were given aspirin 100 mg, clopidogrel 75 mg/ticagrelor 90 mg and heparin 5000 IU for 5-7 days. Patients were followed up for 30 days after discharge, and MACE (Major Adverse Cardiovascular Events) were recorded.

Measurement of treating outcomes

The myocardial infarction thrombolysis (TMI) classification, hemodynamic parameters, thrombotic score (TS) [7], left ventricular ejection fraction (LVEF), CRP level, uric acid, liver and kidney functions, electrocardiogram (ECG), echocardiography and other information of patients before and after the intervention were collected to compare differences in the therapeutic effects (treatment efficacy) and SE of the two treatment methods.

Statistical analysis

Relevant analysis was conducted using the SPSS version 19.0 software (IBM®,

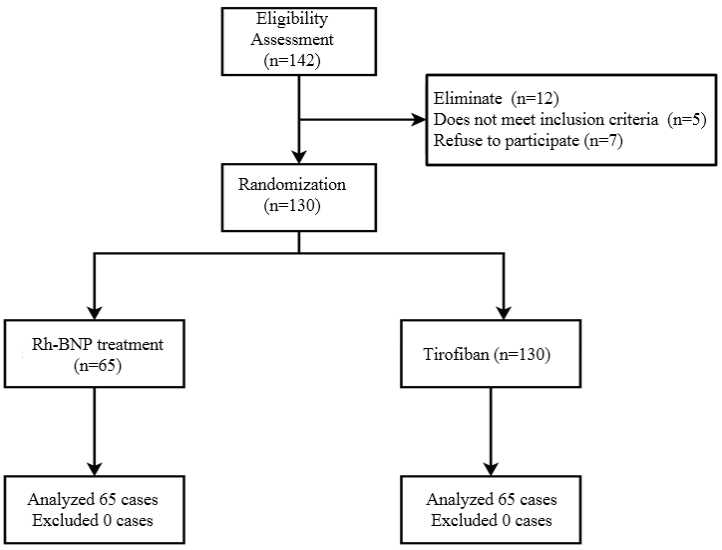

Fig. 1. Research Process.

Armonk, NY). Continuous data was denoted by mean ± standard deviation (SD). The number of cases denotes classified data. The Student test was used to compare the differences between consecutive data sets. Chi-square and Fisher's exact tests were used to determine whether there are differences between different categories of index groups. $p<0.05$ is statistically significant.

RESULTS

Patient baseline characteristics

The analysis of baseline data among the sufferers participating in this experiment did not demonstrate significant differences (SD) in preoperative age, body mass index (BMI), and other indicators. Table 1 demonstrates the details.

No statistically significant differences were among the sufferers participating in this experiment in combined medication (Table 2).

Intervention Information

Table 3 indicates no differences in the number of branches, number of stents, and score of thrombus before the intervention, systolic blood pressure, and other relevant respects. However, after the intervention, the TMI changes in thrombus score levels in the rh-BNP group and other relevant aspects dramatically exceeded those in the TIF group (Table 3). On the other hand, the TMI Frame Count (CTFC), slow flow (SF) incidence, post-intervention thrombus score, stent length, and sodium nitroprusside administration times after correction were dramatically ´lower in the TIFgroup (Table 3).

The effect of rh-BNP or TIF on the treating outcomes of PCI

Twenty-four hours after PCI intervention, creatine kinase (CK), creatine kinase isozyme (CKMB), and the amino-terminal fraction of B-type natriuretic peptide (NT pro-BNP) in the rh BNP group were dramati-

Table 1
Baseline Characteristics.

Characteristic	rh-BNP(n=65)	TIF(n=65)	t/χ^2	*p*
Age (years)	60.19±10.02	58.96±10.14	1.462	0.09
Gender (male, %)	47(72.3)	51(78.5)	-0.613	0.36
BMI(kg/m^2)	25.94±3.54	25.44±3.29	0.837	0.50
Time before balloon dilation(min)	227.98±68.52	232.19±86.43	-0.388	0.63
Killip classification				
Level 1 (n, %)	61(93.8)	60(92.3)	0.117	0.69
Level 2 (n, %)	4(6.2)	5(7.7)		
Smoke (n,%)	41(63.1)	40(61.5)	0.035	0.85
Drink (n,%)	24(36.9)	14(21.5)	3.710	0.06
Hypertension (n, %)	41(63.1)	47(72.3)	1.258	0.27
Level 1 (n, %)	8(12.3)	7(10.8)		
Level 2 (n, %)	16(24.6)	14(21.5)	0.286	0.85
Level 3 (n, %)	17(26.2)	19(29.2)		
Diabetes (n, %)	18(27.7)	21(32.3)	0.328	0.56
Cerebral Infarction (n, %)	8(12.3)	11(16.9)	0.525	0.49

t: t-test; χ^2: Chi-squared test; BMI: body mass index; rh-BNP: B-type recombinant human brain peptide.
TIF: tirofiban.

Table 2
Information on drug combination use.

Characteristic	rh-BNP (n=65)	TIF (n=65)	t/χ^2	*p* value
Ticagrelor (n, %)	59(90.8)	61(93.8)	-	0.39
Statins (n, %)	62(95.4)	61(93.8)	-	0.53
Nitrates (n, %)	45(69.2)	48(73.8)	0.443	0.44
β-blocker (n, %)	57(87.7)	52(80.0)	1.690	0.13
ACEI/ARB	52(80.0)	56(86.2)	1.259	0.29
CCB (n, %)	21(32.3)	22(33.8)	0.884	0.36
PPI (n, %)	48(73.8)	52(80.0)	0.705	0.44
Hypoglycemic drugs (n, %)	21(32.3)	23(35.4)	0.327	0.53

t: t-test, χ^2: Chi-squared test; rh-BNP: B-type recombinant human brain natriuretic peptide; TIF: tirofiban; ACEI: ACE inhibitor; ARB: angiotensin II receptor antagonist; CCB: calcium channel blocker (calcium antagonist); PPI: proton pump inhibitor.

cally lower than in the TIF group. The LEVF changes in the rh-BNP group (RBG) dramatically exceeded those in the TIF group. (Table 4).

However, there were no statistical differences among the sufferers participating in this experiment in CK (p=0.13) and CKMB (p=0.18) at the peak recording time points. The sum STR in the RBG also markedly exceeded that in the TIF group immediately after intervention (Table 5), and there were no differences in sum STR two hours after the intervention (Table 5).

Major Adverse Cardiovascular Events (MACE)

The incidence of angina and HF in the RBG was dramatically lower than in the TIF group (Table 6). On the other hand, in terms of CA occlusion microbleeds, the incidence of TMI microbleeds, the overall utilization of streptokinase, tissue type plasmin activator, and other relevant aspects in the RBG markedly exceeded those in the TIF group (Table 6). Both groups of patients did not experience MI or other severe side effects (Table 6).

Discharge follow-up

After discharge, there was no follow-up loss for 30 days. According to the information shown in Table 7, there were no differences in physiological indicators and MACE among the patients participating in this experiment (Table 7).

DISCUSSION

PCI can markedly unblock the infarcted CA and was chosen as the first-line treatment strategy for STEMI clinical treatment. Recent studies given a large sample suggest that PCI can construct BF in >90% of IRA and restore TMI to level 3 [12]. However, the effect of PCI is offset by some severe side effects. Slow/no BF is a risk element influencing the prognosis of SEMI patients. Some drugs were utilized to enhance the therapeutic effect of PCI to enhance coronary BF after PCI.

Compared to studies with TIF, few people have focused on the influence of rh-BNP on coronary BF after PCI. Guo *et al.* showed that compared to patients treated with PCI alone, rh-BNP can significantly reduce the incidence of slow BF, indicating the potential of rh-BNP to improve BF after PCI [13]. Therefore, this study compared the therapeutic influences of rh-BNP and TIF on PCI-related slow/no flow. The outcomes demonstrated that compared with TIF, administering rh-BNP markedly reduced the occurrence of SF after PCI.

Table 3
Information on treatment outcomes for patients with myocardial infarction with elevation of the segment ST (STEMI) and percutaneous coronary intervention (PCI) patients.

Characteristic	rh-BNP (n=65)	TIF (n=65)	t/χ^2	*p* value
Number of branches				
Single branch (n,%)	8(12.3)	7(10.8)		
Double branches (n,%)	19(29.2)	17(26.2)		
Three branches (n,%)	38(58.5)	41(63.1)	0.286	0.87
IRA distribution				
LAD (n,%)	33 (50.8)	38(58.5)		
LCX (n,%)	10 (15.4)	7(10.8)		
RCA (n,%)	22 (33.8)	20(30.8)	0.977	0.61
TMI level before PCI				
Level 0 (n,%)	19(29.2)	25(38.5)	2.298	0.51
Level 1 (n,%)	8(12.3)	8(12.3)		
Level 2 (n,%)	9(13.8)	11(16.9)		
Level 3 (n,%)	29(44.6)	21(32.3)		
TMI level after PCI				
Level 0 (n,%)	1(1.5)	2(2.3)	-	0.03
Level 1 (n,%)	2(3.1)	7(6.9)		
Level 2 (n,%)	6(9.2)	11(13.1)		
Level 3 (n,%)	56(86.2)	45(77.7)		
CTFC after PCI (FPS)	23.60±4.05	25.57±5.29	-2.381	0.02
Level 3 TMPG after PCI (n,%)	58(89.2)	49(75.5)	4.279	0.04
TS score before PCI	3(2,4)	3(2,4)	-1.45	0.15
TS score after PCI	0(0,1)	1(0,1)	-3.908	<0.001
TS score changes	3(2,3)	1(1,1)	-4.263	<0.001
Support number	1(1,1)	1(1,2)	-0.898	0.37
Support length(mm)	26.4±11.33	31.35±12.93	-2.323	0.02
Thrombotic aspiration during intervention (n,%)	15(23.1)	14(21.5)	0.044	0.83
Intraoperative hypotension (n,%)	5(7.7)	7(10.8)	0.367	0.55
Intraoperative systolic blood pressure (mmHg)	125.58±18.87	122.88±21.06	0.772	0.44
Intraoperative diastolic blood pressure (mmHg)	70.66±5.09	70.69±11.50	-0.2	0.98
HR (n/min)	72.23±8.46	72.58±7.65	-0.25	0.80
SF/no flow (n,%)	9(13.8)	20(30.8)	5.370	0.02
Use of sodium nitroprusside (n,%)	4(6.2)	15(23.1)	-	0.01

t: t-test, $\chi 2$: Chi-squared test; rh-BNP: B-type recombinant human brain natriuretic peptide; TIF: tirofiban; CTFC: corrected TMI frame count; FPS: frames per second; IRA: infarction-related artery; LAD: anterior descending branch of left CA; LCX: left circumflex branch; PCI: primary PCI; RCA: right CA; rh-BNP: B-type recombinant human brain natriuretic peptide; TMI: thrombolysis for MI; TMPG: TMI myocardial perfusion level; TS: thrombotic score; HR: heart rate; SF: slow flow.

Table 4
Effects of two treating methods on ventricular function and ejection fraction.

Characteristic	rh-BNP (n=65)	TIF (n=65)	t/χ^2	*p*
CK peak (U/L)	2108±1452	3562±1609	0.260	0.13
CKMB peak (U/L)	168.4±112.3	206.9±139.2	0.117	0.18
Ln (NT-proBNP)	5.96±0.75	7.43±0.93	0.122	0.15
LEVF	48.32±9.86	52.08±10.04	0.103	0.42

t: t-test, χ^2: Chi-squared test; rh-BNP: B-type recombinant human brain natriuretic peptide; TIF: tirofiban; CK: creatine kinase; CKMB: creatine kinase isozyme; NT-proBNP: N-terminal pro B-type natriuretic peptide.

Table 5
The impact of two treatment methods on the total STR at two hours after PCI surgery.

Characteristic	rh-BNP (n=65)	TIF (n=65)	t/χ^2	*p*
Total STR after PCI surgery				
<30% (n,%)	5(7.7)	12(18.5)		
30%-70% (n,%)	13(21.5)	21(32.3)		
>70% (n,%)	47(70.8)	32(49.2)	6.795	0.03
Total STR at two hours after PCI surgery				
<30% (n,%)	3(4.6)	8(12.3)		
30%-70% (n,%)	9(13.8)	12(18.5)		
>70% (n,%)	53(81.5)	45(69.2)	3.408	0.17

t: t-test, χ^2: Chi-squared test; Rh BNP: B-type recombinant human brain natriuretic peptide; TIF: tirofiban; PCI: primary PCI; STR: ST-segment resolution.

Table 6
The impact of two treatment methods on the total STR at two hours after PCI surgery.

Characteristic	rh-BNP (n=65)	TIF (n=65)	t/χ^2	*p*
Heart failure (n, %)	11(16.9)	23(35.4)	5.735	0.03
Mortality (n, %)	1(1.5)	0(0)	-	0.32
Angina pectoris (n, %)	8(12.3)	18(27.7)	4.808	0.03
TMI level				
Microbleeds (n, %)	17(26.2)	8(12.3)	4.011	0.04
GUSTO				
pyorrhea (n, %)	17(26.2)	8(12.3)	4.011	0.05

t: t-test, χ^2: Chi-squared test; PCI: primary PCI; STR: ST-segment resolution: rh-BNP: B-type recombinant human brain natriuretic peptide; TIF: tirofiban; TMI: thrombolysis myocardial infarction; GUSTO: the application of streptokinase and tissue type plasmin activator in the treatment of coronary occlusion.

In addition, the thrombus score of patients receiving treatments with rh-BNP was evidently lower than that of TIF. It may be due to the more substantial thrombolytic function of rh-BNP on existing thrombi in the CA[14]. Regarding biochemical parameters, the two clinically recognized myocardial function indicators, CK and CKMB, showed significantly lower peak levels in the RBG compared to the TIF group.

Table 7
The impact of two treatment methods on the total STR at two hours after PCI surgery.

Characteristic	rh-BNP (n=65)	TIF (n=65)	t/χ^2	*p*
CK (U/L)	82.50±27.29	80.66±29.18	0.369	0.71
CKMB (U/L)	12.58±6.76	12.63±6.91	0.046	0.95
HSCRP (mg/L)	2.18±1.09	2.52±1.61	1.381	0.16
Ln (NT-proBNP)	5.23±0.85	5.41±1.22	0.941	0.34
LVEF (%)	17(26.2)	8 (12.3)	4.011	0.04
Mortality	0	0	-	-
Secondary MI	0	0	-	-
Treatment Failure	5(7.8)	9(13.8)	1.209	0.26
Angina pectoris	7(10.9)	5(9.3)	0.427	0.55

t: t-test, χ^2: Chi-squared test; PCI: primary PCI; STR: ST-segment resolution. rh-BNP: B-type recombinant human brain natriuretic peptide; TIF: tirofiban; CK: creatine kinase; CK-MB: creatine kinase-myocardial band; NT-proBNP: N-terminal pro b-type natriuretic peptide; LVEF: left ventricular ejection fraction.

At the same time, side effects were absent among the sufferers participating in this experiment at the peak time point [15]. In addition, the NT pro-BNP, which serves as a marker for the degree of myocardial injury, was also lower in the RBG than in the TIF group [16]. These data clearly indicate that rh-BNP has a more substantial protective effect on PCI treatment-related injuries than TIF.

The electrocardiogram examination of the patient's myocardial function revealed that the sum-STR changes in the RBG were superior to those in the TIF group. Previous studies demonstrated a positive correlation between the recovery of myocardial ischemic injury and the recovery of sum-STR [17]. Integrated with the significant changes in LVEF in the RBG, it can be seen that the improvement in the influence of rh-BNP on myocardial function is also more marked than that of TIF. In addition, the incidence of MACE in the RBG was below that in the TIF group, representing rh-BNP's safety in clinical application. This study followed all patients for 30 days after discharge, and the results showed no differences in biochemical, myocardial function, MACE, and other parameters between the two groups of patients, further proving the potential of rh-BNP in improving CA BF after PCI surgery. Existing research also indicates that the influence of rh-BNP on the heart is more pronounced after intervening, but over time, the disparity in treating efficacy in the two drugs decreases. This decrease may be because of the more substantial function of rh-BNP in enhancing microcirculation by dissolving small blood clots [14].

In conclusion, the current research compared the effectiveness of rh-BNP and TIF in preserving STEMI patients from PCI-related ischemia/reperfusion (I/R) injury. The results show that both drugs significantly reduce the occurrence of SF and MCAE and improve myocardial function. Additionally, during the 30-day follow-up, rh-BNP had a more substantial immediate effect on most indicators after the intervention than TIF. The safety of its application was similar, suggesting good potential for clinical use in treating PCI-related SF.

Notably, the study has various limitations. Firstly, it is a retrospective study using case data, potentially introducing bias and limiting the findings' generalizability. Secondly, the sample size is relatively small. Thirdly, the study lacks information on the long-term outcomes of the two treatment

methods, which is crucial for understanding their overall effectiveness and safety.

ACKNOWLEDGMENTS

We want to express our gratitude to everyone who contributed their time, effort, and expertise to make this study successful.

Funding

None

Conflict of interests

There are no conflicting interests

Authors' ORCID number

- Dahuan Shi (DS): 0009-0005-3133-426X
- Xin Li (XL): 0000-0001-7588-3328
- Lantao Yang (LY): 0000-0002-0277-4355
- Chunmei Luo (CL): 0000-0002-8823-8296
- Jing Ma (JM): 0000-0002-6120-5857

Authors contribution

DS, XL: Designed the study work and performed the experiments. LY, CL: Analyzed the data and wrote the manuscript. JM: Drafted and edited the manuscript.

REFERENCES

1. **Domienik-Karłowicz J, Kupczyńska K, Michalski B, Kapłon-Cieślicka A, Darocha S, Dobrowolski P, Wybraniec M, Wańha W, Jaguszewski M.** Fourth universal definition of myocardial infarction. Selected messages from the European Society of Cardiology document and lessons learned from the new guidelines on ST-segment elevation myocardial infarction and non-ST-segment elevation-acute coronary syndrome. Cardiol J 2021;28(2):195-201. *https://doi.org/10.5603%2FCJ.a2021.0036*.
2. **Akbar H, Foth C, Kahloon RA, Mountfort S**. Acute ST-Elevation Myocardial Infarction. StatPearls. Treasure Island (FL) ineligible companies. StatPearls Publishing, Copyright © 2024, StatPearls Publishing LLC.; 2024.
3. **Mechanic OJ, Gavin M, Grossman SA**. Acute Myocardial Infarction. StatPearls. Treasure Island (FL) ineligible companies. StatPearls Publishing, Copyright © 2024, StatPearls Publishing LLC.; 2024.
4. **Ibanez B, James S, Agewall S, Antunes MJ, Bucciarelli-Ducci C, Bueno H, Caforio ALP, Crea F, Goudevenos JA, Halvorsen S, Hindricks G, Kastrati A, Lenzen MJ, Prescott E, Roffi M, Valgimigli M, Varenhorst C, Vranckx P, Widimský P, Group ESD.** 2017 ESC Guidelines for the management of acute myocardial infarction in patients presenting with ST-segment elevation: The Task Force for the management of acute myocardial infarction in patients presenting with ST-segment elevation of the European Society of Cardiology (ESC). Eur Heart J 2017;39(2):119-177. *https://doi.org/10.1093/eurheartj/ehx637*
5. **Elendu C, Amaechi DC, Elendu TC, Omeludike EK, Alakwe-Ojimba CE, Obidigbo B, Akpovona OL, Oros Sucari YP, Saggi SK, Dang K, Chinedu CP.** Comprehensive review of ST-segment elevation myocardial infarction: Understanding pathophysiology, diagnostic strategies, and current treatment approaches. Medicine (Baltimore) 2023;102(43):e35687. *https://doi.org/10.1097%2FMD.0000000000035687*.
6. **Szummer K, Jernberg T, Wallentin L.** From early pharmacology to recent pharmacology interventions in acute coronarysyndromes: JACC State-of-the-Art Review. J Am Coll Cardiol 2019;74(12):1618-1636. *https://doi.org/10.1016/j.jacc.2019.03.531*.
7. **Donisan T, Balanescu DV, Iliescu G, Marmagkiolis K, Iliescu C.** Acute Coronary Syndrome, Thrombocytopenia, and Antiplatelet Therapy in Critically Ill Cancer Patients. In: Nates JL, Price KJ, editors.

Oncologic Critical Care. Cham: Springer International Publishing; 2020. p. 711-732.

8. **Li F, Li H, Luo R, Pei JB, Yu XY.** Lyophilized recombinant human brain natriuretic peptide for chronic heart failure: Effects on cardiac function and inflammation. World J Clin Cases 2023;11(26):6066-6072. *http://dx.doi.org/10.12998/wjcc.v11.i26.6066.*
9. **Zhang S, Wang Z**. Effect of recombinant human brain natriuretic peptide (rhBNP) versus nitroglycerin in patients with heart failure: A systematic review and meta-analysis. Medicine (Baltimore) 2016;95(44):e4757. *https://doi.org/10.1097%2FMD.0000000000004757.*
10. **Zhou Y, Wang X, Yuan H, Wu L, Zhang B, Chen X, Zhang Y.** Impact of recombinant human brain natriuretic peptide on emergency dialysis and prognosis in end-stage renal disease patients with type 4 cardiorenal syndrome. Sci Rep. 2023;13(1):20752. *https://doi.org/10.1038/s41598-023-48125-1.*
11. **Liang L, Tang R, Xie Q, Han J, Li W.** The clinical effect of recombinant human brain natriuretic peptide on asymptomatic periprocedural myocardial injury after percutaneous transluminal coronary angioplasty. Sci Rep. 2020;10(1):15902. *https://doi.org/10.1038/s41598-020-72710-3.*
12. **Kampinga MA, Vlaar PJ, Fokkema M, Gu YL, Zijlstra F.** Thrombus Aspiration during percutaneous coronary intervention in acute non-ST-elevation myocardial infarction Study (TAPAS II)-Study design. Neth Heart J 2009;17(11):409-413. *https://doi.org/10.1007/bf03086293.*
13. **Guo Z, Liu W, Xin S, Nizzati M, Li G.** Follow-up observation of one year's treatment of acute ST-elevated myocardial infarction via reverse thrombolysis combined PCI surgery. J Xinjiang Med Univ. 2017;40(1):4.14.
14. **Zhao L, Zhao Z, Chen X, Li J, Liu J, Li G.** Safety and efficacy of prourokinase injection in patients with ST-elevation myocardial infarction: phase IV clinical trials of the prourokinase phase study. Heart Vessels. 2018;33(5):507-512. *https://doi.org/10.1007/s00380-017-1097-x.*
15. **Zhonghua Z, Xue X, Bing G, Zhi Z.** [2019 Chinese Society of Cardiology (CSC) guidelines for the diagnosis and management of patients with ST-segment elevation myocardial infarction]. Zhonghua xin xue guan bing za zhi. 2019;47(10):766-783. *https://doi.org/10.3760/cma.j.issn.0253-3758.2019.10.003.*
16. **Cao Z, Jia Y, Zhu B.** BNP and NT-proBNP as diagnostic biomarkers for cardiac dysfunction in both clinical and forensic medicine. Int J Mol Sci 2019;20(8):1820. *https://doi.org/10.3390%2Fijms20081820.*
17. **Van 't Hof AW, Liem A, de Boer MJ, Zijlstra F.** Clinical value of 12-lead electrocardiogram after successful reperfusion therapy for acute myocardial infarction. Zwolle Myocardial infarction Study Group. Lancet (London, England). 1997;350(9078):615-9. *https://doi.org/10.1016/s0140-6736(96)07120-6.*

Invest Clin 65(3): 346 - 357, 2024 https://doi.org/10.54817/IC.v65n3a07

The effect of regular exercise combined with quantitative nutritional support on immune function indicators such as CD3+, CD4+, CD8+, and nutritional status in dialysis patients.

Chunfeng Kong[1] and Changdong Zhu[2]

[1]Department of Hemodialysis, Lujiang County People's Hospital, Hefei, China.
[2]Department of Clinical Laboratory, Lujiang County People's Hospital, Hefei, China.

Keywords: hemodialysis; immune function; nutritional status.

Abstract. To study the effect of regular exercise and quantitative nutritional support on dialysis patients' immune function indicators and nutritional status, 100 uremic patients who underwent hemodialysis treatment in our hospital from February 2021 to February 2023 were selected as the study subjects. They were divided into a control group (n=50) that received regular exercise and routine nutritional support, and a research group (n=50) that received regular exercise and quantitative nutritional support. This study compared the baseline levels of nutritional indicators such as prealbumin (PA), transferrin (TF), serum albumin (SAB), and hemoglobin (HB); cellular immune indicators such as CD3+, CD4+, and CD8+; as well as humoral immune indicators such as immunoglobulin A (IgA), immunoglobulin G (IgG), and immunoglobulin M (IgM) at enrollment and after three months of intervention. At the time of enrollment, there were no significant differences in nutritional indicators between the two groups of patients ($p>0.05$), nor in the levels of cellular immune indicators ($p>0.05$) or humoral immune indicators ($p>0.05$). After three months of intervention, nutritional indicators such as PA in all patients in the experiment grew ($p<0.05$), and those in the research group exceeded the control group ($p<0.05$). Similarly, the levels of CD3+ and other cellular immune indicators and the concentrations of IgA and other humoral immune indicators increased in both groups after three months of intervention ($p<0.05$). However, these increases were higher in the research group than in the control group ($p<0.05$). Regular exercise combined with quantitative nutritional support can effectively improve hemodialysis patients' nutritional index levels, nutritional status, immune index levels, and immune function.

Corresponding author: Changdong Zhu. Department of Clinical Laboratory, Lujiang County People's Hospital, Hefei, China. E-mail: zhucd2023@163.com

Efecto del ejercicio regular, combinado con soporte nutricional cuantitativo, sobre indicadores de la función inmune tales como CD3+, CD4+, CD8+, y el estado nutricional en pacientes en diálisis.

Invest Clin 2024; 65 (3): 346 – 357

Palabras clave: hemodiálisis; función inmune; estado nutricional.

Resumen. Para estudiar el efecto del ejercicio regular y el apoyo nutricional cuantitativo sobre los indicadores de función inmune y el estado nutricional de los pacientes en diálisis, se seleccionaron como sujetos de estudio 100 pacientes urémicos que se sometieron a tratamiento de hemodiálisis en nuestro hospital desde febrero de 2021 hasta febrero de 2023. Se dividieron en un grupo control (n=50) que recibió ejercicio regular y apoyo nutricional de rutina y un grupo de investigación (n=50) que recibió ejercicio regular y apoyo nutricional cuantitativo. Este estudio comparó los niveles basales de indicadores nutricionales como prealbúmina (PA), transferrina (TF), albúmina sérica (SAB) y hemoglobina (HB); indicadores inmunes celulares tales como CD3+, CD4+ y CD8+; así como indicadores inmunes humorales como inmunoglobulina A (IgA), inmunoglobulina G (IgG) e inmunoglobulina M (IgM) al momento de la inscripción y después de tres meses de intervención. En el momento del reclutamiento, no hubo diferencias significativas en los indicadores nutricionales entre los dos grupos de pacientes ($p>0,05$), ni en los niveles de indicadores inmunes celulares ($p>0,05$) o indicadores inmunes humorales ($p>0,05$). Después de tres meses de intervención, los indicadores nutricionales como la PA en todos los pacientes del experimento aumentaron ($p<0,05$), y los del grupo de investigación superaron al grupo control ($p<0,05$). De manera similar, los niveles de CD3+ y otros indicadores inmunes celulares y las concentraciones de IgA y otros indicadores inmunes humorales aumentaron en ambos grupos después de tres meses de intervención ($p<0,05$). Sin embargo, estos aumentos fueron mayores en el grupo de investigación que en el grupo control ($p<0,05$). El ejercicio regular combinado con apoyo nutricional cuantitativo puede mejorar eficazmente los niveles de índices nutricionales, el estado nutricional, los niveles de índices inmunológicos y la función inmune de los pacientes en hemodiálisis.

Received: 09-12-2023 Accepted: 02-03-2024

INTRODUCTION

Hemodialysis (HD) is a renal replacement therapy commonly used in patients with advanced or end-stage renal disease. Diabetes nephropathy accounts for a high proportion of HD, which is consistent with the increasing trend of the number of diabetes patients [1]. When the kidneys lose normal function, HD draws the patient's blood out of the body, simulates kidney function through a special filter to remove waste, toxins, and excess water from the body, and then reinfuses the purified blood back into the patient's body to maintain water-electrolyte and acid-base balance. This process can

help patients maintain and improve their quality of life [2]. However, at the same time as treatment, patients may experience complications such as malnutrition [3].

During the HD process, waste and excess water in the patient's body are discharged through a dialyzer, which may increase the patient's metabolic rate and energy consumption. Dialysis patients must limit their intake of substances such as sodium, potassium, and phosphorus during and between treatment periods while also controlling their water intake, which may lead to loss of appetite and reduced intake. When energy intake is insufficient to meet the patient's metabolic needs, it can lead to energy expenditure exceeding the intake, leading to malnutrition [4]. During dialysis, some nutrients and proteins may be removed along with the waste, leading to protein loss. The inflammatory response and chronic inflammatory state during dialysis may lead to metabolic disorders, promote protein breakdown, accelerate protein loss, and lead to malnutrition [5]. The causes of HD malnutrition include both iatrogenic and non-iatrogenic factors. Possible factors related to iatrogenic factors include poor dialysis adequacy and excessive loss of serum albumin during dialysis, while non-iatrogenic factors include poor appetite and insufficient nutrition supplementation. These factors can be changed and incorporated into the nutritional assessment [6].

When dialysis patients are in a state of severe metabolic stress, a sharp decrease in serum albumin and a significant decrease in albumin and hemoglobin are usually observed. These changes are usually accompanied by a deterioration in the overall health status of patients and are unlikely to respond to adjustments in dialysis plans. In such cases, targeted nutritional interventions and protein supplementation must be used during dialysis [7]. Protein-energy malnutrition and deficiency of single nutrients can affect immune responses [8]. When immune cells are activated, they can meet nutritional needs through anaerobic respiration. Signals from adipose tissue limit the activity and quantity of immune cells in nutrient-deficient situations [9]. Under malnutrition, the secretion of adipokines is dysregulated, affecting the activity of immune cells and leading to an increased susceptibility of inflammatory autoimmune reactions to infectious diseases[10]. Long-term protein deprivation correlates the degree of malnutrition in body weight with the antibody response in the humoral immune response [11]. Nutritional metabolism is related to the differentiation and function of various immune cells, and nutritional intervention can manipulate immune cell function. Nutritional intervention can enhance nutritional status, affecting immune cell dynamics [12]. This study applies regular exercise combined with quantitative nutritional intervention to HD patients and analyzes its effectiveness.

PATIENTS AND METHODS

General Information: The research subjects of this study consisted of 100 uremic patients who received HD treatment in our hospital from February 2021 to February 2023. The patients knew the purpose of the research, agreed to participate, and signed an informed consent form. Inclusion criteria: (a) Dialysis time≥6 months. (b) Age≥18 years old. (c) Regular dialysis 2-3 times a week. (d) Comply with the diagnostic criteria for malnutrition in the GLIM Malnutrition Diagnostic Standards - Global Consensus Report in Clinical Nutrition receive nutritional support. (e) Stable conditions, electrolyte disorders, acidosis, and other uremic signs have been effectively controlled. Exclusion criteria: (a) Concomitant acute gastrointestinal diseases. (b) Concomitant malignant tumors and other malignant consumptive diseases. (c) Presented diseases that affect metabolism, such as hyperthyroidism and adrenal diseases. (d) Significant edema of pleural and abdominal effusion. (e) The combination of severe depression and recent poor appetite that led to a decrease in body

mass index. Other exclusion criteria: (a) deterioration of the condition or death during the study. (b) Missing visits. (c) Automatic exit. This study included 100 patients, with no excluded cases. Upon meeting the inclusion criteria, participants were randomly assigned into two groups to ensure comparability and to minimize selection bias. Data were systematically collected at two distinct time points: baseline data at the beginning of the study and follow-up data upon intervention completion. Eighty valid data were collected, and the effective data recovery rate was 100%. There were no significant differences in general information such as gender, age, body mass index, and primary disease between the two groups of patients ($p>0.05$), as shown in Table 1.

Method: A nutritional assessment was conducted on the included patients, and their nutritional status was evaluated based on the Malnutrition Universal Screening Tool (MUST). BMI ≥ 20.0 was scored as 0. A BMI between 18.5 and 20.0 was 1 point. BMI ≤ 18.5 was 2 points, or weight loss within 5% in the past 3-6 months was 0 points. Weight loss between 5% and 10% in the past 3-6 months was 1 point. Weight loss of more than 10% in the past 3-6 months was 2 points. Fasting or consuming food less than five days due to acute illness was 2 points. A score of 0 indicates a low nutritional risk state, and regular nutritional screening is sufficient. A score of 1 indicated a moderate nutritional risk state, requiring recording dietary intake status within three days and repeated screening. A score of 2 or more indicated a high-risk state and required nutritional intervention. After evaluation, the patient's BMI was ≤ 18.5, indicating a high-risk state and requiring nutritional intervention.

Control Group (CG): Regular exercise combined with routine nutritional support. Regular exercise: When patients came to the hospital for treatment, exercise education was carried out, and patients were advised to take moderate walks indoors and outdoors and engage in mild aerobic exercises such as jogging, cycling, and swimming. Exercise should be carried out 2 hours after meals, and loose and breathable clothes suitable for the ambient temperature should be worn. Before and after exercise, measuring the pulse and keeping records was necessary. If there was any discomfort during exercise, it should have to be stopped immediately, and excessive exercise should be avoided. The frequency of exercise was 3-5 times a week, and the heart rate of exercise needed to be 20 times/min higher than the resting rate. Each walk took 2-3 minutes and required 2-3 minutes of rest, with an average of 60-80 steps per minute, alternating. Nutritional support: Based on the patient's condition and dietary habits, it was essential to know

Table 1
Comparison of general information between two groups of patients.

Group	n	Gender		Age (years)	BMI (kg/m^2)	Primary disease			
		Male	Female			Chronic glomerulonephritis	Diabetic nephropathy	Polycystic kidney	Other
Control Group	50	28 (56)	22 (44)	56.56±12.36	18.49±3.21	13 (26)	15 (30)	11 (22)	11 (22)
Research Group	50	30 (60)	20 (40)	57.12±12.40	18.50±3.20	14 (28)	14 (28)	10 (20)	12 (24)
χ^2/t	-	0.164		0.226	0.016		0.163		
p	-	0.685		0.822	0.988		0.983		

Values are expressed as n (%) or X±SD.

how to correctly use scale tools such as salt spoons and oil cups to help patients match their daily meals and master nutritional support. Then, it was necessary to encourage patients to record and grasp their nutritional intake. Weekly dietary surveys needed to be conducted on patients, and timely guidance and supplementation should be provided for any unreasonable situation. It is also necessary to correct unhealthy dietary habits and adjust dietary plans.

Research group (RG): In the study, the rRG received a comprehensive nutritional intervention that included both a specialized nutrient formula and a tailored food plan. The nutritional support was twofold: (a) Specialized Nutrient Formula: The RG was provided with a specially formulated oral nutrient solution designed to meet the specific needs of hemodialysis (HD) patients. The formula composition was based on individual protein and energy requirements. Daily protein needs were calculated at 0.8 to 1.2 grams per kilogram of body weight. Energy requirements for males and females were determined using separate formulas: for males, the formula used was 88.362 + (13.397 × weight in kg) + (4.799 × height in cm) - (5.677 × age in years); for females, the formula was 447.593 + (9.247 × weight in kg) + (3.098 × height in cm) - (4.330 × age in years). The nutrient solution was composed of a blend containing 1-9% protein, 1-20% maltodextrin, 1-10% plant mixed oils, 0.1-1% borage oil, 1-15% corn syrup solids, 1-5% sugar, 1-2% cellulose, 0.1-1% essential minerals, 0.01-0.1% emulsifier, and 0.01-0.05% L-carnitine and L-taurine. The RG members were instructed to consume this nutrient solution 200-250 mL per session, 6-7 times daily, ensuring each feeding was completed within 15-20 minutes and spaced at least two hours apart. (b) Tailored Food Plan: In addition to the nutrient solution, patients in the RG were provided with a food plan tailored to their needs and dietary habits. This plan was not solely based on the consumption of the nutrient solution but was supplemented by regular meals. The food plan aimed to ensure that patients received a balanced diet, taking into account their daily total energy and nutrient requirements. Fat intake was targeted to provide 30% of the total daily calorie intake, and carbohydrates were to account for 50%. Patients were educated on using tools like salt spoons and oil cups to properly portion their meals and were encouraged to maintain a record of their nutritional intake. Weekly dietary surveys were conducted to offer personalized guidance and to make any necessary adjustments to their diet. (c) The combination of the nutrient solution and the tailored food plan was designed to ensure that patients in the RG received adequate nutrition to address their high-risk nutritional state, as identified by the Malnutrition Universal Screening Tool (MUST). Additionally, patients were advised to consume fruit and vegetable juices between feedings, with a hydration goal of 500 mL of water plus the volume of the previous day's urine output. Weekly follow-ups via WeChat phone calls by nurses helped monitor the patient's adherence to the feeding regimen and provided an opportunity for ongoing nursing guidance, including reminders about the importance of nutrient tube maintenance and timely follow-up appointments.

Electronic records of follow-up data.

Outcome Measures

Nutritional status: At the time of enrollment, fasting peripheral venous blood was collected from patients from 6:00 to 7:00 in the morning during the intervention period of three months. After centrifugation, serum was collected for nutritional indicators, including PA, TF, SAB, and HB. PA standard reference range= 0.20-0.40 g/L. TF's typical reference range = 2.5-4.3 g/L. SAB typical reference range = 35-55 g/L. HB normal reference range=110～160 g/L.

Immunity

Cellular immune indicators: At the time of enrollment, the patient's fasting

peripheral venous blood was collected from 6:00 to 7:00 in the morning for cellular immune index testing during the intervention period of three months. The detection indicators include CD3+, CD4+, and CD8+. The normal reference range for CD3+ was 955-2860/μL. CD4+normal reference range= 450~1440/μL. CD8+ normal reference range= 320~1250/μL.

Humoral immune indicators: At enrollment, fasting venous blood was collected from patients at 6:00 to 7:00 in the morning for humoral immune index testing during the intervention period of three months. The detection indicators include IgA, IgG, and IgM, and the normal reference range of IgA is 0.71-3.85 g/L. Normal reference range of lgG =7.0-16.6 g/L. IgM typical reference range = 0.4-3.45 g/L.

Statistical analysis: IBM SPSS 26.0® was used for data processing, and the measurement data was expressed as mean ± standard deviation ($\bar{x}$±SD). According to the Kolmogorov-Smirnov test, the measurement data conformed to a normal distribution, with independent t-tests performed between groups and paired t-tests performed within groups. Graph Pad Prism 8 was used to draw a bar-separated scatter plot of indicator horizontal changes. The number of cases used in technical data, expressed as a percentage (n,%), was subjected to the χ^2 test, and $p<0.05$ was considered statistically significant.

RESULTS

Comparison of nutritional status between the two groups of patients

At the time of enrollment, there was no significant difference in the levels of PA, TF, SAB, and HB nutritional indicators between the two groups of patients ($p>0.05$). After intervention for three months, the levels of nutritional indicators such as PA in all patients in the experiment grew ($p<0.05$), while the RG group exceeded the CG group ($p<0.05$), as shown in Table 2.

Comparison of cellular immune indicators between the two groups of patients

At the time of enrollment, there were no significant differences in the levels of cellular immune indicators such as CD3+, CD4+, and CD8+ between the two groups of patients ($p>0.05$). At the time of intervention for three months, the levels of CD3+ and other cellular immune indicators in both groups of patients increased ($p<0.05$), while the RG exceeded the CG ($p<0.05$), as shown in Table 3.

Table 2
Comparison of nutritional index levels between the two groups of patients.

Group	n	PA (g/L)		TF (g/L)		SAB (g/L)		HB (g/L)	
		Baseline Parameters	At three months of intervention	Baseline Parameters	At three months of intervention	Baseline Parameters	At three months of intervention	Baseline Parameters	At three months of intervention
Control group	50	0.17±0.07	0.30±0.86*	2.30±0.31	2.96±0.26*	33.90±1.07	35.79±3.85*	106.74±8.11	114.85±5.73*
Research group	50	0.16±0.07	0.34±0.57*	2.30±0.33	3.15±0.40*	33.74±1.06	37.11±2.17*	104.82±6.27	117.44±5.16*
t	-	0.256	2.463	0.041	2.170	0.777	2.110	1.325	2.375
p	-	0.799	0.016	0.968	0.032	0.439	0.037	0.188	0.020

PA: pre albumin. TF: transferrin. SAB: serum albumin. HB: hemoglobin.
Values are expressed as X±SD; *p<0.05 compared to levels at admission to the study.

Table 3
Comparison of cellular immune index levels between the two groups of patients.

Group	n	CD3+(μL)		CD4+(μL)		CD8+(μL)	
		Baseline Parameters	At three months of intervention	Baseline Parameters	At three months of intervention	Baseline Parameters	At three months of intervention
Control Group	50	944.74±21.05	974.04±24.64*	441.30±16.31	465.67±27.42*	313.38±14.93	364.68±20.60*
Research Group	50	943.17±25.87	989.20±35.40*	442.11±18.57	479.95±27.49*	310.87±15.41	373.82±16.74*
t	-	0.333	2.487	0.233	2.597	0.827	2.435
p	-	0.740	0.015	0.816	0.011	0.410	0.017

Values are expressed as X±SD *p<0.05 Compared to the time of admission.

Table 4
Comparison of humoral immune index levels between the two groups of patients.

Group	n	lgA (g/L)		lgG (g/L)		IgM (g/L)	
		Baseline Parameters	At three months of intervention	Baseline Parameters	At three months of intervention	Baseline Parameters	At three months of intervention
Control Group	50	0.70±0.06	1.26±0.09*	6.59±1.33	7.34±1.10*	0.39±0.05	1.57±0.08*
Research Group	50	0.68±0.06	1.31±0.10*	6.44±1.21	7.94±1.22*	0.38±0.04	1.62±0.10*
t	-	1.467	2.567	0.620	2.561	0.926	2.640
p	-	0.146	0.012	0.537	0.012	0.357	0.010

IgA: Immunoglobulin A. LgG: Immunoglobulin G. IgM: Immunoglobulin M. Values are expressed as X±SD. *p<0.05 compared to Baseline Parameters.

Comparison of humoral immune indicators between the two groups of patients

At the time of enrollment, a significant difference did not exist in the concentration of IgA, IgG, and IgM humoral immune indicators between the two groups of patients ($p>0.05$). At the time of intervention for three months, the levels of IgA and other humoral immune indicators in both groups of patients increased ($p<0.05$), and the RG exceeded the CG ($p<0.05$), as shown in Table 4.

DISCUSSION

Prealbumin PA, also known as thyroid binding protein, transports thyroid hormones [13]. Its main synthetic organ is the liver. In cases of malnutrition in the body, the synthesis of PA is affected, and its blood level decreases [14]. PA is often used as an essential indicator to evaluate the nutritional status of patients. During dialysis, HD patients excrete a certain amount of protein through dialysis, resulting in protein loss. The side effects of medication, the disease itself, and other factors in patients can lead to loss of appetite and affect dietary intake. Patients can also suffer malnutrition by limiting phosphorus, sodium, and potassium intake to control the fluid balance and avoid material accumulation in the blood [15]. TF is a protein responsible for iron transport, present in plasma and involved in HB synthesis and oxygen transport [16]. It absorbs iron from

the intestines, spleen, and other tissues and transports it to the RBC in the bone marrow, synthesizing hemoglobin [17]. Iron metabolism can be evaluated by monitoring the level of TF in the blood. In cases of malnutrition, TF can undergo a decrease [18]. SAB is a rich protein in the blood synthesized by the liver and reaches the entire body through blood circulation, maintaining a balance between plasma and cells and avoiding the loss and retention of water and nutrients [19]. It participates in the binding and transportation of various substances, binds with free fatty acids, transports fatty acids to cells, participates in immune regulation of the body, and maintains acid-base balance [20]. Changes in SAB levels can reflect the nutritional status of patients. In HD patients with malnutrition, excessive protein loss affects liver protein synthesis, decreasing SAB levels [21]. HB is a Pro present in RBC and an essential component in the blood. It transports oxygen from the lungs to various tissues for oxygen exchange [22], and HB levels are commonly used to assess the degree of anemia in patients. Malnutrition may cause anemia and decreased HB [23]. For HD patients, long-term dialysis treatment may lead to chronic inflammatory reactions and iron loss, affecting RBC generation and HB levels [24].

Table 2 shows that regular exercise and quantitative nutritional support can improve patients' nutritional indicators. Quantitative nutritional intervention can develop personalized nutritional interventions based on the specific nutritional needs of patients, ensuring that patients consume sufficient Pro and other nutrients. Pro is the primary raw material for the synthesis of PA, and sufficient intake of Pro can promote the synthesis of PA. Regular exercise can promote Pro synthesis and increase muscle mass, which is the main storage area for Pro. Increasing muscle mass can increase Pro storage in the body. The pro breakdown can lead to a decrease in PA and transferrin levels. Regular exercise can reduce Pro breakdown, and quantitative nutritional interventions can increase Pro intake, thereby maintaining high Pro levels in patients.

The effect of regular exercise and quantitative nutritional intervention on cellular immune indicators in HD malnutrition patients. CD3+ is a cell surface marker that refers to lymphocytes carrying CD3 antigens. It mainly exists in the expression of T lymphocytes and is a part of T cell receptor complexes. In immunology, cell surface markers are identified and classified to distinguish different types of immune cells, and the number of T cells identified by CD3 labelling can be monitored [25]. CD4+ cells, also known as helper T cells, are critical immune cells in the immune system and influence the regulation and coordination of immune responses in the body [26]. CD4+ are mainly present in the peripheral blood and other parts of lymphatic tissue and participate mainly in the immune response of intracellular and extracellular pathogens, as well as the immune regulation of T cells. It suppresses the immune response through inhibitory cytokines, avoiding excessive immune response and autoimmune reactions [27]. CD8+ are cytotoxic T cells and essential immune cells in the immune system. They kill infected or mutated cells in the body [28]. When the body is invaded by pathogens such as bacteria and viruses, CD8+ cells can recognize and kill infected cells to prevent pathogen transmission [29]. The activity and function of CD8+ play a vital role in the immune system, protecting the body from pathogen infection and tumor invasion [30]. The important subpopulations of lymphocytes play an essential role in the immune response, and malnutrition may impact the immune system, leading to impaired immune function and affecting the level of lymphocyte subpopulations. Thus, malnutrition can lead to a decrease in the number of T cells or impaired function, leading to a decrease in the levels of CD3+, CD4+, and CD8+, affecting the normal regulatory function of the immune system [31]. Table 3 shows that regular exercise combined with

quantitative nutritional support can effectively improve patients' cellular and humoral immune indicator levels. Analyzing the reasons, regular exercise combined with quantitative nutritional intervention can improve immune function and enhance the number and activity of T cells, and regular exercise can enhance the body's immune activity. Quantitative nutritional intervention can provide T cells with the required Pro and micronutrients, thereby increasing cellular immune indicators such as CD3+ levels, helping to enhance T cell function and immune response ability [32].

The effect of regular exercise and quantitative nutritional intervention on humoral immune indicators in HD malnutrition patients. IgA is an immunoglobulin mainly present on the surface of mucous membranes and body fluids, mainly on the surface of mucous membranes such as the respiratory and digestive tracts. It is a barrier to protect the mucosa from pathogen invasion and the first immune barrier. Abnormal levels of IgA may be related to certain immune diseases [33]. IgG is an immunoglobulin in bodily fluids and blood, synthesized by B lymphocytes and secreted during immune activation during infection, mainly involved in humoral immune responses. It can bind to pathogens, neutralize toxins, and activate the immune system, promoting pathogen clearance and destruction [34]. IgM is a crucial component of the humoral immune system and is the immunoglobulin first produced during early infection or initial exposure to antigens. It participates in humoral immunity and can quickly initiate immune responses, especially in early infections. It has a solid ability to agglutinate and activate complement, quickly neutralizing and clearing pathogens, thereby preventing the further spread of infection [35]. Pro is the main component of immunoglobulin [36]. Due to an insufficient supply of Pro, malnutrition patients limit immunoglobulin synthesis, decreasing the levels of related immunoglobulin indicators. Immunoglobulin plays a crucial role in maintaining the body's immune function, and malnutrition, leading to a decrease in immunoglobulin synthesis, may increase the risk of infection in patients. Therefore, providing reasonable nutritional support for HD malnutrition patients is crucial for improving their immune indicators and preventing infection [37,38]. Regular exercise, combined with quantitative nutritional intervention, could markedly enhance the immune index levels of patients, as shown in Table 4. Regular exercise can stimulate immune cell activity and enhance the body's ability to clear pathogens. Quantitative nutritional support ensures patients receive sufficient Pro supply through reasonable dietary adjustments and nutritional supplementation, an important immunoglobulin component. Recombinant Pro intake helps to increase the synthesis of immunoglobulin.

In conclusion, this study observed a significant effect of combining regular exercise with quantitative nutritional support in improving the nutritional indicators of HD malnutrition patients and also tested the levels of humoral and cellular immune indicators. The results show that regular exercise combined with quantitative nutritional support can also help improve immune function and have an auxiliary therapeutic effect on the immune function of HD malnourished patients. Its effect becomes more pronounced with the extension of intervention time. However, the sample size of this study is relatively small, and the specific efficacy needs to be confirmed by expanding the sample size. Secondly, the causes of malnutrition in dialysis patients involve multiple factors and mechanisms. This study only observed changes in nutritional indicators and levels of humoral cellular immune indicators, and its specific mechanisms require further research in animal experiments.

ACKNOWLEDGMENT

We would like to acknowledge the invaluable contributions of all those who supported and assisted in this research.

Conflict of interest

No potential conflict of interest relevant to this article was reported.

Funding

None

Authors' ORCID number

- Chunfeng Kong: 0000-0002-0163-3569
- Changdong Zhu: 0000-0003-1350-5588

Contribution of authors

Both authors contributed equally to this study, and their efforts were equally significant in its completion.

REFERENCES

1. **Elliott DA.** Hemodialysis. Clin Tech Small Anim Pract 2000;15(3):136-148. *https://doi.org/10.1053/svms.2000.18297*.
2. **Himmelfarb J, Ikizler TA.** Hemodialysis. N Engl J Med 2010;363(19):1833-1845. *https://doi.org/10.1056/nejmra0902710*
3. **Jameson MD, Wiegmann TB.** Principles, uses, and complications of hemodialysis. Med Clin North Am 1990;74(4):945-960. *https://doi.org/10.1016/s0025-7125(16)30528-4*
4. **Daugirdas JT.** Hemodialysis adequacy and biocompatibility. Semin Dial 2011;24(5):508-509. *https://doi.org/10.1111/j.1525-139x.2011.00984.x*
5. **Graterol Torres F, Molina M, Soler-Majoral J, Romero-González G, Rodríguez Chitiva N, Troya-Saborido M, Socias Rullan G, Burgos E, Paúl Martínez J, Urrutia Jou M, Cañameras C, Riera Sadurní J, Vila A, Bover J.** Evolving concepts on inflammatory biomarkers and malnutrition in chronic kidney disease. Nutrients 2022;14(20):4297. *https://doi.org/10.3390/nu14204297*
6. **Sahathevan S, Khor BH, Ng HM, Gafor AHA, Mat Daud ZA, Mafra D, Karupaiah T.** Understanding development of malnutrition in hemodialysis patients: A Narrative Review. Nutrients 2020;12(10):3147. *https://doi.org/10.3390/nu12103147*
7. **Piccoli GB, Lippi F, Fois A, Gendrot L, Nielsen L, Vigreux J, Chatrenet A, D'Alessandro C, Cabiddu G, Cupisti A.** Intradialytic nutrition and hemodialysis prescriptions: a personalized stepwise approach. Nutrients 2020;12(3):785. *https://doi.org/10.3390/nu12030785*
8. **Munteanu C, Schwartz B.** The relationship between nutrition and the immune system. Front Nutr 2022;9(1):1082500. *https://doi.org/10.3389%2Ffnut.2022.1082500*
9. **Wensveen FM, Valentić S, Šestan M, Wensveen TT, Polić B.** Interactions between adipose tissue and the immune system in health and malnutrition. Semin Immunol 2015;27(5):322-333. *https://doi.org/10.1016/j.smim.2015.10.006*
10. **Carbone F, La Rocca C, De Candia P, Procaccini C, Colamatteo A, Micillo T, De Rosa V, Matarese G.** Metabolic control of immune tolerance in health and autoimmunity. Semin Immunol 2016;28(5):491-504. *https://doi.org/10.1016/j.smim.2016.09.006*
11. **Carrillo E, Jimenez MA, Sanchez C, Cunha J, Martins CM, da Paixão Sevá A, Moreno J.** Protein malnutrition impairs the immune response and influences the severity of infection in a hamster model of chronic visceral leishmaniasis. PloS one 2014;9(2):e89412. *https://doi.org/10.1371%2Fjournal.pone.0089412*
12. **Okawa T, Nagai M, Hase K.** Dietary intervention impacts immune cell functions and dynamics by inducing metabolic rewiring. Front Immunol 2020;11(1):623989. *https://doi.org/10.3389/fimmu.2020.623989*

13. **Blake CC.** Prealbumin and the thyroid hormone nuclear receptor. Proc R Soc Lond B Biol Sci 1981;211(1185):413-431. *https://doi.org/10.1098/rspb.1981.0015*
14. **Tekgüç H, Özel D, Sanaldi H, Akbaş H, Dursun O.** Prealbumin and retinol binding proteins are not usable for nutrition follow-up in pediatric intensive care units. Pediatr Gastroenterol Hepatol Nutr 2018;21(4):321-328. *https://doi.org/10.5223/pghn.2018.21.4.321*
15. **Chrysostomou S, Stathakis C, Petrikkos G, Daikos G, Gompou A, Perrea D.** Assessment of prealbumin in hemodialysis and renal-transplant patients. J Ren Nutr 2010;20(1):44-51. *https://doi.org/10.1053/j.jrn.2009.04.001*
16. **Gomme PT, McCann KB, Bertolini J.** Transferrin: structure, function and potential therapeutic actions. Drug Discov Today 2005;10(4):267-273. *https://doi.org/10.1016/s1359-6446(04)03333-1*
17. **de Jong G, van Dijk JP, van Eijk HG.** The biology of transferrin. Clin Chim Acta 1990;190(1-2):1-46. *https://doi.org/10.1016/0009-8981(90)90278-z*
18. **Sato M, Hanafusa N, Tsuchiya K, Kawaguchi H, Nitta K**. Impact of transferrin saturation on all-cause mortality in patients on maintenance hemodialysis. Blood Purif 2019;48(2):158-166. *https://doi.org/10.1159/000499758*
19. **Fanali G, di Masi A, Trezza V, Marino M, Fasano M, Ascenzi P**. Human serum albumin: from bench to bedside. Mol Aspects Med 2012;33(3):209-290. *https://doi.org/10.1016/j.mam.2011.12.002*
20. **Fujiwara S, Amisaki T.** Fatty acid binding to serum albumin: molecular simulation approaches. Biochim Biophys Acta 2013;1830(12):5427-5434. *https://doi.org/10.1016/j.bbagen.2013.03.032*
21. **Eriguchi R, Obi Y, Rhee CM, Chou JA, Tortorici AR, Mathew AT, Kim T, Soohoo M, Streja E, Kovesdy CP, Kalantar-Zadeh K.** Changes in urine volume and serum albumin in incident hemodialysis patients. Hemodial Int 2017;21(4):507-518. *https://doi.org/10.1111/hdi.12517*
22. **Gell DA.** Structure and function of haemoglobins. Blood Cells Mol Dis 2018;70(1):13-42. *https://doi.org/10.1016/j.bcmd.2017.10.006*
23. **Topal M, Guney I.** The association of soluble Klotho levels with anemia and hemoglobin variability in hemodialysis patients. Semin Dial 2023;36(2):142-146. *https://doi.org/10.1111/sdi.13122*
24. **Gilbertson DT, Hu Y, Peng Y, Maroni BJ, Wetmore JB.** Variability in hemoglobin levels in hemodialysis patients in the current era: a retrospective cohort study. Clin Nephrol 2017;88(11):254-265. *https://doi.org/10.5414/cn109031*
25. **Chen Q, Yuan S, Sun H, Peng L.** CD3(+) CD20(+) T cells and their roles in human diseases. Hum Immunol 2019;80(3):191-194. *https://doi.org/10.1016/j.humimm.2019.01.001*
26. **Takeuchi A, Saito T.** CD4 CTL, a cytotoxic subset of CD4(+) T cells, their differentiation and function. Front Immunol 2017;8(1):194. *https://doi.org/10.3389/fimmu.2017.00194*
27. **Preglej T, Ellmeier W.** CD4(+) Cytotoxic T cells - phenotype, function and transcriptional networks controlling their differentiation pathways. Immunol Lett 2022;247(1):27-42. *https://doi.org/10.1016/j.imlet.2022.05.001*
28. **Natalini A, Simonetti S, Favaretto G, Peruzzi G, Antonangeli F, Santoni A, Muñoz-Ruiz M, Hayday A, Di Rosa F.** OMIP-079: Cell cycle of CD4(+) and CD8(+) naïve/memory T cell subsets, and of Treg cells from mouse spleen. Cytometry A 2021;99(12):1171-1175. *https://doi.org/10.1002/cyto.a.24509*
29. **Mittrücker HW, Visekruna A, Huber M.** Heterogeneity in the differentiation and function of $CD8^+$ T cells. Arch Immunol Ther Exp (Warsz) 2014;62(6):449-458. *https://doi.org/10.1007/s00005-014-0293-y*
30. **Huff WX, Kwon JH, Henriquez M, Fetcko K, Dey M.** The Evolving Role of CD8(+)CD28(-) Immunosenescent T cells in cancer immunology. Int J Mol

Sci 2019;20(11):2810. *https://doi.org/10.3390/ijms20112810*

31. **Demas GE, Drazen DL, Nelson RJ.** Reductions in total body fat decrease humoral immunity. Proc Biol Sci 2003;270(1518):905-911. *https://doi.org/10.1098/rspb.2003.2341*
32. **Du F, Wu C.** Review on the effect of exercise training on immune function. Biomed Res In 2022;2022(1):9933387. *https://doi.org/10.1155/2022/9933387*
33. **Zemla A.** LGA: A method for finding 3D similarities in protein structures. Nucleic Acids Res 2003;31(13):3370-3374. *https://doi.org/10.1093/nar/gkg571*
34. **Liston A.** The development of T-cell immunity. Prog Mol Biol Transl Sci 2010;92(1):1-3. *https://doi.org/10.1016/s1877-1173(10)92001-2.*
35. **Cursiefen C, Bock F, Clahsen T, Regenfuss B, Reis A, Reis A, Steven P, Heindl LM, Bosch JJ, Hos D, Eming S, Grajewski R, Heiligenhaus A, Fauser S, Austin J, Langmann T.** New therapeutic approaches in inflammatory diseases of the eye - targeting lymphangiogenesis and cellular immunity: Research Unit FOR 2240 Presents Itself. Klin Monbl Augenheilkd 2017;234(5):679-685. *https://doi.org/10.1055/s-0043-108247.*
36. **Masiero A, Nelly L, Marianne G, Christophe S, Florian L, Ronan C, Claire B, Cornelia Z, Grégoire B, Eric L, Ludovic L, Dominique B, Sylvie A, Marie G, Francis D, Fabienne S, Cécile C, Isabelle A, Jacques D, Jérôme D, Bruno G, Katarina R, Jean-Michel M, Catherine P.** The impact of proline isomerization on antigen binding and the analytical profile of a trispecific anti-HIV antibody. MAbs 2020;12(1):1698128. *https://doi.org/10.1080%2F19420862.2019.1698128.*
37. **Pandey VK, Tripathi A, Srivastava S, Pandey S, Dar AH, Singh R, Duraisamy P, Singh P, Mukarram SA.** A systematic review on immunity functionalities and nutritional food recommendations to develop immunity against viral infection. Applied Food Research 2023;3(1):100291. *https://doi.org/10.1016/j.afres.2023.100291.*
38. **Batool R, Butt MS, Sultan MT, Saeed F, Naz R.** Protein–energy malnutrition: A risk factor for various ailments. Crit Rev Food Sci Nutr 2015;55(2):242-253. *https://doi.org/10.1080/10408398.2011.651543.*

Invest Clin 65(3): 358 - 368, 2024 https://doi.org/10.54817/IC.v65n3a08

Impact of a ketogenic diet on intestinal microbiota, cardiometabolic, and glycemic control parameters in patients with Type 2 diabetes mellitus.

Na Lu[1], Xincui Zhou[1] and Fengnian Guo[2]

[1] Department of Colorectal Surgery, South of Guang'anmen Hospital, China Academy of Chinese Medical Sciences, Beijing, China.
[2] Department of Endocrinology, South of Guang'anmen Hospital, China Academy of Chinese Medical Sciences, Beijing, China.

Keywords: ketogenic diet; Type 2 diabetes mellitus; intestinal flora; glucagon like peptide-1; glycosylated hemoglobin.

Abstract. A ketogenic diet (KD), characterized by high fat and low carbohydrate intake, has been proposed as a therapeutic option for Type 2 Diabetes Mellitus (T2DM). One hundred individuals with T2DM were selected and divided into a control group (CG) and an observation (OG) group, with 50 patients in each group, to investigate the effects of a KD on the intestinal flora, Glucagon Like Peptide-1 (GLP-1), and HbA1c levels in T2DM patients. Individuals in the CG were given standard treatment and diet, while patients in the OG were given a KD based on the CG. The blood glucose index, blood lipid index, HbA1c, GLP-1 levels, physical examination, and intestinal flora were compared in both groups. The FPG, HbA1c, two h PG, HOMA-IR TG, TC, and LDL-C levels in the two groups were reduced when compared to those before treatment ($p<0.05$), and the decreases in the OG were more significant than in the CG ($p<0.05$), while the levels of GLP-1 in the two groups were increased compared to those before treatment, those in the OG were significantly increased when compared to the CG ($p<0.05$). After treatment, waist circumference, BMI, body mass, and the levels of *Enterococcus faecalis (E. faecalis)* and *Escherichia coli (E. coli)* of the two groups were reduced compared to indicators before treatment ($p<0.05$), and those in the OG were even lower than those in the CG ($p<0.05$). In conclusion, these findings underscore the KD's potential to act as an efficacious dietary strategy in managing T2DM.

Corresponding author: Fengnian Guo, Department of Endocrinology, South of Guang'anmen Hospital, China Academy of Chinese Medical Sciences, Beijing, 102618, China. E-mail: leidui26492806@163.com

Impacto de una dieta cetogénica en la microbiota intestinal y los parámetros de control cardiometabólico y glucémico en pacientes con diabetes mellitus tipo 2.

Invest Clin 2024; 65 (3): 358 – 368

Palabras clave: dieta cetogénica; diabetes mellitus tipo 2; flora intestinal; péptido-1 similar al glucagón; hemoglobina glicosilada.

Resumen. Una dieta cetogénica (KD), caracterizada por una ingesta alta en grasas y baja en carbohidratos, se ha propuesto como una opción terapéutica para la diabetes mellitus tipo 2 (DM2). Se seleccionaron cien individuos con DM2 y se dividieron en un grupo control (GC) y un grupo de observación (GO), con 50 pacientes en cada grupo, para investigar los efectos de una dieta cetogénica sobre los niveles de la flora intestinal, el péptido similar al glucagón-1 (GLP-1) y la HbA1c en pacientes con DM2. Los individuos del GC recibieron tratamiento y dieta estándar, mientras que los pacientes del GO recibieron el tratamiento estándar similar al GC, más una dieta cetogénica. En ambos grupos se compararon el índice de glicemia, el índice de lípidos en sangre, la HbA1c, los niveles del GLP-1, el examen físico y la flora intestinal. Los niveles de FPG, HbA1c, 2h PG, HOMA-IR TG, TC y LDL-C en los dos grupos se redujeron en comparación con los de antes del tratamiento ($p<0,05$), y las disminuciones en el GO fueron más significativas que en el grupo GC ($p<0,05$), mientras que los niveles de GLP-1 en los dos grupos aumentaron en comparación con los de antes del tratamiento, los del GO aumentaron significativamente en comparación con el GC ($p<0,05$). Después del tratamiento, la circunferencia de la cintura, el IMC, la masa corporal y los niveles de *Enterococcus faecalis (E. faecalis) y Escherichia coli (E. coli)* de los dos grupos se redujeron en comparación con los indicadores antes del tratamiento ($p<0,05$), y los del GO fueron incluso más bajos que los del GC. ($p<0,05$). En conclusión, estos hallazgos subrayan el potencial de la KD para actuar como una estrategia dietética eficaz en el tratamiento de la DM2.

Received: 03-03-2024 Accepted: 13-05-2024

INTRODUCTION

Type 2 Diabetes Mellitus (T2DM) is a chronic metabolic disorder marked by elevated blood sugar levels [1]. T2DM is linked to metabolic syndrome and insulin resistance. It is influenced by genetics, obesity, inactivity, and ethnicity [2, 3]. The prevalence of T2DM varies globally, with a higher incidence in developed countries. As per the most recent report from the International Diabetes Federation (IDF), the worldwide incidence of T2DM among adults stood at 536.6 million individuals (10.5%) in 2021. It is projected that the number of individuals living with diabetes will reach 783.2 million people (12.2%) globally by the year 2045 [4].

From a pathophysiological perspective, T2DM is associated with insulin resistance, wherein the body's cells are less responsive to insulin, and a gradual failure of pancreatic β-cells to compensate for this increased

demand [5]. This dysfunction is reflected in the hallmark signs and symptoms of T2DM, which include polyuria, polydipsia, polyphagia, and weight loss [6].

Long-term complications of T2DM are broad-ranging and include microvascular damage leading to retinopathy, neuropathy, and nephropathy, as well as macrovascular complications such as coronary artery disease, peripheral arterial disease, and cerebrovascular disease [7, 8].

Diagnosis of T2DM is typically confirmed through several tests, including fasting plasma glucose (FPG), 2-hour plasma glucose (2-h PG) during an oral glucose tolerance test (OGTT), and hemoglobin A1c (HbA1c) levels, which reflect the mean blood glucose levels over the previous two to three months [9].

Treatment modalities for T2DM include lifestyle interventions, oral hypoglycemic agents, non-insulin injectables, and insulin therapy [10, 11]. Among the dietary strategies, the KD (a high-fat, adequate-protein, low-carbohydrate diet) has emerged as a potential therapeutic option [12, 13]. This diet aims to induce a state of ketosis, where the body utilizes fat as a primary energy source instead of glucose [14].

The KD has been associated with alterations in the gut microbiota, which play a crucial role in metabolic health [15]. A shift in intestinal flora could potentially influence the incretin hormone glucagon-like peptide-1 (GLP-1), which promotes insulin secretion and improves glycemic control. Furthermore, the KD could influence HbA1c levels, providing a broader metabolic benefit for patients with T2DM [16,17].

However, the literature presents a paucity of comprehensive studies that holistically examine the effects of a KD on both the intestinal microbiota and the serum levels of GLP-1 and HbA1c in patients with T2DM. Therefore, this study aims to explore the effects of a KD on intestinal flora and serum GLP-1 and glycosylated hemoglobin levels in T2DM patients.

PATIENTS AND METHODS

This study was conducted as an interventional study with a randomized controlled trial (RCT) design. The study spanned over six months, from June 2021 to June 2022, at the South of Guang'anmen Hospital.

Based on the random number table method, 100 T2DM patients were selected and divided into a control group (CG) and an observation group (OG), with 50 patients in each group. As shown in Table 1, there were no significant differences between the two groups in general data ($P>0.05$).

Our hospital's Ethics Committee reviewed and approved the study, and patients signed the informed consent form.

Inclusion criteria: ① Patients with T2DM were initially diagnosed through clinical signs and symptoms (polyuria, polydipsia, polyphagia, unexplained weight loss, fatigue,

Table 1
Clinical data of patients.

Group	n	Sex(n)		Age $\bar{x} \pm SD$	BMI (kg/m^2) $\bar{x} \pm SD$
		Male	Female		
CG	50	31	19	53.11±9.69	27.32±5.23
OG	50	32	18	52.64±10.53	27.06±5.56
t/χ^2		0.043		0.232	0.241
p		0.836		0.817	0.810

CG: Control group, OG: Observation group, $\bar{x} \pm SD$: mean ± standard deviation (SD), BMI: Body mass index, t: t-test, χ^2: chi-square test.

and blurred vision), and serological indicators (FPG >7.0 mmol/L or 126 mg/dL; a plasma glucose concentration equal to or exceeding ≥11.1 mmol/L or 200 mg/dL two hours after a 75-g oral glucose tolerance test (OGTT); HbA1c >6.5% or higher was also indicative of T2DM) [18, 19], ② Patients with good treatment compliance; ③Complete and accurate medical records.

Exclusion criteria: ① Patients with other serious diabetic complications such as ketoacidosis; ② Patients with other endocrine diseases; ③ Heart, liver, and kidney failure patients; ④ Patients with drug allergy episodes in the past.

The patients in the CG were given standard treatment: patients were instructed to control their diet, exercise appropriately, quit smoking, and limit alcohol consumption, and blood glucose was closely monitored. Patients in the OG were given a KD based on treatment in the CG. High-protein and low-carbohydrate KD treatment included 1/5-2/5 of fat, 2/5 of protein, 1/5 of carbohydrate, keeping regular three meals. This diet limits carbohydrate intake to around 20-50 grams daily and increases fats such as meat, fish, eggs, nuts, and healthy oils. On the other hand, adjusting protein consumption is also part of this diet; if much protein is consumed, it can be converted to glucose and may slow the transition to ketosis. The intake of fat was rich in ω-3 mainly, such as sardines, salmon, tuna, and other sources of this fat. The amount of drinking water was more than 2000 mL/d, multiple mineral vitamins needed to be supplemented, and the amount of exercise remained at the previous level. Both groups of patients were treated continuously for six months.

Serological indicators

The two groups of patients had 5 mL of fasting peripheral venous blood collected in the morning before and after treatment, centrifuged at 3000 r/min, and the supernatant stored at 4°C. A radioimmunoassay was used to measure fasting blood glucose (FPG) and postprandial blood glucose (2h PG), ELISA was used to detect fasting insulin (FINS), and an insulin resistance index was used to determine insulin resistance (HOMA-IR=(FPG×FINS)/22.5. All the kits were provided by the Shanghai Enzyme Linked Biotechnology Co., Ltd. and operated strictly according to the specifications of the kit instructions. The levels of triglycerides (TG) and total cholesterol (TC) were detected by ELISA, and the levels of low-density lipoprotein cholesterol (LDL-C) were detected by the surfactant clearance method. ELISA detected serum HbA1c and GLP-1 levels.

Physical examination indicators

Intestinal flora

Before and after treatment, 0.1g of fresh feces from the two groups of patients were collected, mixed with normal saline, and inoculated into the culture medium containing aerobic and anaerobic bacteria, respectively. The aerobic bacteria mainly refer to *bifidobacteria* and *lactobacillus*. The culture environment was aerobic; the temperature was set at 37°C, and the time was 48h. Anaerobic bacteria refer to *E. faecalis* and *E. coli*. The air extraction and ventilation method was adopted, and the incubation time was 72h. After the culture, the *BIOLOG* automatic microbial identification system detected the *Bifidobacterium, Lactobacillus, Fecal Enterococcus, and E. coli* levels.

Statistical methods

IBM SPSS 20.0® was used for statistical analysis, and the counting data were χ^2. The measurement data were expressed by mean ± standard deviation (Mean±SD) and compared by the t-test. The difference was statistically significant when $p<0.05$

RESULTS

Blood glucose indicators in each group

There was no difference ($p>0.05$) in blood glucose between the two groups before treatment. After treatment, the levels

of FPG, 2h PG, and HOMA-IR in both groups were reduced compared to those before treatment ($p<0.05$), and those in the OG were even more reduced than those in the CG ($p<0.05$), as shown in Table 2.

Blood lipid indexes in each group

Blood lipid indexes between the two groups were no different before treatment ($p>0.05$). After treatment, the levels of TG, TC, and LDL-C in the two groups were reduced compared to those before treatment ($p<0.05$), and the levels in the OG were even more reduced than those in the CG ($p<0.05$) (Table 3).

HbA1c and GLP-1 levels in each group

Before treatment, HbA1c and GLP-1 levels between the two groups were no different ($p>0.05$); after treatment, those in the two groups were raised compared to those before treatment, and the levels of HbA1c in the CG were higher than those in the OG ($p<0.05$). The concentration of GLP-1 in the OG was higher than in the CG after six months of treatment ($p<0.05$), as shown in Table 4.

Physical examination indexes in each group

Before treatment, the two groups' waist circumference, BMI, and body mass were no different ($p>0.05$). After treatment, waist circumference, BMI, and body mass of the two groups were reduced compared to those before treatment, and the indicators of the OG were even more reduced than in the CG ($p<0.05$) (Table 5).

Comparison of intestinal flora in each group

Before treatment, the intestinal flora between the two groups was no different

Table 2
Blood glucose indicators in each group before and after six months of treatment.

Group	N	FPG (mmol/L)		2h PG (mmol/L)		HOMA-IR	
		Before	After	Before	After	Before	After
CG	50	8.45±1.24	7.29±0.98*	13.01±1.72	10.22±1.47*	3.86±0.72	2.87±0.55*
OG	50	8.32±1.07	6.57±1.01*	12.83±1.66	8.63±1.25*	3.77±0.67	2.43±0.48*
t		0.561	3.618	0.533	5.827	0.647	4.262
p		0.576	0.000	0.596	0.000	0.519	0.000

CG: Control group, OG: Observation Group, FPG: Fasting Plasma Glucose, 2h PG: 2-hour Postprandial Glucose, HOMA-IR: Homeostatic Model Assessment of Insulin Resistance, t: t-test, values are expressed as Mean±SD *: $p<0.05$ compared with the patients in this group before treatment.

Table 3
Blood lipid indexes in each group before and after six months of treatment.

Group	N	TG		TC		LDL-C	
		Before	After	Before	Before	Before	After
CG	50	2.57±0.61	1.97±0.42*	5.23±0.96	4.41±0.91	3.69±1.02	3.01±0.76*
OG	50	2.53±0.57	1.62±0.38*	5.21±1.13	3.94±0.77	3.63±0.95	2.65±0.41*
t		0.339	4.370	0.095	2.788	0.304	2.948
p		0.736	0.000	0.924	0.006	0.762	0.004

CG: Control group, OG: Observation group, TG: triglyceride, TC: total cholesterol, LDL-C: low-density lipoprotein cholesterol. Values are expressed as mmol/L. t: t-test, *: $p<0.05$ compared with the patients in this group before treatment, * $p<0.05$.

Table 4
HbA1c and GLP-1 levels in each group before and after six months of treatment.

Group	N	HbA1c (%)		GLP-1 (μ mol/L)	
		Before	After	Before	After
CG	50	8.41±1.12	7.51±1.09*	6.72±0.88	11.34±1.11*
OG	50	8.53±1.18	6.64±0.87*	6.64±0.52	14.43±2.28*
t		0.522	-4.411	-0.553	8.616
p		0.603	0.000	0.581	0.000

CG: Control group, OG: Observation group, HbA1c: hemoglobin A1c, GLP-1: glucagon-like peptide 1, t: t-test, * p<0.05 compared with the patients in this group before treatment.

Table 5
Physical examination indexes in each group before and after six months of treatment.

Group	N	Weight (kg)		BMI (kg/m^2)		Waist circumference (cm)	
		Before	After	Before	After	Before	After
CG	50	90.02±10.80	72.14±9.63*	30.58±2.81	25.70±1.42*	98.63±3.41	86.84±3.25*
OG	50	89.12±10.72	67.76±9.58*	30.46±2.92	24.25±1.35*	98.56±3.35	80.62±2.20*
t		-0.418	-2.280	-0.209	-5.233	-0.104	-11.207
p		0.677	0.025	0.835	0.000	0.918	0.000

CG: Control group, OG: Observation group, BMI: body mass index, t: t-test, *: p<0.05 compared with the patients in this group before treatment.

Table 6
Intestinal flora in each group before and after six months of treatment.

Group	N	*Bifidobacterium*		*Lactobacillus*		*E. faecalis*		*E. coli*	
		Before	After	Before	After	Before	After	Before	After
CG	50	7.54±0.95	8.15±0.86*	6.93±0.99	7.58±0.82*	8.22±0.83	7.42±0.72*	9.46±1.15	8.16±1.18*
OG	50	7.62±1.14	8.82±0.76*	6.84±0.92	8.12±0.93*	8.16±0.76	6.56±0.77*	9.64±1.23	7.24±0.87*
t		0.381	4.128	-0.471	3.080	-0.377	-5.769	0.756	-4.437
p		0.704	0.000	0.639	0.003	0.707	0.000	0.452	0.000

CG: Control group, OG: Observation group. Values are expressed as lgCFU/g, t: t-test, *: p<0.05 compared with the patients in this group before treatment.

(p>0.05). After treatment, the levels of *Bifidobacterium* and *Lactobacillus* in the two groups were increased compared to those before treatment, and those in the OG were higher than in the CG (p<0.05). After treatment, the levels of *E. faecalis* and *E. coli* in the two groups were reduced to those before treatment (P<0.05), and the levels in the OG were even lower than those in the CG (p<0.05) (Table 6).

DISCUSSION

The ketogenic diet (KD) has been increasingly studied for its potential therapeutic effects in various health conditions, including type 2 diabetes mellitus (T2DM) [20]. T2DM is a chronic condition characterized by insulin resistance and impaired glucose metabolism [21]. This study aimed to investigate the impact of a KD on the intestinal

microbiota and the serum levels of glucagon-like peptide-1 (GLP-1) and glycosylated hemoglobin (HbA1c) in patients with T2DM.

The present study's findings suggest that patients with T2DM who followed a KD for six months exhibited significant improvements in their serum levels of GLP-1 and HbA1c, as well as their blood glucose and lipid profiles, compared to the control group receiving standard treatment. Additionally, there were notable changes in the composition of the intestinal microbiota, with an increase in beneficial bacteria such as *Bifidobacterium* and *Lactobacillus*, and a decrease in potentially harmful bacteria like *E. faecalis and E. coli*.

Several studies have investigated the impact of a KD on weight, blood glucose levels, and lipid profiles in patients with T2DM. In line with the present study, the research findings suggest that a KD can induce positive changes in these parameters, offering potential benefits for managing T2DM. Li *et al.*'s study results show that following a KD can lead to a decrease in fasting blood glucose and glycosylated hemoglobin levels in T2DM patients, which indicates an improvement in blood glucose management [22]. Zhou *et al.*[23] also conducted a meta-analysis to investigate the role of KD in controlling body weight and managing blood sugar in overweight patients with T2DM. The results show that the KD significantly reduces body weight, reduces waist circumference, reduces glycosylated hemoglobin and triglycerides, and increases high-density lipoproteins (HDL)[23].

Additionally, the improvement in lipid profiles, particularly the reduction in triglyceride levels, is corroborated by Yuan *et al.* [24]. The KD's impact on lipid profiles, especially triglyceride levels, is likely due to its effects on insulin secretion and lipid metabolism. By reducing carbohydrate intake and increasing fat intake, the diet leads to a decrease in insulin secretion, which in turn reduces the conversion of excess carbohydrates into triglycerides in the liver [25]. Additionally, the diet's high-fat content provides a source of energy that is less likely to be stored as triglycerides in adipose tissue, further contributing to the reduction in triglyceride levels [26].

The efficacy of insulin action is ensured through a cellular signalling cascade, which encompasses membrane insulin receptors (IRS) and intracellular proteins (PI3K and AKT). Critical for the uptake of plasma glucose into tissues, these interactions between proteins play a vital role. Conversely, deficiencies in cellular signal transduction and insulin responses to insulin stimulation (IR) can disrupt glucose regulation, consequently contributing to the onset of T2DM [27]. The reduction in carbohydrate intake in a KD induces a state of nutritional ketosis, which alters the body's metabolism, leading to improved blood glucose levels and insulin sensitivity [28, 29]. In line with the present study, a systematic study by Huang *et al.* revealed that the ketogenic diet can improve insulin sensitivity in individuals with type 2 diabetes, with the most significant effect resulting from a ketogenic diet paired with exercise [30]. The study by Paoli *et al.* also confirms these findings and states that a ketogenic diet can improve blood sugar control and insulin sensitivity [31].

The reduction in HbA1c levels in the observation group supports the results of a study by Rafiullah *et al.,* which concluded that very low-carbohydrate ketogenic diets effectively reduce HbA1c in individuals with T2DM [32]. A recent systematic review and meta-analysis conducted by Zaki *et al.* [33] found that low carbohydrate (LCD) and KD positively impact glucose regulation in individuals with Type 2 Diabetes. Nevertheless, the analysis indicated that ketogenic diets demonstrate notably higher effectiveness in lowering HbA1c levels (− 1.45%) when compared to LCD (− 0.27%) [33].

The results of the present study showed that the ketogenic diet increases the serum level of GLP-1 in diabetic patients. GLP-1 is a hormone produced by the intestines that helps regulate blood sugar levels and stimu-

lates insulin secretion [34]. Widiatmaja *et al*. conducted a study to analyze the long-term effect of KD on the serum levels of adiponectin and IGF-1 in rats. The results showed that long-term KD increases serum adiponectin levels and does not affect serum IGF-1 levels [35]. This finding is contrary to the results of the present study, which could be due to the type of participants and the type of study. Since human studies on this parameter have not been conducted in people with a KD diet, it is necessary to investigate this matter further.

Finally, the present study showed that KD improves intestinal microbiota. KD improves *Bifidobacterium* and *Lactobacillus* levels and reduces *E. faecalis* and *E. coli* levels in the intestine. Previous studies have also shown that a very low-calorie ketogenic diet (VLCKD) can lead to significant changes in gut microbiota composition in drug-naïve patients with T2DM and obesity. One study compared the effects of VLCKD and a hypocaloric Mediterranean diet (MD) on gut microbiota in patients with T2DM and obesity. The results showed that the VLCKD group had more significant changes in gut microbiota composition [36]. The study of Paoli *et al*. also supports this idea and results [37]. Since the number of studies in this field is limited, more studies are recommended.

In conclusion, this study confirms that a ketogenic diet significantly outperforms standard dietary treatments for type 2 diabetes mellitus over six months. It more effectively lowers blood glucose levels, improves lipid profiles, reduces body weight and waist circumference, and beneficially alters gut microbiota. These findings highlight the ketogenic diet's potential as a superior dietary intervention for managing type 2 diabetes.

Authors' ORCID number

- Na Lu: 0000-0001-5222-6675
- Xincui Zhou: 0009-0000-5661-531X
- Fengnian Guo: 0009-0008-8713-8833

Contributions of authors

All authors were involved in data collection, article design, interpretation of results, review, and manuscript preparation.

Conflict of interests

The authors declare no conflict of interest.

Funding

None.

REFERENCES

1. **Han Y, Kim D-Y, Woo J, Kim J**. Glu-ensemble: An ensemble deep learning framework for blood glucose forecasting in type 2 diabetes patients. Heliyon 2024;10:e29030.
2. **Sahu MK, Tiwari SP**. Epidemiology, pathogenesis and treatment of diabetes: A comprehensive review. World J Diabetes Res Pract 2024;1(1):1-9.
3. **Szablewski L**. Insulin resistance: the increased risk of cancers. Curr Oncol 2024;31(2):998-1027. *https://doi.org/10.3390/curroncol31020075"31020075*
4. **Yan Y, Wu T, Zhang M, Li C, Liu Q, Li F**. Prevalence, awareness and control of type 2 diabetes mellitus and risk factors in Chinese elderly population. BMC Public Health 2022;22(1):1382. *https://doi.org/10.1186/s12889-022-13759-9"12889-022-13759-9*
5. **Dludla PV, Mabhida SE, Ziqubu K, Nkambule BB, Mazibuko-Mbeje SE, Hanser S, Basson AK, Pheiffer C, Kengne AP**. Pancreatic β-cell dysfunction in type 2 diabetes: Implications of inflammation and oxidative stress. World J Diabetes 2023;14(3):130-146. *https://doi.org/10.4239%2Fwjd.v14.i3.130"3.130*.
6. **Galdón Sanz-Pastor A, Justel Enríquez A, Sánchez Bao A, Ampudia-Blasco FJ**. Current barriers to initiating insulin therapy in individuals with type 2 diabetes. Front Endocrinol 2024;15:1-11. *https://doi.org/10.3389/fendo.2024.1366368"2024.1366368*

7. **Vlacho B, Rossell-Rusiñol J, Granado-Casas M, Mauricio D, Julve J**. Chapter 1 - Overview on chronic complications of diabetes mellitus. In: Mauricio D, Alonso N, editors. Chronic Complications of Diabetes Mellitus: Academic Press; 2024. p. 1-10.
8. **Mansour A, Mousa M, Abdelmannan D, Tay G, Hassoun A, Alsafar H**. Microvascular and macrovascular complications of type 2 diabetes mellitus: Exome wide association analyses. Front Endocrinol 2023;14:1143067. *https://doi.org/10.3389%2Ffendo.2023.1143067"2023.1143067*
9. **El Sayed NA, Aleppo G, Aroda VR, Bannuru RR, Brown FM, Bruemmer D, Collins BS, Hilliard ME, Isaacs D, Johnson EL, Kahan S, Khunti K, Leon J, Lyons SK, Perry ML, Prahalad P, Pratley RE, Seley JJ, Stanton RC, Gabbay RA, on behalf of the American Diabetes Association.** 2. Classification and Diagnosis of Diabetes: Standards of Care in Diabetes-2023. Diabetes Care 2023;46(1):S19-S40 *https://doi.org/10.2337%2Fdc23-S002"002*
10. **Tourkmani AM, Alharbi TJ, Rsheed AMB, Alotaibi AF, Aleissa MS, Alotaibi S, Almutairi AS, Thomson J, Alshahrani AS, Alroyli HS, Almutairi HM.** A hybrid model of in-person and telemedicine diabetes education and care for management of patients with uncontrolled Type 2 diabetes nellitus: findings and implications from a multicenter prospective study. Telemedicine Reports 2024;5(1):46-57. *https://doi.org/10.1089/tmr.2024.0003"2024.0003*
11. **Garedow AW, Jemaneh TM, Hailemariam AG, Tesfaye GT**. Lifestyle modification and medication use among diabetes mellitus patients attending Jimma University Medical Center, Jimma zone, south west Ethiopia. Sci Rep 2023;13(1):4956. *https://doi.org/10.1038%2Fs41598-023-32145-y"-y*
12. **Firman CH, Mellor DD, Unwin D, Brown A**. Does a ketogenic diet have a place within diabetes clinical practice? Review of current evidence and controversies. Diabetes Ther 2024;15(1):77-97. *https://doi.org/10.1007%2Fs13300-023-01492-4" 13300-023-01492-4.*
13. **Zhu H, Bi D, Zhang Y, Kong C, Du J, Wu X, Wei Q, Qin H**. Ketogenic diet for human diseases: the underlying mechanisms and potential for clinical implementations. Signal Transduct Target Ther 2022;7(1):11. *https://doi.org/10.1038%2Fs41392-021-00831-w"-w*
14. **Masood W, Annamaraju P, Khan Suheb MZ, Uppaluri KR**. Ketogenic Diet. StatPearls. Treasure Island (FL): StatPearls Publishing LLC; 2024.
15. **Wu J, Yang K, Fan H, Wei M, Xiong Q**. Targeting the gut microbiota and its metabolites for type 2 diabetes mellitus. Front Endocrinol 2023;14:1-12. *https://doi.org/10.3389/fendo.2023.1114424"2023.1114424*
16. **Lin Y**. The role of ketogenic diet in gut microbiota. Highl Sci Eng Technol 2022;19:36-43.
17. **Koutentakis M, Kuciński J,** Świeczkowski **D, Surma S, Filipiak KJ, Gąsecka A**. The ketogenic effect of SGLT-2 inhibitors-beneficial or harmful? J Cardiovasc Dev Dis 2023;10(11):465. *https://doi.org/10.3390%2Fjcdd10110465"10110465*
18. **Sadat A**. Alarming surge in early-onset Type 2 diabetes: A global catastrophe on the horizon. Touch REV Endocrinol 2023;19(2):7-8. *https://doi.org/10.17925%2FEE.2023.19.2.5"2023.19.2.5*
19. **Committee ADAPP**. 2. Classification and Diagnosis of Diabetes: Standards of Medical Care in Diabetes—2022. Diabetes Care 2021;45(Supplement_1):S17-S38. *https://doi.org/10.2337/dc22-S002"002*
20. **Chandgude D, Tambat P, Tale V**. A comprehensive review on keto diet on management of Type 2 diabetes and obesity. J Chem Health Risks 2024;13(4):609-614.
21. **Galicia-Garcia U, Benito-Vicente A, Jebari S, Larrea-Sebal A, Siddiqi H, Uribe KB, Ostolaza H, Martín C**. Pathophysiology of Type 2 diabetes mellitus. Int J Mol Sci 2020;21(17):6275. *https://doi.org/10.3390%2Fijms21176275"21176275*
22. **Li S, Yuan S, Lin G, Zhang J**. Effects of a two meals-a-day ketogenic diet on newly diagnosed obese patients with type 2 diabetes mellitus: a retrospective ob-

servational study. Medicine (Baltimore). 2023;102(43):e35753. *https://doi.org/10.1097%2FMD.0000000000035753" 00000 00000035753*

23. **Zhou C, Wang M, Liang J, He G, Chen N**. Ketogenic diet benefits to weight loss, glycemic control, and lipid profiles in overweight patients with Type 2 diabetes mellitus: A meta-analysis of randomized controlled trails. Int J Environ Res Public Health 2022;19(16):10429. *https://doi.org/10.3390%2Fijerph191610429"191610429*
24. **Yuan X, Wang J, Yang S, Gao M, Cao L, Li X, Hong D, Tian S, Sun C**. Effect of the ketogenic diet on glycemic control, insulin resistance, and lipid metabolism in patients with T2DM: a systematic review and meta-analysis. Nutr Diabetes 2020;10(1):38. *https://doi.org/10.1038/s41387-020-00142-z"-z*
25. **Vidić V, Ilić V, Toskić L, Janković N, Ugarković D**. Effects of calorie restricted low carbohydrate high fat ketogenic vs. non-ketogenic diet on strength, body-composition, hormonal and lipid profile in trained middle-aged men. Clin Nutr 2021;40(4):1495-1502. *https://doi.org/10.1016/j.clnu.2021.02.028"2021.02.028*
26. **Patikorn C, Saidoung P, Pham T, Phisalprapa P, Lee YY, Varady KA, Veettil SK, Chaiyakunapruk N**. Effects of ketogenic diet on health outcomes: an umbrella review of meta-analyses of randomized clinical trials. BMC Medicine 2023;21(1):196. *https://doi.org/10.1186/s12916-023-02874-y"-y*
27. **Yang Q, Vijayakumar A, Kahn BB**. Metabolites as regulators of insulin sensitivity and metabolism. Nat Rev Mol Cell Biol 2018;19(10):654-672. *"https://doi.org/10.1038/s41580-018-0044-8"41580-018-0044-8*
28. **Dowis K, Banga S**. The potential health benefits of the ketogenic diet: A narrative review. Nutrients 2021;13(5):1654. *"https://doi.org/10.3390%2Fnu13051654"13051654*
29. **Yang Z, Mi J, Wang Y, Xue L, Liu J, Fan M, Zhang D, Wang L, Qian H, Li Y**. Effects of low-carbohydrate diet and ketogenic diet on glucose and lipid metabolism in type 2 diabetic mice. Nutrition 2021;89:111230. *"https://doi.org/10.1016/j.nut.2021.111230"2021.111230*
30. **Skow SL, Jha RK**. A ketogenic diet is effective in improving insulin sensitivity in individuals with Type 2 diabetes. Curr Diabetes Rev 2023;19(6):e250422203985. *"https://doi.org/10.2174/1573399818666220425093535"15733998186662204250935 35*
31. **Paoli A, Bianco A, Moro T, Mota JF, Coelho-Ravagnani CF**. The effects of ketogenic diet on insulin sensitivity and weight loss, which came first: the chicken or the egg? Nutrients 2023;15(14):3120. *"https://doi.org/10.3390%2Fnu15143120"15143120*
32. **Rafiullah M, Musambil M, David SK**. Effect of a very low-carbohydrate ketogenic diet vs recommended diets in patients with type 2 diabetes: a meta-analysis. Nutr Rev 2022;80(3):488-502. *"https://doi.org/10.1093/nutrit/nuab040"040*
33. **Zaki HA, Iftikhar H, Bashir K, Gad H, Fahmy AS, Elmoheen A**. A comparative study evaluating the effectiveness between ketogenic and low-carbohydrate diets on glycemic and weight control in patients with type 2 diabetes mellitus: a systematic review and meta-analysis. Cureus 2022;14(5). *"https://doi.org/10.7759/cureus.25528"25528*
34. **Müller TD, Finan B, Bloom SR, D'Alessio D, Drucker DJ, Flatt PR, Fritsche A, Gribble F, Grill HJ, Habener JF, Holst JJ, Langhans W, Meier JJ, Nauck MA, Perez-Tilve D, Pocai A, Reimann F, Sandoval DA, Schwartz TW, Seeley RJ, Stemmer K, Tang-Christensen M, Woods SC, DiMarchi RD, Tschöp MH**. Glucagon-like peptide 1 (GLP-1). Mol Metab 2019;30:72-130. *"https://doi.org/10.1016%2Fj.molmet.2019.09.010"2019.09.010*
35. **Widiatmaja DM, Lutvyani A, Sari D, Kurniasari H, Meiliana I, Fasitasari M, Yamaoka Y, Rejeki P**. The effect of long-term ketogenic diet on serum adiponectin and insulin-like growth factor-1 levels in mice. J Basic Clin Physiol Phar-

macol 2021;33(5):1-11. *"http://dx.doi.org/10.1515/jbcpp-2021-0287"2021-0287*

36. Deledda A, Palmas V, Heidrich V, Fosci M, Lombardo M, Cambarau G, Lai A, Melis M, Loi E, Loviselli A, Manzin A, Velluzzi F. Dynamics of gut microbiota and clinical variables after ketogenic and mediterranean diets in drug-naïve patients with Type 2 diabetes mellitus and obesity. Metabolites 2022;12(11):1092. *"https://doi.org/10.3390%2Fmetabo12111092"12111092*

37. Paoli A, Mancin L, Bianco A, Thomas E, Mota JF, Piccini F. Ketogenic diet and microbiota: friends or enemies? Genes 2019;10(7):534. *"https://doi.org/10.3390/genes10070534"10070534*

Invest Clin 65(3): 369 - 377, 2024 https://doi.org/10.54817/IC.v65n3a09

Prediction of the individual response to treatment of skeletal Class II malocclusions and their long-term stability. A Case Report.

Sergio Duarte-Inguanzo[1,2], Aurora Duarte-López[3], Olga Zambrano[4] and Jesús A. Luengo-Fereira[5]

[1] Unidad Académica de Odontología, Universidad Autónoma de Zacatecas, Ciudad de Zacatecas, México.
[2] División de Estudios para Graduados, Facultad de Odontología, Universidad del Zulia. Maracaibo, Venezuela.
[3] Facultad de Odontología Unidad Saltillo, Maestría en Ortodoncia, Universidad Autónoma de Coahuila, México.
[4] Instituto de Investigaciones, Facultad de Odontología, Universidad del Zulia. Maracaibo, Venezuela.
[5] Unidad Académica de Odontología, Universidad Autónoma de Zacatecas, Ciudad de Zacatecas, México.

Keywords: Class II; Herbst appliance; Baccetti and Franchi model.

Abstract. Non-surgical correction of class II skeletal malocclusions begins at an early age, during the growth and development of the jaw. Treatments tend to be relatively long and generate financial commitments for the family. Predicting the success and stability of the results can be helpful for parents who wish to know about the prognosis and make the right decision to start treatment. This work reports the findings of the prediction of the response to treatment of a skeletal class II malocclusion and its long-term stability in a thirteen-year-old male patient. The individual prediction cephalometric model of Baccetti and Franchi was applied. According to this indicator, the treatment of this patient would result in "a great response". The patient was treated with a Herbst-type fixed mandibular anterior projection appliance, followed by brackets for the final detailing of the occlusion. Sixteen years later, after finishing treatment, the correction of the Class II malocclusion, the overbite and the harmony in the profile with the projection of the mandible forwards are maintained by the increase in the total mandibular length (13 mm), and through the opening of the angle between the ramus and mandibular body from 122° to 128°. In conclusion, the individual prediction cephalometric model applied, particularly in this case report, allowed us to accurately predict the excellent response and stability of the facial, dental and skeletal results of the class II skeletal malocclusion treatment.

Corresponding author: Sergio Duarte-Inguanzo. Privada Los Pinos No. 7, Colonia Cañada de la Bufa, Guadalupe, Zacatecas, México. México. Phone: +52-492-9229924. E-mail: sergio.duarteinguanzo@hotmail.com

Predicción de la respuesta al tratamiento de las maloclusiones Clase II esqueléticas y su estabilidad a largo plazo. Presentación de un caso.

Invest Clin 2024; 65 (3): 369 – 377

Palabras clave: cefalometría; aparato de Herbst, Modelo de Baccetti y Franchi.

Resumen. La corrección no quirúrgica de las maloclusiones esqueléticas clase II se inicia en las edades tempranas, durante el crecimiento y desarrollo de la mandíbula, suelen ser tratamientos relativamente largos y generar compromisos financieros para la familia. Predecir el éxito y la estabilidad de los resultados puede resultar útil a los padres que desean saber sobre el pronóstico y tomar la decisión para iniciar el tratamiento. Este trabajo reporta los hallazgos de la predicción de la respuesta al tratamiento de una maloclusión clase II esquelética y su estabilidad a largo plazo, en un paciente masculino, de trece años de edad. Se aplicó el modelo cefalométrico de predicción individual de Baccetti y Franchi, y según este indicador, el tratamiento tendría "*una gran respuesta*". El paciente fue tratado con un aparato de proyección anterior mandibular fijo tipo Herbst y apliques ortodóncicos para el detallado final de la oclusión. Dieciséis años después de finalizado el tratamiento, se mantuvo la corrección de la maloclusión Clase II, la sobremordida horizontal y la armonía en el perfil con la proyección de la mandíbula hacia adelante, mediante el aumento de la longitud total mandibular (13 mm), y por medio de la apertura del ángulo entre rama y cuerpo mandibular de 122° a 128°. En conclusión, el modelo cefalométrico de predicción individual aplicado particularmente en este reporte de caso permitió predecir de manera acertada la buena respuesta y estabilidad de los resultados faciales, dentales y esqueletales del tratamiento de la maloclusión esquelética clase II.

Received: 28-01-2024 *Accepted: 13-05-2024*

INTRODUCTION

Class II malocclusion or skeletal distoclusion significantly impacts function and facial aesthetics. The prevalent diagnostic finding in this type of malocclusion is mandibular skeletal retrusion, which is challenging to treat and has a high risk of relapse.[1]

Various functional/orthopedic devices for treating this malocclusion, among which the Herbst and the Twin-Block, stand out and have shown remarkable effectiveness [2]. In a systematic review, Cozza *et al.* reported substantial variabilities in the results of class II treatments attributed to the type of device used, duration of treatment, patient cooperation, time of intervention, and the inherent characteristics of the patient [3]. Similarly, Canut and Arias report that patients' response to this malocclusion treatment varies significantly. Moreover, the nature of the variations that induce the resolution of Class II with functional devices is still unclear [4]. Petrovic *et al.,* in addition to other authors, affirm that the effects of Class II therapy are much more effective when carried out during the peak of mandibular growth [5-7]. Saadia and Valencia report that if the therapy is applied

when biological events occur during growth and craniofacial development processes, it will have a more effective impact and less tendency to relapse [8]. The success in treating skeletal malocclusions is determined by the extent to which the correction is stable in the long term [8,9]. Al Yami *et al.* reported variable results between good and moderate stability in 10-year post-treatment follow-ups [10]. Likewise, Bondemark *et al.,* in a study on the post-treatment stability of Class II orthopedic therapies with Herbst-type appliances in patients who received the treatment during the pubertal growth peak, reported good stability regarding facial characteristics; however, they found recurrence regarding the molar and canine relationship [11].

Ruf and Pancherz report that the correction of skeletal Class II is more effective if the Herbst appliance is combined with multibracket treatment; in this way, a more significant occlusal correction is achieved, and they report stability for two years' post-treatment [12]. Tulloch *et al.* reported that in younger patients treated, less recurrence was observed than in those who received treatment at an older age [13]. Failure can occur individually to different treatments and similar protocols, even in patients who receive treatment under ideal conditions [8,9]. The possibility of predicting with greater certainty the prognosis of the results of a skeletal Class II treatment and its long-term stability could be an invaluable tool for the clinician.

Previous studies have tried to find specific predictors to anticipate a successful treatment; however, they have yet to be systematically validated [14-16]. Some authors affirm that a Class II patient at the peak of pubertal growth with a closed gonial angle of the mandible will react successfully to functional orthopedic treatment [7,17]. In this regard, Baccetti and Franchi proposed a cephalometric model to predict individually the response to treatment of a skeletal Class II malocclusion with functional jaw orthopedics. They analyzed various cephalometric parameters, noting that only the angular relationship between the ramus and the mandibular body represents the indicator with predictive power [18].

This work aimed to report the prediction of the response to treatment of a skeletal Class II malocclusion and its long-term stability using the Baccetti and Franchi cephalometric model [18].

CASE PRESENTATION

This is the case of a 13-year-old male patient who attended the orthodontic service at the Piezzo Dental Clinic in Zacatecas, Mexico. Informed consent to participate in the study was obtained from the patient and his representatives, and the authorization to publish his photograph in this study. He presented with no medical history of interest, euryprosopic facial type, a symmetrical, slightly enlarged lower facial third, convex profile, short chin-neck distance, lip incompetence, open nasolabial angle, and closed mentolabial angle (Fig. 1a). Permanent dentition, Class II molar and bilateral canine, 14 mm overjet, and 30% overbite. A triangular symmetric upper dental arch; square asymmetric lower arch, upper and lower crowding; a severe curve of Spee (Fig. 2a); and cervical vertebral maturation stage CS3 [19].

The cephalometric analysis determined a skeletal Class II mandibular hypoplasia[20] (Fig. 3a). The value of the predictive angular measurement (Co-Go-Me°) was 122°; therefore, according to the model, the patient would have a "great response" to treatment[18] (Fig. 4).

The patient was treated with a fixed Herbst-type mandibular anterior projection appliance with bands for one year and five months to position the mandible in a molar and canine Class I (Fig. 2b) and a straight profile until the end of the mandibular growth peak CS4 and the beginning of CS5[19], at 14 years and eight months of age (Fig. 1b). In the second phase, complete brackets were placed for one year, and Class

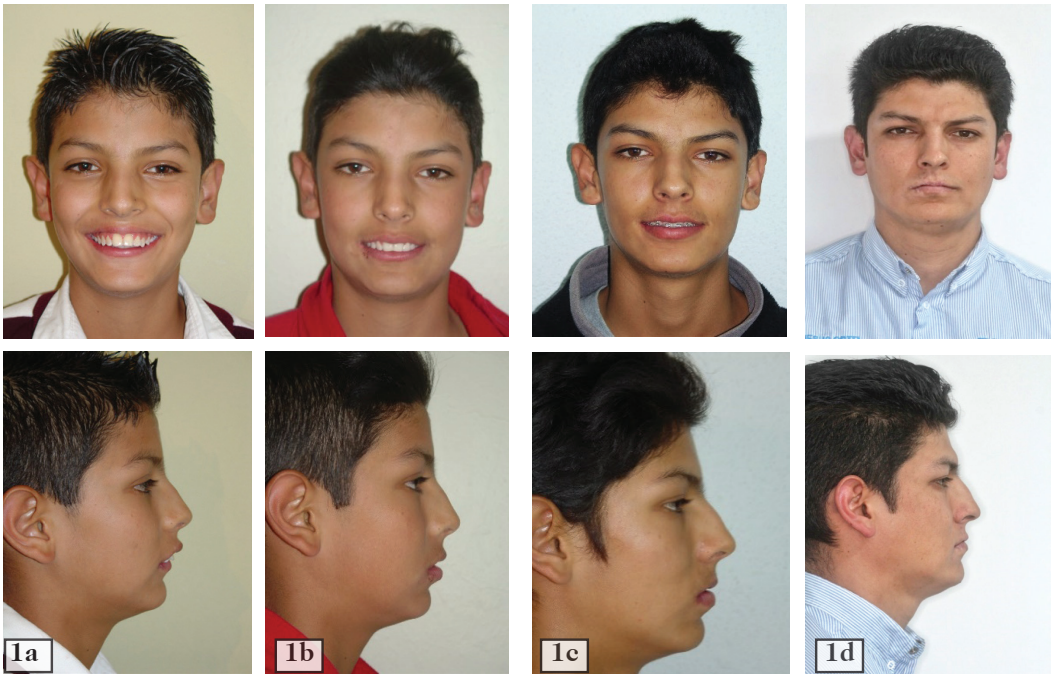

Fig. 1. Front and profile photographs: (1a) pre-treatment at 13 years and three months of age; (1b) after Herbst therapy at 14 years and eight months of age; (1c) at the end of bracket treatment at 15 years and eight months of age; (1d) 16 years after treatment completion at 31 years and nine months of age.

Fig. 2. Intraoral photographs, Right Lateral, Frontal, and Left Lateral Views: (2a) Pre-treatment at 13 years and three months of age; (2b) after Herbst therapy at 14 years and eight months of age; (2c) at the end of bracket treatment at 15 years and eight months of age; (2d) 16 years after treatment completion at 31 years and nine months of age.

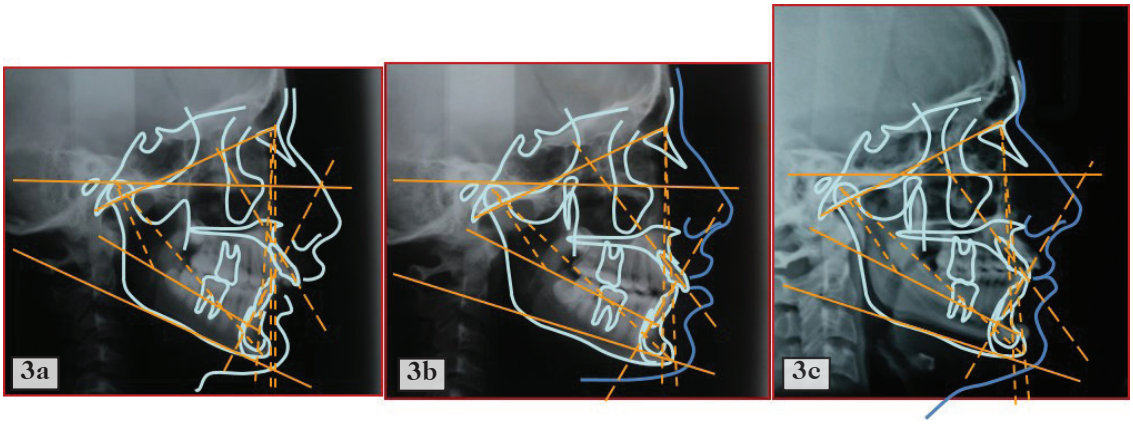

Cephalometric Measurements	Norma	Initial pre-treatment measurement (3a)	End of treatment measurement (3b)	16 years post-treatment (3c)
Convexity (A/B-Pg)	2mm	9mm	1mm	-1mm
Maxillary Deepness (PoOr-NaA)	90°	89°	89°	90°
Facial Deepness (Po-Or/N-Pg)	87°	75°	86°	88°
Mandibular Plane (Go-Me/Po-Or)	26°	30°	27°	29°
Upper Incisor / N-A	22°	25°	25°	23°
Lower Incisor / Mandibular Plane	90°	84°	89°	92°
Mandibular Arch (Dc-XI/XI-Pm)	29°	34°	28°	30°
Mandibular Body Lenght(XI-Pm)	69 mm	67 mm	68mm	70mm
Total Mandibular Length (Co-Gn)	132mm	121mm	131mm	134mm

Fig. 3. (3a) Initial Cephalometry; (3b) After treatment; (3c) 16 years post-treatment…

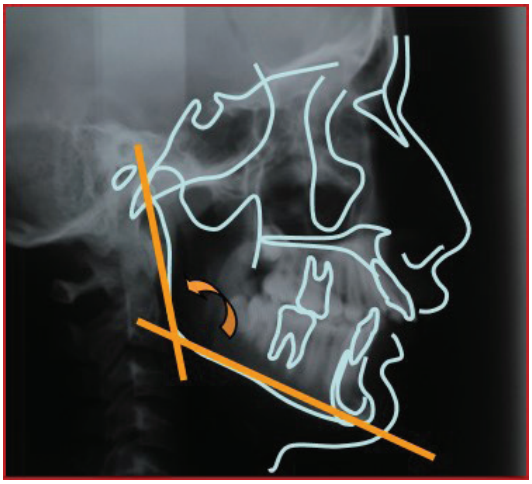

Favorably Response

Co-Go-Me 122°

The measure of the prediction was 122°, 2° below 124°, which means it will have a great response to treatment.

Fig. 4. Tracing of the Condylion, Gonion, Menton (Co-Go-Me) planes to form the predictive angle according to Baccetti and Franchi's individual prediction cephalometric model.

II intermaxillary ligatures were used for four months (Fig. 2c). The profile and facial harmony were further improved at the end of this phase (Fig. 1c). Finally, a containment period was carried out for one year with Hawley-type removable retainers, worn 24 hours a day for six months, followed by six months of only night use, and the patient was discharged. Appointments were held every three years to monitor the stability of the results.

Intraorally, the molar and canine Class II changed to Class I (Fig. 2c). Post-treatment cephalometry, in general terms, showed a remarkable correction of skeletal Class II and harmonization in profile [20]. Most notable was the 6° increase in angulation between the ramus and the mandibular body, thus increasing the total mandibular length by 10 mm (Fig. 3b).

At the age of 31 years, new records were taken: extra orally, greater harmony was observed in the facial contour, proportioned thirds, and straight and balanced profile (Fig. 1d). Intra orally, a Class I molar and canine occlusion with solid interdigitation on both sides, 2 mm overjet, and 30% overbite were observed (Fig. 2d).

Cephalometrically, a relevant value was the increase in total mandibular length of 3 mm in these 16 years after finishing the treatment, thus maintaining a balanced profile [20] (Fig. 3c).

A superimposition shows us that 16 years after treatment, the total mandibular length alone increased by 3 mm more, reaching a total increase of 13 mm since the beginning of treatment (Fig. 5).

DISCUSSION

This paper reports the prediction of the response to treatment and its long-term stability by applying the Baccetti and Franchi [18] model in an adolescent with skeletal class II malocclusion, treated with a Herbst-type fixed appliance and the use of brackets for the final detailing of the occlusion.

The study by Baccetti and Franchi [18] identified the Co-Go-Me angle with a predictive power of 80.4% reliability. According to this model, a Co-Go-Me angle between 124° and 128.5° will respond favorably to orthopedic therapy; a Co-Go-Me angle greater than 128.5° will react unfavorably to therapy; and those patients who initially present a Co-Go-Me angle of less than 124° will have a great response to treatment; however, these authors did not present long-term stability results. In the present report, this measure (122°) correctly predicted the largely favorable response to treatment.

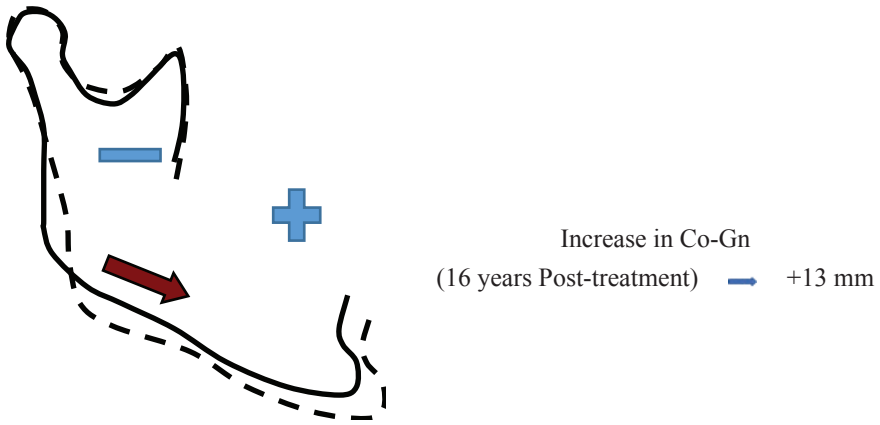

Fig. 5. Superimposition of the mandible (Continuous line: 13 years three months of age - Dotted line: 31 years nine months of age).

This prediction model determines that the shape of the mandible, specifically the angular relationship between the ramus and the body, plays a more critical role as an indicator of treatment prognosis than the position of the mandible in relation to other craniofacial structures. Other authors report similar findings [14,15].

Van Limborgh and Enlow [21] described that the mandible has growth control with a more significant genetic load than the maxilla; therefore, there is less possibility of changes under environmental influences. However, the rotations between the ramus and mandibular body and the redirection of condylar growth are susceptible to changes determined by environmental factors or therapeutic actions [21]. In skeletal Class II malocclusion due to mandibular hypoplasia, the therapeutic solution is the elongation of the mandible to bring forward its body and the chin, and this can be achieved by generating, with the treatment, a descending intra-matrix rotation between the ramus and the mandibular body; that is, opening precisely the angle between these two structures, consequently increasing the distance between the condyle and the chin, and therefore increasing the total mandibular length[2]. So, if the mandible initially presents an open angle between the ramus and the body, the prognosis could be unfavorable, since it would have less possibility of opening further and lengthening the mandible forward (it is as if a hinge were opening). Therefore, it is necessary that this angle initially be closed [5].

Cozza *et al.* suggest that a closed mandibular angle before treatment correlates with evidence of better responsiveness to orthopedic treatment to increase total mandibular length and vice versa. At the start of treatment, a patient with an open angle between the ramus and the mandibular body will be less likely to attain elongation through orthopedic therapy [3]. Likewise, Petrovic *et al.* state that the potential responsiveness to orthopedic therapy aimed at stimulating growth in the mandibular condyle is significantly more significant in the presence of anterior growth rotation of the mandible than in a posterior growth rotation [5]. In the case of the current study, the patient initially presented a significantly closed Co-Go-Me mandibular angle and a notable anterior rotation of the mandible. On the other hand, Proffit and Saadia define a good response to orthopedic therapy as one that is maintained in the long term [8,9]. Canut *et al.* state that there is a high risk of recurrence in skeletal Class II treatments; however, in some cases, it is possible to maintain stable long-term favorable treatment results, free of recurrence and containment [4].

In the case described in this report, after completing the comprehensive treatment, the patient only used removable retainers for one year with discontinuous use over time. The remaining time, the patient remained free of containment and relapse.

Ruf and Pancherz report good results in occlusal correction and stability of the treatment of skeletal Class II; they attribute this to the simultaneous application of full bracket and Herbst appliances [12]. In the patient of the present report, occlusal correction and excellent stability were achieved by combining complete brackets and Herbst. Ruf and Pancherz[12] made the stability evaluation two years after treatment, unlike in the case presented in this report, where the evaluation was performed 16 years after finishing the treatment.

Bondemark reports post-treatment stability in facial characteristics but not in occlusion or cephalometric data [11]. The present report maintained favorable facial, dental, and cephalometric changes; moreover, a better and more detailed occlusal interdigitation was achieved with time. This refinement was self-formed. Likewise, the facial profile reached a better balance and harmony, so it can be inferred that growth and development alone have the capacity for self-improvement in cases like this when they are helped at a specific moment through a treatment that creates a suitable scenario.

Tulloch *et al*. state that the earlier the age at which treatment is started, the more stable it will be, and vice versa [13]. This statement sounds somewhat ambiguous since they do not mention the specific age. In our case, Herbst therapy was started at the beginning of the CS3 [19] mandibular growth peak.

In conclusion, Baccetti and Franchi's prediction model for Class II malocclusion correction predicted the response to treatment in this particular patient, which was confirmed and resulted in long-term stable facial and dental skeleton changes.

ACKNOWLEDGMENT

We thank Dr. Humberto Martínez for his contribution to editing and translating the manuscript and Carlos E. Duarte-Hernández for searching bibliographic references.

Funding

This study was not funded.

Conflicts of interest

The authors reported no potential conflict of interest.

Authors' ORCID number

- Sergio Duarte-Inguanzo (SD): 0009-0008-7877-5574
- Aurora Duarte-López (AD): 0009-0005-0386-1046
- Olga Zambrano (OZ): 0000-0003-4867-2351
- Jesús A. Luengo-Fereira (JL): 0000-0002-2780-5496

Authors' contribution

SD: Treatment and clinical and radiographic follow-up of the case. Conception, design, analysis, and interpretation of data, editing, review, and approval of the final version of the manuscript to be published. Funding support. AD: Analysis and interpretation of data, editing, review, and approval of the final version to be published. OZ: Conception, design, analysis, and interpretation of data, editing, critical review, and approval of the final version to be published. JL: Analysis and interpretation of data, critical review, and approval of the final version to be published.

REFERENCES

1. **Enlow D.** Crecimiento Maxilofacial 1993 Edt. McGraw Hill.
2. **McNamara JA, Bookstein F**. Skeletal and dental changes following functional therapy on class II patients. Am J Orthod 2009;88:91-110.
3. **Cozza P, Baccetti T, Franchi L, De Toffol L, McNamara JA Jr.** Mandibular changes produced by functional appliances in Class II malocclusion: a systematic review. Am J Orthod Dentofacial Orthop. 2006;129(5): 599.e1-12.
4. **Canut J, Arias S.** Evaluación a largo plazo de evolución de tratamientos de maloclusiones división 2 Clases II. Eur J Orthod 2000;21:377-386.
5. **Petrovic A, Stutzmann J, Lavergne J.** Mechanism of craniofacial growth and modus operandi of functional appliances: a cell-level and cybernetic approach to orthodontic decision making. In: Carlson DS, ed. Craniofacial Growth Theory and Orthodontic Treatment. Ann Arbor, Mich: Center for Human Growth and Development, The University of Michigan; 1990:13–74. Craniofacial Growth Monograph Series; Monograph 23.
6. **Hägg U, Pancherz H**. Dentofacial orthopaedics in relation to chronological age, growth period and skeletal development. An analysis of 72 male patients with Class II division 1 malocclusion treated with the Herbst appliance. Eur J Orthod. 1988;10:169–176.

7. **Faltin K, Faltin RM, Baccetti T, Franchi L, Ghiozzi B, McNamara Jr JA**. Long-term effectiveness and treatment timing, Angle Orthod 2009;73:221-230.
8. **Saadia M, Valencia R**: Dentofacial Orthopedics in the Growing Child; Understanding Craniofacial Growth in the management of Malocclusions. Edt. Wiley Blackwell, 2022.
9. **Proffit W, Fields H**. Ortodoncia Contemporánea. Elsevier, 2019; 87-91
10. **Al Yami EA, Kuijpers-Jagtman A, van´t Hof M**. Stability of orthodontic treatment outcome: follow-up until 10 years postretention. Am J Orthod Dentofacial Orthop 1999;115(3):300-304.
11. **Bondemark L, Holm A, Hansen K, Axelsson S, Mohlin B, Brattstrom V, Paulin G, Pietila T.** Long- term stability of orthodontic treatment and patient satisfaction. A systematic review. Angle Orthod 2007;77(1):181-191.
12. **Ruf S, Pancherz H.** Herbst/multibracket appliance treatment of Class II division 1 malocclusions in early and late adulthood: a prospective cephalometric study of consecutively treated subjects. Eur J Orthod 2006;28:352-360.
13. **Tulloch JF, Phillips C, Koch G, Proffit W.** The effects of early intervention on skeletal pattern Class II malocclusion: a randomized clinical trial. Am J Orthod Dentofacial Orthop 1997;111(4):391-400.
14. **Charron C.** Recherche d´élements prognostiques quant a l'efficacite´ de l'Activateur en occlusion de classe II d'Angle. Orthod Fr. 1989;60:685–693.
15. **Cretella E, Franchi L, Gastaldi G, Giuntini V, Lione R, Cozza P, Pavoni C.** Development of a prediction model for short-term success of functional treatment of Class II malocclusion. Int J Environ Res Public Health 2020;17(12):4473.
16. **Ahlgren J, Laurin C**. Late results of activator treatment: a cephalometric study. Br J Orthod. 1976;3:181–187.
17. **Patel HP, Moseley HC, Noar JH**. Cephalometric determinants of successful functional appliance therapy. Angle Orthod. 2002;72:410–417.
18. **Baccetti T, Franchi L**. Cephalometric mandibular features for the prediction of individual outcomes of Class II treatment including functional jaw orthopedics. Am J Orthod Dentofacial Orthop 2012;43(7):112-128.
19. **Baccetti T, Franchi L**. The Cervical Vertebral Maturation (CVM) method for the assessment of optimal treatment timing in dentofacial orthopedics. Semin Orthod 2005;11(3):119-129.
20. **Duarte S.** Atlas de Cefalometría. Análisis clínico y práctico. Ed. Amolca, 2003:119-147.
21. **Van Limborgh F, Enlow D.** Rotations and increase mandibular, genetic appearance. Angle Orthod 1997;23:112-145.

Invest Clin 65(3): 378 - 386, 2024 https://doi.org/10.54817/IC.v65n3a10

Prediction of the individual response to treatment of skeletal Class III malocclusions and their long-term stability. A Case Report.

Sergio Duarte-Inguanzo[1, 2], *Aurora Duarte-López*[3], *Olga Zambrano* [4] *y Jesús A. Luengo-Fereira*[5]

[1] Unidad Académica de Odontología, Universidad Autónoma de Zacatecas, Ciudad de Zacatecas, México.
[2] División de Estudios para Graduados, Facultad de Odontología, Universidad del Zulia. Maracaibo, Venezuela.
[3] Facultad de Odontología Unidad Saltillo, Maestría en Ortodoncia, Universidad Autónoma de Coahuila, México.
[4] Instituto de Investigaciones, Facultad de Odontología, Universidad del Zulia. Maracaibo, Venezuela.
[5] Unidad Académica de Odontología, Universidad Autónoma de Zacatecas, Ciudad de Zacatecas, México.

Key words: Class III; facial mask; craniofacial growth.

Abstract. Predicting the outcome of the treatment and its stability over time is an invaluable tool for the clinician when initiating therapy for correction of class III skeletal malocclusions. This work reports the predicted response to treatment of a 5-year-old female patient with skeletal Class III malocclusion and its long-term stability. The individual prediction cephalometric model of Baccetti and Franchi was applied in this case. As a result of the predictive equation, an individual value of -0.958 was obtained (norm = -0.4065), which predicted a "very good response to treatment". The Class III malocclusion and anterior crossbite were corrected, and the profile was harmonized with rapid maxillary expansion (RME) and a facemask projecting the maxilla forward 12 mm, in addition to the mandible's 9° total downward rotation. After 15 years and three months of completing the treatment, the stability of the results was confirmed. In conclusion, the individual prediction cephalometric model used in this case report allowed us to accurately predict the results in facial, skeletal and dental changes and the long-term stability of the treatment of class III skeletal malocclusion.

Corresponding author: Sergio Duarte-Inguanzo. Privada Los Pinos No. 7, Colonia Cañada de la Bufa, Guadalupe, Zacatecas, México. Zip Code: 98619. México. Phone: +52-492-9229924. Email: sergio.duarteinguanzo@hotmail.com

Predicción de la respuesta al tratamiento de las maloclusiones clase III esqueléticas y su estabilidad a largo plazo. Presentación de un caso.

Invest Clin 2024; 65 (3): 378 – 386

Palabras clave: Clase III; máscara facial; crecimiento craneofacial.

Resumen. Predecir el resultado del tratamiento y su estabilidad en el tiempo es una herramienta invaluable para el clínico al iniciar una terapia para la corrección de las maloclusiones esqueléticas clase III. Este trabajo reporta los hallazgos de la predicción de la respuesta al tratamiento y su estabilidad a largo plazo en una paciente femenina de 5 años de edad con maloclusión Clase III esquelética. Se aplicó el modelo cefalométrico de predicción individual de Baccetti y Franchi y se obtuvo como resultado de la ecuación predictiva un valor individual de -0.958 (norma= -0.4065), lo cual predijo una "*muy buena respuesta al tratamiento*". Se corrigió la maloclusión Clase III, la mordida cruzada anterior y se armonizó el perfil con expansión rápida maxilar (ERM) y una máscara facial mediante la proyección de la maxila 12 mm hacia adelante, además de la rotación descendente total de la mandíbula 9°. Después de 15 años y 3 meses de finalizado el tratamiento se confirmó la estabilidad de los resultados. En conclusión, el modelo cefalométrico de predicción individual utilizado en este reporte de caso permitió predecir de manera acertada los resultados en los cambios faciales, esqueletales y dentales y la estabilidad a largo plazo del tratamiento de la maloclusión esquelética clase III.

Received: 28-01-2024 Accepted: 13-05-2024

INTRODUCTION

Class III skeletal malocclusion, due to its characteristics, gives a hard aspect and the appearance of a severe and rigid person. In fact, in comics, bad guys are attributed a profile of this type. However, these malocclusions are generally easy to diagnose and treat in growth-development patients. It is common for parents to notice them by their appearance alone; that is, class III is evident and is also friendly in its therapeutic response in most cases [1].

They can present with alterations in various structures [2]. however, relapse is a phenomenon that develops frequently. To be considered a successful therapy, good results need to be maintained in the long term. The response to treatment and its stability vary from patient to patient, so some patients are predestined to orthopedic failure and surgical treatment in adulthood [3-5].

The facemask is one of the most effective orthopedic therapies. However, failure can occur even in correctly applied treatments and with cooperative patients in some cases, generating frustration in the patient and the clinician [6]. This context places the dentist at a disadvantage; there is a need to know when to start the treatment, which cases will be corrected successfully and which will not, the conditions that determine good results, and their long-term stability. Saadia M. affirms that if the therapy is applied

when the biological events occur during the growth and craniofacial development process (during the primary and early mixed dentitions), it will have a more effective impact and have less tendency to relapse[7]. The authors Zere *et al.* and Campbell state that applying these treatments in the prepubertal stage is necessary [8,9]. Tweed described two different patterns of Class III malocclusion that predict the outcome of the treatment: a favorable pattern characterized by hypodivergent growth and an unfavorable pattern characterized by hyperdivergent growth [10]. Wendl *et al.* analyzed differences between patients with Class III malocclusion treated with success or failure, finding that an increased maxillary intermolar width has a higher risk of recurrence and treatment failure [11]. Paoloni *et al.* report that the width of the dental arch and the length of the upper sagittal arch in primary dentition are predictors of prognosis; when the length of the arch is decreased and the intermolar dimension is increased, there will be a greater risk of recurrence [12]. Thamira *et al.* and Zentner *et al.* reported that the gonial angle, ramus dimensions, and the mandibular body were determining factors between those who responded well or poorly to Class III treatment. The treatments were done with commonly used fixed and removable devices and combinations. An evaluation of the retention of the results was not provided [13,14]. Björk reports that a closed angulation of the skull base in patients with class III malocclusion is an unfavorable condition in the prognosis of long-term treatment [15].

Some cephalometric indicators predict treatment prognosis based on different variables, achieving different confidence levels. The most frequently studied variables are the gonial angle, Witts assessment, ramus length, the inclination of the lower incisors with respect to the mandibular plane, and the SNB angle [11,16].

Baccetti and Franchi proposed a model of cephalometric variables that individually predicts the response to treatment of skeletal Class III malocclusions treated with rapid maxillary expansion (RME) and facemask[17]. This predictive model is based on three cephalometric measurements: the vertical length of the mandibular ramus (Co-Go), the skull base angle (Ba-T and SBL), and the angle of the mandibular plane and cranial base (PM-SBL). When applying the results of these cephalometric measurements to an equation generated with the multivariate statistical method at the beginning of treatment, an individual value is obtained, which, when compared to the established norm (-0.4065), can predict the degree of therapeutic success or failure [17] (Fig. 1).

The present work describes the findings of the prediction of the response to treatment with rapid expansion and facial mask of a skeletal Class III malocclusion and its long-term stability using the Baccetti and Franchi predictive method [17].

CASE PRESENTATION

This is the case report of a 5-year-old female patient who attended the orthodontic service at the Piezzo Clinic in Zacatecas, Mexico. After explaining the study's purpose, her parents signed a consent form and approved the publication of her photographs in this paper.

The patient presented no medical history of interest, with an euryprosopic, symmetrical, and levelled facial type. She had a slightly decreased lower third, concave profile with an evident anteroposterior deficiency in the middle third and an increased chin-neck distance (Fig. 2a). The patient had primary dentition with the absence of dental organ 51, physiological spaces present, a -6mm severe anterior crossbite, bilateral edge-to-edge posterior occlusion, exaggerated or severe mesial step, bilateral class III canine relationship, and 0% overbite. (Fig. 3a).

The cephalometric analysis [18] revealed a concave skeletal Class III profile with maxillary retroposition and mandibular upward rotation (Fig. 4a).

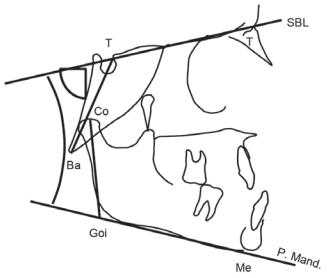

T	Tuberculum Sellae
SBL	Stable Basicranial Line
Co	Condylion
Ba	Basion
Goi	Gonion Intersection
Me	Menton
P. Mand.	Mandibular plane

Coefficients		
(Co-Goi	x	0.2282)
+ (Ba-T-SBL	x	0.205)
+ (Mand P. –SBL	x	0.120)
-*Constant*		- 29.784
= Individual Value		"X"
Norm Critical Value		-0.4065

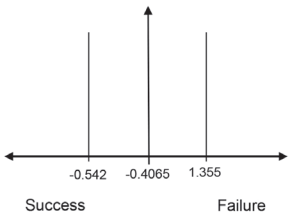

Fig. 1. (Procedure): Cephalometric Measurements of the predictive model of Baccetti and Franchi, and predictive model equation and critical value.

Fig. 2. Front and profile photographs: Initial, five years-seven months old (2a), four months after starting maxillary protraction, five years 11 months old (2b), end of orthopedic treatment, nine years 11 months old age (2c), facial characteristics 15 years three months post-treatment, 25 years two months old (2d).

When calculating the predictive value of the Baccetti and Franchi model for Class III, the result was –0.958. According to this indicator, the patient would have "a great response" to the treatment [17] (Fig. 5).

The patient was treated with rapid maxillary expansion (RME) using a fixed Hyrax-type expander for three weeks, with daily activation, and maxillary protraction therapy with a facemask, starting at cervi-

Fig. 3. Intraoral photographs: Initial, five years seven months of age (3a), four months after beginning maxillary protraction, five years 11 months of age (3b), end of orthopedic treatment, nine years 11 months of age (3c), occlusal characteristics, 15 years three months post-treatment, 25 years two months old (3d).

cal maturation stage SC1 [19], at five years and seven months of age, with constant use of 16 hours a day for a year, positive results were manifested from the first four months (Figs. 2b and 3b). She then continued using the facemask occasionally for periods of three months, with a break of approximately eight months to control relapse until the end of the maxillary growth peak, cervical maturation stage SC3 [19] and ending at nine years 11 months, with a total treatment time of four years and four months. A straight, harmonious, and proportionate profile was obtained (Fig. 2c), achieving a bilateral Class I molar and canine relationship and a positive overbite of 2 mm (Fig. 3c).

The post-treatment cephalometry [18] quantified the improvement in the characteristics of the skeletal profile. The most notable being the 9° forward relocation of the maxilla, as well as the relocation of the chin backward, due to the sum of the downward rotations between ramus and body, 4° the mandibular arch, and 9° the mandibular plane. At the end of this orthopedic phase, the patient was nine years and 11 months old (Figs. 2c, 3c, and 4b). The parents were satisfied with this result and decided not to proceed with a second multibracket phase for the final correcting details.

New records were taken when the patient was 25 years old. A symmetrical face was observed with properly proportioned thirds, a harmonious contour, and a straight and balanced profile (Fig. 2d). Intraorally, the overjet and overbite remained stable. Likewise, in an anteroposterior direction, the class I molar relationship and the bilateral class I canine relationship achieved at the end of treatment were maintained without recurrence up to the end of the follow-up period. The anterior lower spaces were maintained, while the upper ones were closed (Fig. 3d).

In cephalometry [18], relevant changes were the increases in maxillary height and AFAI that combined with a stable maxillary depth (91°) and the increase in the measurement of the mandibular arch (4°) in the 15 years after completing the treatment (Fig. 4c). They further improved the balance and

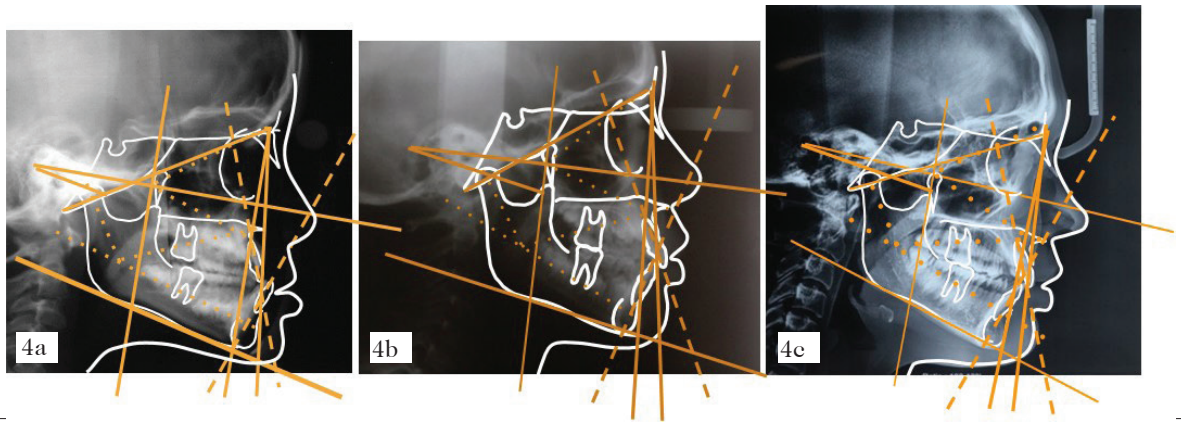

Cephalometric Measurement	Norma / Patient pretreatment (4a)	Norma / Patient Ends of orthopedic (4b)	Norma / Patient 15.3 years posttreatment(4c)
Convexity	2mm/ -7mm	2mm/ 5mm	2mm/3mm
Maxillary depth	90° / 83°	90° / 92°	90° / 91°
Facial depth	87° / 89°	87° / 86°	87° / 88°
Mandibular body length	61mm / 60 mm	65mm / 64 mm	69 / 70 mm
Mandibular plane	26° / 19°	26° / 28°	26° / 27°
Maxillary height	51° / 44°	53° / 54°	57° / 58°
Lower Anterior Facial Height (LAFH)	47° / 41°	47° / 48°	47° / 50°
1 upper/ N-A	22° / 21°	22° / 23°	22° / 23 °
1 lower / N-B	25° / 24°	25° / 25°	25° / 25°
Mandibular arch	26° / 31°	26° / 27°	28.5° / 31°
Cranial deflection	27°/ 24°	27°/ 24°	27°/ 24°
Posterior facial height	55mm/ 51mm	56.4mm/ 54mm	58.5mm/ 57mm

Fig. 4. Cephalometric analysis: Initial at five years seven months of age (4a). End phase 1, at nine years 11 months of age (4b). Measurements at 25 years two months of age (4c).

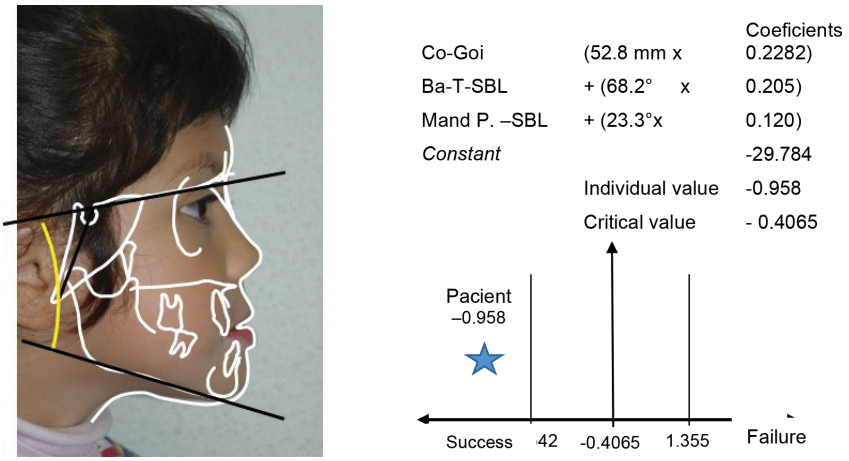

Fig. 5. Application of the individual prediction model at the beginning of treatment. According to this result, it would have a great response and stability.

symmetry in the profile and the lower third, adjusting with the self-consolidation of the permanent dentition (Fig. 3d).

DISCUSSION

Skeletal Class III treatments in children are very rewarding because they are imposing on most patients. However, there are some cases that, due to their characteristics, require surgical treatment when they reach adulthood [1].

The Baccetti and Franchi cephalometric prediction model for Class III identifies three variables with a predictive power of 83.3% reliability [17]. Orthopedic treatment will be unfavorable when there is: a) an acute angle of the skull base (Ba- T and the SBL), b) an open angle between the mandibular plane and the cranial base (PM-SBL), and c) a long mandibular ramus (Co-Goi) [17], (Fig. 1). It is worth mentioning that these authors only included the stability results after a follow-up of six years post-treatment. In the present case report, this model correctly predicted the favorable response to treatment after 15 years.

In skeletal Class III, the therapeutic solution is based mainly on the anterior repositioning of the maxilla and downward mandibular rotation, thus increasing the anterior inferior facial height (AFAI) [4]. Westwood *et al.* states that all orthopedic force is more effective when applied in the same direction of displacement due to bone growth [6]. By nature, the direction of displacement during the growth of the upper jaw is forward and downward (perpendicular to the anterior cranial base) [20]. So, if the anterior cranial base presents an inclination upwards (open skull base angle), we will have a better response to the orthopedic maxillary protraction. Furthermore, if the mandible has a counterclockwise rotation (closed mandibular plane angle) and a vertically short ramus, there will be a better response to the effect of the facial mask, thus obtaining a straighter profile and a more proportionate and balanced face and vice versa [6]. These considerations give meaning to the cephalometric measurements of the predictive model of Baccetti and Franchi since they evaluate precisely these variables. In addition, they include structures governed by genetics, such as the skull base, and others that can be modified by the environment, such as the maxilla and mandible [21], which makes it more systematic and distinguishes it from the others. This statement coincides with that of Batagel [2] and Björk [15], who report that a closed angulation of the skull base is an unfavorable condition in the prognosis of long-term treatment. The patient presented an open cranial base angulation in this report.

The other two variables analyzed by this prediction model are the vertical length of the ramus and the mandibular rotation through the distance from Co to Goi and the angle between the mandibular plane (PM) and the skull base (SBL), respectively. A short vertical ramus and a decreased mandibular plane angle may indicate a lack of vertical growth in the middle and lower third of the face [18]. So, if these measurements within the predictive equation result in a figure below the critical value or norm, it will be reasonable that the response is good since protraction therapy will cause downward rotation of the jaw, increasing the vertical and generating a straighter profile and a better proportion in the dimensions of the face.

Tweed and Nardoni *et al.* report that the hypo-divergent facial growth pattern predicts success, and the hyper-divergent pattern predicts treatment failure [10,16]. This conclusion is reasonable since one of the effects generated by the biomechanics of facial mask therapy is the downward rotation of the jaw, thus increasing the facial vertical. The patient presented in this work had a hypo-divergent facial pattern. The importance of vertical skeletal relationships in determining the prognosis of early treatment of Class III malocclusions has also been emphasized by Franchi *et al.* [22], who found that patients

with a large angle between the mandibular and palatal planes in the primary dentition ended up with less favorable long-term results. Tahmina *et al*. and Zentner *et al*. agree with this predictive cephalometric model regarding the height of the mandibular ramus since they also identified the height of the ramus and the dimensions of the mandibular body as discriminating factors between those who responded well or poorly to the treatment [13,14]. The patient in this report had decreased posterior facial height and a vertically short ramus.

Some research has reported other types of predictive variables based on the dimensions of the dental arches. Paoloni *et al*. and Franchi *et al*. report that the width of the dental arch and the length of the upper sagittal arch in primary dentition are predictors of prognosis. When the arch length decreases and the inter-molar dimension increases, there will be a greater risk of recurrence [12,22]. In the present case, the patient had primary dentition at the beginning of the treatment; the transverse dimension of the upper arch was decreased, with an adequate arch length. Hence, the excellent treatment results and long-term stability coincided with the findings of these authors [12,22]. In the present case, the structural characteristics were corrected with the treatment and generated self-improvement and stability of long-term results, which was considered a successful treatment. Surprisingly, in this patient, 15 years and three months after treatment, her clinical and cephalometric records still showed specific favorable self-regulated changes, which allows us to think that in some skeletal Class III malocclusions, craniofacial growth and development are capable of improving on its own. Their conditions exceeded our expectations.

In conclusion, the individual prediction cephalometric model of the authors Baccetti and Franchi for Class III malocclusion, applied in the present report, predicted the success of the treatment of this particular patient and could be confirmed not only with the results in the facial-skeletal and dental changes but also with its long-term stability within the 15 years post-treatment follow-up.

ACKNOWLEDGMENT

We thank Dr. Humberto Martínez for his contribution to editing and translating the manuscript and Carlos E. Duarte-Hernández for searching bibliographic references.

Funding

This study was not funded.

Conflicts of interest

The authors reported no potential conflict of interest.

Authors' ORCID number

- Sergio Duarte-Inguanzo (SD): 0009-0008-7877-5574
- Aurora Duarte-López (AD): 0009-0005-0386-1046
- Olga Zambrano (OZ): 0000-0003-4867-2351
- Jesús A. Luengo-Fereira (JL): 0000-0002-2780-5496

Authors' contribution

SD: Treatment and clinical and radiographic follow-up of the case. Conception, design, analysis, and interpretation of data, editing, review, and approval of the final version of the manuscript to be published. Funding support. AD: Analysis and interpretation of data, editing, review, and approval of the final version to be published. OZ: Conception, design, analysis, and interpretation of data, editing, critical review, and approval of the final version to be published. JL: Analysis and interpretation of data, critical review, and approval of the final version to be published.

REFERENCES

1. **Saadia M, Valencia R:** Dentofacial Orthopedics in the Growing Child; Understanding Craniofacial Growth in the management of Malocclusions. Edt. Wiley Blackwell, 2022.
2. **Batagel J.** The etiological factors in class III malocclusion. Eur J Orthod 1993;15(5):347-370.
3. **Plasencia E.** Retención y Recidiva Ortodoncia clínica y Terapéutica. Madrid: Masson;2000, p 665-667.
4. **Faltin K, Faltin RM, Baccetti T, Franchi L, Ghiozzi B, McNamara Jr JA**. Long-term effectiveness and treatment timing, Angle Orthod 2009;73:221-230.
5. **Thilander B.** Treatment of Angle Class III malocclusion with chin cap. Trans Eur Orthod Soc 1963;39:384-398.
6. **Westwood PV, McNamara JA, Baccetti T, Franchi L, Sarver DM**. Long-term effects of Class III treatment with rapid maxillary expansion and facemask therapy followed by fixed appliances. Am J Orthod Dentofacial Orhop 2003;123:306-320.
7. **Saadia M:** Dentofacial Orthopedics for the Growing Child. Barcelona: Espaxs; 1999, p 7.
8. **Zere E, Chaudhari P, Sharan J**. Developing Class III malocclusions: Challenges and solutions. Clin Cosmet Investing Dent 2018;10:99-116.
9. **Campbell P**. The dilemma of Class III treatment. Early or late? Angle Orthod. 1983;53(3):175-191.
10. **Tweed C.** Clinical Orthodontics. Vol 2. Saint Louis: CB Mosby Company 1966.
11. **Wendl B, Kamenica A, Droshl H, Jakse N, Weiland F, Wendl T, Wendl M**. Restrospective 25 year follow up of treatment outcomes in angle class III patients: success versus failure. J Orofac Orthop 2017;78(2):129-136.
12. **Paoloni V, Razza F, Franchi L, Cozza P**. Stability prediction of early orthopedic treatment in Class III malocclusion: morphologic discriminant analysis. Prog Orthod 2021;22(1):34.
13. **Tahmina K, Tanaka E, Tanne K.** Craniofacial morphology in orthodontically treated patients of Class III malocclusion with stable and unstable treatment outcomes. Am J Orthod Dentofacial Orthop 2000;117:681-690.
14. **Zentner A, Doll GM, Peylo SM**. Morphological parameters as predictors of successful correction of Class III malocclusion. Eur J Orthod 2001;23:383-392.
15. **Björk A**. Variations in the growth pattern of the human mandible: longitudinal radiographic study by the implant method. J Dent Res 1989;42:400-411.
16. **Nardoni D, Siquieira D, Cardoso M, Filho L**. Cephalometric variables used to predict the success of interceptive treatment with rapid maxillary expansion and face mask. A longitudinal study. Dental Press J Orthod. 2015;20(1):85-96.
17. **Baccetti T, Franchi L, McNamara J**. Cephalometric variables predicting the longterm success or failure of combined rapid maxillary expansion and facial mask therapy. Am J Orthod Dentofacial Orthop 2004;126(1):16-22.
18. **Duarte S**: Atlas de Cefalometría, Análisis clínico y práctico. Caracas: Amolca; 2003, p 119-147.
19. **Baccetti T, Franchi L**. The Cervical Vertebral Maturation (CVM) method for the assessment of optimal treatment timing in dentofacial orthopedics. Semin Orthod 2005;11(3):119-129.
20. **Enlow D**. Crecimiento Maxilofacial 1993 Edt. McGraw Hill.
21. **Van Limborg F, Enlow D**. Rotations and increase mandibular, genetic appearance. Angle Orthod 1997;23:112-145.
22. **Franchi L, Baccetti T, Tollaro I.** Predictive variables for the outcome of early functional treatment of Class III malocclusion. Am J Orthod Dentofac Orthop 1997;112(1):80-86.

Invest Clin 65(3): 387 - 402, 2024 https://doi.org/10.54817/IC.v65n3a11

Efectos biológicos y terapéuticos de *Cibotium barometz*, planta de la medicina tradicional: Revisión exploratoria.

José Luis Rivas-García[1], Nayely Torres-Gómez[1], Luisa Elena Silva-De Hoyos[1] y Liliana Argueta-Figueroa[2]

[1] Tecnológico Nacional de México, Instituto Tecnológico de Toluca. Colonia Agrícola Bellavista, Metepec, Estado de México, México.

[2] CONAHCyT, Tecnológico Nacional de México, Instituto Tecnológico de Toluca. Colonia Agrícola Bellavista, Metepec, Estado de México, México.

Palabras clave: cibota; Gou-ji; Penghawar Djambi; helecho lanudo; medicina complementaria.

Resumen. El propósito de esta revisión es brindar un panorama actual de la evidencia de los efectos biológicos y terapéuticos de *Cibotium barometz* y su potencial para tratar diversas afecciones. La presente revisión se realizó siguiendo las directrices de PRISMA-ScR. La búsqueda se llevó a cabo en las bases de datos PubMed, Scopus, Web of Science y Embase así como en Google Académico. La información extraída de los estudios se sintetizó de forma cualitativa. A través de la búsqueda se encontraron un total de 902 registros, de los cuales, después del proceso de selección se evaluaron 17 artículos en texto completo, pero sólo 14 artículos cumplieron los criterios de elegibilidad y fueron incluidos en esta revisión. Las actividades biológicas y terapéuticas de *Cibotium barometz* reportadas son como antioxidante, antimicrobiano, antiviral, pretratamiento anticancerígeno, estimulación de la proliferación de condrocitos, osteoprotector y hepatoprotector. La evidencia encontrada sugiere que *C. barometz* posee diversos efectos biológicos y terapéuticos tanto *in vitro* como *in vivo*, motivo por el cual resulta un tópico relevante que podría considerarse para establecer una mayor cantidad de estudios de caracterización fitoquímica, así como estudios clínicos que aporten una evidencia sólida y determinen otros posibles usos terapéuticos.

Autor de correspondencia: Liliana Argueta-Figueroa. CONAHCyT, Tecnológico Nacional de México, Instituto Tecnológico de Toluca. Colonia Agrícola Bellavista, Metepec Estado de México, México. Tel (+52)7222087200. Correo electrónico: l_argueta_figueroa@hotmail.com

Biological and therapeutic effects of *Cibotium barometz*, traditional medicinal plant: A scoping review.

Invest Clin 2024; 65 (3): 387 – 402

Keywords: cibota; Gou-ji; Penghawar Djambi; woolly fern; complementary medicine.

Abstract. This review aims to provide a current overview of the evidence for the biological and therapeutic effects of *Cibotium barometz* and its potential to treat various conditions. The present review was performed following the PRISMA-ScR guidelines. The search used PubMed, Scopus, Web of Science, Embase databases, and Google Scholar. The information extracted from the studies was synthesized qualitatively. Through the search, 902 records were found, of which, after the selection process, 17 full-text articles were evaluated, but only 14 articles met the eligibility criteria and were included in this review. The reported biological and therapeutic activities of Cibotium barometz are antioxidant, antimicrobial, antiviral, anticancer pretreatment, stimulation of chondrocyte proliferation, osteoprotective, and hepatoprotective.The evidence found suggests that C. barometz has various biological and therapeutic effects both *in vitro* and *in vivo*, which is why it is a relevant topic that could be considered to establish a more significant number of phytochemical characterization studies, as well as clinical studies that provide solid evidence and determine other possible therapeutic uses.

Recibido: 10-03-2024 Aceptado: 24-06-2024

INTRODUCCIÓN

Cibotium barometz (Linn.) J. Sm. (*C. barometz)*, conocida comúnmente como "cibota", "helecho lanudo", "helecho chivo" o "Penghawar Djambi" es un helecho arborescente perteneciente a la familia *Cibotiaceae*, que puede alcanzar hasta 3 metros de altura y tiene una rizoma denso y leñoso, con raíces que asemejan pelos de color dorado amarillento formado por tricomas multicelulares de tipo lanoso [1]. *C. barometz* es originaria de China y se encuentra distribuida en este país, así como en Malasia y la India; además, se ha adaptado bien al clima subtropical, y frecuentemente, dada su configuración estética, en muchos otros países se utiliza como planta de ornato [2].

C. barometz ha sido llamada Planta Tartárica Barometz, formando parte de leyendas mitológicas. En este sentido, se creía que era mitad animal, mitad vegetal, el fruto era un cordero unido al helecho a través de un cordón umbilical, y ambos morían cuando la oveja comía todas las hojas. El mito surge porque si se observa el helecho sin hojas, el rizoma al revés se asemejaría a un cordero con los tallos de las frondas asemejando las patas [1,3]. La configuración de *C. barometz* consiste en un rizoma monopodal con un tallo subterráneo, el cual crece en dirección horizontal produciendo raíces; y de una parte aérea, que consiste en un tallo con hojas que crece en cada yema o nudo del rizoma. Debido a esta configuración, los rizomas se encuentran en crecimiento continuo y la propagación de la planta es relativamente sencilla [4].

Los pelos de color dorado en el rizoma y las partes jóvenes de *C. barometz* y otras es-

pecies de *Cibotium* se han utilizado en China por sus propiedades astringentes para detener el sangrado. Además, en el continente asiático se utiliza un extracto del rizoma conocido como "Gou ji", al cual se le atribuyen propiedades antiinflamatorias y analgésicas siendo una de las hierbas más utilizadas en las fórmulas que se prescriben para el tratamiento de la osteoporosis en China [1]. También se emplea como un antirreumático, para fortalecer la columna vertebral, para el tratamiento de poliuria y leucorrea, así como para tratar heridas y ulceras promoviendo la cicatrización. Desde la perspectiva de la Medicina Tradicional China se ha postulado que el *C. barometz* ayuda a fortalecer el riñón, fortalecer el hígado, expulsar el viento, eliminar la humedad y flema [4].

En la actualidad, la evidencia acerca del uso de extractos provenientes de plantas ha ido creciendo, así como sus aplicaciones, no solo para la búsqueda de nuevas biomoléculas sino para aprovechar sus compuestos bioactivos como agentes reductores y estabilizadores en la síntesis de nanoestructuras [5,6]. Por lo cual, es importante la organización, sistematización y síntesis de la evidencia a través de los lineamientos de establecidos en la medicina basada en evidencia [7]. Además, la terapéutica a basada en remedios naturales fue reconocida en la Cumbre Mundial de la Organización Mundial de la Salud sobre Medicina Tradicional, en la que se analizaron las formas a través de las cuales, las medicinas tradicionales, complementarias e integradoras ayudan a hacer frente a los problemas de salud [8]. Por lo tanto, el estudio de los compuestos activos de las plantas es relevante para caracterizar y entender los mecanismos de acción de los fitocompuestos, puede permitir la identificación de nuevas moléculas bioactivas, así como proveer de evidencia científica al uso de plantas para tratar afecciones, o por el contrario, señalar su potencial toxicidad si fuera el caso, y cuáles son las áreas de oportunidad para su uso en la medicina complementaria [9].

Por lo tanto, el objetivo de esta revisión exploratoria es proporcionar un panorama actual de la evidencia de las actividades biológicas y terapéuticas reportadas, y adicionalmente, de los fitocompuestos que posee *C. barometz*.

METODOLOGÍA

Diseño del estudio. La presente revisión sistemática se realizó siguiendo las recomendaciones para revisiones exploratorias (scoping reviews) de la declaración PRISMA-ScR [7].

Criterios de elegibilidad y características de los estudios incluidos. Los criterios de elegibilidad fueron artículos con texto completo en idioma inglés o español, publicados en cualquier momento del tiempo. Dichos artículos deben tener diseño de estudios clínicos, *in vivo* o *in vitro*; y deben proveer información acerca las actividades biológicas y terapéuticas, y opcionalmente, de los fitocompuestos que posee *C. barometz.* Los criterios de exclusión fueron otras revisiones de la literatura y *C. barometz* en formulación con otros compuestos.

Estrategia de búsqueda y bases de datos usadas. La búsqueda se llevó a cabo en noviembre de 2022 y fue actualizada en marzo de 2023. Las palabras clave y los algoritmos de la estrategia de búsqueda usados se muestran en la Tabla 1. Dos revisores se encargaron de la búsqueda en las bases de datos PubMed, Scopus, Web of Science y Embase, así como en Google Académico. Adicionalmente, se realizó una búsqueda manual en la bibliografía de los estudios incluidos en la presente revisión.

Selección de los estudios. Los registros identificados en la búsqueda fueron tamizados a través de la lectura del título y el resumen para determinar si debían de ser analizados a texto completo, seleccionado aquellos que cumplían con los criterios de elegibilidad y se excluyeron los que no satisfacían dichos criterios.

Tabla 1
Estrategia de búsqueda en las bases de datos.

Base de datos	Algoritmo de búsqueda
PubMed	(“Cibotium barometz (L.) J. Sm.” OR “Cibotium barometz” OR “barometz”) AND (“bioactive compounds” OR “biological effect” OR “phytotherapeutic” OR antibacterial OR anti-inflammatory OR antioxidant OR “wound healing” OR “dressing” OR “osteogenic” OR “hepatoprotective”)
Scopus	TITLE-ABS-KEY (“Cibotium barometz L. J. Sm.” OR “Cibotium barometz” OR “barometz”) AND (“bioactive compounds” OR “biological effect” OR “phytotherapeutic” OR “antibacterial” OR “anti-inflammatory” OR “antioxidant” OR “wound healing” OR “dressing” OR “osteogenic” OR “hepatoprotective”)
Web of Science	(ALL=((“Cibotium barometz L. J. Sm.” OR “Cibotium barometz” OR “barometz”) ALL=((“ “bioactive compounds” OR “biological effect” OR “phytotherapeutic” OR “antibacterial” OR “anti-inflammatory” OR “antioxidant” OR “wound healing” OR “dressing” OR “osteogenic” OR “hepatoprotective”)
Embase	(“Cibotium barometz (L.) J. Sm.” OR “Cibotium barometz” OR “barometz”) AND (“bioactive compounds” OR “biological effect” OR “phytotherapeutic” OR antibacterial OR anti-inflammatory OR antioxidant OR “wound healing” OR “dressing” OR “osteogenic” OR “hepatoprotective”)
Google académico	(“Cibotium barometz (L.) J. Sm.” OR “Cibotium barometz” OR “barometz”) AND (“bioactive compounds” OR “biological effect” OR “phytotherapeutic” OR antibacterial OR anti-inflammatory OR antioxidant OR “wound healing” OR “dressing” OR “osteogenic” OR “hepatoprotective”)

Proceso de recolección y síntesis de los datos. Los datos relevantes de los artículos incluidos fueron registrados, tomando en consideración el diseño del estudio, la metodología, y los resultados. Dos revisores de manera independiente se encargaron de la obtención de los datos, así como la organización y síntesis de la información.

RESULTADOS

Al realizar la búsqueda se encontraron un total de 902 registros. Después de descartar los duplicados, al revisar el título y el resumen de los registros se determinó si parecían cumplir los criterios de elegibilidad, en caso positivo se descargaron y evaluaron 19 artículos de texto completo, sin embargo, únicamente 16 artículos satisfacían por completo los criterios y fueron incluidos en la presente revisión. En la Fig. 1 se muestra el proceso de selección y tamizaje de los estudios incluidos. Dichos artículos fueron exclusivamente estudios con diseño *in vitro* e *in vivo*, ya que no se encontraron estudios clínicos. Tres estudios fueron excluidos con razones: dos estudios debido a que el texto completo se encuentra únicamente en idioma chino [10,11] y otro artículo debido a que fue retractado [12]. En la Tabla 2 se encuentra un resumen de los estudios con actividad terapéutica o biológica incluidos en el presente trabajo.

Compuestos fitoquímicos de *C. barometz*

El análisis cualitativo del rizoma de *C. barometz* a través de extractos con diferentes solventes (hexano, cloroformo, acetato de etilo, etanol, metanol y agua) mostró que los extractos contenían diversos compuestos bioactivos tales como antraquinonas, flavonoides, fenoles, taninos, fitoesteroles y triterpenoides. El extracto de acetato de etilo (un éster) exhibió mayor actividad antioxidante y capacidad de absorción de radicales de oxígeno, al parecer esto se debe a los polifenoles no flavonoides, además, dicho

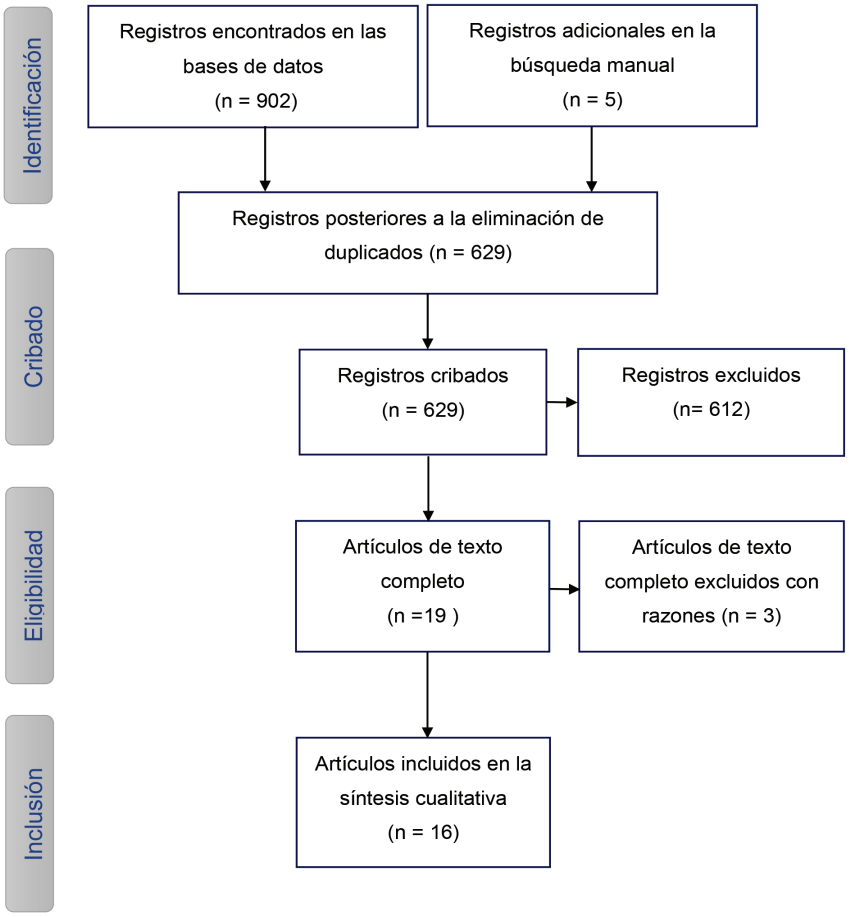

Fig. 1. Diagrama de flujo PRISMA del proceso de selección de los estudios.

extracto tuvo mayor actividad antifúngica y antibacteriana. El análisis cuantitativo, utilizando cromatografía de gases acoplada a espectrometría de masas, reveló la presencia de 1-nonadeceno, Z-5-nonadeceno, octacosanol y 1-tetracosanol/1-heneicosanol, los cuales contribuyen parcialmente a los efectos antioxidante y antimicrobiano del rizoma de *C. barometz* [13]. Por otra parte, mediante cromatografía electrocinética micelar se identificaron en *C. barometz* cinco compuestos: ácido protocatequiico, aldehído protocatequiico, ácido cafeico, jeringatina y vainillina [14].

En otros estudios, como los del grupo de investigación de Xie y col. [11,15,16] se han enfocado en la identificación de glucósidos a través de extracto etanol:agua 1:1 y una posterior hidrólisis ácida, y su potencial aplicación terapéutica se describe más adelante.

En un estudio realizado por Chen y col.[17] se identificaron los componentes claves del rizoma de *C. barometz* a través de cromatografía de líquidos acoplada a espectrometría de masas, entre los cuales están 1,3,7-trihidroxi-2-(3-metilbut-2-enil) xantona, cochinchinol a, cochinchinol b, cudraflavanona b, cudraxantona q, aspidinol, kaempferol y 6-desoxijacareubina.

En un estudio llevado a cabo por Kim y col. [18] determinaron que los fitocompuestos presentes en el rizoma de *C. barometz* en extracto alcohólico fueron ácido protocatequiico, hidrato de (+)-catequina, ácido p-cumárico, ácido elágico, ácido clorogénico, ácido cafeico y ácido ferúlico.

Tabla 2
Características de los estudios incluidos.

Estudio y diseño	Elementos de prueba	Extracto	Parámetros evaluados
Actividad antioxidante, antibacterial y antiviral			
Wen y col. (2011) *in vitro*	Actividad antiviral en SARS-CoV en células Vero E6	Extracción acuosa de *C. barometz* por ultrasonido, filtrado y el residuo fue extraído en metanol por ultrasonido y liofilizado.	Viabilidad celular usando el método de MTT Inhibición de la replicación viral Ensayo de inhibición de la proteasa 3CL de SARS-CoV
Lai y col. (2012) *in vitro*	Actividad antioxidante Actividad antibacterial (probada en 8 cepas bacterianas[1])	Extracto metanólico de hojas de *C. barometz*, y liofilización.	Ensayo antioxidante DPPH• Poder reductor de Fe^{3+} Contenido de fenoles totales Ensayo de blanqueamiento de betacaroteno Actividad de inhibición de la tirosinasa Halos de inhibición
Mai y col. (2012) *in vitro*	Actividad antioxidante	Extracto metanólico utilizando el método Soxhlet, del rizoma de *C. barometz*	Ensayo antioxidante DPPH• ABTS•+ $•O_2$ •OH Poder reductor de Fe^{3+} Poder reductor de Cu^{2+} Contenido de fenoles totales Contenido de ácido cafeico
Zarib y col. (2018) *in vitro*	Actividad antioxidante	Extractos obtenidos por maceración en ciclohexano, diclorometano, acetato de etilo, o metanol, del rizoma de *C. barometz*	Ensayo antioxidante DPPH• ABTS•+ Contenido de fenoles flavonoides totales Poder reductor de Fe^{3+}
Heng y col. (2020) *in vitro*	Actividad antibacterial (probada en 11 microorganismos[2]) Actividad antioxidante	Extractos del rizoma de *C. barometz* con hexano, cloroformo, acetato de etilo, etanol, metanol o agua, liofilizado.	Detección cualitativa de fitoquímicos Ensayo antioxidante DPPH• Poder reductor de Fe^{3+} Ensayos antibacterianos y antifúngicos
Pretratamiento anticancerígeno			
Shi y col. (2020) *in vitro*	Efecto sensibilización quimioterapéutica en células U87 de glioblastoma humano	Extracto etanólico del rizoma en polvo de *C. barometz*, desproteinización por el método de Sevag y papaína; y liofilización.	Contenido de sacáridos Viabilidad celular ROS intracelular

Tabla 2. CONTINUACIÓN

Estudio y diseño	Elementos de prueba	Extracto	Parámetros evaluados
Tratamiento para la atrofia muscular			
Kim, y col. (2023) *in vitro*	Atrofia muscular inducida por dexametasona en un modelo celular *in vitro* utilizando miotubos C2C12	Extracto etanólico del rizoma de *C. barometz*	Viabilidad celular con MTT en células C2C12. Efecto en los miotibos de las células C2C12.
Estimulación de la proliferación de condrocitos			
Fu, y col. (2017) *in vitro*	Modelo *in vitro* de proliferación de condrocitos	Fracciones de polisacáridos obtenidos del rizoma de *C. barometz*	Viabilidad celular con MTT Reacción en cadena de la polimerasa cuantitativa con transcripción inversa Western blot
Actividad osteoprotectora			
Cuong, y col. (2009) *in vitro*	Modelo de inhibición de la formación de osteoclastos	Fracciones de glucósidos obtenidos del rizoma de *C. barometz*	Masa ósea Recambio óseo Fuerza del tejido óseo Marcadores bioquímicos de resorción ósea Flexión de tres puntos Microarquitectura del hueso trabecular
Zhao, y col. (2011) *in vivo*	Actividad osteoprotectora en ratas Sprague-Dawley	Extracto etanólico al 70% del rizoma de *C. barometz*	Densidad mineral ósea total en el fémur Marcadores de recambio óseo (osteocalcina, la fosfatasa alcalina, desoxipiridinolina y niveles en orina de Ca y P) Resistencia ósea Microarquitectura trabecular
Huang, y col. (2018a) *in vitro*	Actividad osteoprotectora en la línea celular derivada de calvaria de ratón MC3T3-E1	Fracciones de polisacáridos obtenidos del rizoma de *C. barometz* (CBBP-2 y CBBP-3)	Fosfatasa alcalina
Huang, y col. (2018b) *in vivo*	Actividad osteoprotectora en ratas Sprague-Dawley	Fracciones de polisacáridos obtenidos del rizoma de *C. barometz* (CBBP-1)	Densidad mineral ósea Contenido mineral óseo Expresión de ARNm del factor de transcripción 2
Huang, y col. (2020) *in vitro*	Evaluación de la proliferación, diferenciación y mineralización de células preosteoblásticas	Fracciones de polisacáridos obtenidos del rizoma de *C. barometz* (CBP70-1-1 y CBP70-1-2)	Viabilidad celular Actividad de fosfatasa alcalina Ensayo basado en rojo de alizarina

Tabla 2. CONTINUACIÓN

Estudio y diseño	Elementos de prueba	Extracto	Parámetros evaluados
Prevención de osteoartritis			
Chen, y col. (2022) *in vitro* e *in vivo*	Viabilidad celular de SW1353. Modelo de osteoartritis de rodilla por el método de Hulth en ratas Sprague-Dawley (n=6/grupo)	Decocción por 1 hora tres veces, se agregó etanol anhidro, centrifugación, destilación a presión, secado por aspersión, congelación a -20ºC.	Viabilidad celular con MTS. Evaluación histológica. Concentraciones de MMP-1, MMP-3. MMP-13. COX_2 y PGE_2. Efecto en la vía NFκB.
Actividad hepatoprotectora			
Xie, y col. (2017) *in vitro*	Modelo *in vitro* de daño hepático agudo inducido por acetaminofén (APAP) en la línea celular HepG2	Extracto etanólico al 50% del rizoma de *C. barometz* e hidrólisis ácida	Viabilidad celular usando el método de MTT
Li, y col. (2019) *in vitro*	Modelo *in vitro* de daño hepático agudo inducido por acetaminofén (APAP) en la línea celular HepG2	Extracto etanólico al 50% del rizoma de *C. barometz* e hidrólisis ácida	Viabilidad celular usando el método de MTT

[1]Micrococcus luteus, Bacillus cereus, Staphylococcus aureus, Escherichia coli, Pseudomonas aeruginosa, Salmonella choleraesuis, Enterobacter aerogenes y Klebsiella pneumoniae, [2]Bacillus cereus, Staphylococcus aureus, Acinetobacter baumannii, Escherichia coli, Klebsiella pneumoniae, Pseudomonas aeruginosa, Candida albicans, Candida krusei, Candida arapsilosis, Cryptococcus neoformans y Aspergillus fumigatus. DPPH• (radical 1, 1-difenil-2-picrilhidrazilo), BCB (Beta-carotene bleaching assay) ABTS•+ (radical de sal diamónica del ácido 3-etilbenzotiazolina-6-sulfónico), •O2- (radical anión superóxido), •OH (radical hidroxilo), Trolox (± -6 -hidroxil -2,5, 7, 8-tetramethlychromane-2-carboxyl acid), BHA (butilhidroxianisol), MTT (bromuro de 3-(4,5-dimetiltiazol-2-il)-2,5-difeniltetrazolio), ROS (especies reactivas de oxígeno), MTS [3-(4,5-dimetiltiazol-2-il)-5-(3-carboximetoxifenil)-2-(4-sulfofenil)-2H-tetrazolio].

Li y col. [19] reportaron los compuestos de *C. barometz* encontrados a través de ChemMapper, los cuales fueron más de 60 compuestos, entre los cuales destacan ácido esteárico, ácido hexadecanoico, piperitona, aldehído protocatequiico, vainillina, glucopiranósido, ácido-9-octadecenoico, éster metílico del ácido linolénico, éster metílico del ácido 3-O-cafeoilquínico, isoflavona de soja, fenacetina, linalool, 1,3-di-acido O–cafeoilquínico, kaempferol, aldehído protocatéquico, quercetina, anetol, glucopiranósido, entre otros; asimismo, a través de un análisis farmacológico en red utilizando el software Cytoscape para determinar la intersección compuesta de enfermedades-objetivos apuntando a que el principal compuesto activo de *C. barometz* para la artritis es 3,5-dimetil-4-hidroxibenzaldehído.

Recientemente se ha reportado por Ji y col. [20] que *C. barometz* produce una variedad de triterpenos bioactivos y sus metabolitos, así como la vía biosintética de estos triterpenos, encontrando que los genes relacionados están altamente expresados en el rizoma. Este trabajo es relevante porque los triterpenos y sus metabolitos, como los triterpenoides y las saponinas triterpenoides, desempeñan funciones esenciales en la fisiología de las plantas, especialmente en la defensa de

las plantas contra plagas y fitopatógenos invasores, además de potencialmente ser útiles para el desarrollo de nuevos fármacos.

Efectos biológicos y terapéuticos reportados

a) Antioxidante, antimicrobiano y antiviral

Lai y col. [21] evaluaron la capacidad antioxidante, la inhibición de la tirosinasa y el efecto antimicrobiano en bacterias grampositivas y gramnegativas del extracto de las hojas *C. barometz*; y encontraron que posee actividad antioxidante, probablemente debido a la presencia de compuestos fenólicos, pero una débil inhibición de la tirosinasa (35%). En la prueba de difusión en disco únicamente se formaron halos de inhibición con *Staphylococcus aureus* y *Bacillus cereus* (con altas concentraciones, siendo de 500 y 1000 μg/mL, respectivamente), mientras que *Micrococcus luteus*, *Escherichia coli*, *Pseudomonas aeruginosa*, *Salmonella cholerasius*, *Enterobacter aerogenes* y *Klebsiella pnemona* fueron resistentes.

Mai y col. [22] determinaron que el rizoma de *C. barometz* posee actividad antioxidante *in vitro* que podría ser atribuible a la presencia de compuestos fenólicos tales como el ácido cafeico, el ácido protocatequiico, el kaempferol y la oniquina.

Zarib y col. [23] determinaron el solvente idóneo para obtener el mayor contenido fenólico total y contenido flavonoide total utilizando solventes de diferentes polaridades, encontrando que el mayor contenido fenólico total se observó con el extracto de acetato de etilo, seguido de extracto en metanol, extracto en diclorometano y extracto de ciclohexano. En ese mismo orden resultó la actividad eliminadora de radicales (ABTS+) y la capacidad reductora de iones metálicos (Fe^{3+}).

Heng y col. [13] obtuvieron extractos de los pelos de rizoma con diferentes solventes comparando su actividad antioxidante y antimicrobiana. La actividad antioxidante de captación de radicales DPPH• del extracto obtenido en acetato de etilo resultó muy similar al estándar utilizado en la prueba (ácido ascórbico), seguido de los extractos con etanol, metanol y agua; en cambio, los obtenidos con cloroformo y hexano tuvieron porcentajes antioxidantes significativamente menores. En lo que se refiere a la actividad antimicrobiana, el extracto de acetato de etilo fue el único que mostró actividad antibacteriana frente a *Bacillus cereus, Staphylococcus aureus, Acinetobacter baumannii, Escherichia coli, Klebsiella pneumoniae y Pseudomonas aeruginosa*, sin embargo, tuvo un efecto fue bacteriostático en contacto con *E. coli* y *K. pneumoniae*; observando que las bacterias gramnegativas fueron menos susceptibles que las grampositivas. Todos los extractos exhibieron actividad antifúngica, pero a concentraciones mayores que las utilizadas para la inhibición bacteriana. El extracto con acetato de etilo también exhibió mayor inhibición del crecimiento de las levaduras probadas, pero con *A. fumigatus* fue únicamente fungistático. Potencialmente las propiedades antioxidantes y antimicrobianas del extracto con acetato de etilo se deben a los polifenoles no flavonoides y a los alcoholes alifáticos que encontraron 1-heneicosanol, 1-tetracosanol, octacosanol.

En lo que respecta a la actividad antiviral, Wen y col. [24] reportaron que el extracto del rizoma de *C. barometz* inhibe al coronavirus SARS-CoV sin afectar la viabilidad celular de las células huésped (Vero E6), mostrando una inhibición de la actividad de la proteasa 3CL de SARS-CoV.

b) Pretratamiento anticancerígeno

Shi [25] investigaron el efecto actividad de sensibilización quimioterapéutica de los polisacáridos de *C. barometz* en una línea celular de glioblastoma (U87). Los extractos obtenidos fueron dos tipos de polisacáridos: procesados y crudos; en los primeros, utilizaron calentamiento a 80°C; y, los segundos fueron sin calor. Estos polisacáridos como tratamiento previo al fármaco de elección

(temozolomida) redujeron significativamente la viabilidad celular de U87; particularmente, los polisacáridos crudos mostraron una mejor actividad que los polisacáridos procesados, lo cual tendría una repercusión en la clínica ya que podría reducirse la dosis de la temozolomida y por tanto su toxicidad, sin disminuir su eficacia.

c) Tratamiento para la atrofia muscular

En un modelo *in vitro,* Kim y col. [18] probaron el extracto etanólico de *C. barometz* y determinaron que la regulación negativa de la proteína de miosina de cadena pesada (MyHC) inducida por dexametasona aumentó con el extracto, así como la longitud y el ancho de los miotubos. Además, el número de núcleos teñidos localizados en miotubos positivos para MyHC aumentaron significativamente. Por lo cual, dicho extracto podría ser potencialmente útil para aliviar la sarcopenia.

d) Estimulación de la proliferación de condrocitos

Fu [26] realizaron un estudio *in vitro*, en el cual aislaron condrocitos de las rodillas de ratas Sprague–Dawley para probar los polisacáridos obtenidos del rizoma de *C. barometz* a través de un ensayo de viabilidad celular, observando un aumento en la proliferación de condrocitos de manera dosis-dependiente. Además, encontraron que la estimulación de la proliferación de los condrocitos ocurre mediante la promoción de la transición del ciclo celular G1/S.

e) Actividad osteoprotectora

De acuerdo con la medicina tradicional china, el riñón es responsable de la nutrición de los huesos y también ayuda en las funciones gonadales [27]. De esta forma, *C. barometz* contribuiría en la nutrición de los huesos a través de su efecto sobre los riñones, por lo que algunos autores buscaron evidencia científica que soportara este efecto osteoprotector.

Un estudio *in vitro* realizado por Cuong y col. [28] identificó los fitocompuestos de *C. barometz,* algunos de estos no habían sido descritos previamente como cibotiumbarosida B, cibotiglicerol B y galactopiranósido y se caracterizó un compuesto previamente identificado en otros seres vivos, el corcoionósido C. Además, se probó la inhibición de la formación de osteoclastos, para lo cual se obtuvieron macrófagos primarios derivados de la médula ósea del fémur y la tibia de ratones; y también se estimuló la generación de osteoclastos, resultado que los compuestos antes mencionados tuvieron una alta inhibición de la formación de osteoclastos, particularmente el cibotiglicerol B (97%).

Adicionalmente se encontraron cuatro estudios pertenecientes al mismo grupo de investigación. En el primero, Zhao y col. [29] probaron un extracto etanólico al 70% del rizoma de *C. barometz* en un modelo *in vivo* de pérdida ósea inducida por ovariectomía, las hembras fueron asignadas a grupos con 1) tratamiento con vehículo (control); 2) tratamiento con estradiol (25 g/kg/día); 3) tratamiento con extracto de *C. barometz* a diferentes dosis (100, 300 ó 500 mg/kg/día) y 4) grupo de procedimiento quirúrgico simulado. La administración de estradiol o del extracto de *C. barometz* durante 16 semanas comenzó a las 4 semanas posquirúrgicas. El extracto de *C. barometz* evitó la disminución de la densidad mineral ósea total, lo que estuvo acompañado por una disminución significativa en la remodelación esquelética y de los niveles de los marcadores de recambio óseo. Asimismo, este estudio mostró que el extracto de *C. barometz* podría mejorar la resistencia ósea previniendo el deterioro de la microarquitectura trabecular. Posteriormente, Huang y col. [30] evaluaron la actividad osteoprotectora de *C. barometz, in vitro.* Para esto, extrajeron, aislaron y purificaron los polisacáridos crudos solubles alcalinos del rizoma de *C. barometz*, obteniendo dos fracciones llamados CBBP-2 y CBBP-3. CBBP-2 mostró actividad en los niveles de fosfatasa alcalina y promovió la mineralización osteogénica. En otro estudio subsecuente, Huang y col. [31] en un modelo de ratas ovariectomi-

zadas probaron los efectos osteoprotectores del CBBP-1, el cual aumentó significativamente el contenido mineral óseo y la densidad mineral ósea, mejorando las propiedades biomecánicas del tejido óseo. Además, las células osteoblásticas MC3T3-E1 tratadas con CBBP-1 aumentaron la expresión de ARNm del factor de transcripción 2 relacionado con runt, osterix, osteopontina, osteocalcina y sialoproteína ósea, lo que indica que CBBP-1 puede estimular la diferenciación osteoblástica. Más adelante, en un estudio *in vitro,* Huang y col. [32] aislaron polisacáridos crudos de *C. barometz*, identificando dos polisacáridos homogéneos (CBP70-1-1 y CBP70-1-2). Los experimentos de los efectos de CBP70-1-1 y CBP70-1-2 revelaron que promueven la proliferación, diferenciación y mineralización de las células MC3T3-E1, incluso mejor que las células bajo tratamiento con estradiol.

f) Prevención de osteoartritis

Chen y col. [17] llevaron a cabo un experimento en un modelo de osteoartritis con ratas utilizando un extracto del rizoma de *C. barometz*. En este estudio, las células SW1353 tratadas a concentraciones de 100 a 500 μg/mL, con o sin IL-1β, no mostraron disminución en la viabilidad celular. En la evaluación histológica se encontró evidencia que sugiere que podría aliviar significativamente el cartílago degeneración en dicho modelo de osteoartritis. También encontraron que el extracto puede inhibir significativamente la alternancia anormal de COX_2 ARNm y PGE_2 con efecto dosis dependiente. Además, reportaron que dicho extracto puede suprimir notablemente la expresión de MMP-1, MMP-3 y MMP-13 en el ARNm. Por último, en lo que concierne al efecto en la vía de señalización NFκB, se reportó que NFκB p65 se translocaba a los núcleos desde el citoplasma después de haber sido pretratado con IL-1β, y que una dosis alta del extracto puede suprimir en cierta medida la translocación nuclear de NFκB p65.

g) Actividad hepatoprotectora

Xie y col. [15] aislaron del rizoma de *C. barometz* cinco glucósidos de hemiterpeno no identificados previamente, cibotiumbarósidos *E*, *F*, *G*, *H* e *I*; y dos glucósidos de hemiterpeno, previamente identificados. Los cibotiumbarósidos *F* e *I* exhibieron una notable actividad hepatoprotectora contra el daño hepático agudo inducido por acetaminofén (APAP) *in vitro,* resultando incluso más efectivos que el control positivo hepatoprotector, el biciclol. Sin embargo, siete glucósidos de hemiterpeno resultaron inactivos en los ensayos de citotoxicidad, neuroprotección, antidiabéticos y antiinflamatorios.

Li y col. [16] probaron *in vitro* el efecto hepatoprotector de algunos glucósidos obtenidos de *C. barometz,* empleando una metodología similar al estudio de Xie y col. [15], e informaron que algunos de los compuestos aislados de podrían reducir significativamente el daño celular HepG2 inducido por APAP, incluso más que el biciclol.

DISCUSIÓN

La evidencia encontrada en los estudios incluidos en la presente revisión de *C. barometz* apunta a múltiples efectos biológicos y terapéuticos, uno de los efectos más estudiados es el antioxidante. Una de las consideraciones importantes acerca del efecto antioxidante reportado es que depende, además de las características propias de la planta en sí, del método de extracción utilizado [4], por lo que aún hace falta establecer cuál es la metodología idónea. Los antioxidantes son compuestos que inhiben o reducen los efectos provocados por los radicales libres y los compuestos oxidantes. Los antioxidantes fenólicos actúan como captadores de radicales libres, y a veces, como quelantes de metales, tanto en el paso de iniciación como en la propagación del proceso oxidativo [33]. En este trabajo se ha encontrado evidencia de que *C. barometz* posee fitocompuestos con efecto antioxidante, lo que proveería de evidencia

científica al uso que se le da dado a dicho extracto en la medicina tradicional china [34]. Además, se ha reportado, al menos *in vitro,* como potencial anticancerígeno; este efecto protector podría estar relacionado con las propiedades antioxidantes de *C. barometz*, pero hace falta más investigación para dicha aplicación [35]. Plausiblemente, el efecto antioxidante podría promover la cicatrización de heridas de forma indirecta.

En la esta revisión se encontró que no hay suficiente evidencia para determinar si existe o no actividad antimicrobiana de *C. barometz* y para la cicatrización de heridas. En el estudio de Lai y col. [21] se reportó la concentración en la que se observa un halo de inhibición pero no se llevó a cabo la determinación de la concentración mínima inhibitoria. La prueba de difusión en disco depende por completo de la capacidad para difundirse en el agar la sustancia probada, por lo cual no es el método más adecuado para afirmar que existe actividad antimicrobiana. En cambio, en el estudio realizado por Heng y col. [13] se encontraron las concentraciones mínimas inhibitorias de todos los microorganismos probados, pero no la concentración mínima letal. Dados estos resultados, y la escasa evidencia encontrada en esta revisión, es probable que el efecto de *C. barometz* sea la disminución del crecimiento microbiano.

Por otro lado, el efecto de la temperatura para la obtención de extractos es importante, pero es un parámetro poco estudiado en los extractos de *C. barometz,* considerando que los extractos utilizados en la medicina tradicional se llevan a cabo por infusión acuosa. En diversos estudios incluidos se utilizó metanol, el cual se ha reportado que es un solvente adecuado para la extracción de polifenoles de plantas frescas debido a su capacidad para inhibir la acción de las polifenoloxidasas que podrían afectar la actividad antioxidante, ya que este solvente puede evaporarse con facilidad [36].

Al menos en la fase experimental *in vitro* e *in vivo*, los resultados de los estudios apuntan que el extracto de *C. barometz* promueve de manera pronunciada la expresión de genes marcadores relacionados con la osteogénesis, mediante la activación de la vía de señalización de las proteínas morfogenéticas óseas, y dicha vía promueve la formación ósea. Por lo tanto, *C. barometz* podría ser empleado como un potencial tratamiento complementario para la prevención y el tratamiento de la osteoporosis posmenopáusica [29,31].

Mediante estudios en animales fue reportado que *C. barometz* tiene un efecto hepatoprotector, lo cual también ha sido sustentado desde la medicina tradicional china. En este sentido, plausiblemente se puedan desarrollar formulaciones con *C. barometz* que intervengan en el tratamiento integral de estas patologías.

Desde hace varias décadas, aprovechando las propiedades de *C. barometz*, se cuenta una preparación comercial para uso profesional odontológico. Inicialmente se conoció como Alvogyl® (Septodont, Francia) y se usaba como apósito postexodoncia por su efecto hemostático, analgésico y antimicrobiano, el cual contenía pelos de *C. barometz* y otros agentes activos, sin embrago, esta formulación generó preocupación acerca de la seguridad del paciente debido a posibles reacciones alérgicas al yodoformo. Debido a esto, actualmente se distribuye como Alveogyl®, una reformulación de este apósito utilizando las fibras provenientes de *C. barometz* y otros compuestos como eugenol, lauril sulfato de sodio, carbonato de calcio, aroma de menta y excipientes [37]. Reportes indican que Alveogyl® se ha utilizado de forma tópica para la prevención y tratamiento local de la osteítis alveolar con buenos resultados y alta tolerabilidad [38,39], por lo que se emplea de forma cotidiana gracias a su fácil colocación y eficacia. Aunque se buscaron estudios clínicos que incluyeran apósitos únicamente formulados con *C. barometz* no se encontraron, lo cual indica que hace falta investigación al respecto.

Aunque la revisión sistemática permite analizar de manera crítica la evidencia científica reportada [40], en la presente no se encontraron estudios clínicos o ensayos clí-

nicos aleatorizados que pudieran proveer de la evidencia científica más alta. Casi todos extractos encontrados fueron preparados a través de métodos que no son semejantes a la forma de infusión o decocción como se utilizan en la medicina tradicional, por lo cual no hay evidencia de que su uso en estos preparados tenga un efecto terapéutico. Únicamente se encontraron estudios *in vivo* e *in vitro*, los cuales son útiles para conocer las bases científicas y mecanismos de acción de los objetos de estudio, pero que no muestran una evidencia definitiva y robusta sobre el efecto terapéutico o la potencial toxicidad en humanos [41].

Por tanto, la evidencia apunta a que *C. barometz* exhibe diversos efectos biológicos tanto *in vitro* como *in vivo* con potencial para tratar diversas afecciones. Los efectos reportados de *C. barometz* fueron como antioxidante, antimicrobiano, antiviral, pretratamiento anticancerígeno, estimulación de la proliferación de condrocitos, osteoprotector y hepatoprotector. La investigación actual deja en manifiesto los amplios usos de las plantas que han sido empleadas en la medicina tradicional, por lo que más estudios pueden dar pie a ensayos clínicos que deriven en nuevas opciones terapéuticas.

AGRADECIMIENTO

LAF agradece al Programa Investigadoras e Investigadores por México del CONAHCyT, LESDH agradece por la beca posdoctoral CONAHCyT, asimismo todos los autores agradecen a la División de Estudios de Posgrado e Investigación del Tecnológico Nacional de México/Instituto Tecnológico de Toluca por el apoyo otorgado.

Financiamiento

Ninguno.

Declaración de conflicto de intereses

Ninguno.

Número ORCID de los autores

- José Luis Rivas-García (JLGR): 0000-0003-4849-7370
- Nayely Torres-Gómez (NTG): 0000-0002-3945-2552
- Luisa E. Silva-De Hoyos (LESDH): 0000-0002-8511-2284
- Liliana Argueta-Figueroa (LAF): 0000-0002-1044-6757

Contribución de los autores

JLGR y LAF: Conceptualización, metodología y supervisión.• JLGR, NTG, LESDH, LAF: Recolección, síntesis y análisis de datos. • LAF. Escritura y preparación del manuscrito original.• LAF. Revisión y edición del manuscrito.

REFERENCIAS

1. **Bissanti G**. *Cibotium barometz*: Un Mondo Ecosostenibile; 2023 [02/03/2023]. Disponible en: https://antropocene.it/es/2023/02/01/cibotium-barometz-3/.
2. **Abraham S, Thomas T**. Ferns: A Potential Source of Medicine and Future Prospects. In: Marimuthu J, Fernández H, Kumar A, Thangaiah S, editors. Ferns: Biotechnology, Propagation, Medicinal Uses and Environmental Regulation. Singapore: Springer Nature; 2022. p. 345-378.
3. **Appleby JH**. The Royal Society and the Tartar lamb. Notes Rec R Soc Lond. 1997;51(1):23-34. *https://doi.org/10.1098/rsnr.1997.0003.*
4. **Lim TK**. *Cibotium barometz*. Edible Medicinal and Non-Medicinal Plants. 2015:82-91. *https://doi.org/10.1007/978-94-017-7276-1_4.*
5. **Ávila-Avilés RD, Argueta-Figueroa L, García-Contreras R, Vilchis-Nestor AR.** Synthesis of biogenic silver and gold nanoparticles from *Anemopsis californica* extract with antibacterial and cytotoxic activities. Mater Today Commun 2024; 38:108071. Disponible en: *https://doi.org/10.1016/j.mtcomm.2024.108071.*

6. **Morales-Luckie RA, Lopezfuentes-Ruiz AA, Olea-Mejía OF, Argueta-Figueroa L, Sanchez-Mendieta V, Brostow W, Hinestroza JP**. Synthesis of silver nanoparticles using aqueous extracts of *Heterotheca inuloides* as reducing agent and natural fibers as templates: *Agave lechuguilla* and silk. Mater Sci Eng, C 2016;69:429-436. *https://doi.org/10.1016/j.msec.2016.06.066.*
7. **Tricco AC, Lillie E, Zarin W, O'Brien KK, Colquhoun H, Levac D, Moher D, Peters MDJ, Horsley T, Weeks L, Hempel S, Akl EA, Chang C, McGowan J, Stewart L, Hartling L, Aldcroft A, Wilson MG, Garritty C, Lewin S, Godfrey CM, Macdonald MT, Langlois EV, Soares-Weiser K, Moriarty J, Clifford T, Tunçalp Ö, Straus SE.** PRISMA Extension for Scoping Reviews (PRISMA-ScR): Checklist and Explanation. Ann Intern Med 2018;169(7):467-473. *https://doi.org/10.7326/M18-0850.*
8. **World Health Organization** - Traditional Medicine Global Summit 2023 [01/02/2024]. Disponible en: https://www.who.int/publications/m/item/who-traditional-medicine-summit-2023-meeting-report--gujarat-declaration.
9. **Gurib Fakim A**. Medicinal plants: Traditions of yesterday and drugs of tomorrow. Mol Aspects Med 2006;27(1):1-93. *https://doi.org/10.1016/j.mam.2005.07.008.*
10. **Xu G, Sun N, Zhao MJ, Ju CG, Jia TZ**. Study on decoction's effect of different processed rhizomes of *Cibotium barometz* on retinoic acid induced male rats osteoporosis. Zhongguo Zhong Yao Za Zhi. 2014;39(6):1011-1015.
11. **Xie MP, Li L, Lu AQ, Zheng YP, Zang CX, Sun H, Wang SJ**. Phenolic acid and glycosides from rhizomes of *Cibotium barometz*. Chin Tradit Herb Drugs 2016;47(2):194-199. *https://doi.org/10.7501/j.issn.0253-2670.2016.02.002.*
12. **Al-Wajeeh NS, Hajrezaie M, Al-Henhena N, Kamran S, Bagheri E, Zahedifard M, Saremi K, Noor SM, Ali HM, Abdulla MA**. The antiulcer effect of *Cibotium barometz* leaves in rats with experimentally induced acute gastric ulcer. Drug Des Devel Ther 2017;11:995-1009. *https://doi.org/10.2147/DDDT.S107018.*
13. **Heng YW, Ban JJ, Khoo KS, Sit NW**. Biological activities and phytochemical content of the rhizome hairs of *Cibotium barometz* (Cibotiaceae). Ind Crops Prod 2020;153:112612. *https://doi.org/10.1016/j.indcrop.2020.112612.*
14. **Wang L, Xu H, Yu L, Zhu Z, Ye H, Liu L, Li X, Peng J**. Simultaneous separation and analysis of five compounds in *Cibotium barometz* by micellar electrokinetic chromatography with large-volume sample stacking. Separations 2021;8(9):147. *https://doi.org/10.3390/separations8090147.*
15. **Xie MP, Li L, Sun H, Lu AQ, Zhang B, Shi JG, Zhang D, Wang SJ**. Hepatoprotective hemiterpene glycosides from the rhizome of *Cibotium barometz (L.) J. Sm*. Phytochemistry 2017;138(1):128-133. *https://doi.org/10.1016/j.phytochem.2017.02.023.*
16. **Li L, Xie M-P, Sun H, Lu A-Q, Zhang B, Zhang D, Wang S-J**. Bioactive phenolic acid-substituted glycoses and glycosides from rhizomes of *Cibotium barometz*. J Asian Nat Prod Res 2019;21(10):947-953. *https://doi.org/10.1080/10286020.2018.1563076.*
17. **Chen G-Y, Wang Y-F, Yu X-B, Liu X-Y, Chen J-Q, Luo J, Tao Q-W**. Network pharmacology-based strategy to investigate the mechanisms of *Cibotium barometz* in treating osteoarthritis. Evid Based Complement Alternat Med 2022;2022:1826299. *https://doi.org/10.1155/2022/1826299.*
18. **Kim NH, Lee JY, Kim CY**. Protective role of ethanol extract of *Cibotium barometz* (*Cibotium* Rhizome) against dexamethasone-induced muscle atrophy in C2C12 myotubes. Int J Mol Sci 2023;24(19). *https://doi.org/10.3390/ijms241914798.*
19. **Li Y, Zhang N, Peng X, Ma W, Qin Y, Yao X, Huang C, Zhang X**. Network pharmacology analysis and clinical verification of Jishe Qushi capsules in rheumatoid arthritis treatment. Medicine (Baltimore)2023;102(34):e34883.*https://doi.org/10.1097/md.0000000000034883.*

20. **Ji Z, Fan B, Chen Y, Yue J, Chen J, Zhang R, Tong Y, Liu Z, Liang J, Duan L**. Functional characterization of triterpene synthases in *Cibotium barometz*. Synth Syst Biotechnol 2023;8(3):437-444. *https://doi.org/https://doi.org/10.1016/j.synbio.2023.06.005*.
21. **Lai HY, Lim YY, Tan SP**. Antioxidative, tyrosinase inhibiting and antibacterial Activities of leaf extracts from medicinal ferns. Biosci Biotechnol Biochem 2009;73(6):1362-1366. *https://doi.org/10.1271/bbb.90018*.
22. **Mai W, Chen D, Li X**. Antioxidant activity of Rhizoma Cibotii *in vitro*. Adv Pharm Bull 2012;2(1):107-114. *https://doi.org/10.5681/apb.2012.015*.
23. **Zarib ANM, Zollappi ANH, Abidin MZ, Rahim MBHA, Gani SA, Hamid M, Khayat ME**. Total phenolic, total flavonoid and antioxidant activity of extract from rhizome of *Cibotium barometz* prepared by various solvents. Malays J Biochem Mol Biol 2018;21(2):17-22.
24. **Wen CC, Shyur LF, Jan JT, Liang PH, Kuo CJ, Arulselvan P, Wu JB, Kuo SC, Yang NS**. Traditional Chinese medicine herbal extracts of *Cibotium barometz*, *Gentiana scabra*, *Dioscorea batatas*, *Cassia tora*, and *Taxillus chinensis* inhibit SARS-CoV replication. **J Tradit Complement Med** 2011;1(1):41-50. *https://doi.org/10.1016/S2225-4110(16)30055-4*.
25. **Shi Y, Wang X, Wang N, Li FF, You YL, Wang SQ**. The effect of polysaccharides from *Cibotium barometz* on enhancing temozolomide–induced glutathione exhausted in human glioblastoma U87 cells, as revealed by 1H NMR metabolomics analysis. Int J Biol Macromol 2020;156:471-484. *https://doi.org/10.1016/j.ijbiomac.2020.03.243*.
26. **Fu C, Zheng C, Lin J, Ye J, Mei Y, Pan C, Wu G, Li X, Ye H, Liu X**. *Cibotium barometz* polysaccharides stimulate chondrocyte proliferation in vitro by promoting G1/S cell cycle transition. Mol Med Rep 2017;15(5):3027-3034. *https://doi.org/10.3892/mmr.2017.6412*.
27. **Peng Z, Xu R, You Q**. Role of traditional Chinese medicine in bone regeneration and osteoporosis. Front Bioeng Biotechnol 2022;10:911326. *https://doi.org/10.3389/fbioe.2022.911326*.
28. **Cuong NX, Minh CV, Kiem PV, Huong HT, Ban NK, Nhiem NX, Tung NH, Jung JW, Kim HJ, Kim SY, Kim JA, Kim YH**. Inhibitors of osteoclast formation from Rhizomes of *Cibotium barometz*. J Nat Prod 2009;72(9):1673-1677. *https://doi.org/10.1021/np9004097*.
29. **Zhao X, Wu ZX, Zhang Y, Yan YB, He Q, Cao PC, Lei W**. Anti-osteoporosis activity of *Cibotium barometz* extract on ovariectomy-induced bone loss in rats. J Ethnopharmacol 2011;137(3):1083-1088. *https://doi.org/10.1016/j.jep.2011.07.017*.
30. **Huang D, Zhang M, Chen W, Zhang D, Wang X, Cao H, Zhang Q, Yan C**. Structural elucidation and osteogenic activities of two novel heteropolysaccharides obtained from water extraction residues of *Cibotium barometz*. Ind Crops Prod 2018;121:216-225. *https://doi.org/10.1016/j.indcrop.2018.04.070*.
31. **Huang D, Zhang M, Yi P, Yan C**. Structural characterization and osteoprotective effects of a novel oligo-glucomannan obtained from the rhizome of *Cibotium barometz* by alkali extraction. Ind Crops Prod 2018;113:202-209. *https://doi.org/10.1016/j.indcrop.2018.01.034*.
32. **Huang D, Hou X, Zhang D, Zhang Q, Yan C**. Two novel polysaccharides from rhizomes of *Cibotium barometz* promote bone formation via activating the BMP2/SMAD1 signaling pathway in MC3T3-E1 cells. Carbohydr Polym 2020; 231:115732. Disponible en: *https://doi.org/10.1016/j.carbpol.2019.115732*.
33. **Virgili F, Marino M**. Regulation of cellular signals from nutritional molecules: a specific role for phytochemicals, beyond antioxidant activity. Free Radic Biol Med 2008;45(9):1205-1216. *https://doi.org/10.1016/j.freeradbiomed.2008.08.001*.
34. **Pomarón C**. Dietética en los síndromes de riñón y vejiga. Rev Int Acupunt 2012;6(2):77-82. *https://doi.org/10.1016/S1887-8369(12)70057-1*.

35. **Williams Ibarra J, Carrero Y, Vargas JH, Acosta M**. Capacidad pro-apoptótica *in vitro* de *Valeriana rígida y Valeriana decussata* sobre una línea celular de cáncer de mama. Invest Clín 2022;63(4):376-387. *https://doi.org/10.54817/IC.v63n4a05.*
36. **Lim YY, Quah EPL**. Antioxidant properties of different cultivars of *Portulaca oleracea*. Food Chem 2007;103(3):734-740. *https://doi.org/10.1016/j.foodchem.2006.09.025.*
37. **Kalsi HK, Major R, Jawad H**. Alvogyl or Alveogyl? Br Dent J 2020;229(4):211. *https://doi.org/10.1038/s41415-020-2073-x.*
38. **Ehab K, Abouldahab O, Hassan A, Fawzy El-Sayed KM**. Alvogyl and absorbable gelatin sponge as palatal wound dressings following epithelialized free gingival graft harvest: a randomized clinical trial. Clin Oral Investig 2020;24(4):1517-1525. *https://doi.org/10.1007/s00784-020-03254-z.*
39. **Assari AS, Alrafie HS, Al Ghashim AH, Talic FN, Alahmari AM, Al Manea MY, Alrashdan RY**. Effectiveness of different socket dressing materials on the postoperative pain following tooth extraction: a randomized control trial. J Med Life 2022;15(8):1005-1012. *https://doi.org/10.25122/jml-2022-0140.*
40. **Torres-Rosas R**. Generalidades de la elaboración de la revisión sistemática en acupuntura. Rev Int Acupunt 2022;16(3):100192. *https://doi.org/https://doi.org/10.1016/j.acu.2022.100192.*
41. **Manzo-Toledo A, Torres-Rosas R, Mendieta-Zerón H, Arriaga-Pizano L, Argueta-Figueroa L**. Hydroxychloroquine in the treatment of covid-19 disease: A systematic review and meta-analysis. Med J Indones 2021;30(1):20-32. *https://doi.org/10.13181/mji.oa.205012.*

Investigación Clínica
Vol. 65 Nº 3 / September 2024
Bilingual - Abstracts in Spanish and English

Contents

Investigación Clínica
Vol. 65 Nº 3 /Septiembre 2024
Bilingüe - Resúmenes en Español e Inglés

Contenido